ZANCO
Journal of Pure and Applied Sciences

زانکۆی سەلاحەدین - هەولێر
Salahaddin University-Erbil

Volume 31, Number 6, 2019

RESEARCH PAPER

An Analysis of Causes and Factors Affecting Change Orders Occurrence in Construction Projects in Iraq

Khalil Ismail Wali[1] and Nazik Imad Saber*[2]

[1,2]Department of civil, College of Engineering, Salahaddin University-Erbil, Kurdistan Region, Iraq.

A B S T R A C T:

One of the most important problems facing the construction management process is the occurrence of change orders, which became inevitable in every construction project and the magnitude of these variations varies considerably from project to project. Considerably causing different effects to the project like changes in cost, time, quality, and completion schedule. The objective of this study is analyzing change orders causes related to owner, contractor, consultant and other causes and their effects on project cost for the Kirkuk governorate-Iraq selected as a case study for the purpose of this paper. The Relative Importance Index (RII) methodology was used to analysis the collected data. The case study analysis focused on the selection of 12 construction projects and a questionnaire administered to professionals in the construction industry in Iraq. According to the questionnaire analysis of 40 questions and based on RII ranking was found that the top most ten significant causes of the change orders come to the poor project management in the first rank. Whereas, change in the country's economic conditions comes in the second rank, contractor's lack of experience and mistakes during construction stage, poor cost estimation, quality assurance and control, poor performance of contract and subcontractor, the contractor's financial difficulties, the lack of required skills, unrealistic project durations and design errors and omissions, and finally the collision between contract documents.

INTRODUCTION :

Change orders have many definitions depending on different researches one of which is that the change order is a written order to the contractor, signed by the owner, and issued after execution of the contract, authorizing a change in the work or an adjustment in the contract sum or the contract time. Every change that is done to the project leads to the impact on time and cost of the project. Change order brings a problem to all parties included in the project and in most of the cases are causes of the contractual disputes. There are many reasons that a change order can be issued such as errors and omissions on design, market conditions, slow delivery of the required material and other similar factors.

The construction projects related change orders and the subsequent conflicts are the main causes of major problems in the industry such as delays in project completion, increase in cost, and defects in quality. A change may be because of an addition, deletion, or revision of the project scope (Naoum, 1994).

Sun and Meng (2009) reviewed and combined existing literature on project change causes and effects developed two classifications for change causes and change effects, and illustrated how the taxonomies can be used during the project change management process.

The essential elements in any construction projects are the triple constraint factors (cost, time and quality) Due to many causes, these elements can significantly differ from the premier evaluation of contract in terms of these elements. The reasons could be changed in the specification, scheduling, or any other contract documents.

When change occurs, it brings many negative impacts to both parties (contractor and owner) also effected on all stage of project specific when the change occur in execution stage because it is effected on the productivity of labor, tools, equipment, and so on and maybe causes dispute for manager and site engineer (Halwatura and Ranasinghe, 2013).

Change order on a construction project is a work that added to or deleted from the original scope of work of a contract which alters the original contract amount or completion date, unavoidably a change order represents a problem on the project in terms of additional cost, or additional time or both. Change orders play a significant role in construction because they have a great impact on cost, schedule, quality, safety, and productivity. So, they are one of the major causes of project failure (Desai et al., 2015).

It is rarely to finish or closeout a construction project without a change which usually emerges as a consequence of some reasons attributed to the two signed parties that are participating or engage in contract documents or the parties that take part in the project execution. Upon recognizing its structure, the change is contractually legalized by the issuance of a change order, which is a script detailing the scope of the change and its effect on both cost and time. If no approved is arrive the parties of the project on the change, it turnovers into an allegation or contention that have an influence on execution stage of the project and effect on project successfully completion (Alaryan, 2014).

The causes behind project changes are mostly, communication inefficiency of not being in time and being ineffective, improper integration, ambiguity, environment changes, and aggregation of project complexity. The substantial effects of change orders on the projects time period and on the direct and indirect involved cost factors can be assessed from a project management standpoint (Lokhande and Ahmed, 2015).

Most of the change orders issued during the construction period are major causes of time and cost overruns, disruption, and disputes. In some cases, change orders cause confusion and lead to a detrimental effect on the environment. Yet, no unique method is available for avoiding or managing them effectively (Alnuaimi et al., 2009).

The main objectives of the study were to identify the causes of change orders in construction projects, using a case study analysis and rank them based on the number of occurrences and percentage to determine their effects on the occurrence of change orders in construction projects in Iraq. Hence, Kirkuk Governorate projects selected as a case study for the purpose of this study.

2. THE LITERATURE REVIEW

Wu et al. (2004) concluded that the key reasons for change orders in Taiwan were poorly implemented design drawings, policy changes and new management requests are not essential causes of change orders.

Alnuaimi et al. (2009) discussed change orders in public construction projects in Oman by investigating causes of variations, studying their effects on the project, identifying the beneficial parties, and suggesting remedies to alleviate related problems.

Mohammad et al. (2010) investigated the most significant causes contribute to the variation orders in the in in in the States of Selangor, Malaysia. The result concluded that owner is the main cause of the change orders in the building projects and recommended that owner should have appropriate planning and alternatives before starting a project in order to avoid variation order during the construction phase.

A change order is an official document that is used to adjust the approved contractual agreement and develops as a part of the project's forms. The conclusion of these authors study showed that conflicts between contract documents, lack of participation in the design phase, always vary the project objective is one of the strong reason causing change orders. The change orders reduced by good communication through contract preparation, good project implementation planning of following activities and keep good connection among all parties. The owner should take all the benefits of consultancy selected to the projects (Keane et al., 2010).

Enshassi et al. (2010) analyzed the reasons of variation orders in construction projects in the Gaza Strip. The results showed that causes related to the consultant are the main significant reasons of variation orders followed by the factors related to the owner.

Priyantha et al. (2011) identified the causes, nature, and effects of variations in

highways construction in Sri. The results revealed the higher number of cost overrun projects than the number of cost reduction projects. According to the analysis, it is identified that change causes at least a 9.9% mean change of first contract sum. Thus, it can be said that the effects of variation are visible in the form of cost overruns in highways project.

Halwatura and Ranasinghe (2013) focused on the causes of change orders in road projects in Sri Lanka. The research identified that poor estimation is the main cause of variation orders in the road construction industry. For instance, the consultants do not accomplish adequate studies at the initial investigation and design phase.

Han (2014) examined the effects of change orders in infrastructure projects in the cost aspects. Regardless of sighting different contract processes or what so ever, contract change orders (CCO) are yet predictable due to unexpected utility conflicts, unpredicted geology, and other unforeseen conditions. No matter of the project location and condition, the CCO undesirably affects the project in aspects of the cost.

Jadhav and Bhirud (2015) revealed that the key causes of change orders in construction projects in Pune are owner changes, additional work and adjustment to prior work and the second main reason is the absence of contractor participation in the design phase. It may lead to a lack of understanding design at the time of the construction stage. The other causes are unrealistic design periods, the lack of communication between the contractor and the consultants. The most significant effects of change orders increase the cost of the projects.

Msallam et al. (2015) studied the change orders in highway projects in Jordan which are the main severe problems in the highway projects. Variation order is any change and modification to the contractual forms of a project by the owner or the owner's representative, it can be an activity that is deleted or added to the original contract document, which modifies the original contract quantity or completion date. This study focused on the causes and impacts of change orders on time and cost also found that the main effects of variation orders are time delays, cost overrun, increase in overhead expenses, turnover of professionals and project team.

Sadrija (2016) carried out a study to find the causes and effects of change orders on project cost for the Albanian infrastructure project. As a result, was found out that the main cause of the change order is significant changes in the quantities of work and the main effect was found to increase in the cost of the project.

3. MATERIALS AND METHODS
3.1 Questionnaire Survey

The questionnaire designed and prepared taking in consideration the site engineer idea, owners, contractors, and consultant and their experience in construction help us in order to conclude in this survey all the required data to perform an effective survey. The questionnaire survey is prepared with the detailed understandable question in order to create an easily answered survey for the respondents.

3.2 Data Gathering and Evaluation

The questionnaire survey was prepared and distributed to professional personnel who have dealt with project changes in their professional experience. The survey was distributed to 46 people with different professions from which 100 % distributed to the civil engineers of different profiles and different years of experience and 15 companies (contractors and engineers). From the 46 surveys, 40 surveys were returned back completed meaning that 87 % of the people which were part of this survey answered.

A ranking procedure is used for the above causes starting from one which the one that produces most of the change orders up to the five which is the one that produces less the change orders. Otherwise, they can be classified from 1-5 as very high influence up to the no influence.

3.3 Survey the Change Order Occurrence in 12 Projects in Kirkuk Governorate:

The case study analysis was carried out for 12 project documents from recently completed mostly public projects comprises highway and building projects in Kirkuk Governorate in Iraq. The survey revealed that the change orders occurrence in the cost of the projects ranged from 0.03% to 28.8% due to various causes as listed in Table1.

Table 1: Survey of change occurring in Cost of 12 Projects in Kirkuk Governorate

No.	Name of Project	Name of Company	Type of the project	Initial Contract cost ID	Final cost ID	Percentage of change in project cost	Cause of the change
1	Construction of Shoraw bridge	Naseh Saaid Company	Highway project	4,027,831,200	4,195,389,200	4.16	Added paint task that not mentioning it in original detection and for the aesthetic site has been added this task for being in the entrance of the city and for the needed site to the necessary traffic tags with plastic pipes to connect the water to the garden.
2	Building School of 12 Classes	Al-arz al-khzraa Company	Building project	495,006,000	519,166,000	4.88	Because of design requirement
3	Rehabilitation and expand Reyaz Sailo	Qaws al-borj Company	Industrial project	418,995,000	432,945,000	3.33	According to work requirement
4	Construction of fountain in the entrance of Hawija Township	Direct execution	Highway project	43,383,750	52,063,750	20	To complete the required works because some of the activities were not mentioned in the tender
5	Development Erbil entrance/second stage	Khwakorek Company	Highway project	2,728,000,000	3,515,930,000	28.8	Adding concrete work for supporting walls to present low and high areas on both sides of the new road because of exposing the road.
6	Construction of Shewasor bridge with 260m (length)	Hana and Palkana Company	Highway project	11,097,100,000	9,759,800,000	-12.05	Re-design and cutting pieces of rock to reach the required levels according to the master plan
7	Building School of 12 Classes in al-Tanak	Domez and Mohammed Ismail Company	Building project	794,608,000	800,608,000	0.75	Because of decline the natural area level for school site from the street level by 120cm
8	Building six Schools with six classes in Taza, Laylan and Moltaqa districts.	Al-Wataniya Al-Aalamya Company	Building project	1,194,146,000	1,240,637,000	3.9	To raise the building level higher than street level according to client requirements.
9	Construction of second corridors for main ways (Mosul, Fatha and Laylan)	Dal and Saqr Al-Manara Company	Highway project	19,810,055,000	22,155,374,000	11.84	Due to design requirements
10	Building department of the school building	Dalta Al-Neel Al-Azraq Company	Building project	2,498,858,500	2,674,473,500	7.02	Because of failure in soil testing report and re-design the building foundation according to consultant office instructions
11	Rehabilitation and expand Kirkuk Sailo	Benaa Al-Motaqbal Company	Industrial project	373,000,000	374,800,000	0.48	According to the work needed and construction design requirement
12	Building school of 18 classes	Borj Al-Saaa Company	Building project	1,383.360.000	1,383,740,000	0.03	To treat groundwater problem around the building, squares and reservoirs

3.4 Relative importance index

For the analyzing of the survey questionnaire the relative importance index method will be used following the below formula: (Gundecha, 2012)

$RII = \dfrac{\sum W}{A*N}$ $\qquad$ $(0 \leq RII \leq 1)$

From which the characters have the below meaning:

$RII - Relative\ Importance\ Index\ RII \sum W - Weight\ given\ to\ each\ factor\ by\ the\ reposndents\ and\ ranges\ from\ 1\ to\ 5.$
$(A) - is\ the\ highest\ weight\ (in\ this\ study\ 5)\ and$
$(N) - total\ number\ of\ (40)$

Example of calculating the RII as listed in Table 3 as follows:

$W = a_1*n_1 + a_2*n_2 + a_3*n_3 + a_4*n_4 + a_5*n_5$
$= 1*1 + 2*9 + 3*12 + 4*14 + 5*4 = 131$

$RII = \dfrac{131}{5*40} = 0.655$

4. Data Analysis

4.1 Respondents Personal Profile

The survey showed the profile of respondents for five items in Table 2.

Table 2: Personal Information

Personal information	Categories	Percent
1. Age Group (years)	18-24	5
	25-34	35
	35-44	27.5
	Over 45	32.5
2. Experience (years)	Under 5	7.5
	5_9	32.5
	10_19	30
	Over 20	30
3. Position	Owner	2.5
	Consultant	17.5
	Contractor	22.5
	Site Engineer	42.5
	Project Manager	15
4. The time has been in his present position (years)	Less than 2	15
	2_5	22.5
	6_9	20
	Over 10	42.5
5. The main type of construction work	Highway	20
	Building	50
	Industrial	15
	water resources	10
	Other	5

4.2 Overall Evaluation of Causes of Change order

Based on the analysis performed for the survey questionnaire using the relative importance index method RII of the Change order is shown in Table 3.

Table 3: Analysis of Change Order Causes

	Causes of change order	1	2	3	4	5	∑W	RII	Rank
No.	**A. Causes due to Owner**								
1	Additional works.	1	9	12	14	4	131	0.655	25
2	Acceleration of work by owner.	2	8	20	7	3	121	0.605	31

3	Lack of information given to the contractor.	4	2	10	21	3	137	0.685	18
4	Poor cost estimation.	0	3	7	19	11	158	0.790	4
5	Owner's change of planning because of financial issues.	2	5	14	15	4	134	0.670	20
6	Owner Interference.	3	9	19	7	2	116	0.580	36
7	Owner satisfaction factor.	7	10	16	5	2	105	0.525	38
8	Change in specifications.	1	7	14	15	3	132	0.660	24
9	Poor owner briefing or the clarity of requirement.	0	6	23	9	2	127	0.635	28
	B. Causes due to Contractor								
10	The lack of required skills.	0	5	9	18	8	149	0.745	8
11	The scope of work for the contractor is not will defined.	0	5	15	16	4	139	0.695	12
12	Poor project management.	0	5	4	15	16	162	0.810	1
13	Differing site conditions.	1	8	21	9	1	121	0.605	31
14	Contractor's lack of experience and mistakes during construction stage.	0	2	11	13	14	159	0.795	3
15	Poor performance of Contract and subcontractor.	0	4	9	16	11	154	0.770	6
16	The contractor's financial difficulties.	0	2	14	13	11	153	0.765	7
17	Conflict between contract documents.	0	3	16	11	10	148	0.740	9
18	Time needed to rectify defects.	0	7	11	19	3	138	0.690	13
	C. Causes due to Consultants								
19	Poor coordination between consultant and contractors or subcontractor.	0	8	14	15	3	133	0.665	24
20	Unrealistic project duration and design errors and omissions.	1	3	13	12	11	149	0.745	8
21	Non-conformity of designs with governmental regulations and laws.	0	8	12	14	6	138	0.690	13
22	Quality assurance/control	0	2	14	11	13	155	0.775	5
23	Failure to perform design and supervision effectively by consultant.	1	4	17	17	1	133	0.665	23
24	Failure by consultant supervision and coordination with his junior team.	4	7	15	10	4	123	0.615	30
25	Poor working drawing details or non-complete drawing or specification.	1	4	17	12	6	138	0.690	13
26	Lack of project ideas and information given to the designer.	2	3	19	14	2	131	0.655	25
27	Techniques change (If time between design and construction is long).	2	8	14	12	4	128	0.640	27
28	Non-conformity of designs with the requirements of the employer.	0	6	27	4	3	124	0.620	29
29	Lack of consultant experience about availability of materials or equipment.	2	2	15	18	3	138	0.690	13
	D. Other Causes								
30	Political pressure.	3	10	17	6	4	118	0.590	35

31	Inappropriate overall organizational structure linking to the project.	0	10	22	5	3	121	0.605	31
32	Problems on work place, unfamiliarity with local condition and safety consideration.	0	7	16	13	4	134	0.670	20
33	Unavailability of resources.	2	6	14	10	8	136	0.680	19
34	Unexpected conditions and weather conditions.	1	6	15	10	8	138	0.690	13
35	Problem with neighbors.	1	14	10	13	2	121	0.605	31
36	Mistakes and discrepancies in contract document	0	7	10	19	4	140	0.70	11
37	Corruption and illegal agreements.	2	3	16	17	2	134	0.670	20
38	Accident during construction.	4	12	14	6	4	114	0.570	37
39	Change in the country's economic conditions.	0	1	8	20	11	161	0.805	2
40	Change in government regulations and laws.	0	6	9	16	9	148	0.740	9

4.3 Top Ten Significant change order cause

According to the ranking process the analysis, result revealed that the top ten significant factors causes of the change orders are: the poor project management, change in the country's economic conditions, contractor's lack of experience and mistakes during construction stage, poor cost estimation, quality assurance/control, poor performance of Contract and subcontractor, the contractor's financial difficulties, the lack of required skills, unrealistic project durations and design errors and omissions, and conflict between contract documents with RIIs of 0.810, 0.805, 0.795, 0.790, 0.775, 0.770, 0.765, 0.745, 0.745, 0.740respectively.

4.4 Evaluation and Ranking of change order causes related to specified parties:

The ranking of cause of change orders related to specified parties are shown in Table 4. The most significant cause of change orders related to the owner which comes in the first rank is poor cost estimation followed by owner's change of planning because of financial issues which come in the second rank.

The most significant factor cause of change orders in projects due to the contractor is poor project management followed by contractor's lack of experience and mistakes during construction

stage. The third one is the poor performance of contract and subcontract.

The most significant factor cause change orders in projects due to consultant is quality assurance/ control followed by unrealistic project durations and design errors and omissions. The later effected cause of change order is Non-conformity of designs with governmental regulations and laws, Poor working drawing details or non-complete drawing or specification.

The most significant factor cause change orders in projects due to other causes is change in the country's economic conditions followed by, a change in government regulations and laws and mistakes and discrepancies in contract document.

Table 4: Ranking the Change Order Causes

Causes related to Owner									
	Additional works	Acceleration of work by owner	Lack of information given to the contractor	Poor cost estimation	Owner's change of planning because of financial issues	Owner interference	Owner satisfaction	Change in specification	Poor owner briefing or the clarity of requirement
Mean	3.28	3.08	3.43	3.95	3.35	2.90	2.65	3.30	3.18
Std. Deviation	1.012	.888	1.059	.876	1.001	.955	1.051	.939	.747
Ranking	5	7	3	1	2	8	9	4	6

Causes related to Contractor									
	The lack of required skills	The scope of work for the contractor is not well defined	Poor project management	Differing site conditions	Contractor's lack of experience and mistakes during the construction stage	The poor performance of contract and subcontract	The contractor's financial difficulties	The collision between contract documents	Time needed to rectify defects
Mean	3.73	3.48	4.05	3.03	3.98	3.85	3.83	3.70	3.45
Std. Deviation	.933	.847	1.011	.800	.920	.949	.903	.939	.876
Ranking	5	7	1	9	2	3	4	6	8

Causes related to Consultant										
	The lack of coordination between consultant and contractors or subcontractors	Unrealistic project durations and design errors and omissions	Non-conformity of designs with governmental regulations and laws	Quality assurance/ control	Failure to perform design and supervision effectively by the consultant.	Failure by consultant supervision and coordination with his junior team	Poor working drawing details or non-complete drawing or specification	Lack of project ideas and information given to the designer	Techniques change (If the time between design and construction is long)	Non-conformity of designs with the requirements of the employer	Lack of consultant experience about the availability of materials or equipment
Mean	3.33	3.73	3.45	3.88	3.33	3.08	3.45	3.28	3.20	3.10	3.45
Std. Deviation	.888	1.037	.986	.939	.797	1.11	.959	.877	1.043	.744	.904
Ranking	4	2	3	1	4	8	3	5	6	7	3

	Political pressure	Inappropriate overall organizational structure linking to the project	Problems on the workplace, unfamiliarity with local condition and safety	Unavailability of resources	Unexpected problems and weather conditions	Problem with neighbors	Mistakes and discrepancies in the contract document	Corruption and illegal agreements	Accident during construction	Change in the country's economic conditions	Change in government regulations and laws
Causes related to Other Factors											
Mean	2.95	3.03	3.35	3.40	3.45	3.03	3.50	3.35	2.85	4.03	3.78
Std. Deviation	1.061	.832	.893	1.128	1.061	1.000	.906	.893	1.122	.768	.974
Ranking	8	7	6	5	4	7	3	6	9	1	2

The illustration of responsibility of change order occurrence causes in terms average mean shown in a form of radar diagram in Fig.1 revealed that causes related to contractors are in the first rank causes at an average mean of 3.677, the consultant comes in the second rank in average of 3.389, and the owner comes in the fourth rank.
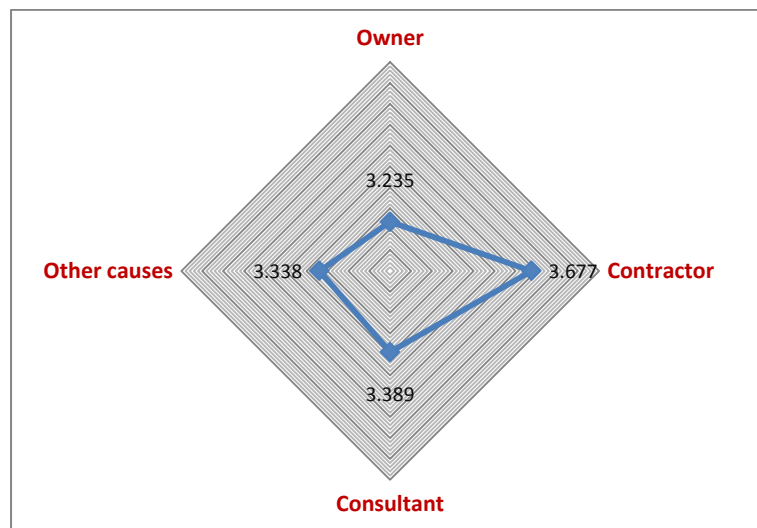
Figure 1: The average mean for the responsibility of change orders causes.

4.5 Fishbone diagram for causes and effect of projects change orders:

The Fishbone diagram also known as cause and effect or the Ishikawa diagram is an analysis tool that used to determine the potential root causes of a problem. This analysis also provides a systematic way for examining the effects of the causes that involve to those effects (Watson, 2004).
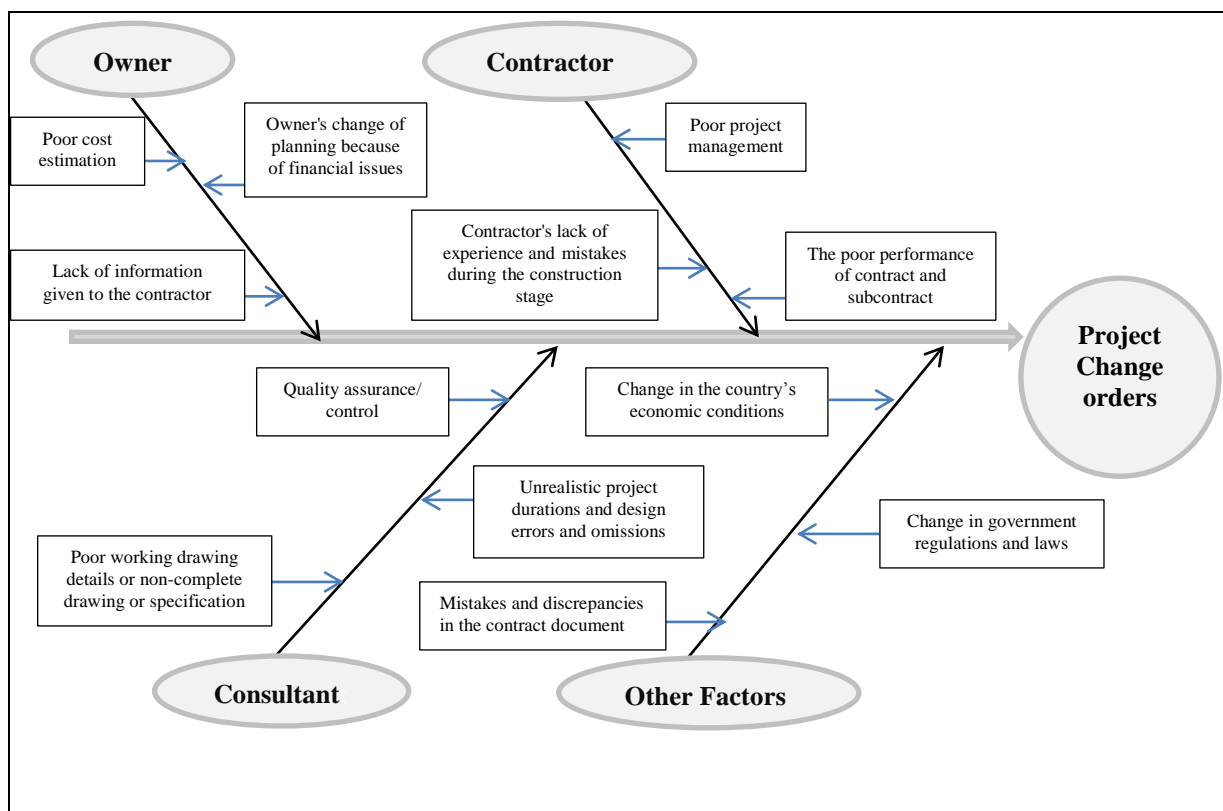
Figure 2: Fishbone diagram for causes and effect of change orders due to specified parties.

The fishbone diagram revealed the root causes of change orders due to owner, contractor, consultant, and other causes factors.

4.6 Reliability test:

To test the reliability of collected data used in this study and to examine how closely the interrelated the variables, SPSS program used to determine Cronbach's Alpha for 40 variables included in the questionnaire survey as shown below. The result of the analysis shows the Cronbach's Alpha was 0.861 > 0.7 hence checking the reliability of collected used for the purpose of this study.

Cronbach's Alpha	N of Items
.861	40

4.7 Comparison of the results of this study with other researches findings

The comparison between the findings of this study and other studies carried out in various countries conducted in terms of the top five significant causes of the change orders. Table 5 shows that in Iraq the main cause of change orders was, poor project management that compared to the other countries in Kuwait change of plans by owner is the main cause of change orders. In Jordan change of schedule is the main cause, in Gaza Strip lack of materials and equipment spare parts due to closure is the main cause of change orders and in Sri Lanka, poor estimation is the main cause of change orders that comes in the fourth rank in Iraq

		N	%
Cases	Valid	40	100.0
	Excluded[a]	0	.0
	Total	40	100.0

a. List wise deletion based on all variables in the procedure.

Table 5: Comparison of Top Five Significant Change Order Causes

Current study-Iraq (2018)	Kuwait (Alaryan, 2014)	Jordan (Msallam et al., 2015)	GAZA STRIP (Enshassi et al., 2010)	Sri Lanka (Halwatura and Ranasinghe, 2013)
Poor project management	Change of plans by owner	Change of schedule	Lack of materials and equipment spare parts	Poor Estimation
Change in the country's economic conditions.	Change of project scope by owner	Ambiguous design details	Change in design by consultant	Unforeseen site conditions
Contractor's lack of experience and mistakes during the construction stage.	Problems on site, errors	Change of plan or scope	Lack of consultant's knowledge of available materials	Political pressure
Poor cost estimation.	Omission in design	Conflict between contract documents	Errors and omission in design	Poor investigation
Quality assurance/control	Poor design and poor working drawing details	Lack of coordination	Conflicts between contract documents	Client-initiated variations

5. Conclusions

From the results and analysis of this research, study revealed that the most significant causes of change orders in Iraq were the poor project management followed by a change in the country's economic conditions and contractor's lack of experience, poor cost estimation, and quality assurance/control. At the same time, it was founded that the most significant causes of change orders occurrence related to the owner were poor cost estimation, owner's change of planning because of financial issues and lack in information given to the contractor. The most significant causes of change orders related to the contractor were; poor project management, contractor's lack of experience and mistakes during the construction stage and lack of information given to the contractor. Whereas, the most significant causes of change orders related to consultant were, quality assurance/ control, unrealistic project durations and design errors and omissions and non-conformity of designs with governmental regulations and laws. On other hand, the most significant causes of change orders are due to other causes were change in the country's economic conditions, change in government regulations and laws and mistakes and discrepancies in the contract document. The fishbone diagram also revealed the root causes of change orders due to owner, contractor, consultant, and other causes factors. Therefore, this study provides benefits to various parties involved in the construction sector in order to focus on the factors and causes of change order occurrence during the design stage and construction planning and management process.

References

ALARYAN, A. 2014. Causes and effects of change orders on construction projects in Kuwait. *International Journal of Engineering Research and Applications,* 4**,** 01-08.

ALNUAIMI, A. S., TAHA, R. A., AL MOHSIN, M. & AL-HARTHI, A. S. 2009. Causes, effects, benefits, and remedies of change orders on public construction projects in Oman. *Journal of Construction Engineering and Management,* 136**,** 615-622.

DESAI, N., PITRODA, J. & BHAVSAR, J. J. 2015. A review of change order and assessing causes affecting change order in Construction. *International academic Research for Multidisciplinary,* 2**,** 152-162.

ENSHASSI, A., ARAIN, F. & AL-RAEE, S. 2010. Causes of variation orders in construction projects in the Gaza Strip. *Journal of Civil Engineering and Management,* 16**,** 540-551.

GUNDECHA, M. 2012. Study of Factors Affecting Labor Productivity at a building construction Project in the USA. Web Survey.

HALWATURA, R. & RANASINGHE, N. 2013. Causes of variation orders in road construction projects in Sri Lanka. *ISRN Construction Engineering,* 2013.

HAN, N. 2014. *Quantifying Causes, Schedule, and Cost Impacts of Change Orders:" Is Alternative Contracting Really Effective?".*

JADHAV, O. U. & BHIRUD, A. N. 2015. An Analysis Of Causes and Effects Of Change Orders On Construction Projects In Pune. *International Journal of Engineering Research and General Science,* 3.

KEANE, P., SERTYESILISIK, B. & ROSS, A. D. 2010. Variations and change orders on construction projects. *Journal of legal affairs and dispute resolution in engineering and construction,* 2**,** 89-96.

LOKHANDE, M. A. & AHMED, F. S. Y. 2015. Assessing Consequences of Change Request Impact in Construction Industry of YEMEN: An Explorative Likert-Scale Based Survey Design. *Management,* 5**,** 141-147.

MOHAMMAD, N., ANI, A. C., RAKMAT, R. & YUSOF, M. 2010. Investigation on the causes of variation orders in the construction of building project–a study in the state of Selangor, Malaysia. *Journal of Building Performance,* 1.

MSALLAM, M., ABOJARADEH, M., JREW, B. & ZAKI, I. 2015. Controlling Of Variation Orders in Highway Projects in Jordan. *Journal of Engineering and Architecture,* 3**,** 95-104.

NAOUM, S. G. 1994. Critical analysis of time and cost of management and traditional contracts. *Journal of Construction Engineering and Management,* 120**,** 687-705.

PRIYANTHA, T., KARUNASENA, G. & RODRIGO, V. 2011. Causes, Nature and Effects of variations in Highways. *Built-Environment Sri Lanka,* 9.

SADRIJA, E. 2016. *CHANGE ORDER CAUSES, EFFECTS, CONTROLS AND THEIR IMPACT ON PROJECT COST IN ALBANIAN INFRASTRUCTURE PROJECTS.*

SUN, M. & MENG, X. 2009. Taxonomy for change causes and effects in construction projects. *International Journal of Project Management,* 27**,** 560-572.

WATSON, G. 2004. The legacy of Ishikawa. *Quality Progress,* 37**,** 54.

WU, C. H., HSIEH, T. Y., CHENG, W. L. & LU, S. T. 2004. Grey relation analysis of causes for change orders in highway construction. *Construction management and economics,* 22**,** 509-520.

RESEARCH PAPER

The Radar Coverage Estimation under Multiple Antennas and Targets

Arazoo Mustafa Aziz[*]

[*]Department of Electrical, College of Engineering, Salahaddin University-Erbil, Kurdistan Region, Iraq

A B S T R A C T:
   Choosing the suitable antenna type for a particular application has importance in meeting the desired system objects. In this paper the comparative studies between three different types of antenna, which are phased array, planar array and parabolic reflector, have been investigated based on their suitability as a basic radiating element for radar coverage. The radiation characteristics and size of the radiating structures that makes them a good candidate for the radar coverage, and second part radar coverage at different targets (objects). Radar Cross Section RCS of rectangular flat plat as simple target, and missile and aircraft as complex targets have been molded.
   The radar coverage of the Erbil International Airport (EIA) for Ultra High Frequency (UHF) band applications, in high resolutions, detect large target, and long range are estimated and considered as study case with different antennas and target or radar cross sections (RCS) for multipath/lobbing pattern.

1. INTRODUCTION:

The performance of radar system depends not only on the radar's design parameters but also on a number of other factors which have to be accounted for when assessing or predicting. The factors can be judged by maximum range, transmitted power, antenna size, target size (RCS), atmospheric effects, clutter (environment) and receiver noise (AL-Samerai *et al.*, 1988).

The simple radar equation based on free-space propagation, in most cases, far from accurate results and must be modified to account for multipath propagation and atmospheric refraction. The performance of radars is often assessed posteriori by flying known targets on predetermined trajectories and measuring the

detection ranges by the radar of interest installed on the chosen site. This is a time-consuming and costly method. A priori prediction of the performance of radar is to be sited in a suitable position chosen on the basis of information gained from maps obtained (Yossra *et al.*, 2002).

The antenna is one of the most critical parts of a radar system. It transfers the transmitter energy to signals in space with a required pattern. This process is applied in an identical way on reception. A graphic representation of the relative distribution of the radiated power in space is called a radiation pattern. Investment in the antenna therefore brings direct results in terms of system performance (Le *et al.*, 2014).

The electromagnetic (EM) theory lets the RCS measurement of targets that can be mathematically well defined, considering its size and physical forms. In practical this statement refers to targets with simple geometries. The solutions for simple targets are very important for two reasons, first reason, these objects can be considered as reference targets and they can be created and used

---

* **Corresponding Author:**
Arazoo Mustafa Aziz
E-mail: arazoo .aziz @su.edu.krd
Article History:
Received: 07/05/2019
Accepted: 09/08/2019
Published: 05/12 /2019

Aziz. A /ZJPAS: 2019, 31 (6): 13-22

14

as calibration references to measure complex geometry targets; second reason, approximations of equations used to determine the RCS of complex geometry targets can be made by detailed information of the behavior of targets of simple geometries and their combinations (Miacci *et al.*, 2002).

The estimation of RCS has been the field of focus in the recent years for various purposes. The research of radar cross section (RCS) of simple and complex objects is certainly Significant to identify targets such as aircrafts, rockets, ships and other objects, with the purpose of improving their radar visibility in various frequency ranges (Burgess *et al.*, 1988). Radar cross section diagrams are usually difficult to understand due to fact that they are two dimensional representations of three dimensional objects. Moreover, the difficulty in interpreting RCS diagrams is depend upon the geometry of the target and, sometimes on the techniques used to measure or calculate the RCS (Gottapu *et al.*, 2017).

In this study, focuses on three arrangements of antennas, the planar array, phased array and parabolic reflector, also three types of target, rectangular flat plat, missile and aircraft in Erbil international airport (EIA) are considered and selected as case study to check for optimal radar coverage and optimal detection probabilities applicable for UHF-band frequencies. Simulations are made for different antennas and targets for multipath/lobbing pattern.

2. RADAR RANGE EQUATION

The maximum radar range R_{max} is the distance beyond which the target cannot be detected in equation (1) (Merrill *et al.*, 2001).

$$R_{max} = \sqrt[4]{\frac{P_t G^2 \lambda^2 \sigma}{(4\pi)^3 S_{min}}} \quad (1)$$

The symbols are P_t = transmitted signal power, G = is the gain of antenna, λ = wavelength, σ =target radar cross section , S_{min} = minimum detectable signal as shown in Figure (1).
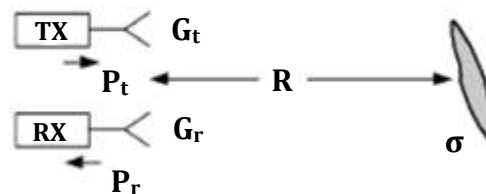

Figure 1: Basic of radar range equation.

3. ANTENNA FAR-FIELD

The maximum range of a radar system depends in large part on the average power of its transmitter and the physical size of its antenna. Based on the distance away from the face of antenna, two regions are identified. Near field, ray emitted have spherical wave fronts (David *et al.*, 2005). Fraunhofer regions, the wave fronts can be locally represented by plane waves Figure (2).
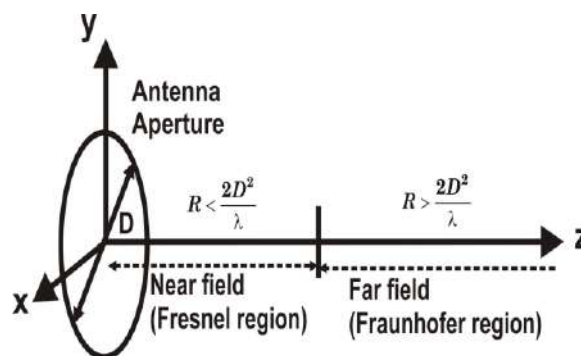

Figure 2: Near and far fields of antenna.

3.1. Parabolic Antenna

Antennas based on parabolic reflectors are the most common type of the directive antennas while a high gain is required. The main advantage is that they can be made to have gain and directivity as large as required. The main disadvantage is that big dishes are difficult to mount and are likely to have a large windage.

A dish antenna consists of one circular parabolic reflector and a point source situated in the focal point of reflector. Antenna converts a spherical wave irradiating from the point source into a plane wave. Conversely, all the energy received by the dish from a distant source is reflected to a focal point. Point P is defined by range R and angular position (β, φ) Figure (3). The aperture factor at P is given by equation (2) (Bassem *et al.*, 2004):

Aziz. A /ZJPAS: 2019, 31 (6): 13-22

15

$$E(\beta, \phi) = E(\beta) = \pi r^2 \frac{J_{1(Kr\sin\beta)}}{Kr\sin\beta} \qquad (2)$$

Where r is the aperture radius, J_1 is the Bessel function. The electric field is independent of ɸ due to the circular symmetry Ove the aperture.
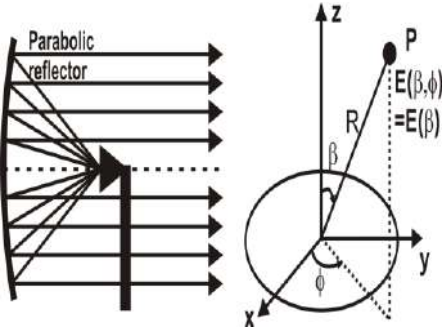

Figure 3: Parabolic dish antenna model.

3.2. Phased Array Antenna

An array is a composite antenna formed from two or more basic radiator elements. The elements could be dipoles, dish reflectors synthesize narrow directive beams that may be steered. Phased arrays use electronic steering by controlling the phase or amplitude scaling of current feeding the array elements (Christian *et al.*, 1997).

3.2.1. Linear Array Antennas

The array factor is a function of number of elements, distance, phases and magnitudes. With direction sine $\sin\beta$ is calculated in equation (3) (Bassem et al., 2000).

$$E(\sin\beta) = \sum_{i=1}^{N} e^{j(i-1)(kd\sin\beta)} \qquad (3)$$

Where $k = \frac{2\pi}{\lambda}$.

The power radiation pattern is calculated using equation (4):

$$G(\sin\beta) = |E_n(\sin\beta)|^2 = \frac{1}{N^2}\left(\frac{\sin((NKd\sin\beta)/2)}{\sin((Kd\sin\beta)/2)}\right)^2 \quad (4)$$

As shown in Figure (4), steering the main beam into the direction $\sin\beta_0$ is accomplished by making the phase difference between two adjacent elements equal to $kd\sin\beta_0$ by equation (5) (Bassem *et al.*, 2000).

$$G(\sin\beta) = \frac{1}{N^2}\left(\frac{\sin((NKd/2)(\sin\beta - \sin\beta_0))}{\sin((Kd/2)(\sin\beta - \sin\beta_0))}\right)^2 \quad (5)$$
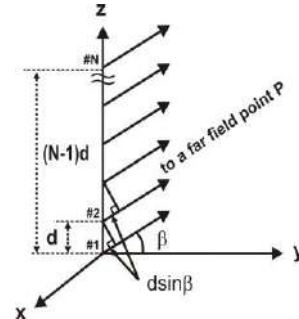

Figure 4: Uniform linear arrays.

3.3. Planar Array Antenna

Planar arrays are more versatile; they provide more symmetrical patterns with lower side lobes, much higher directivity (narrow main beam). They can be used to scan the main beam toward any point in space (Nawroz *et al.*, 2008).

The array factor of a rectangular planar array show in Figure (5) and equation (6) (Xing *et al.*, 2001).

$$AF_n(\theta, \phi) = \left\{\frac{1}{M}\frac{\sin\left(M\frac{\psi_x}{2}\right)}{\sin\left(\frac{\psi_x}{2}\right)}\right\}\left\{\frac{1}{N}\frac{\sin\left(N\frac{\psi_x}{2}\right)}{\sin\left(\frac{\psi_x}{2}\right)}\right\} \quad (6)$$

Where

$$\psi_x = Kd_x \sin\theta \cos\phi + \beta_x \qquad (7)$$
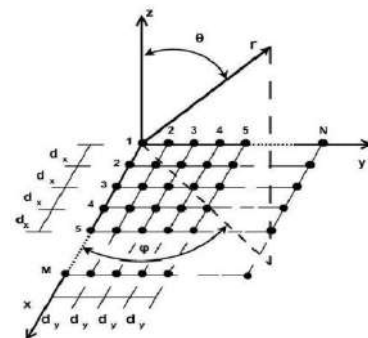
$$\psi_y = Kd_y \sin\theta \cos\phi + \beta_y \qquad (8)$$

Figure 5: Planner array geometry.

Aziz. A /ZJPAS: 2019, 31 (6): 13-22

16

4. RCS OF DIFFERENT TARGETS

4.1. Simple Targets

The geometry shapes such as sphere, ellipsoid, cylinder, circular flat plate, rectangular flat plate, triangular, truncated cone for computing RCS are considered as simple targets. For determining RCS of simple targets using Physical Optics (Swathi *et al.*, 2013).

RCS of complex targets can be computed by relating the model as a collection of simple targets who's RCS are known. The complete RCS is obtained by summing the contributions from individual simple targets.

4.1.1. RCS of Rectangular Flat Plat

Consider a perfectly conducting rectangular flat plate in the x-y plane as shown in Figure 6. The two sides of the plate are denoted by 2a and 2b. For a linearly polarized incident wave in the x-z plane, the horizontal and vertical backscattered RCS are (David *et al.*, 2005).

$$\sigma = \frac{4\pi a^2 b^2}{\lambda^2} \left(\frac{\sin(ak\sin\theta\cos\phi)}{ak\sin\theta\cos\phi} \frac{\sin(bk\sin\theta\sin\phi)}{bk\sin\theta\sin\phi} \right)^2 \quad (9)$$
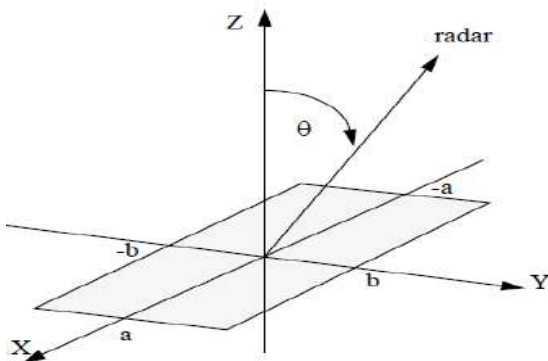

Figure 6: Rectangular flat plat geometry.

4.2. RCS OF Missile and Aircraft

RCS of complex targets is calculated by describing the target as a collection of simple models whose RCS are known. The total RCS for missile is obtained by summing the contributions from individual simple targets that of Cylinder, Cone formulations as shown in Figure (7) (Mauro *et al.*, 2008) and aircraft target contain several

simple targets as shown in Figure (8) (Gao *et al.*, 2008).

The main difficulty for RCS prediction of complex targets using high-frequency techniques is the computation of surface and line integrals over an arbitrary shape.
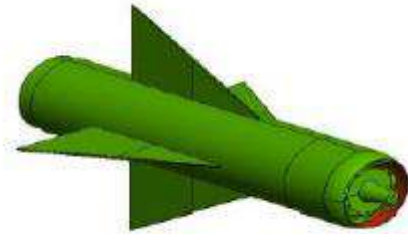

Figure 7: Missile target.

Figure 8: Aircraft target.

5. ERBIL INTERNATIONAL AIRPORT

As mentioned, Erbil International Airport location is selected as case study to check for optimal radar coverage applicable for UHF-band frequencies using two-dimensional (2D) and detection map contours (DMC) coverage representations. Simulations are made for different considerable antennas and targets. The investigation area, Erbil International Airport location, is situated in Erbil city Kurdistan Region of northern Iraq, approximately elevation 413m northeast of the city of Erbil. The selected area is in great importance site economically and geographically of Erbil city. Figure (9) represents the selected geographical position are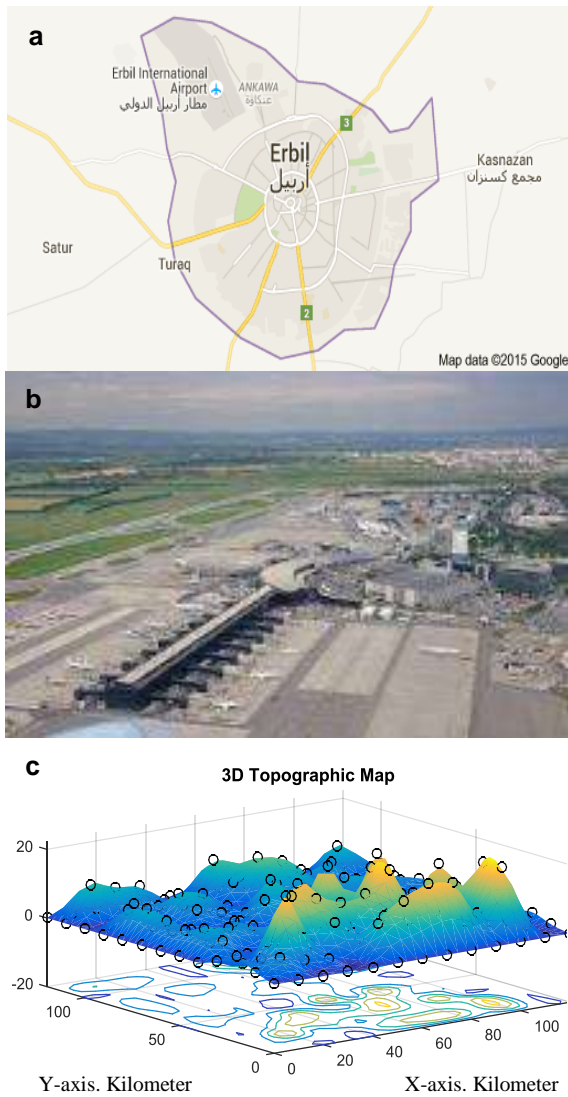a at latitude from 36.229168N and longitude from 43.993610 (https://latitude.to/articles-by-country/iq/iraq/9488/erbil-international-airport).

Aziz. A /ZJPAS: 2019, 31 (6): 13-22

17

Figure 9: (a) Global Positioning System (GPS) Erbil city Map (b) EIA and (c) Digital map of Erbil Airport.

The specifications of the measured radar base station are; transmitting signal power is 2200kw, vertical beamwidth is 1.3degree, antenna power gain is 34dB, transmitting frequency is 2GHz, polarization is vertical, and type of beam is Cosecant pencil beam for long rang at low altitude.

6. SIMULATION, RESULTS AND DISCUSSION

6.1. Calculation RCS for Different Targets

The size of a target as "seen" by radar is not always related to the physical size of the target. The measure of the target size as observed by radar is called the radar cross section.

In this study, the measurement of RCS of three types of targets, depending on the size of the targets and radar frequencies used, three targets as related in the Simple and complex targets. RCS of rectangular flat plat is one type of simple targets is plotted in dbsm (RCS can also be expressed in decibels referenced to a square meter which equals 10 log (RCS in m^2)) versus aspect angle as shown in Figure (10) is 1dbsm smaller than the RCS for the complex targets are missile and aircraft as shown in Figures (11) and (12) are 28dbsm and 60dbsm respectively using Matlab simulation, aspect angles $0 \leq \theta \leq 90$, $a = b = 10.16$cm and freguency = 2GHz. Meaning that the size of target is large the RCS is large. Fundamental equation for the RCS of a perfectly reflecting surface of area A when viewed directly by the radar $\sigma = \frac{4\pi A^2}{\lambda^2}$.
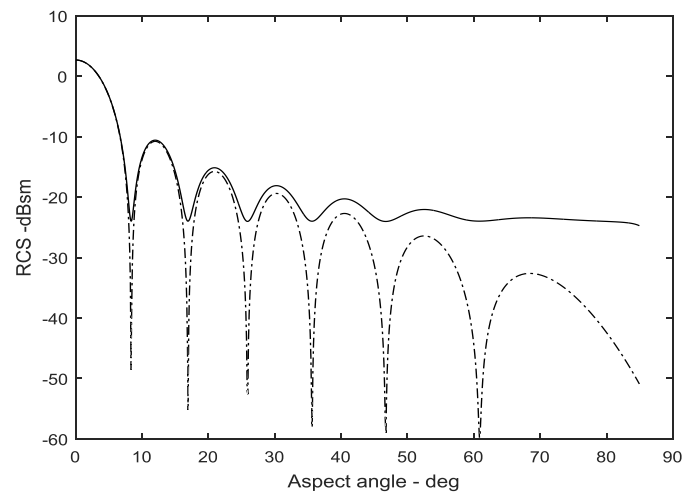

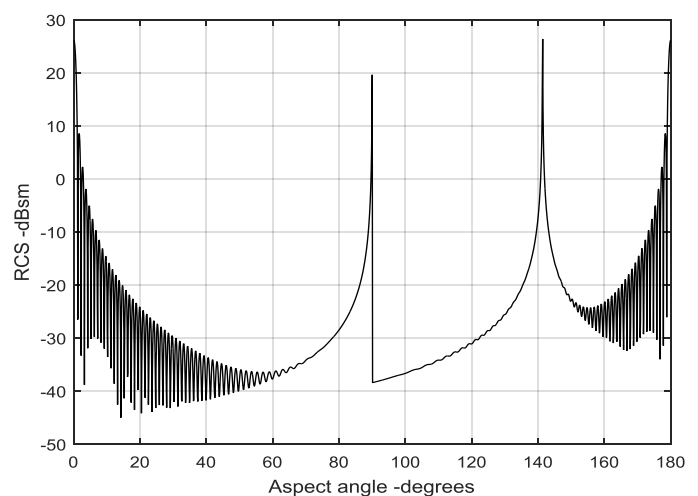**Figure 10:** RCS for a rectangular flat plate.

Figure11: RCS of missile.
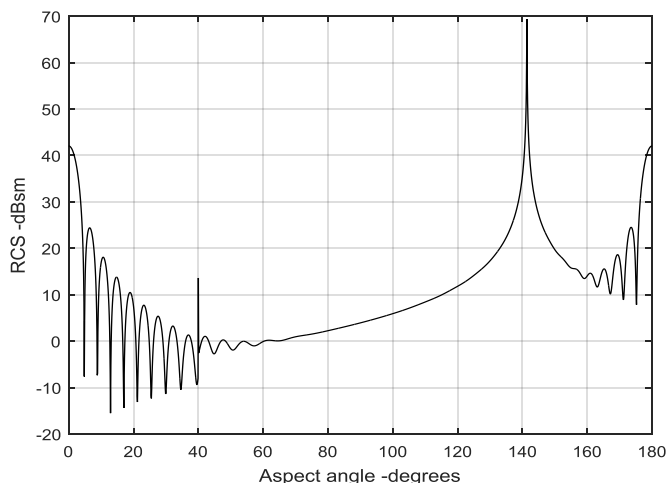
Aziz. A /ZJPAS: 2019, 31 (6): 13-22

18

Figure 12: RCS of aircraft.

6.2. Two Dimensional Radar Coverage (2DRC) for Multiple Antennas and Targets

The radar coverage has been tested for different types of target where Figure (13) shows different lobbing pattern, which are aircraft, missile and rectangular flat plat. The maximum range is 250km when the target is aircraft and it decreases to 160Km and 130km when the target becomes missile and rectangular flat plat respectively. The reduction is due to the One of the parameters that affects the radar equation and maximum range is the type of target meaning radar cross section (σ). Different target produce different radar cross sections give different ranges and heights. When increasing the radar cross section the maximum range increases, vice versa, as shown in equation (1) $\left(R_{max} \propto \sqrt[4]{\sigma}\right)$, which showed that if the RCS is increased 4 times, the maximum range will be increased (Shant et al., 2003), RCS of aircraft is $6m^2$ meaning that when detect the aircraft using UHF, but when target are missile and rectangular flat plat the RCS is $0.5m^2$ and $0.1m^2$ using large frequency UHF-band. Also it is clear from the results the effects of changing the RCS is greatly appeared in the case of lobbing pattern (Arazoo et al., 2016), for the three types of target which are used in this work. Therefore the classification of targets can be obtained depending on the radar coverage of each target when other parameters are fixed.

In order to study the lobbing pattern and the dead zones between lobes it is important to use different type of antenna. Figure (13), (14) and (15) shows that the whole lobbing pattern is

decreased when the type of antenna is changed from antenna which is parabolic, phased array and planar array. The maximum range is 250km when the type of antenna is planner array and it decreases to 225Km and 190km when the antenna becomes phased array and parabolic respectively, when the target is aircraft. Also the number of lobes in the case of antenna = parabolic is greater than that of antenna =planar array and phased array this gives higher probability of detecting of the targets because the distances between lobes decreased, with antenna of planar array, the number of lobes is lower and probability of detection is less because the distances between adjacent lobes are bigger (Qaysar et al., 2011). In this paper the suitable antenna is planar array because number of lobes is low and detected long rang at low altitude, but parabolic detected short range high altitude, as shown in Table (1).
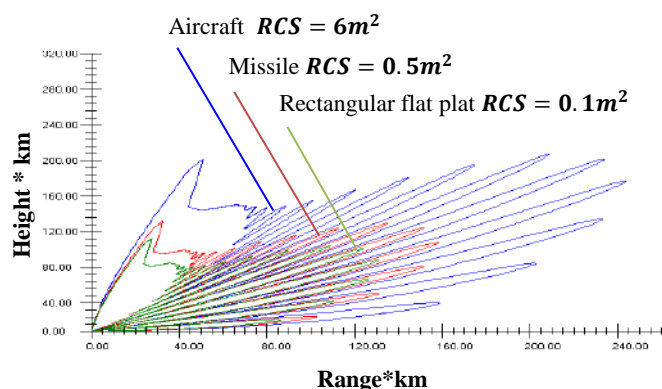

Figure 13: The 2D radar cosecant pencil beam coverage using planar array antenna using different targets, vertical polarization for lobbing pattern.
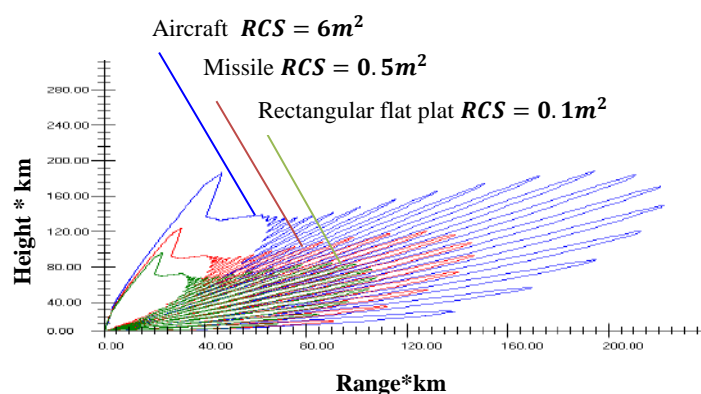

Figure 14: The 2D radar cosecant pencil beam coverage using phased array antenna using different targets, vertical polarization for lobbing pattern.
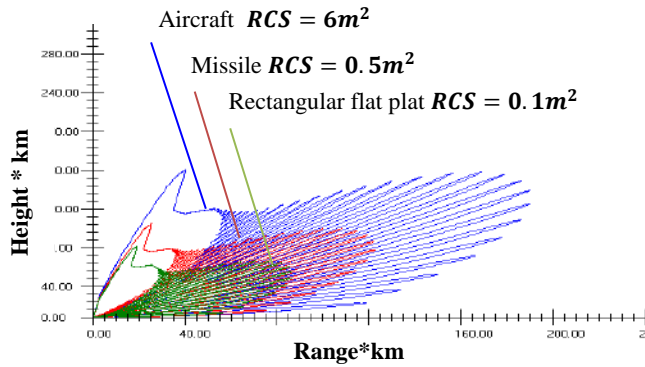
Aziz. A /ZJPAS: 2019, 31 (6): 13-22

19

Figure 15: The 2D Radar Cosecant pencil beam coverage using parabolic reflector antenna using different targets, vertical polarization for lobbing pattern.

Table (1): 2D Radar Coverage Results.

Targets	Planar array	Phased Array	Parabolic Reflector
Aircraft and RCS= 6 m²	R_{max}=250km	R_{max}=225km	R_{max}=190km
Missile RCS=0.5 m²	R_{max}=160km	R_{max}=145km	R_{max}=120km
Rectangular flat plat and RCS= 0.1 m²	R_{max}=130km	R_{max}=105km	R_{max}=85km
Ability to Steer-Beam	Yes ability	Yes ability	Not ability
No. of. Lobes	Is low	Is Medium	Is larger

6.3. Detection Map Contours (DMC) Radar Coverage for Multiple Antennas and Targets

This package simulates the detection of targets in three dimensions when introducing three-dimensional topography using Visual C++ language package. This model computes and plots DMC of constant probability of detection at different heights around the radar's site for 360o azimuth angle, for different types of antenna, different target model.

The lowest target height given from the input data is 3km depending on these height consecutive computations for determining the target height and ground range are performed.

The ray elevation angle to the terrain peak and the ray elevation angle to the target at the considered azimuth angles are computed. If the ray elevation angle to the target is less than that to the terrain peak in the considered azimuth then the ray elevation equals the peak angle else computing of target range which is performed and repeated for 360o azimuth angles.

The results obtained in the present work show the effects of three types of antenna on the interference propagation (multipath propagation) and the three types of target are examined. Figure (16) is obtained for transmitting frequency=2GHz and transmitting power of 2200 KW, and the type of target is aircraft where the heights of the receiver are assumed to be 6 altitudes beginning from first height=3km from the center of the DMC diagram. In this figure the resultant field is computed from the direct and reflected components, and for this reason different DMCs are obtained. The difference in the array factor of each type of antennas as shown in Figure (16a, 16b and 16c) produces different detection map contours.

The DMC contours for planar array Figure (16a) have a maximum range of 225km, which is greater than that for phased array, which is 180km as shown in Figure (16b). The last case is greater than that for the parabolic reflector see Figure (16c), the maximum range is 140km and the type of target is aircraft at the same azimuth angle of 278o and the same receiver height of 8km.

One can notice that the detection map contours obtained for different antennas and targets are the same in shape but they have different detection ranges. All the contours for different heights are for the same ground, and this reflects the height of the ground irregularities.

The comparison of the three DMCs in Figure (17a, 17b and 17c) shows that at receiver height 8km and the target is missile, the DMC diagrams for the planar array produce greater ranges when compared with those of the phased array and parabolic reflector for the same receiver height and directions. But at higher receiver heights and higher elevation angles, the differences between the DMC diagrams of the planar array and phased array decrease at higher elevation angles. The parabolic reflector gives the lower maximum detection range, and these results coincide with the results of the two dimension coverage

Aziz. A /ZJPAS: 2019, 31 (6): 13-22

20

obtained in Figure (13), (14), and (15). Increasing the detection receiver height from 3km to 8km. Figure (18) is the type of target is rectangular flat plat. From in this figure it is seen that when the type of antenna is planar array greater maximum detection range is 100km obtained when this is compared with the case of phased array in figure18b. The maximum detection range in this case is 55km. The smaller ranges obtained when change to parabolic reflector the maximum range is 41km as shown in Figure18c.These results are also similar to the results obtained for the two dimension coverage shown in Figure (13), (14), and (15) and the results obtained by previous studies. The greater ranges obtained when increasing the RCS to 0.1 m2 and 6m2 as shown in Table (2), are due to the obvious decrease of the RCS (change type of target) and the effects of the size of target at higher heights and higher elevation angles. Also, the best antenna is planar array because number of lobes is lower than phased array and parabolic reflector, and the range is long when the target is aircraft. When the target is aircraft the RCS is large we need long range to detected and need low frequency as compared to missile and rectangular.

Table (2): Three Dimensional (3D) or DMC Radar Coverage Results at Target Height is 8km.

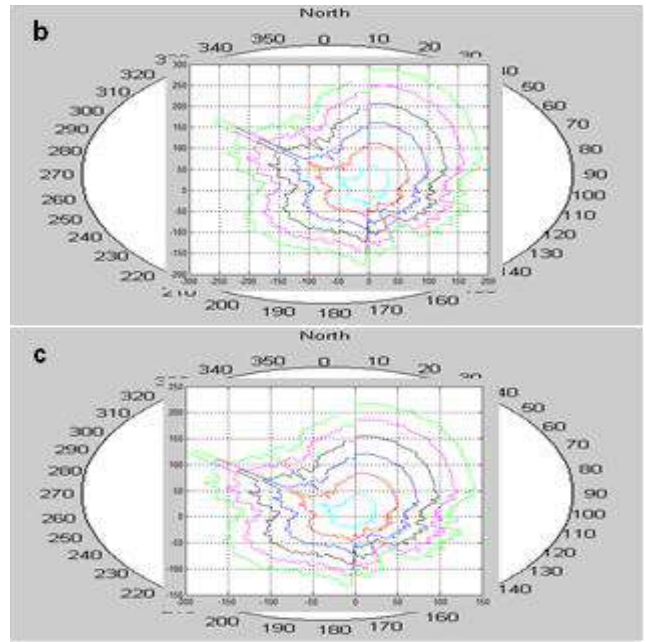| Targets	Planar array	Phased Array	Parabolic Reflector
Aircraft and RCS= 6 m^2	R_{max}=225km	R_{max}=180km	R_{max}=140km
Missile RCS=0.5 m^2	R_{max}=125km	R_{max}=80km	R_{max}=65km
Rectangular flat plat and RCS= 0.1 m^2	R_{max}=100km	R_{max}=55km	R_{max}=41km
Ability to Steer-Beam	Yes ability	Yes ability	Not ability
No. of. Lobes	Is low	Is Medium	Is larger

Figure 16: DMC radar coverage for aircraft target, RCS= 6m2, f=2GHz and vertical polarization; a. planar array antenna, b. phased array antenna, c. parabolic reflector antenna.
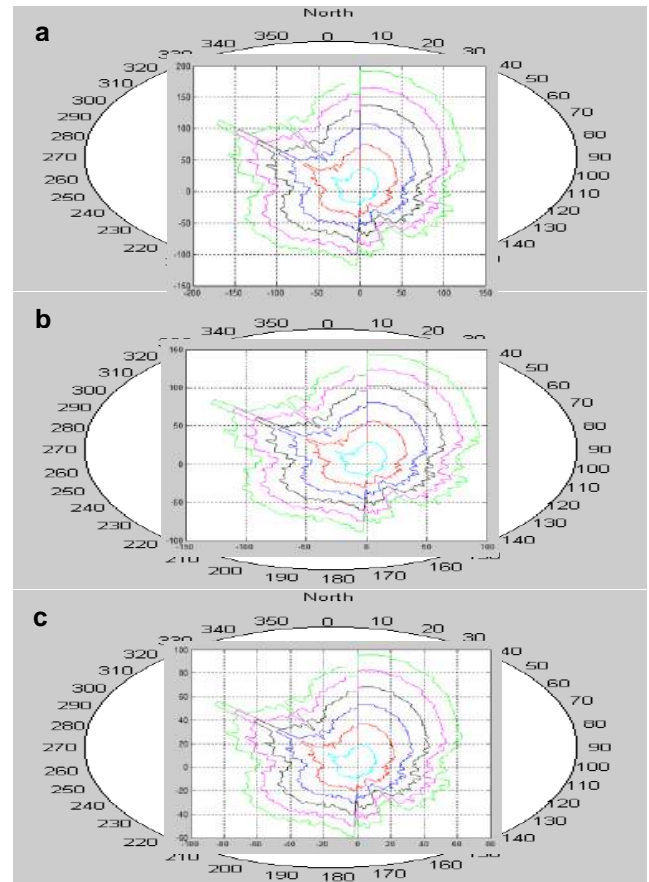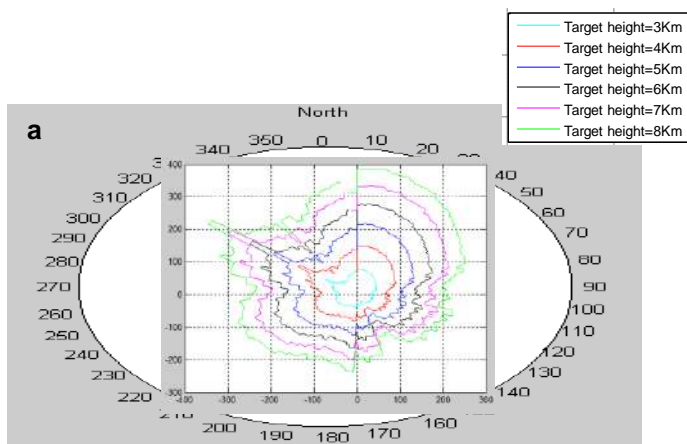

Figure 17: DMC radar coverage for missile target, RCS= 0.5m2, f=2GHz vertical Polarization; a. planar array antenna, b. phased array antenna, c. parabolic reflector.
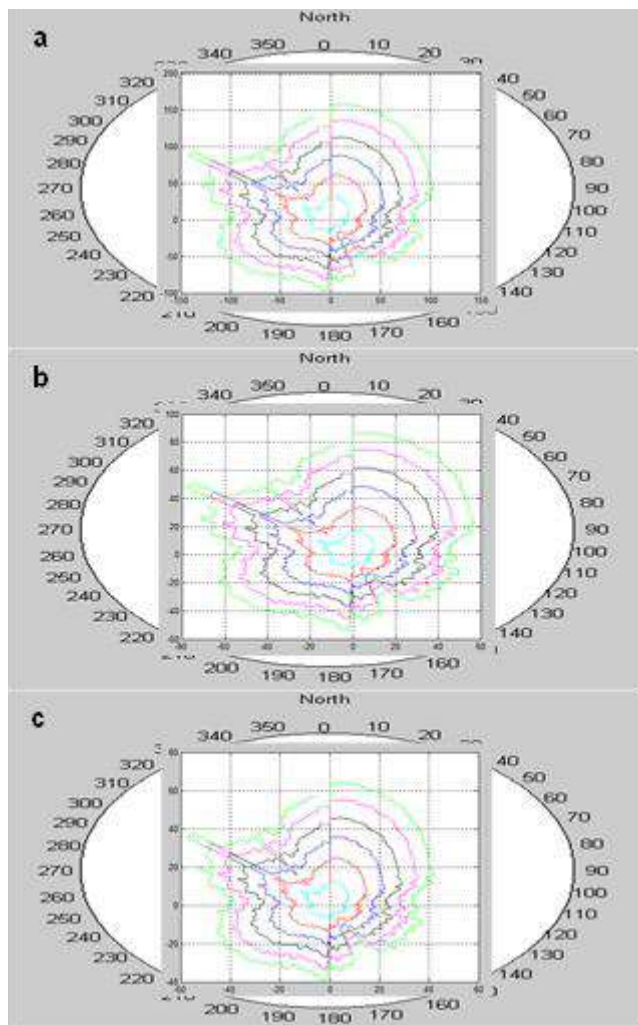
Aziz. A /ZJPAS: 2019, 31 (6): 13-22

21

Figure 18: DMC radar coverage for rectangular flat plat target, RCS= 0.1m2, f=2GHz and vertical polarization; a. planar array antenna, b. phased array antenna, c. parabolic reflector antenna.

7. CONCLUSION

Based on the simulation results, we conclude that the planar and phased array antenna have more advantages than the parabolic antenna. For planner and phased array antenna, it is flexible to steer its radiation pattern to any designed angle with only change in phased shifting or amplitude scaling. In comparison with the parabolic antenna, we cannot steer the radiation pattern without steering the whole antenna, however parabolic antenna is usually very big and which impacts the inertial and friction. Furthermore, the results show that the planar array yields much reduction of number lobe levels, half power beamwidth and grating lobes compared to linear array phased array antenna and parabolic.

The RCS analysis of the rectangular flat plat which represents a simple target and, missiles and aircraft which represent complex targets are both related to the size of the targets.

Simulation results showed and indicated that targets are more easily detected for larger RCS, since it reflects a limited amount of radar energy and it will increase the coverage area. As a consequence, increasing the target size (RCS) will decrease number of pattern lobes, increase number of dead zones, and the radar coverage will increase. So, for obtaining larger coverage and optimal detection probabilities in Erbil International Airport anticlines, it is confirmed to use the different targets based on the radar specifications.

Acknowledgements

References

AL-Samerai, K. S. 1988. Modeling of Radar Wave Propagation. M.Sc. Theses, University of Technology, Iraq.

Arazoo, M. A., Jalil, A. H., Diary, R. S. 2016. The Radar Coverage Studies and Simulation for Bana Bawi Anticlines in Erbil City-Kurdistan Region of Northern Iraq. *ZANCO Journal of Pure and Applied Sciences,* 28, 2, 22-29.

Bassem, R. M. 2000. Radar Systems Analysis and Design using Matlab.3rd Edition. Chapman and Hall/CRC, 1st edition, US.

Bassem, R. M. Atef, Z. E. 2004. Matlab Simulations for Radar Systems Design. Chapman & Hall /CRC, US.

Burgess, L. R., Berlekamp, J. 1988. Understanding Radar Cross-Section Measurements. Microwaves Systems News and Communications Technology, 54-61.

Christian, W. 1997. Radar Basics. Germany.

David, J. 2005. Microwave Devices & Radar, Lecture notes. Naval Postgraduate School.

Gottapu, S. B. R., Swathi N., Srikanth K., Kota, R. 2017. Monostatic Radar Cross Section Estimation

Aziz. A /ZJPAS: 2019, 31 (6): 13-22

22

of Missile Shaped Object Using Physical Optics Method. *IOP Conference Series: Materials Science and Engineering*, 225 (1), 012278.

Gao, Z., Wang, M. 2008. An Efficient Algorithm for Calculating Aircraft RCS Based on the Geometrical Characteristics. *Chinese Journal of Aeronautics*, 21, 296-303.

https://latitude.to/articles-bycountry/iq/iraq/9488/erbil-international-airport.

Le, Q. T., Do, Q. L., Nguyen, X. T. 2014. Study Comparative of Parabolic and Phased Array Antenna.VNU *Journal of Science: Mathematics – Physics*, 30, 3, 31-36.

Mauro, A. A., Inácio, M. M., Marcelo, A.S. M., Mirabel, C. R. 2008. Radar Cross Section of Simple and Complex Targets in the C-band: A Comparison between Anechoic Chamber Measurements and Simulations. *Piers online*, 4, 7, 791-794.

Merrill, I. S. 2001. Introduction to Radar System. McGraw – Hill higher education New York, 3rd edition.

Nawroz, I. H. 2008. Modeling of Radar Wave Propagation by using planar array and beam forming Techniques. M.Sc. Thesis, Salahaddin University, Iraq

Miacci, M. A. S. 2002. Experimental Measurements of the Microwave Backscattering of Single Shapes Targets. Master of Science – ITA, Brazil.

Qaysar, S. M., Nawroz, M. H. 2011. Modeling of Radar Wave Propagation by Using Planar Array Antenna. *ZANCO Journal of Pure and Applied Sciences*. 23, 1.

Shant, K. A. 2003. Computer Simulation of Radar Coverage and Radar Monitor. Ph.D. Thesis, University of Technology, Iraq.

Swathi, N. 2013. RCS Computation of Shapes Obtained by Cascading Simple Objects Using PO Method and Results Obtained Using Matlab Simulation Software. *International Journal of Electronics and Communication Technology*, 4(2), ISSN 2230-7109.

Xing, W. 2001. Design Considerations of a New Type all Solid-State Phased Array 3D Radar. IEEE, Nanjing Research, Institute of Electronics Technology.

Yossra, H. A. 2002. Modeling of three –Dimensional Radar Coverage of land Topography. M.Sc. Thesis, University of Technology, Iraq.

RESEARCH PAPER:

Study of Crumb Rubber Modified Local Asphalts Using Classical Tests

Diyar Nadhim Hasan Shwan[*,1], Aso Faiz Saeed Talabany[1]

[1] Department of Civil Engineering, College of Engineering, Salahaddin University-Erbil, Kurdistan Region, Iraq.

A B S T R A C T:
The rapid growth of population and industrialization levels around the world requires higher number of vehicles for transportation and better road qualities, on one hand, on the other hand this growth causes a huge number of scrap tires. Incorporating scrap tires into the asphalt pavements will help in saving the environment beside improving some of its properties and recycle the scrap tires. This study investigates the effect of Crumb Rubber Modifier (CRM) on the asphalt properties using classical tests. Different percentages of CRM by weight of the asphalt was added to three locally produced asphalts of different sources and grades. The results of this study show that higher CRM contents lead to decrease penetration and ductility values, while it causes increase of the softening point, elastic recovery and penetration index. Higher softening point and elastic recovery indicate better resistance against rutting and high temperature deteriorations, higher penetration index indicates lower temperature susceptibility and better road life performance.

1. INTRODUCTION:

Crumb Rubber is a general term that describes scrap tires that have been cut and reduced in size into fine granular particles for use in asphalt pavements as a modifying material. In the last decades, the rapid growth of industrialization levels and population have been caused in increased demand of transportation particularly higher number of vehicles in the developing and industrialized countries. This growth, in addition to other waste products, generates a huge number of used tires every year. According to ETRMA (2011), about 1.5 billion tires are sold globally every year. Finally, most of these tires fall into the category of scrap tires. One of the worrying environmental issues is how to deal with these used tires.

In General, the purpose of adding CRM to asphalt is to enhance some of its properties such as lower temperature susceptibility, better fatigue and permanent deformation resistance. The enhancement of the CRM asphalt properties depends on the interaction process between the asphalt and the CRM to a great extent, where a viscous gel is formed due to the swelling of the CRM particles, resulting in a higher viscosity of the CRM asphalt.

The CRM properties that can affect the interaction process are chemical composition, production process, specific surface area and particle size (Heitzman, 1992). CRM can be obtained from tires by two major methods: (1) Ambient, is a method of processing scrap tires where the tire is processed or ground at the normal room temperature using special tools; (2) Cryogenic, is a grinding method in which liquid nitrogen of temperature less than -80 C° is used to freeze the scrap tires until the rubber is brittle, then a hammer mill is used to shatter the frozen rubber into small particles. The CRM produced

---

* **Corresponding Author:**
Diyar Nadhim Hasan Shwan
E-mail: diyarnadhem@gmail.com

with this method has smoother particles and relatively smaller surface area.

The reaction between the asphalt and the CRM is made up of two simultaneous processes: absorption of the oily materials in the asphalt into the polymeric chains of the rubber, on one hand, on the other hand, partial digestion of the CRM into the asphalt. (Navarro et al., 2007, TREDREA, 2006) mentioned that after adding 15% of CRM to the asphalt, only a range of 2 to 4 percentage is dispersed or dissolved in the asphalt.

CRM reaction with asphalt is a time-temperature dependent process. If the time is too long or the temperature is too high, the swelling will continue to a point where, swelling is replaced by devulcanisation/depolymerisation because of long exposure to high temperatures which causes the dispersion of the CRM into the asphalt (Presti, 2013).

The swelling process of CRM particles governs the improvements of the asphalt properties. Due to the absorption of the maltenes components of the asphalt, CRM particles can swell three to five times its original size (Peralta et al., 2010, Vonk and Bull, 1989). This leads to increase the asphaltenes proportion in the asphalt binder, consequently increase its viscosity.

The mechanism nature via which the interaction between the CRM and the asphalt happens has not been completely characterized. Heitzman (1992) stated that the interaction is a non-chemical reaction which doesn't cause the dissolving of the rubber particles in the asphalt binder. Instead, the absorption of the oily phase materials and swelling of the CRM particles lead to decrease the free space between the rubber particles, as a result increase the viscosity of the asphalt. Bahia and Davies (1994) stated that the higher viscosity of the asphalt cannot be only resulted from the presence of swollen rubber particles.

(Mashaan et al., 2011, Mashaan and Karim, 2013) showed that the increase in the mixing temperature leads to higher softening point, Brookfield Viscosity, complex shear modulus and elastic recovery values, whereas the longer mixing time has no significant effect on CRM modified asphalt properties in the case of 30 and 60 minutes. (Moreno et al., 2011, Shen and Amirkhanian, 2005) indicated that the mixing time shows an insignificant difference in the optimal binder content selection.

Mashaan et al. (2011) studied the effect of different CRM contents on the rheological, physical properties and rutting resistance of CRM modified asphalts. The results of the study showed that higher CRM content leads to decrease the penetration, ductility and phase angle values, whereas causes to increase the elastic recovery, complex modulus, loss modulus and storage modulus. Increased elastic recovery indicates a better resistance against rutting deformation which occurs in asphalt pavements due to high traffic volume and loading.

Lee et al. (2008) studied the performance properties of CRM modified asphalts with different CRM contents and processing methods using SUPERPAVE rheological tests of asphalt. They used CRM from passenger car scrap tires processed with two different methods, one source used cryogenic grinding method and the other used ambient grinding method. The results of the study show that the ambient grinding method is more effective in decreasing the temperature susceptibility and increasing the viscosity while there is no statistically significant difference between these two methods in the fatigue cracking and m-value (slope of stiffness curve at 60 seconds in Bending Beam Rheometer test).

Sebaaly et al. (2003) conducted a study to evaluate the rheological behavior of CRM modified asphalts at low temperatures. The study included three different sizes of CRM, four asphalt types and three CRM contents. The results of the study showed that CRM size has no significant effect on the low temperature properties of the asphalt. Also, he motioned that some combinations of CRM content and size may either improve or jeopardize the low temperature performance grade of the asphalt.

The objective of this study is to discover the effect of adding four different percentages of CRM on the properties of locally produced asphalts of two different sources and two different grades using classical asphalt tests.

2. MATERIALS AND METHODS

2.1. Materials

2.1.1 Asphalt binders:

In this Study three types of locally produced asphalts are used, two asphalts with different grades (source A grade 40-50 and source B grade 50-70) from Lanaz refinery which is located in Erbil, and the third type of asphalt (source C grade 50-70) from Phoenix refinery which is located in Arbat-Sulaymaniyah. Table 1 shows the

characteristics of the three original asphalts from sources A, B and C.

Table 1 Properties of the original asphalts.

Test Method		Source A*	Source B*	Source C**
Penetration at 25 ℃	ASTM D5	43	55	56
Ductility at 25 ℃	ASTM D113	>150 Cm	>150 Cm	120 Cm
Elastic Recovery at 25 ℃	ASTM D6084	9 %	8 %	20 %
Softening Point	ASTM D36	52 ℃	49 ℃	50 ℃
Penetration after RTFO test at 163 ℃	ASTM D2872	20	24	24
Loss on heat	ASTM D2872	0.63 %	0.84 %	0.60 %
Flash Point	ASTM D92	320 ℃	270 ℃	255 ℃

*From Lanaz refinery.

**From Phoenix refinery.

2.1.2 Crumb Rubber

The CRM used in this study is from truck scrap tires obtained from a special factory from Baghdad-Iraq that uses special tools and devices to cut and shred scrap tires into small particles at normal room temperature. Figure 1 shows microscopic image (40x) of CRM modified asphalt for different CRM contents for source C (Phoenix refinery, grade 50-70), in which the CRM particles are shown in the form of black spots. Table 2 shows the gradation of CRM used in this study and CRM from two other studies for the purpose of comparison (Lee et al., 2008, Shen et al., 2009).
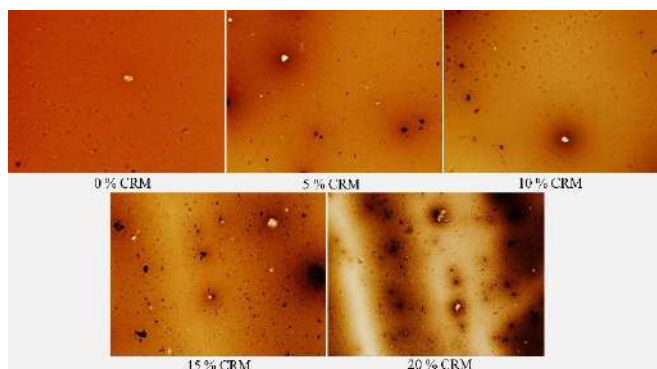

Figure 1: Microscopic image (40x) of CRM modified asphalt with different CRM contents for Source

Table 2 Gradation of CRM.

Sieve Size (mm)	This Study	Lee et al. 2008	Shen et al. 2009
0.6	100	100	100
0.425	-	83	60.8
0.3	72	74	19.3
0.18	-	42	13.1
0.15	24	9	11.1
0.075	1	0	0

2.2 Experimental Works

The asphalt batches preparation was made by mixing the original asphalts with different CRM percentages (0,5,10,15 and 20% by weight of the asphalt). The mixing process continued for 30 minutes at 180 C° with 950 rpm mixer speed. For the three asphalt types and the five different CRM contents, the total number of prepared asphalt batches in this study is 15. For each test a minimum of three samples are tested. The flow chart in Figure 2 summarizes the experimental works.
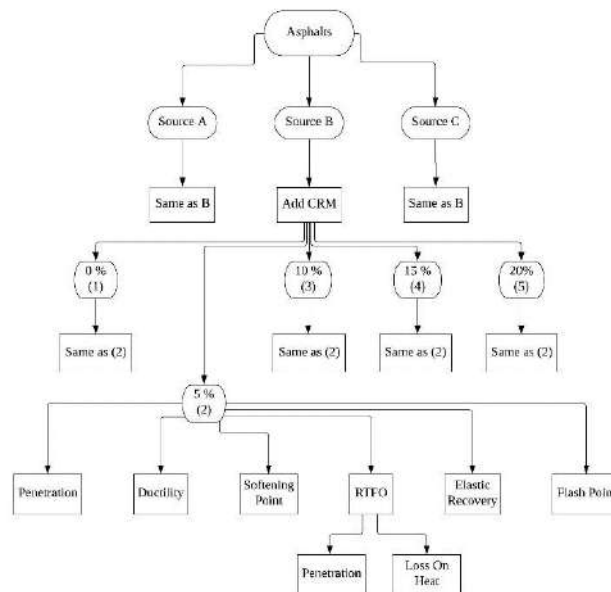
Figure 2: Flow Chart of Experimental Work Procedure

3. RESULTS

The classical asphalt test results were used to show the effect of CRM content on the basic properties of asphalt are shown in Figure 3 through Figure 7 and Tables 3 and 4.

The results of penetration, ductility, softening point, elastic recovery, flash point and RTFO are measured directly from the tests, while the penetration index results are calculated using equations (1) and (2) from penetration value at 25 C° and the softening point (Ehinola et al., 2012).

$$PI = \frac{20(1-25A)}{(1+50A)} \quad \ldots\ldots (1)$$

$$A = \frac{\log(pen\ at\ 25\ ℃) - \log 800}{25 - ASTM\ Softening\ Point} \quad \ldots\ldots (2)$$

PI= Penetration index.

A= Temperature susceptibility.
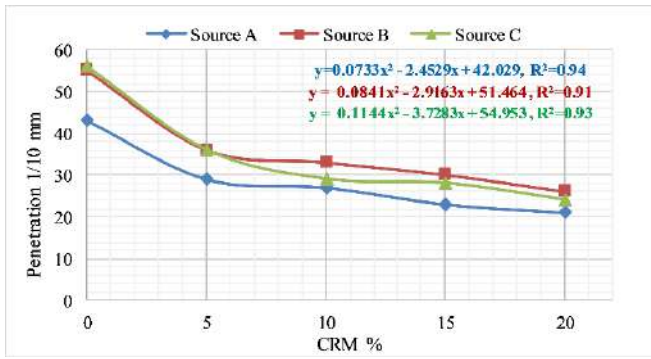
(a)
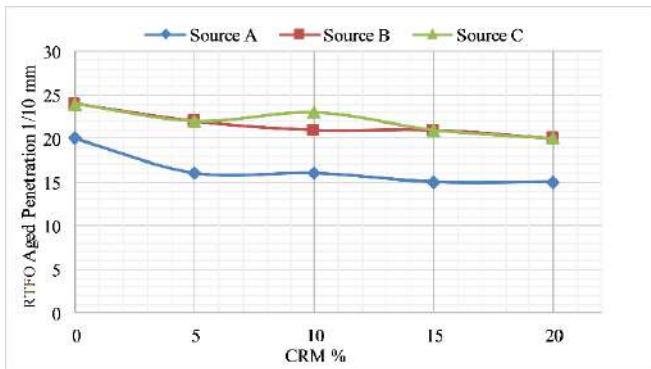
(b)

Figure 3: Penetration Value for different CRM contents: (a) Original asphalt, (b) RTFO aged asphalt.
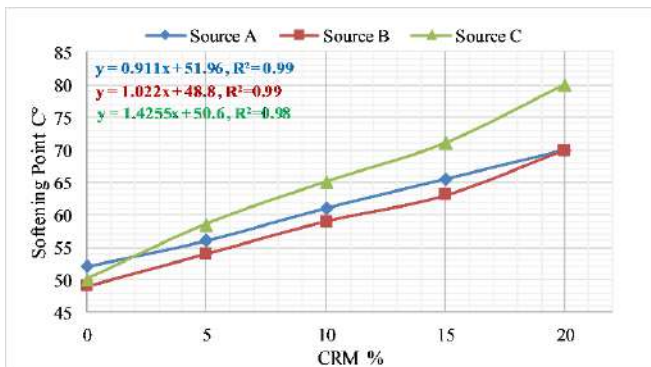
Figure 4: Softening Point test results for different CRM contents.
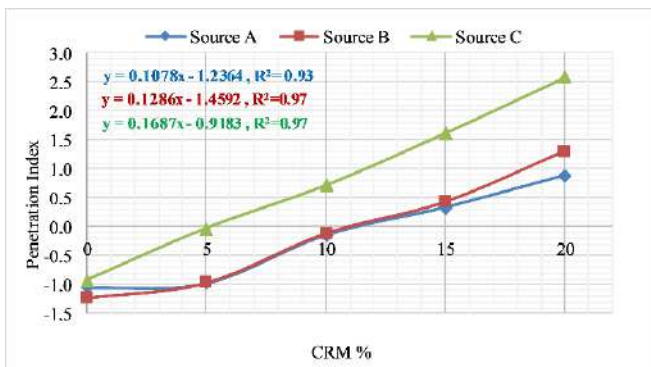
Figure 5: Penetration Index for different CRM contents.
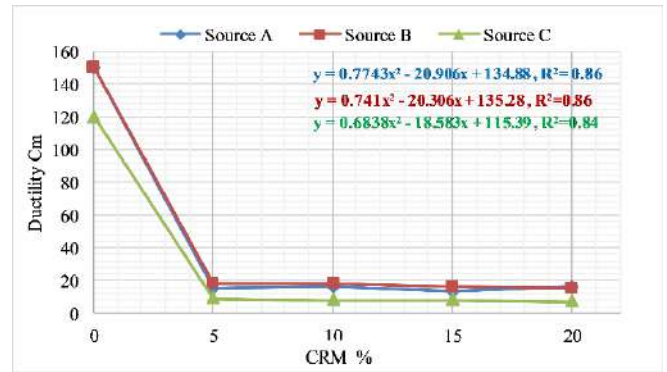
Figure 6: Ductility test results for different CRM contents.
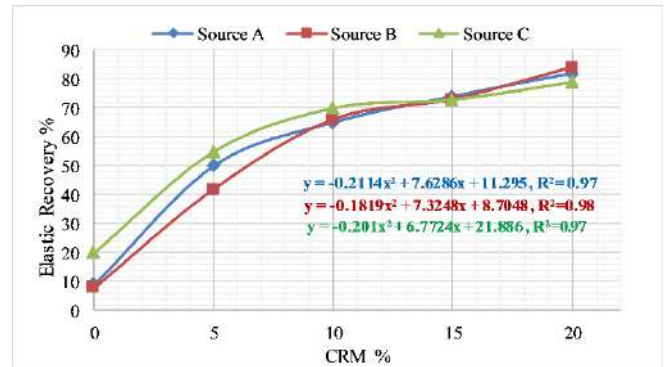
Figure 7: Elastic Recovery test for different CRM contents.

Table 3 Flash Point test results for different CRM contents.

CRM %	Flash Point C°		
	Source A	Source B	Source C
0	320	270	255
5	312	300	270
10	310	292	262

Table 4 Percent of Loss on Heat for different CRM contents.

CRM %	Percent of Loss on Heat		
	Source A	Source B	Source C
0	0.63	0.84	0.60
5	0.48	0.59	0.67
10	0.43	0.62	0.96
15	0.60	0.67	0.89

4. DISCUSSIONS

4.1 Penetration

The penetration value decreases by the increasing of CRM content (see Figure 3 (a)). The reduction in the penetration value is resulted from the stiffening of the asphalt due to the absorption of the light materials by CRM particles and the digestion of CRM into the asphalt. The percentage

of reduction in the penetration value after adding 20% of CRM is equal to 51%, 53% and 57 % for sources A, B and C, respectively. This high reduction in the penetration value should be considered before using such modified asphalts in road pavements, because if the asphalt is too stiff causes thermal cracking of the pavement in cold weathers.

The statistical analysis shows that the correlation coefficients between CRM content and penetration value for sources A, B and C are equal to -0.89, -0.89 and -0.86 respectively.

The penetration results of this study have a similar trend to the results of studies conducted by other researchers (Mashaan et al., 2011, Nejad et al., 2012, Paulo and Jorge, 2008).

4.2 Softening Point

The results show that the effect of adding CRM differs according to the source of the asphalt. As seen in Figure 4, there is almost a linear increase of the softening point by incorporating and increasing the CRM content for the three sources of asphalt. The regression formulas for sources A and B show that for every 1% increase in CRM content, the softening point increases about 1 C° degree, while for source C, the softening point increases about 1.5 C° degree for every 1% of CRM added. The correlation coefficients between CRM content and softening point for sources A, B and C are equal to 0.99, 0.99 and 0.99, respectively.

Similar to this study, other studies show that the softening increases by increasing the CRM content (Dantas Neto et al., 2003, Mashaan and Karim, 2013, Nejad et al., 2012). Higher softening points indicate stiffer asphalts having the ability to improve its elastic deformation recovery, in addition, the higher the softening point indicates the better rutting resistance of the binder.

4.3 Penetration Index PI

As Figure 5 indicates, the penetration index increases by increasing the CRM content. The PI value for 0% CRM content of the sources A, B and C are approximate values, while after adding 20% of CRM the PI values reach 0.88, 1.3 and 2.58 for sources A, B and C, respectively. This means that CRM content has a greater effect on source C than sources A and B.

The higher penetration index means that the asphalts have less temperature susceptibility, asphalts with less temperature susceptibility are more resistant against low temperature cracking and rutting (Nejad et al., 2012). The correlation coefficient values for the sources A, B and C are equal to 0.96, 0.98 and 0.98, respectively.

4.4 Ductility

Ductility test provides a measure of tensile properties of asphalt. It is a measure of the elongation in centimeters of a standard specimen of asphalt before breaking at a temperature of 25 C°. As illustrated in Figure 6, the ductility test loses about 90% of its value in a sudden decrease from 150 Cm to 15 Cm after adding 5% of CRM to sources A and B, and loses 93% of its value in a sudden decrease from 120 Cm to 9 Cm for the same CRM content for source C. The results show that CRM contents higher than 5% have no significant effect on ductility values. This dramatic decrease is resulted from the absorption of the oily materials in the asphalt by the CRM particles. The statistical analysis shows a correlation coefficient of -0.70, -0.72 and - 0.70 for sources A, B and C, respectively.

The results of this study and Nejad et al. (2012) show a sudden decrease in the ductility value due to the incorporation of CRM into the asphalt, while Mashaan et al. (2011) shows that increased CRM content causes a gradual decrease in the ductility value.

4.5 Elastic Recovery

Figure 7 shows the effect of CRM content on elastic recovery for the three asphalt sources. The elastic recovery increases by increasing the CRM content. The elastic recovery of the three sources of asphalts almost has the same trend and behavior by increasing the CRM content. The elastic recovery at 20% CRM content has approximate values for sources A, B and C, which is about 80%. Statistical analysis shows that CRM content has a high correlation coefficient of 0.92, 0.95 and 0.90 with the elastic recovery for asphalt sources A, B and C, respectively.

Asphalt is a viscoelastic material; higher values of elastic recovery indicates that the asphalt has a better ability to recover its original shape after the application of loads. Higher values of elastic recovery mean a better resistance against rutting deformation and fatigue cracking. The results of this study have a corresponding trend to

the results of studies conducted by (Mashaan et al., 2011, Nejad et al., 2012).

4.6 Flash Point

According to ASTM D92 (2016) Flash Point "is the lowest temperature of the test specimen at which application of an ignition source causes the vapors of the test specimen to ignite under specified conditions of test". This test covers the safety concerns against fire occurring of asphalt while heating at mix plant, spreading and compaction stages. Table 3 shows that the flash points are according to the Iraqi and ASTM standards (>232 ℃).

The test of flash point was made for CRM contents of 0%,5% and 10% because for higher CRM contents, the high temperatures caused to introduce bubbles on the surface of the sample and prevented the flash occurring.

4.7 Penetration After Rolling Thin Film Oven Test (RTFO)

Figure 3 (b) shows the penetration values after short term aging by RTFO test. The penetration decreases after the short term aging as a result of the RTFO test conditions. The RFTO test simulates the aging of the asphalt binder at mix plant, in this test the asphalt is subjected to a temperature of 163 ℃ and oxidation by hot airflow for 85 minutes that causes the loss of the light materials through volatilization. The results of the penetration for the original and RTFO aged asphalts shows that the penetration Aging Ratio (PAR) decreases by increasing the CRM content.

4.8 Loss On Heat

Table 4 shows the percentages of loss on heat of the asphalt binders due to the volatilization of the light materials in the RTFO test. The results show that CRM content has no obvious effect on loss on heat percentage.

5. CONCLUSIONS

From the results of adding CRM to three types of asphalt of different sources and grades, it can be concluded that:

1. The results of the three asphalt sources have similar trends by increasing the CRM content in penetration, ductility and elastic recovery tests, while the CRM content has a greater effect on Source C than Sources A and B in softening point test and penetration index values.

2. The penetration value has an inverse relationship with the CRM content in the asphalt, in which the penetration values for original asphalt decreases gradually, losing about 50% of its original value at 20% CRM content.
   The penetration of RTFO aged asphalts also decreases by increasing the CRM content, losing about 25% of its original value at 15% CRM content. The CRM content has a greater effect on the original asphalt than the RTFO aged asphalt due to the hardening of the asphalt and volatilization of its light materials.

3. Adding 20% CRM to the asphalt causes a dramatic decrease in the ductility property of the asphalt and losing about 90% of its value, whereas leads to increase its elastic recovery property to about 80%, which indicates a higher ability of the asphalt to recover its original shape after deformations due to high traffic volume and loading.

4. Asphalts modified with CRM have lower temperature susceptibility and better resistance of rutting and high temperatures due to the higher softening point and penetration index.

5. According to the results of this study, CRM has no obvious effect on flash point and loss on heat test results.

References

BAHIA, H. U. & DAVIES, R. 1994. Effect of crumb rubber modifiers (CRM) on performance related properties of asphalt binders. Asphalt paving technology, 63, 414-414.

D92, A. 2016. Standard test method for flash and fire points by Cleveland open cup tester. Annual Book of Standards.

DANTAS NETO, S. A., FARIAS, M. M. D., PAIS, J. C., PEREIRA, P. A. & SANTOS, L. P. Properties of asphalt-rubber binders related to characteristics of the incorporated crumb rubber. Asphalt Rubber 2003 Conference, 2003. 297-310.

EHINOLA, O. A., FALODE, O. A. & JONATHAN, G. 2012. Softening point and Penetration Index of bitumen from parts of Southwestern Nigeria. Nafta, 63, 319-323.

ETRMA. 2011. End of life tyres [Online]. Available: http://www.etrma.org/uploads/Modules/Documents manager/brochure-elt-2011-final.pdf [Accessed May 19,2019.

HEITZMAN, M. 1992. Design and construction of asphalt paving materials with crumb rubber modifier. Transportation Research Record, 1339.

LEE, S.-J., AKISETTY, C. K. & AMIRKHANIAN, S. N. 2008. The effect of crumb rubber modifier (CRM) on the performance properties of rubberized binders in HMA pavements. Construction and Building Materials, 22, 1368-1376.

MASHAAN, N. S., ALI, A. H., KARIM, M. R. & ABDELAZIZ, M. 2011. Effect of crumb rubber concentration on the physical and rheological properties of rubberised bitumen binders. International journal of the physical sciences, 6, 684-690.

MASHAAN, N. S. & KARIM, M. R. 2013. Investigating the rheological properties of crumb rubber modified bitumen and its correlation with temperature susceptibility. Materials Research, 16, 116-127.

MORENO, F., RUBIO, M. & MARTINEZ-ECHEVARRIA, M. 2011. Analysis of digestion time and the crumb rubber percentage in dry-process crumb rubber modified hot bituminous mixes. Construction and Building Materials, 25, 2323-2334.

NAVARRO, F., PARTAL, P., MARTÍNEZ- BOZA, F. & GALLEGOS, C. 2007. Influence of processing conditions on the rheological behavior of crumb tire rubber- modified bitumen. Journal of applied polymer science, 104, 1683-1691.

NEJAD, F. M., AGHAJANI, P., MODARRES, A. & FIROOZIFAR, H. 2012. Investigating the properties of crumb rubber modified bitumen using classic and SHRP testing methods. Construction and Building Materials, 26, 481-489.

PAULO, A. & JORGE, C. 2008. Laboratory optimization of continuous blend asphalt rubber. Proceedings of 3rd European Pavement and Asset Management EPAM, 3.

PERALTA, J., SILVA, H. M., MACHADO, A. V., PAIS, J., PEREIRA, P. A. & SOUSA, J. B. 2010. Changes in rubber due to its interaction with bitumen when producing asphalt rubber. Road Materials and Pavement Design, 11, 1009-1031.

PRESTI, D. L. 2013. Recycled tyre rubber modified bitumens for road asphalt mixtures: A literature review. Construction and Building Materials, 49, 863-881.

SEBAALY, P. E., GOPAL, V. T. & EPPS, J. A. 2003. Low temperature properties of crumb rubber modified binders. Road materials and pavement design, 4, 29-49.

SHEN, J. & AMIRKHANIAN, S. 2005. The influence of crumb rubber modifier (CRM) microstructures on the high temperature properties of CRM binders. The International Journal of Pavement Engineering, 6, 265-271.

SHEN, J., AMIRKHANIAN, S., XIAO, F. & TANG, B. 2009. Influence of surface area and size of crumb rubber on high temperature properties of crumb rubber modified binders. Construction and Building Materials, 23, 304-310.

TREDREA, P. 2006. Specification framework for polymer modified binders and multigrade bitumens.

VONK, W. & BULL, A. Phase phenomena and concentration effects in blends of bitumen and cariflex TR. Proceedings of the 7th International Roofing Congress, 1989.

RESEARCH PAPER

Intelligent System for Screening Diabetic Retinopathy by Using Neutrosophic and Statistical Fundus Image Features.

Bazhdar N. SH. Mohammed[1], Raghad Z. Yousif [1]

[1]Department of Physics, College of Science, Salahaddin University-Erbil, Kurdistan Region, Iraq

A B S T R A C T:

Diabetic retinopathy (DR) is considered as one of the global diseases of blindness, especially for aged people. The main reason behind this disease is the complication of diabetes in retinal blood vessels. Usually, the early warning signs are not observed. Screening is an important key for the diagnosis of early stages of diabetic retinopathy. In this work, a new technique for automatically screening three categories; Normal, Non-Proliferative Diabetic Retinopathy (Non-PDR), and Proliferative Diabetic Retinopathy (PDR) disease is presented that is may help doctors and physicians to make a preliminary decision. Neutrosophic set (NS) domain based on statistical features, Gray Level Cooccurrence Matrix (GLCM), Gray Level Run Length Matrix (GLRLM), and difference statistics were used for features extraction. More than thirty statistical textural features derived from the NS set domain and spatial domain have been tested using a features selection scheme named one-way analysis of variables (ANOVA1) with significance value (p<0.001). After feature selection, about sixteen features were passed the test and introduced to the classification stage which is made up of three techniques Multi-class support vector machine (MUSVM), Naïve Bayes (NB), and Decision Forest (DF) classifiers. Over 50 images from each category were downloaded from Digital Retinal Images for Vessel Extraction (DRIVE) database. The performance resulted for this proposed method shows the system robustness in identifying each stage of diabetic retinopathy within the accuracy, sensitivity, and specificity about 95.5%, 100%, and 93.3% respectively. The results of this method were compared with other considered systems. The fair comparison of results shows system superiority and can be used in clinical observation.

INTRODUCTION:

Automatic screening of DR used by the doctors as a second aim for detection and identification the stages of this disease with more accurate and precise ways. DR is one of the most prevalent worldwide diseases that leading cause of blindness due to the damage blood vessels in the eye from elevated blood sugar (Salz and Witkin, 2015).

It can be treated if the diagnosis shows that patient with diabetes that holds early signs of retinopathy otherwise it will be ended with a complete loss of vision. The most common form of DR can be classified onto two stages; Non-proliferative and Proliferative (Skaggs *et al.*, 2017).

The main symptoms are usually observed in Non-PDR stage; microaneurysm dots, haemorrhages, cotton and wool spots, hard exudate, loops, venous bleeding, and Capillary leakage causes Diabetic Macular Edema (DME).

Early diagnosis in Non-proliferative can prevents vision loss in human beings. In contrast, Proliferative is the most advanced stage. It occurs

* **Corresponding Author:**
Bazhdar Noureddin Sheikh Mohammed
E-mail: bazhdar.sh.mohammed@su.edu.krd

Mohammed. B. *and* Yousif .R/ZJPAS: 2019, 31 (6): 30-39

31

when the retina starts to grow abnormal blood vessels. This is called Neovascularization (NVE). The formation of these new vessels is easy fragile and either make few dark floaters if they bleed little and If they bleed a lot, blood diffuses through the vitreous chamber then might cause loss of visual capacity (Dodson, 2007). Figure 1, depicts a comparison between the symptoms in Non-PDR and PDR cases in DR.
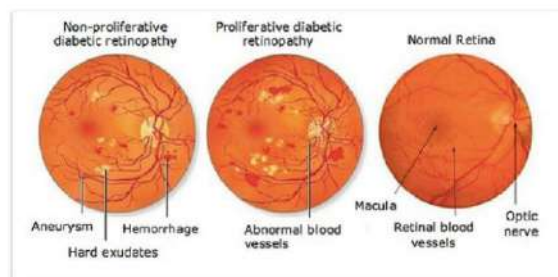

Figure1: The symptoms of Non-PDR and PDR.

Screening Programmed reduces the workload which usually the physicians faced and plays an important role in quality assurance tasks. Medical image analysis allows scientists and ophthalmologists to make a better decision about the stage of this disease. Many screening techniques in the last years have been devoted to detect automatically and classify stages DR, such as fundus photography, fluorescein angiography, B-scan ultrasonography and monochromatic photography (Salz and Witkin, 2015).This technology is called Computer Aided Diagnosis (CAD).

CAD provides useful information about the nature and status of the effect of diabetes on the eye (Verma *et al.*, 2011). Till now there has been no single modality software exist to satisfy all requirements for automatically screening. Recently many algorithms have been developed to diagnose image. Besides, increasing the number of patients, the detection methods have to be increased as well. The goodness of any screening method is determined by how accurate this technique to address the different stages of DR.

The main objective this work is presenting an artificial intelligence system to detect DR cases according to three classes: Normal, Non-PDR and PDR based on Neutrosophic set domain and statistical set domain that make the

ophthalmologists and doctors give a better decision to the patients about the phases of the disease.

1. MATERIALS AND METHODS

In this work, 150 (1240x1488) fundus images divided into three different sets of Normal, Non-PDR, and PDR classes were used. 50 images are defined as Normal. 50 images are Non-PDR and last 50 images are PDR. The digital images have been collected from the DRIVE database project (Staal *et al.*, 2004).All the images have been accepted and reviewed by expert ophthalmologists. Figure 2, represents the flow chart diagram of the proposed method which splits mainly into two structures offline and real-time system.

First of all, in an offline method, the collecting data went through image pre-processing stage. The images from each category (Normal, Non-PDR, and PDR) were resized to (576x576) to reduce processing time. Secondly, all the images were changed from RGB to grayscale, to get uniform intensity before denoising them by the median filter. Then the images were enhanced with adaptive histogram equalization to increase their visual quality and contrast (Gonzalez and Woods, 2003).

After, the statistical and textural features from each fundus image were extracted in spatial and NS domain. In the spatial domain the gray level was by two techniques; GLCM, and GLRLM. From GLCM probabilistic distribution was generated to derive difference statistics features. From NS domain, the images were derived based upon True (T), Indeterminate (I), and False (F). Later all matrices were introduced to the stage of statistical features extraction and calculation at the output of this stage. The feature vector (Fv) was produced to easy describe important characteristics from images. Then, the all features were analyzed by using ANOVA1.

In ANOVA1 test, only those features are remained that make the images clinically significant. To test the powerful of suggested method the data were split onto training\testing sets. Finally, the performance measurements

Mohammed. B. *and* Yousif .R/ZJPAS: 2019, 31 (6): 30-39

32

used to evaluate the ability of the method and different image arguments. Besides, in a real-time system, the fundus photographs undergo the same pre-processing. During analyzing, significant features are selected from them and a feature

three

vector is formed for each image before introducing to the proposed classifiers to give a decision about each image individually either it belongs to Normal, Non-PDR, or PDR.
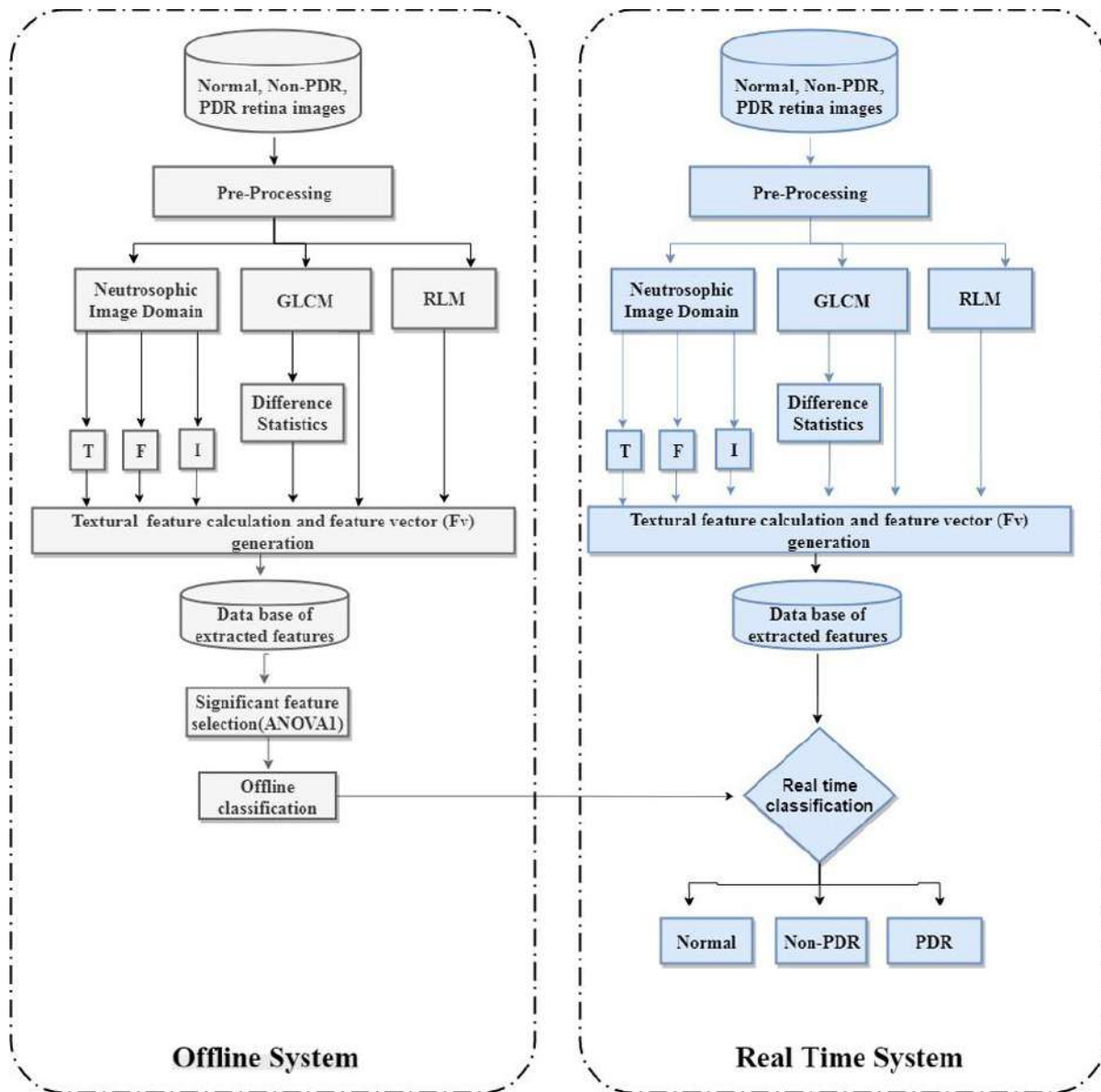
Figure 2: Block diagram of proposed method.

1.1 Extraction features

The main purpose of extracting features from the data is to increase the differentiate images, reduce the original data characteristics during the analysis process, and improves the accuracy of classification output (Ahmed, 2016, Yaba, 2016). The features from the data were extracted by performing: Neutrosophic and Statistical features.

1.1.1 Neutrosophic Image Feature Extraction

The Neutrosophic concept is a branch of philosophy was found by Smarandache and it has been employed widely in some branch of sciences especially founds impressively in image processing like medical image segmentation (Smarandache, 2005). A Neutrosophic set domain studies the origin, nature, and scope of neutralizing and their interactions with different ideational spectra. In NS,an image becomes more

Mohammed. B. *and* Yousif .R/ZJPAS: 2019, 31 (6): 30-39

33

suitable and uniform for the human viewer. The probability in NS image (PNS) can be represented in three components; T, I and F., which means that the pixel is T% true, I% indeterminate and F%

false. T, I and F are functions undertaken by any known or unknown parameters. Each component has a value of [0, 1]. Figure. 3, Shows T.F, I and Homogeneity domain.
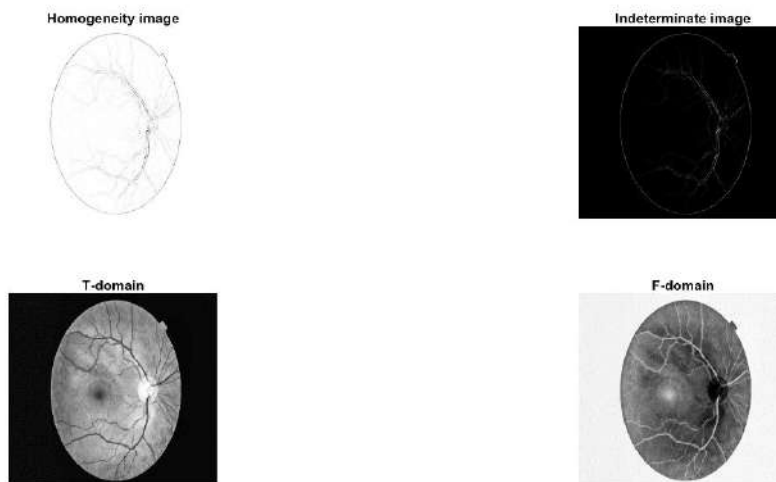
Figure 3: True, False, Indeterminacy, and Homogeneity components for DR image.

Any pixel P in image domain is defined as P(T,I,F) then pixel p(i,j) in image domain is transformed into the Neutrosophic set domain p(i,j)={T(i,j),I(i,j),F(i,j)}, where T(i,j),I(i,j) and F(i,j) are values for each membership. The intensity of the pixel (i,j) can be shown as g(i,j). Let U be a universe of discourse,and W is a set in U composed of light pixels. Each part of the transformation algorithm can be defined as (Salama *et al.*, 2017) (Eisa, 2014):

$$\overline{g(i,j)} = \frac{1}{w \times w}\sum_{n=i-\frac{w}{2}}^{i+\frac{w}{2}} \sum_{n=j-\frac{w}{2}}^{j+\frac{w}{2}} g(m,n) \tag{1}$$

$$T(i,j) = \frac{\overline{g(i,j)}-g_{min}}{g_{max}-g_{min}} \tag{2}$$

$$I(i,j) = \frac{\delta(i,j)-\delta_{min}}{\delta_{max}-\delta_{min}} \tag{3}$$

$$F(i,j) = 1 - t(i,j) \tag{4}$$

$$\delta(i,j) = |\ g(i,j) - \overline{g(i,j)}\ | \tag{5}$$

Where (g(i,j)) is the local mean value of the pixels of the window size in the level domain and δ(i,j) homogeneity value of T at (i,j). Homogeneity describes the local information, especially in segmented image. Neutrosophic images appeared by three matrices: object, edge, and background. In common probability white pixel values for object part, the probability of non-white pixel values for background membership, and for limit between a
non-white and white probability of the boundary was proposed. Neutrosophic set features for a

particular component is described by three set of features; GLCM. RLM, and Difference statistics features and described each one according to T,F, and I components (Salama et al., 2017):

Entropy feature; it measures the disorder of an image. When the elements are not uniform to each other then they make of entropy increase.

$$En_{NS} = En_T + En_F + En_I \tag{6}$$

$$En_T = \sum_{i=1}^{N}\ \sum_{j=1}^{N} P_T(i,j)lnP_T(i,j) \tag{7}$$

$$En_F = \sum_{i=1}^{N}\ \sum_{j=1}^{N} P_F(i,j)lnP_F(i,j) \tag{8}$$

$$En_I = \sum_{i=1}^{N}\ \sum_{j=1}^{N} P_I(i,j)lnP_I(i,j) \tag{9}$$

Contrast feature; it measures the illuminance level between the pixels, or color that makes an object to be distinguished.

$$CO_{NS} = CO_T + CO_F + CO_I \tag{10}$$

$$CO_T = \sum_{i=1}^{N}\ \sum_{j=1}^{N}\ (i-j)^2 P_T(i,j) \tag{11}$$

$$CO_F = \sum_{i=1}^{N}\ \sum_{j=1}^{N}\ (i-j)^2 P_F(i,j) \tag{12}$$

$$CO_I = \sum_{i=1}^{N}\ \sum_{j=1}^{N}\ (i-j)^2 P_I(i,j) \tag{13}$$

Energy feature; it measures the quantity of elements which corresponds to the mean squared value of the signal.

$$En_{NS} = E_T + E_F + E_I \tag{14}$$

$$E_T = \sqrt{\sum_{i=1}^{N}\ \sum_{j=1}^{N} P_T(i,j)^2} \tag{15}$$

$$E_F = \sqrt{\sum_{i=1}^{N}\ \sum_{j=1}^{N} P_F(i,j)^2} \tag{16}$$

Mohammed. B. *and* Yousif .R/ZJPAS: 2019, 31 (6): 30-39

34

$$E_I = \sqrt{\sum_{i=1}^{N} \sum_{j=1}^{N} P_I(i,j)^2} \qquad (17)$$

Homogeneity feature; it measures how much closes the surrounding distribution elements to the diagonal of the image matrix.

$$HO_{NS} = HO_T + HO_F + HO_I \qquad (18)$$

$$HO_T = \sum_{i=1}^{N} \sum_{j=1}^{N} \frac{P_T(i,j)}{1+|i-j|} \qquad (19)$$

$$HO_F = \sum_{i=1}^{N} \sum_{j=1}^{N} \frac{P_F(i,j)}{1+|i-j|} \qquad (20)$$

$$HO_I = \sum_{i=1}^{N} \sum_{j=1}^{N} \frac{P_I(i,j)}{1+|i-j|} \qquad (21)$$

1.1.2 Statistical Features

In an extraction features step, GLCM, GLRLM, and difference statistics were used for combinations the intensity of pixels value. GLCM used as two dimensional matrices of joint probabilities corresponding to the relative frequency of occurrence of pairs, with a distance d between them in a given direction (Alsmadi, 2017). Some of the statistical features were utilized in this paper are Homogeneity, Energy, Entropy Contrast, Symmetry, Correlation, and Momentum 1, Momentum 2, Momentum 3, Momentum 4, Angular 2nd Momentum Difference, Contrast Difference, Mean Difference, Entropy Difference, Short Run Emphasis, Long Run Emphasis, Run Percentage, Gray Level Non-Uniformity, and Run Length Nonuniformity.

Haralick developed a set of texture features from GLCM for an image to measure both first and second order statistics (Haralick *et al.*, 1973, Haralick, 1979). Gray level co-occurrence matrix (GLCM) for an image of size M x N is represented as(Acharya *et al.*, 2011):

$$C_d(i,j) = |\{(p,q),(p+\Delta x, q+\Delta y): I(p,q) = i, I(p+\Delta x, q+\Delta y) = j\}| \qquad (22)$$

Where i, j defined as spatial coordinates, position operator $d = (\Delta x, \Delta y)$, the below equation used to find the grayscale probability of a pixel at $(\Delta x, \Delta y)$:

$$P_d(i,j) = \frac{C_d(i,j)}{\sum C_d.(i,j)} \qquad (23)$$

1.2 Classifiers

Neural Network is presumed as one of the most powerful technique that widely applied on many biomedical processes to recognizing types of disease and classify them to test a constructed models or diagnostic systems based on mathematical operations (Ismail and Yaba, 2015). To guess the output classes according to Normal, Non-PDR, and PDR, three classification methods were suggested: MUSVM, NB, and DF classifier.

1.2.1 Multi-Class support vector machine (MUSVM)

In general, SVM is a nonlinear learning algorithm with high generalization ability to classify images. It performs to classify problems of two groups of sets. SVM classifier determines the best hyperplane which distinguishes between each positive and negative training sample (Chamasemani and Singh, 2011). Multi-class classification problems usually are handled to categorize the features according to more than two binary categories (k >2). To solve MUSVM problems, normally the feature variables in a feature vector are proportional to the number of labels. In common two special approaches are available: one-versus-rest (Hong and Cho, 2008) and one-versus-one (Milgram *et al.*, 2006). These two strategies can split the multi-class problem to multiple binary classification subproblems for training data set. The output training set can be set up to carry out predictions about a test sample (Chamasemani and Singh, 2011).

1.2.2 Naïve Bayesian (NB)

The NB model is a heavily simple and effective method in machine learning. It can predict class labels form on a strong conditional independence assumption. Therefore, the probability of one feature does not make any effect on the other independence assumptions (Mukherjee and Sharma, 2012). The NB algorithm depends on the information of the comparable restricted pixels that already classified in training sets. Suppose C, are classes and m refers to possible classes $C = \{C_1, C_2, C_3, ..., C_m\}$ for the domain of training set D in n-dimensional vector $D = \{D_1, D_2, D_3, ..., D_n\}$. The classifier model estimates that $X \in D_i$ if and only if it has the maximum posteriori probability conditioned on D (Noronha *et al.*, 2014).

$$P(C_i|D) > P(C_j|D) \quad , \quad 1 \le j \le m, \quad j \ne i \qquad (24)$$

Mohammed. B. *and* Yousif .R/ZJPAS: 2019, 31 (6): 30-39

35

By applying Bayes' rule to calculate the probability of a document D in a class C:

$$P(C_j|D) = \frac{P(D|C_j)P(C_j)}{P(D)} \qquad (25)$$

Where P(D) has constant size for all classes, while only $P(D|C_j)P(C_j)$ required to be maximized.

2.1.1 Decision Forest (DF)

The random decision it is an attractive tree predictor tool for appraising image regression. It is decided by the distribution of trees separately and the correlation between them to operate datasets (Breiman, 2001). The main point of the tree is randomly select observations and specified features in a feature vector to produce multiple decision trees from the number of trees and then average the results. After that, the algorithm will select the class before are they restricted through bagging technique. Bagging algorithm is used to show de-correlation between training sets in order to decrease the variance of the model (James *et al.*, 2013).

1.3 Performance Measurements

To weigh the effectiveness of proposed method, the confusion matrix (error matrix) tool was employed as a statistical performance to evaluate the classification model(Stehman, 1997). The parameters such as Accuracy, Sensitivity, Specificity, Precision, and F1-Score are computed for each iteration (Trevethan, 2017):

$$\text{Sensitivity} = \frac{T_p}{T_p + F_N} * 100 \qquad (26)$$

$$\text{Specificity} = \frac{T_N}{F_p + T_N} * 100 \qquad (27)$$

$$\text{Accuracy} = \frac{T_p + T_N}{T_p + T_N + F_p + F_N} * 100 \qquad (28)$$

$$\text{Precision} = \frac{T_p}{T_p + F_p} * 100 \qquad (29)$$

$$\text{F1\_score} = \frac{2T_p}{2T_p + F_p + F_N} * 100 \qquad (30)$$

Where, TP, TN, FP and FN represent True Positive, True Negative, False Positive, and False Negative, respectively. The train and test data sets were split into three-fold cross-validation as represented in Table 1.

Table 1. Splitting the input data into the training and testing sets.

Cross folds	Splitting ratio
1st training	30% Training 70% Testing
2nd training	70% Training 30% Testing
3rd training	30% Training (Random) 70% Testing

To predict the output classifier the input fields were specified into class labels. Classes with their corresponding labeled number are represented in Table 2. One-way analysis of variance (ANOVA1) was performed to select the succeeded features among all applying features (Hogg and Ledolter, 1987). It is usually a comparison method to indicate how close or far away from the means between the groups and within the groups. ANOVA decision represents the probability of occurrence (p-value) value. If the p-value is too small or near to zero, in this case, the null hypothesis is rejected and suggests that at least one sample means among all tested groups is significantly different as compared to the other samples mean (Acharya *et al.*, 2009).

Table 2. Class labels

Classes	Numbers
Normal	1
Non-PDR	2
PDR	3

2. RESULTS

Among 38 applied features after preb processing step, 16 features were selected by ANOVA1 with their p-values <0.001 to increase the accuracy of the method and to become more suitable to overcome the case of the disease. The succeeded features have been shown in Table 3.

Table 3. List of selected features according to their p-values.

Features Name	Feature Number	p-value
NS-Energy	2	3.7767815e-07
NS-Symmetry	5	2.7919764e-05
NS-Correlation	6	8.5578876e-13
NS-Moment 3	9	1.6331283e-05
NS-Short Run Emphasis	11	6.5423865e-07
NS-Run Percentage	13	8.5175199e-09
NS-Gray Level Non-Uniformity	14	0.00081359183
NS-Run Length Non-Uniformity	15	6.4482585e-08

Mohammed. B. *and* Yousif .R/ZJPAS: 2019, 31 (6): 30-39

36

NS-Angular Second Moment	16	4.3907629e-05
NS-Contrast Difference	17	1.2192163e-08
NS-Mean Difference	18	3.7640087e-08
NS-Entropy Difference	19	3.1124333e-07
Homogeneity	20	3.3957011e-06
Entropy	22	6.4770609e-14
Angular Second Moment	35	4.4096184e-05
Entropy	38	1.3581388e-17

Box graph usually is used to test and show relationships between categorical variables to provide more information about the samples. In Figure 4, two successive features are drawn which retrieved from Table 3, to show a difference between the groups means. From both, a clear separation seen that corresponds to statistically significant features to differentiate between the DR cases in clinical observation.
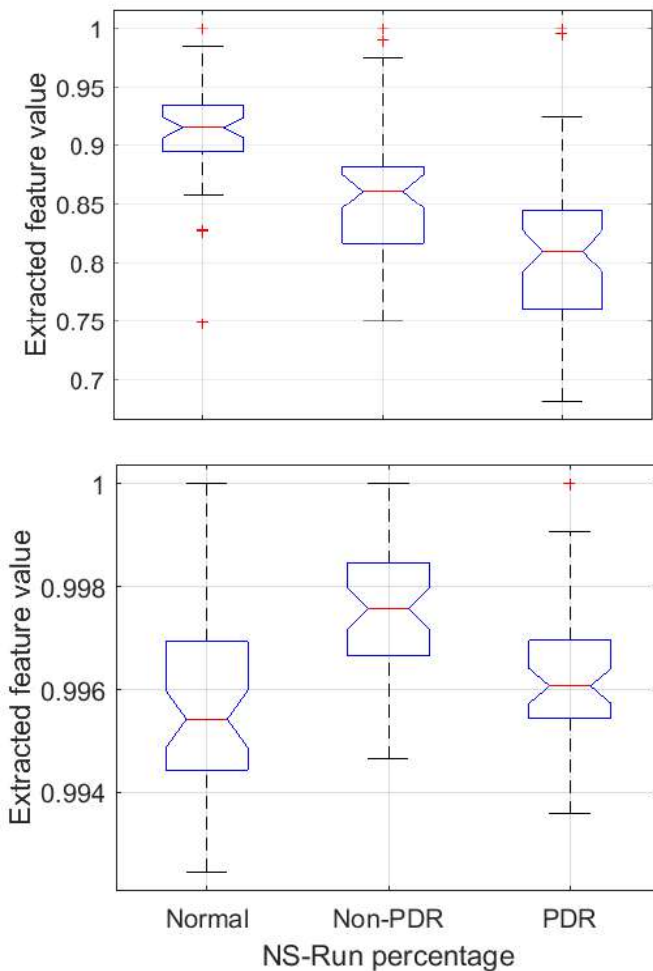
Figure 4: Box graph for two passed features: Entropy and NS-Run percentage.

Tables 4 and 5, illustrate four measurements; Accuracy (Acc), Sensitivity (Se), Specificity (Sp), and Precision (Pre) which found in a confusion matrix to show the best correctness results among final results of suggest method which were classified according to previously mentioned classification techniques. From Table 4, represents the outcome results when only the spatial domain was used to extract features, the ability of the system was poor to distinguish the differences between the stages due to the low percentage values of classification measurements. In contrast, in Table 5, there is a significant increase of performance classification has been seen after the features were extracted from both spatial and Neutrosophic domain which gives suitable output for clinical observation.

Table 4. Performance measurements for each classification method without NS features.

Classification Methods	Training Sets	Acc (%)	Sn (%)	Sp (%)	Pre (%)
MUSVM	1	75.2	91.4	67.1	58.1
	2	71.1	96.6	56.7	53.8
	3	47.6	100	21.4	38.8
Naïve Bayes	1	54.2	91.4	35.7	41.5
	2	68.9	86.7	60	52
	3	40.9	100	51.1	36
Decision forest	1	63.8	80	55.7	47,4
	2	77.8	80	76.6	63.1
	3	41.9	91.2	43.8	36.4

Table 5. Performance measurements for each classification method with NS features.

Classification Methods	Training Sets	Acc (%)	Sn (%)	Sp (%)	Pre (%)
MUSVM	1	93.3	88.6	95.7	91.1
	2	95.5	100	93.3	88.2
	3	93.3	94.3	92.8	86.8
Naïve Bayes	1	72.3	80	68.5	56
	2	86.6	93.3	83.3	73.8
	3	72.3	80	68.5	56
Decision forest	1	82.8	82.8	82.8	70.7
	2	93.3	93.3	93.3	87.5
	3	81.9	100	72.8	64.8

Figure 5, represents the comparison between the accuracy of the method with and without NS-domain. In MUSVM the accuracy raised to more than 95.5 %, while it was about 75% before applying NS. While, In NB classification, the final outcome changes about 70% and nearly 87% for both NS and without NS. Additionally, the accuracy increased by approximately 14% in DF and finally reached 93.3%.

Mohammed. B. *and* Yousif .R/ZJPAS: 2019, 31 (6): 30-39

37

The table of confusion matrix is drawn in Figure 6, describes the superior of the method due to the less inequality between actual and predicted data set classes. Among the all estimations less than %6 error occurred. In Contrast, best performance measurement achieved from MUSVM classifier for diagnosis the preferred stages in diabetic retinopathy with average accuracy about 95.5%.
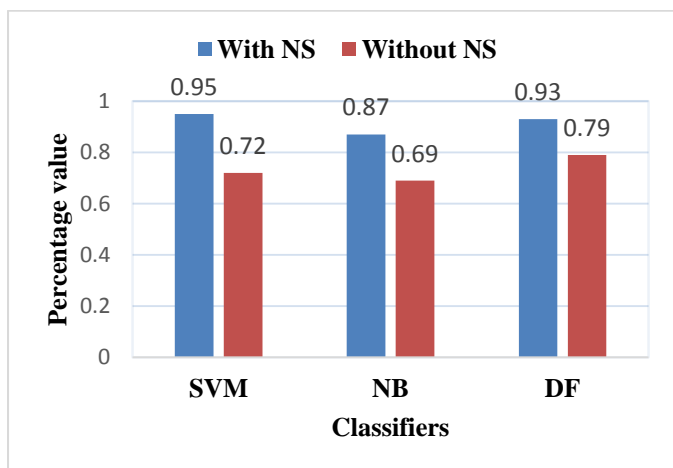
Figure 5. Accuracy improvement by NS-domain.
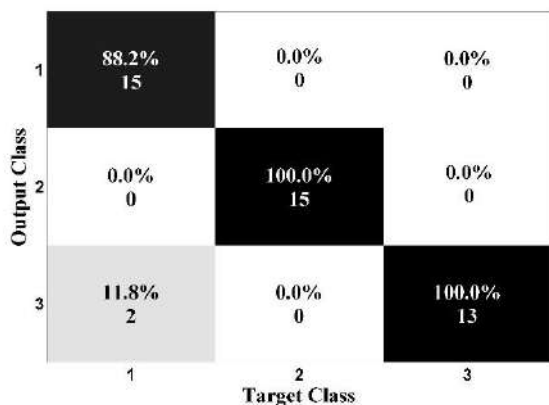
Figure 6: Confusion matrix table.

3. DISCUSSION

Many authors suggested different methods to automatically classify the DR stages. Nayak et al., applied two texture features; Area of blood vessels and exudate area on 140 fundus images contain Normal, Non-PDR, and PDR cases to extract the main different characteristics between the images. The data was classified by ANN classifier (Nayak *et al.*, 2008).To analyze the abnormal signs from

early stage of DR with normal stage , Reza et al., extracted hard exudate, cotton and wool spots, and large plaque of hard exudate from 60 images and classify them according to Normal, Mild, Moderate, and severe stages. To find the information gain within the method, Decision support system was used (Reza and Eswaran, 2011). Five texture features were extracted from 238 fundus images that divided onto Normal, Non-PDR, PDR, and macular edema. In this work, the features were fed into SVM classifier to evaluate the performance the model (Acharya *et al.*, 2012). Nornoha et al., used fundus retinal images to classify 272 fundus images according to normal, mild glaucoma and sever glaucoma by using feature-based machine learning classification approach. For this aim, 3rd order cumulant features was used. Then, the images fed into 10-fold cross validation technique and tested by SVM classifier (Noronha et al., 2014). In another work has been done by Mane et al., hybrid features named holo-entropy features applied on 130 fundus images to

extract retinal blood vessel area and optic disk region on a set of images which contain Normal and DR images. Finally, the images were classified by using decision tree classification technique (Mane and Jadhav, 2017). An automated classification method approached by Islam et al., to classify 180 fundus images according to normal and PDR. In this approach, bag of words model with Speeded Up Robust Features utilizes; 87 images contain microaneurysms, haemorrhages hard exudates, and soft exudates. For a classification purpose, the data split into %65 and %35 training-testing sets. The performance achieved by SVM classifier (Islam *et al.*, 2017).Table 6, represents a list contains a performance measurement comparison between some recently related works and our approached method for automatically diagnosis DR.

4. CONCLUSIONS

Diabetic retinopathy is a global disease of vision loss. It happens in the retina in the back of the eye due to the complication of diabetes inside blood vessels. It ends with blindness if left untreated. Screening is a key part of the diagnosis of early stages of that disease. In this

Mohammed. B. *and* Yousif .R/ZJPAS: 2019, 31 (6): 30-39

38

paper a new way offered to automatically classify fundus images according to Normal, Non-PDR, and PDR groups. The standard images are available in DRIVE project database. The images were extracted using statistical and textural features based on neutrosophic set domain. About thirty-eight features in both domains were applied on images to generate a feature vector. Among them, only sixteen succeeded features selected by ANOVA1 which are viable in medical practice. The collected features were undergone MUSVM, NB, and DF classification models after the data was split into training and testing sets by using three-fold cross validation technique. After analyzing the dataset, the results in MUSVM classifier represented that the suggested method able to classify the DR images with best performance measurement: accuracy 95.5%, sensitivity 100%, and specificity 93.3%. So, the system can be used

as a second tool by ophthalmologists to check DR.

Conflict of Interest

There is no conflict of interest.

Table 6. Comparison between related works.

Author (Year)	No. of images	Features	Performance	Acc (%)	Sn (%)	Sp (%)	Detection
(Nayak et al., 2008)	140	Texture	ANN	93	90	100	Normal, Non-PDR, and PDR
(Reza and Eswaran, 2011)	60	Hard and soft exudate area	Decision support system	97.2	100	97	Non-PDR
(Acharya et al., 2012)	238	Texture Analysis	SVM	-	98.9	89.5	Normal, Non-PDR, PDR, and Edema
(Noronha et al., 2014)	272	Higher order statistics	NB	92.6	100	92	Normal, mild, and moderate\severe
(Mane and Jadhav, 2017)	130	Hybrid holo-entropy, and wavelet	DF	97	96.7	96.4	Normal and abnormal
Islam et al., (2017)	180	Speeded Up Robust Features	SVM	94.4	94.8	94	Normal and DR
Our proposed method	150	Neutrosophic and Statistical	MUSVM	95.5	100	93.3	Normal, Non-PDR, and PDR

References

ACHARYA, U. R., LIM, C. M., NG, E. Y. K., CHEE, C. & TAMURA, T. 2009. Computer-based detection of diabetes retinopathy stages using digital fundus images. *Proceedings of the institution of mechanical engineers, part H: journal of engineering in medicine,* 223**,** 545-553.

ACHARYA, U. R., NG, E. Y.-K., TAN, J.-H., SREE, S. V. & NG, K.-H. 2012. An integrated index for the identification of diabetic retinopathy stages using texture parameters. *Journal of medical systems,* 36**,** 2011-2020.

AHMED, R. M. 2016. Using Logistic Regression to Distinguish Between Fatty and Fibroid Masses in Medical Imaging (Ultrasound Image). *ZANCO Journal of Pure and Applied Sciences,* 28**,** 193-201.

ALSMADI, M. K. 2017. An efficient similarity measure for content based image retrieval using memetic

Mohammed. B. *and* Yousif .R/ZJPAS: 2019, 31 (6): 30-39

39

algorithm. *Egyptian journal of basic and applied sciences,* 4**,** 112-122.

BREIMAN, L. 2001. Random Forests. *Machine Learning,* 45**,** 5-32.

CHAMASEMANI, F. F. & SINGH, Y. P. 2011. Multi-class support vector machine (SVM) classifiers--an application in hypothyroid detection and classification. Bio-Inspired Computing: Theories and Applications (BIC-TA), 2011 Sixth International Conference on,. IEEE, 351-356.

DODSON, P. M. 2007. Diabetic retinopathy: treatment and prevention. *Diabetes and Vascular Disease Research,* 4**,** S9-S11.

EISA, M. 2014. A new approach for enhancing image retrieval using neutrosophic sets. *International Journal of Computer Applications,* 95.

GONZALEZ, R. & WOODS, R. 2003. Digital Image Processing 2nd ed: Pearson Education.

HARALICK, R. M. 1979. Statistical and structural approaches to texture. *Proceedings of the IEEE,* 67**,** 786-804.

HARALICK, R. M., SHANMUGAM, K. & DINSTEIN, I. H. 1973. Textural features for image classification. *IEEE Transactions on systems, man, and cybernetics,* 3**,** 610-621.

HOGG, R. & LEDOLTER, J. 1987. Engineer statistics. *England: MacMillan Publishing Company.*

HONG, J.-H. & CHO, S.-B. 2008. A probabilistic multi-class strategy of one-vs.-rest support vector machines for cancer classification. *Neurocomputing,* 71**,** 3275-3281.

ISLAM, M., DINH, A. V. & WAHID, K. A. 2017. Automated diabetic retinopathy detection using bag of words approach. *Journal of Biomedical Science and Engineering,* 10**,** 86.

ISMAIL, H. J. & YABA, S. P. 2015. Enhanced Accuracy and Reliability of ER and PR Immunohistochemistry Scoring Using ANN from Digital Microscope Images. *ZANCO Journal of Pure and Applied Sciences,* 27**,** 69-80.

JAMES, G., WITTEN, D., HASTIE, T. & TIBSHIRANI, R. 2013. *An introduction to statistical learning*, Springer.

MANE, V. M. & JADHAV, D. V. 2017. Holoentropy enabled-decision tree for automatic classification of diabetic retinopathy using retinal fundus images. *Biomedical Engineering/Biomedizinische Technik,* 62**,** 321-332.

MILGRAM, J., CHERIET, M. & SABOURIN, R. "One against one" or "one against all": Which one is better for handwriting recognition with SVMs? tenth international workshop on Frontiers in handwriting recognition, 2006. SuviSoft.

MUKHERJEE, S. & SHARMA, N. 2012. Intrusion detection using naive Bayes classifier with feature reduction. *Procedia Technology,* 4**,** 119-128.

NAYAK, J., BHAT, P. S., ACHARYA, R., LIM, C. M. & KAGATHI, M. 2008. Automated identification of diabetic retinopathy stages using digital fundus images. *Journal of medical systems,* 32**,** 107-115.

NORONHA, K. P., ACHARYA, U. R., NAYAK, K. P., MARTIS, R. J. & BHANDARY, S. V. 2014. Automated classification of glaucoma stages using higher order cumulant features. *Biomedical Signal Processing and Control,* 10**,** 174-183.

REZA, A. W. & ESWARAN, C. 2011. A decision support system for automatic screening of non-proliferative diabetic retinopathy. *Journal of medical systems,* 35**,** 17-24.

SALAMA, A., EISA, M. & FAWZY, A. 2017. A Neutrosophic Image Retrieval Classifier. *International Journal of Computer Applications,* 170**,** 975-8887.

SALZ, D. A. & WITKIN, A. J. 2015. Imaging in diabetic retinopathy. *Middle East African journal of ophthalmology,* 22**,** 145.

SKAGGS, J. B., ZHANG, X., OLSON, D. J., GARG, S. & DAVIS, R. M. 2017. Screening for Diabetic Retinopathy Strategies for Improving Patient Follow-up. *North Carolina medical journal,* 78**,** 121-123.

SMARANDACHE, F. 2005. *A Unifying Field in Logics: Neutrosophic Logic. Neutrosophy, Neutrosophic Set, Neutrosophic Probability: Neutrsophic Logic. Neutrosophy, Neutrosophic Set, Neutrosophic Probability*, Infinite Study.

STAAL, J., ABRAMOFF, M. D., NIEMEIJER, M., VIERGEVER, M. A. & VAN GINNEKEN, B. 2004. Ridge-based vessel segmentation in color images of the retina. *IEEE Trans Med Imaging,* 23**,** 501-9.

STEHMAN, S. V. 1997. Selecting and interpreting measures of thematic classification accuracy. *Remote sensing of Environment,* 62**,** 77-89.

TREVETHAN, R. 2017. Sensitivity, specificity, and predictive values: foundations, pliabilities, and pitfalls in research and practice. *Frontiers in public health,* 5**,** 307.

VERMA, K., DEEP, P. & RAMAKRISHNAN, A. 2011. Detection and classification of diabetic retinopathy using retinal images. India Conference (INDICON), 2011 Annual IEEE, IEEE, 1-6.

YABA, S. P. 2016. Breast cancer detection system based oncomprehensive wavelet features of mammogram images and neural network. *ZANCO Journal of Pure and Applied Sciences,* 27**,** 47-58.

RESEARCH PAPER

A review of the Effects of Magnetic Field on main blood cells: in vivo and in vitro experiments.

Bestoon T. Mustafa[1], Sardar P. Yaba[2], Asaad H. Ismail[3]

[1,2,3]Department of Physics, College of Education, Salahaddin University-Erbil, Kurdistan Region, Iraq

A B S T R A C T:

Background: Magnetic field has being used in diagnostics for decades such as MRI. Sources of magnetic field were found in electronic devices and may emit extremely low intensity of magnetic field. Beside the daily use of electronic devices, there are some concerns regarding to side effects of magnetic field produces on living cells. Main Blood cells parameters were considered, and Red blood cells have targeted as the main and most affected by magnetic field. Concerns to blood, any abnormality in shape, aggregation, count may cause inflammations or chronic diseases such as anemia.

Objective: In this review, we evaluated the previous works carried out to investigate the effect of static and time varying magnetic fields on rheological properties (blood parameters, viscosity and DNA strand break) of blood between periods from 1980-2019. We provided up-to-date state of research articles and the latest progress. Different intensities of magnetic fields (week, moderate and strong) were looked at.

Result: Seventy two published research articles were reviewed. This shortened to thirty eight articles in respect to our goal. The chosen articles studied the biological effect of magnetic field on human and animal in vivo and in vitro experiments. A few theoretical studies were pointed to. Inconsistent results were compared.

Conclusion: Magnetic fields can be static or time varying as frequency is not zero. Blood counts responded to external magnetic field with altering in counts, aggregations, change in viscosity and DNA strand break. RBCs aggregation increased as blood is affected by magnetic field. Whole blood viscosity enhanced the aggregation of red blood cells. Raise in aggregation changed the time flow of blood in microcirculations.

1. INTRODUCTION

Magnetic fields (MF) can be static or pulsed (time varying field). Static magnetic field (SMF) is known as a zero hertz, whereas, pulsed magnetic field (PMF) has non-zero frequency. SMF is generated using a DC current or obtained from a permanent magnet whereas the direction of charges is constant. The strength of SMF intensity is classified into categories: week magnetic field

[Vergallo and Dini, 2018]. PMF is generated from alternating current in which the direction of the field varies regarding to the frequency. The PMF of extremely low frequency (ELF) is known as a field with frequency below 300 Hz [Hashish et al., 2008].

Sources of MF are varieties. Moderate sources of SMFs include transportation system (electric trains, metro, trams, cars,…ect), industrial process (aluminum production) and some medical diagnostic machines. A 2 mT of SMF produces inside trams exposing users living cells. SMF and PMF were detected in metros and cars [Halgamuge et al., 2010, Chadwick and Lowes, 1998]. MRI generates a high SMF. ELF-EMF produces in heaters, high voltage

* **Corresponding Author:**
Bestoon T. Mustafa
E-mail: bestoon.mustafa@su.edu.krd

Mustafa. B. *et al.* /ZJPAS: 2019, 31 (6): 40-50

41

transmission lines, some household appliances and domestic installations.

Research articles revealed influences of ELF on blood cells [Dasdog et al., 2002, Salem et al., 2005, Amara et al., 2006 and Zaghloul, 2011]. The effects of chemical substances on biological system were introduced intensively. [Qader and Hawezy, 2019, Maulood and Mahmud, 2016]. Yet, the biological effect of non-ionization radiation is controversial [Ismail, H., 2015]. The effect of MF on living cells, red blood cells (RBCs) aggregations, rotations and magnetizations [Iino, 1997 and Sağdilek et al., 2012], DNA single and double stand break [Ali, 2018 and McCann, 1998], viscosity of blood [Kenjereš, 2008 and Mohaseb et al., 2017], heating, body weight, oxidative stress, blood pressure, brain tissue, circulation system, blood proteins, PH and ect. were studied. Similar and contradict results were introduced. Most of in vivo radiobiological experiments were conducted on rats and mice. Therefore, a few studies were conducted on human. The results are controversial.

Blood is known as a biomagnetic fluid due to excising positively and negatively charged particles and molecules such as proteins and erythrocytes. The negatively and positively molecules are due to unbounded (or free) electrons in outermost shells. Existing electrically charged molecules can be a reason where rheological properties of blood respond to MF. Blood parameters can act as paramagnetic or diamagnetic. However, RBCs act in two different ways: paramagnetic or diamagnetic, depending on their oxygenated state [Bansi et al., 2018].

RBCs are large molecules with mean volume of (90 μm^3) and major diameter of (8 μm) [Haik et al., 2001]. They surrounded with a special membrane which allows the cells to bend and stretch while they are passing through tiny blood vessels [Ye et al., 2016 and Kizilova et al., 2018]. Inside RBCs, there is tremendous number of hemoglobin (Hb). Hemoglobins are molecules carrying oxygen and carbon dioxides. Each Hb has four binding sites attached to iron molecules. Hemoglobin iron molecules can be another reason where RBCs can behalf as paramagnetic [Haik et al., 2001].

To study the effect of MF on blood cells, a wide range of researches were conducted

theoretically and practically. Investigations have shown RBCs are aligning in a direction of applied external magnetic field (magnetization). The same behavior was approved to platelets (PLTs) [Bansi et al., 2018]. PLTs and RBCs aggregations were also investigated [Keating et al., 2008 and Keating et al., 2011]. Generally, there are a multiple types of aggregation recognized. First, in normal blood itself, specific particles and molecules intermediate closing cells or aggregations. This is called rouleaux. The second is closing or aggregating molecules in blood under the effect of an external force (MF). Regarding to the effect of magnetic field, temperature stability must be preserved.

2. RED BLOOD CELLS AGGREGATION

Aggregation is the main effect causes blood viscosity [Iino, 1997]. Under no effect of magnetic field, limited range of RBCs aggregations were investigated in vivo and in vitro experiments. These types of aggregations are called rouleaux formation and they are reversible [Rmpling et al., 2004, Bäumler et al., 1999 and Kizilova et l., 2018]. The process of rouleaux formation and disassociation are continuous. Explaining the aggregation pattern can be simple. Tiny molecules and proteins exist in blood and contribute in rouleaux formation [Iino, 1997 and Sağdilek et al., 2012].

In this review, we highlight important results of published research articles regarding to the effect of MFs on blood parameters and rheological properties, published from period 1980-2019. Red blood cell aggregation, WBCs, PLTs, blood viscosity and DNA strand break are considered. Effects of SMF and time-varying MF effects will be discussed.

3. LITERATURE REVIEW

Blood flow and microcirculation were studied intensively during last decades. In vitro and in vivo experiments showed variations of blood flow under the effect of MF. The effect of SMF on blood flow of mice was investigated by [Xu et al., 2001]. Tibialis anterior muscle blood was measured using fluorescence epi-illumination system. An exposure of SMF as small as 1 mT for

Mustafa. B. *et al.* /ZJPAS: 2019, 31 (6): 40-50

42

10 min increased the blood velocity in range of 20% to 45% at 45 min post exposure. However, no increase was seen during the exposure. The same experiment was repeated for time varying MF (50 Hz). Compare to SMF, blood velocity has raised 26% during the exposure. At lower exposure (0.3 mT), both SMF and time varying MF showed zero effect. Exposed animals with SMF at 10 mT changed the blood velocity simultaneously, from 15% to 45% from the beginning to the end of the exposure respectively. The researchers set 1 mT as the threshold valued of hematological change in mice blood.

A similar research was carried out by [Gmitrov et al., 2002] using a higher dosage of MF. They studied the effect of SMF on blood circulation of cutanous tissue in ear lobe of rabbit. Irradiation with MF at 0.25 T during 40 min increased 20% to 40% of the blood flow velocity in microcirculation in the tissue. This is in compare to control samples. The changes started significantly after 10 min of exposure and continued till 20 min after exposure. Concluded that, at a high dosage of exposure, SMF starts to alter flow velocity during exposure.

Peripheral hemodynamic was examined under the effect of 8 T by [Ichioka et al., 1998]. The in vivo experiment observed changes in microcirculatory hemodynamic of dorsal skin of rats using videomicroscopy. Blood flow rate raised 17% at post exposure, 1-5 min after exposure. However, the flow returned to its normal condition after 10 min of exposure. The same researchers [Ichioka et al., 2000] curried out another experiment and studied the whole blood flow property. A field intensity of 8 mT was used. In compare to their previous experiment, changes of blood flow started during exposure simultaneously. They concluded that blood flow of skin reduces at the baseline and returns to baseline 20 min after exposure.

[Schuhfried et al., 2005] studied the effect of time varying magnetic field on microcercuation and temperature alteration of volunteer human feet. Low dose-low frequency (100 µT, 30 Hz) and a higher dose-low frequency (8.4 mT, 10 Hz) field were exposed to 12 healthy male and female volunteer. Treatments were applied to individuals for one week similarly at the same time every day. Both microcirculation and temperature were measured from great joys and dorsum of the foot every 5 min during and 5-10 min after exposure.

For both conditions of exposure, a decrease in microcirculation and temperature drop was reported. However, no significant changes of blood parameters were seen. As a conclusion, exposure did not improve microcirculation in healthy human. At the same pattern, [Lim et al., 2009] has studied the temperature dependence shear stress on aggregation. Shear rate examined at 4, 10, 20, 30 and 40 ^{0}C. Shear rate decreased as temperature increased.

Blood flow was examined under a higher dosage of MF. [Ueno et al., 1986] studied the time varying MF effect on blood flow using laser Doppler flowmeter. Hands of volunteers exposed with magnetic field (16, 32 and 48 mT, 3.8HZ). Blood flow reduced at exposure of 32 and 48 mT. This result shows the non-similar pathological effect of PMF and SMF at a higher intensity as shown by [Gmitrov et al., 2002].

A change of blood viscosity alters blood flow rate and velocity in blood vessels. Viscosity of blood was studied under the effect of MF. Blood viscosity was measured directly or indirectly. In addition, time flow of blood in capillary tubes was also studied as a mirror of blood viscosity. The effect of SMF on human blood viscosity was studied by [Haik et al., 2001]. They measured time flow of blood using capillary tube (3 mm in diameter) considered change in blood viscosity. The tube was set between sources of MF. First, time flow of blood was measured under the effect of gravity and then under the effect of SMF. Increasing the field intensity increased time flow continuously. The 10 T of SMF decreased blood flow rate by 30%. They believe that this reduction is due to an increase in blood viscosity under the effect of SMF. The torque exerted by the SMF will increase association of plasma particles to aggregate RBCs which causes blood viscosity to increase. This result is inconsistent to that shown by [Ueno et al., 1986] using a closely similar MF exposure as they present the flow rate increases under the effect of SMF.

Blood viscosity dependency on high SMF was examined by [Yamamoto et al., 2004]. Oxygenated blood samples were collected from healthy human. 1.5 T has applied to blood samples passing through an Ostwald viscometer tube. Results showed an increase of blood viscosity. They believe that oxygenated blood and shear rate of blood flow selects the status of blood

Mustafa. B. *et al.* /ZJPAS: 2019, 31 (6): 40-50

43

viscosity. Additionally, 1.5 T can alter the blood flow rate.

Relative blood viscosity can be measured easily using classic techniques or tools. [Elblbesy, 2014] has measured relative blood viscosity using a syringe. Easily, 2 mL of blood was loaded into a 5 mL syringe and allowed the blood to flow under normal gravitation. The time of flow was measured. The same experiment was repeated for de-ionized water and then relative blood viscosity was measured. This method can be used to study the effect of magnetic field on blood flow by leaving the syringe between two magnets, similar technique as used by [Haik at al., 2001].

Blood viscosity can also be measured using digital viscometer or rheometers such as microviscometer of brookfied viscometers. The advantage of using digital viscometers is that where small amount of blood samples are required and also results can be achieved more accurately. Blood viscosity can also be measured under different shear rates. Brookfield DV-III Programmable Rheometer was used to measure blood viscosity directly [Baieth, 2008] for blood collected from albino rats at in-vivo experiments. Sixteen coils were used to form a setup of magnetic field. The field was exposed to rats directly and bloods were collected after exposure. Blood viscosity reduced as magnetic field exposure increased. 0.3, 0.5 and 1 mT (50Hz) changed the blood viscosity continuously in compare to control samples. This result is inconsistent to that shown by [Haik et al., 2001] used SMF. Shear rate reduced as viscosity increased. RBCs counts and HTC percentages increased significantly as animals' espoused under 0.5 mT.

One mathematical model studied the effect of non-uniform magnetic field on blood flow [Kenjereš, 2008]. The effect of MF on Oxygenated and deoxygenated blood were examined. A cylinder with a size similar to arties programmed to study the blood flow time. A 10 T of MF affected oxygenated blood slightly and less significantly than that of de-oxygenated blood, due to the fact that magnetic susceptibility of deoxygenated blood is higher than that of oxygenated blood. Blood viscosity was measured experimentally under the effect of SMF using rheometers of different shear rates [Marcinkowska, 2013]. The experiment was performed in vitro for healthy blood samples. No significant changes reported.

In another experiment blood viscosity has determined for human blood samples under different shear rates. A rheometer was used. Relative blood viscosity reduced under the effect of magnetic fields. Drookfield DV-lll viscometer was also used by [Mohaseb et al., 2007] to measure the blood viscosity. Rats were exposed to 0.3 mT (50 Hz) for 21 and 45 days. Both groups of espoused animals showed a significant increase of whole blood viscosity compare to control samples. Their result was obtained using optical microscopic images.

Blood viscosity of polycythemia disease was examined under 1.5 T MRI magnetic field [Kadhim et al., 2016]. The U-tube viscometer and mathematical formula were employed to extract the viscosity of blood samples. Exposure time was extended from 1 min to 21 min. Samples were collected from unhealthy men ages between 28-48 years old. The results showed a decrease of blood viscosity as magnetic field is increased. The 1 and 15 min of exposure resulted the maximum alteration.

Hematological parameters such as RBCs, WBCs and PLTs counts were studied under the effect of MF. Abnormality of blood cell counts cause cardiovascular diseases. An Increase of leukocyte counts cooperate an increase of death risk caused by ischemic heart disease with 65%. Blood viscosity and oxygen supply causes by haemoglobin concentration and associate with ischemic heart disease in men [Maulood, 2018]. [Dasdog et al., 2002] studied PMF effect on blood rheological properties. 16 male wielders (subjected 3-4 hrs per day and each has experienced 10 years fin welding) and 14 healthy males (as control group) were participated. Samples were selected with no chronic diseases and all having regular life style. The result shows a significant difference in hematocrit. However, other blood parameters such as RBCs, WBC and PLTs are almost similar to that of control groups.

Treating blood with micro molecules are paid attention in hematological research area. The effect of SMF (one hr per day for 30 selective days) on blood parameters were studied by [Salem at al., 2005] for blood of albino rats with and without zinc treatment. Untreated Rats and treated rats with zinc were exposed to SMF. Blood

Mustafa. B. *et al.* /ZJPAS: 2019, 31 (6): 40-50

44

samples were withdrawn and examined. Inconsistent to that shown by [Dasdog et al., 2002], the results showed an increase in blood parameters: Hb, WBCs, RBCs. The hematocrit has not changed. WBCs and PLTs have not increased under the zinc treatment. Hematocrit is almost unchanged with zinc or without zinc treatment. This result drives the rule of zinc molecules to resist alteration of blood parameters under the force produced by SMF.

Wistar rats were exposed with 128 mT of SMF in a duration of one hr/ 30 [Amara et al., 2006]. Groups of a six wistar rats were prepared under ambient condition. Each group was exposed for a selective week or weeks. The first week of exposure did not change the body weight and blood parameters significantly. From the second week till 14 days, body weight and blood parameters started to change rapidly. By the end of the month, the average body weight reduced from 215-200 gr. WBCs, RBCs, Hb, Ht% and PLTs have changed from $11.35 \pm 0.16 - 13.68 \pm 1.42$, $7.29 \pm 0.03 - 7.82 \pm 0.15$, $11.98 \pm 0.15 - 13.2 \pm 0.26$, $34.06 \pm 0.32 - 35.37 \pm 0.69$ and $566.33 \pm 15.08 - 626 \pm 14.04$ respectively.

A similar experiment was conducted by [Chater et al., 2006]. 128 mT of a SMF applied on Wistar Pregnant rats at day 6 to day 19, each day for 1 hr. Thirteen days of exposure changed some blood properties: hematocrit increased by 6%, Hb by 12%, and blood glucose increased. Releasing insulin decreased and that leads to diabetes. Body weight reduced slightly due to MF exposure. RBCs changed from 7.36 ± 0.24 to 7.78 ± 0.48, WBCs changed from 10.61 ± 0.72 to 10.28 ± 0.37.

[Cakir et al., 2009] has studied the hematological properties of blood in vivo experiments under the effect of extremely low frequency MF. Female wistar rats were divided into a control and two exposed groups (50 days and 100 days). Each group was irradiated with 0.97 mT for 3 hrs a day. Hb and eosinophil were decreased significantly for 50 days exposure in compare to control group. Body weight, lymphocyte, monocyte, leukocyte, neutrofil, and basophil, counts have not changed significantly. RBCs have reduced slightly under the effect for 50 days ($7.77 \pm 0.27 - 6.76 \pm 1.9$). Therefore, RBC has increased slightly after 100 days of exposure ($7.34 \pm 1.27 - 7.59 \pm 0.54$). WBCs reduced slightly for 50 and 100 days of exposure.

[Hashish et al.,2008] have studied the biological effect of whole body exposure of SMF (2.9 mT) and ELF-EMF (50 Hz) on mice at in vitro experiment. They designed two systems of exposure: one SMF and anther ELF-EMF. Mice were exposed with either field equally for 30 days. In some of the obtained results they showed that mice loss weights similarly under the effect of both exposure. Total protein reduced significantly. Blood parameters reduced similarly under the both fields: PLTs and monocytes counts, peripheral lymphocytes and T and B lymphocytes levels. They concluded that both fields produce physiological disturbances in mice. both fields altered blood parameters similarly. For example, WBCs changed from 4.87 ± 0.53 (control) to 4.47 ± 0.59 and 3.67 ± 0.45 under the effect of SMF and ELF-EMF respectively. Losing body weight may be due to MF or some other biological factors such as loosing body fluid or proteins.

A similar MF as [Chaterst al., 2006] and [Amara at al., 2006] was used by [Sihem et al., 2006] to study the biochemical and hematological parameter changes under the effect of SMF in rats. Rats were exposed directly at in vivo experiments with 128 mT for one hour per day during 10 days. Hb and HCT have risen in compare to control groups. RBCs, WBCs, PLTs increased significantly. $7.26 \pm 0.31(10^{12}/L)$ to 8.09 ± 0.58 $(10^{12}/L)$, 7.81 ± 0.73 $(10^{9}/L)$ to $9.12 \pm 0.91(10^{9}/L)$ and 536.10 ± 36.92 $(10^{9}/L)$ to $783.02 \pm 53.78(10^{9}/L)$ respectively. They believe that the change in Hb is related to magnetic force on RBCs.

[Wyszkowska et al., 2018] studied extremely low frequency time varying MF (7 mT and 50 Hz) effect on hematological parameters in vivo experiments. Groups of rats were exposed to MF for 1 hr/7 days and another group for 24 hrs. The 24 hrs exposure caused WBCs, lymphocytes, haematocrit and haemoglobin to increase. Therefore, one hr exposure for 7 days did not alter measured hematological parameters.

Decades ago, [Battocletti et a., 1981] exposed rhesus monkeys with 2 T of magnetic field. Monkeys with age one and half and two years were chosen. Animals divided into sub groups and irradiated for 63, and 67 hrs. Blood samples were taken before irradiation, after irradiation immediately and two weeks after irradiation. WBCs, neutrophils and lymphocytes changed considerable. Neutrophils increased two

Mustafa. B. *et al.* /ZJPAS: 2019, 31 (6): 40-50

45

folds for the exposed animals. Lymphocytes reduced to half and WBCs decreased by 50% due to exposure and increase after the exposure.

[Mohammed, 2017] has studied the effect of low SMF on biological properties of rats in vivo experiments. Each group of animal was irradiated for 2 hr/day and from 2 days to 7 days period in sequence. Erythrocytes were reduced from an insignificant to a significant from 2 days to 7 days of exposure respectively. The most significant changes was reported at 7 days of exposure, RBCs counts from 3.8 ± 0.07 to 3.0 ± 0.03.

[Strieth et al., 2008] performed an experiment on Syrian golden hamsters to examine the RBCs velocity flow in muscle capillaries during exposure of SMF. They showed that the short time of exposures with 150 mT reduces the RBCs velocity and segmental blood flow in tumor microvessels significantly.

Red blood cells are main cause of increasing blood viscosity. [Iino, 1997] studied the RBCs aggregations (called erythrocyte sedimentation rate- ESR) and sedimentations under the effect of static magnetic field. Blood was withdrawn from male healthy human. ESR enhanced slightly in a saline solution, and significantly in plasma under the effect of 6.3 T. Blood parameter responded MF 20 min from the exposure. The sedimentation has increased continuously in respect of time. Ht level reduced as ESR increased. They believe that the MF causes the cell orientation and thus Enhanced ESR.

0.2 mT time varying MF (50 Hz) was applied on albino rats to examine the RBCs variation [Ali et al., 2003]. Four groups of animal were prepared, A (Control), B (exposed for 15 days) and C (for 30 days) continuously. Group D rats were suicide after 45 days to study the effect of post exposure. Their result showed the elasticity of erythrocyte membrane and permeability decreased and, Hb structure and RBCs physiological structure changed. Irregular shape starting to grow up as time of exposure increases.

Time varying magnetic field effect on PLTs aggregation was studied [Sağdilek et al., 2012]. A 50 Hz - 1 mT and 6 mT was applied. Blood were collected from healthy human and exposed for 90 min and 120 min. Measurement was taken for control and exposed blood samples. Results show an increase of aggregation at 1 mT only. They concluded that the magnetic fields act as an activation of PLTs aggregation.

[Fasshauer et al., 2018 and Brand et al., 2015] examined the effect of MIR on DNA double strand break. They found no evidence where MRI causes DNA double strand break. [Selmaoui et al., 1996] studied the effect of time varying magnetic field (10 μT, 50 Hz) on blood parameters and blood immunity components. Humans were exposed to MF for 24 hrs, continuously. Their result shows no effect of low frequency magnetic field on blood immunity and functions.

Impact of homogeneous static magnetic fields on biological system has studied by [Milovanovich et al., 2016]. SMF has exposed on Male Swiss Webster mice with different orientation to see the effect of SMF at varies orientations. 128 mT was generated using cyclotron. Each group of animal has exposed for 5 days and each day for 1 hr. Results showed the obvious effect of SMF on some specific organs and blood parameters with different orientations rather than whole body. This depends on the field orientation to the same degree. The upward exposure of the field reduced counts of WBCs and serum lymphocytes. Inflammations increased in kidney. Granulocytes dropped down in spleen. However, the only downward exposure produced inflammation in liver and serum granulocytes dropped down.

RBCs and PLTs orientation has observed under 4 T and 3 T of magnetic fields [Yamagishi, 1990]. The degree of orientation increased in respect to MF. PLTs has fully oriented at 3mT. There is an insignificant difference between oxygenated and deoxygenated RBCs unless; both were saturated at 6T. Similar result was found theoretically by [Riberiro et al., 1981]. [Higashi et al., 997] also showed the cell orientation occur under the effect of high MF.

Table 1 summarizes the data collected from the reviewed literature of the effect of MF on rheological properties of blood in vivo and in vitro experiments. The effects are mainly connected to the main blood parameters such as RBCs, WBCs and PLTs, DNA strand break and blood viscosity. The outcome shows that certain intensities of MF can change the blood counts significantly, alter blood viscosity as well as enhance cell

Mustafa. B. *et al*. /ZJPAS: 2019, 31 (6): 40-50

46

orientations. There is no significant clue of the impact of MF on DNA strand break.

Table 1. literature works; effect of MF on blood rheological properties

Study reference	Sample type	Study parameter –field types	Effect
Amara et al., (2006)	Male wistar rats - in vivo	SMF 128 mT (1 hr/day) during 5 days)	WBC increased insignificantly RBC increased insignificantly PLT and HB increased insignificantly Ht increased insignificantly Water consumption increased Body weight increased
		SMF 128 mT (1 hr/day) during 30 days)	WBC increased by 17% RBC increased by 7% PLT and HB increased by 10% Ht increased Water consumption increased Body weight increased
Haik et al., 2001	Human blood - in vitro	SMF: 1 Tesla to 10 Tesla	Blood flow Time reduced continually Blood viscosity increased
Fasshauer et al., 2018	Human blood - in vivo	SMF: 3 T MRI source	No evidence of DNA double strand break.
Brand et al., 2015	Human blood - in vivo	SMF: 3 T MRI source	No evidence of DNA double strand break.
Selmaoui et al., 1996	Human blood - in vivo	ELF-MF (50 Hz, 10 μT)	No evidence of effect on blood components and blood immunity components.
Chater et al., 2006	Wistar Pregnant rats - in vivo	SMF (128 mT for 13 days)	WBC reduced slightly RBC increased slightly PLT increased slightly Hb increased slightly Ht increased considerably.
Strieth et al., 2008	Golden hamsters - in vivo	SMF (149 - 580 mT)	RBCs velocity reduced
Lino, 1997	Human blood - male - in vitro	SMF: 6.3 T	ESR and sedimentation increase as the function of time Htc reduced as a function of ESR.
Ali et al., 2003	Albino rats - in vivo	0.2 mT, 50 Hz	elasticity of erythrocyte membrane and permeability decreased RBCs irregularity increases
Sağdilek et al., 2012	Human blood- in vitro	1 mT and 6 mT for 1.5 and 2 hrs	Platelet aggregation increased
Yamamoto et al., 2004	Human blood- in vitro	1.5 T	Blood viscosity increased Shear rate changed
Milovanovich et al., 2016	Male Swiss Webster mice -	SMF: 128 mT - orientation effect	Upward exposure: WBCs counts and serum lymphocytes

Mustafa. B. *et al.* /ZJPAS: 2019, 31 (6): 40-50

47

	in vitro		reduced, Inflammations increased in kidney, PLTs counts reduced , Hb increased Downward exposure: produced inflammation in liver and serum granulocytes dropped , PLTs counts reduced, Hb increased
Baieth, 2008	Albino rats - in vivo	0.3 mT, 0.5 mT and 1 mT (50 Hz)	Viscosity reduced as magnetic field increased. Shear rate increased as magnetic field increased RBCs cunts and Ht increased under 0.3mT, 0.5 mT but decreased under 1 mT
Kenjereš, 2008	Mathematical model	10 T	Blood flow changed insignificantly
Marcinkowska, 2013	Human blood samples - in vitro	-------------------	Relative blood viscosity reduces as a function of applied magnetic field.
Mohaseb et al., 2017	Albino rats - in vivo	0.3 mT (50Hz).	Blood viscosity increased significantly after 21 and 45 days of exposure
Mohammed, 2017	Albino rats - in vivo	0.8 mT (50Hz)	RBCs reduced significantly Hemoglobin content reduced significantly
Kadhim et al., 2016	Human blood samples with polycythemia disease	1.5 T (1 min- 21min) SMF	Blood viscosity decreased as time of exposure increased.
Haik et al., 2001	Human blood: in-vitro	1-10 T	Blood flow decreased and viscosity increased by 30%
Okano and Ohkubo, 2001	Rabbits	1 mT (30 min) SMF	Vasodilatation reduced significantly Vasomotion enhanced Blood pressure reduced Vasoconstriction reduction in smooth muscle

4. CONCLUSIONS

Blood rheological properties were reviewed under the effect of MF. SMF and time

Mustafa. B. *et al.* /ZJPAS: 2019, 31 (6): 40-50

48

varying magnetic fields resulted impacts mainly on blood parameters, viscosity and blood flow. A few in vivo and in vitro research articles introduced no effect of low dosage MF on blood rheology. However, most of the published research articles revealed the side effect of MF at low, intermediate and high intensity of exposure. RBCs aggregation enhanced, red cell shapes altered as they tend to orient parallel to applied MF. No evident found where DNA strand break enhances under reviewed intensity of magnetic field. White and Red blood cells were found as accepting the highest responded blood parameters to MF. One research found an increase of 17% and 7% of WBCs and RBCs counts respectively as they exposed to a moderate MF. As blood behaves differently in response to applied MF, we believe that a continuous and sequence research is required to investigate the most effective exposure line of magnetic field on blood in vitro and in vivo worlds.

Conflict of Interest: The authors declared that they have no conflicts of interest.

References

Ali, E.A.M., 2018. Effect of 50 Hz, 0.85 mT Magnetic Fields on Some Biochemical Parameters. *Global Journal of Physics*, 7(1), pp.708-715.

Ali, F.M., S. Mohamed, W. and Mohamed, M.R., 2003. Effect of 50 Hz, 0.2 mT magnetic fields on RBC properties and heart functions of albino rats. *Bioelectromagnetics: Journal of the Bioelectromagnetics Society, The Society for Physical Regulation in Biology and Medicine, The European Bioelectromagnetics Association*, 24(8), pp.535-545.

Amara, S., Abdelmelek, H., Salem, M.B., Abidi, R. and Sakly, M., 2006. Effects of static magnetic field exposure on hematological and biochemical parameters in rats. *Brazilian Archives of biology and technology*, 49(6), pp.889-895.

Baieth, H.A., 2008. Physical parameters of blood as a non-Newtonian fluid. *International journal of biomedical science: IJBS*, 4(4), p.323.

Bansi, C.D.K., Tabi, C.B., Motsumi, T.G. and Mohamadou, A., 2018. Fractional blood flow in oscillatory arteries with thermal radiation and magnetic field effects. *Journal of Magnetism and Magnetic Materials*, 456, pp.38-45.

Battocletti, J.H., Salles-Cunha, S., Halbach, R.E., Nelson, J., Sances Jr, A. and Antonich, F.J., 1981. Exposure of rhesus monkeys to 20 000 G steady magnetic field: Effect on blood parameters. *Medical physics*, 8(1), pp.115-118.

Bäumler, H., Neu, B., Donath, E. and Kiesewetter, H., 1999. Basic phenomena of red blood cell rouleaux formation. *Biorheology*, 36(5, 6), pp.439-442.

Brand, M., Ellmann, S., Sommer, M., May, M.S., Eller, A., Wuest, W., Engert, C., Achenbach, S., Kuefner, M.A., Baeuerle, T. and Lell, M., 2015. Influence of cardiac MR imaging on DNA double-strand breaks in human blood lymphocytes. *Radiology*, 277(2), pp.406-412.

Cakir, D.U., Yokus, B., Akdag, M.Z., Sert, C. and Mete, N., 2009. Alterations of hematological variations in rats exposed to extremely low frequency magnetic fields (50 Hz). *Archives of medical research*, 40(5), pp.352-356.

Chadwick, P. and Lowes, F., 1998. Magnetic fields on British trains. *The Annals of occupational hygiene*, 42(5), pp.331-335.

Chater, S., Abdelmelek, H., Pequignot, J.M., Sakly, M. and Rhouma, K.B., 2006. Effects of sub-acute exposure to static magnetic field on hematologic and biochemical parameters in pregnant rats. *Electromagnetic biology and medicine*, 25(3), pp.135-144.

Dasdag, S., Sert, C., Akdag, Z. and Batun, S., 2002. Effects of extremely low frequency electromagnetic fields on hematologic and immunologic parameters in welders. *Archives of Medical Research*, 33(1), pp.29-32.

Elblbesy, M.A., 2014. Plasma viscosity and whole blood viscosity as diagnostic tools of blood abnormalities by using simple syringe method. *Medical Instrumentation*, 2(1), p.5.

Fasshauer, M., Krüwel, T., Zapf, A., Stahnke, V.C., Rave-Fränk, M., Staab, W., Sohns, J.M., Steinmetz, M., Unterberg-Buchwald, C., Schuster, A. and Ritter, C., 2018. Absence of DNA double-strand breaks in human peripheral blood mononuclear cells after 3 Tesla magnetic resonance imaging assessed by γH2AX flow cytometry. *European radiology*, 28(3), pp.1149-1156.

Gmitrov, J., Ohkubo, C. and Okano, H., 2002. Effect of 0.25 T static magnetic field on microcirculation in rabbits. *Bioelectromagnetics*, 23(3), pp.224-229.

Haik, Y., Pai, V. and Chen, C.J., 2001. Apparent viscosity of human blood in a high static magnetic field. *Journal of Magnetism and Magnetic Materials*, 225(1-2), pp.180-186.

Halgamuge, M.N., Abeyrathne, C.D. and Mendis, P., 2010. Measurement and analysis of electromagnetic fields from trams, trains and hybrid cars. *Radiation protection dosimetry*, 141(3), pp.255-268.

Mustafa. B. *et al.* /ZJPAS: 2019, 31 (6): 40-50

49

Hashish, A.H., El-Missiry, M.A., Abdelkader, H.I. and Abou-Saleh, R.H., 2008. Assessment of biological changes of continuous whole body exposure to static magnetic field and extremely low frequency electromagnetic fields in mice. *Ecotoxicology and environmental safety*, *71*(3), pp.895-902.

Higashi, T., Ashida, N. and Takeuchi, T., 1997. Orientation of blood cells in static magnetic field. *Physica B: Condensed Matter*, *237*, pp.616-620.

Ichioka, S., Iwasaka, M., Shibata, M., Harii, K., Kamiya, A. and Ueno, S., 1998. Biological effects of static magnetic fields on the microcirculatory blood flowin vivo: a preliminary report. *Medical and Biological Engineering and Computing*, *36*(1), pp.91-95.

Ichioka, S., Minegishi, M., Iwasaka, M., Shibata, M., Nakatsuka, T., Harii, K., Kamiya, A. and Ueno, S., 2000. High-intensity static magnetic fields modulate skin microcirculation and temperature in vivo. *Bioelectromagnetics: Journal of the Bioelectromagnetics Society, The Society for Physical Regulation in Biology and Medicine, The European Bioelectromagnetics Association*, *21*(3), pp.183-188.

Iino, M., 1997. Effects of a homogeneous magnetic field on erythrocyte sedimentation and aggregation. *Bioelectromagnetics: Journal of the Bioelectromagnetics Society, The Society for Physical Regulation in Biology and Medicine, The European Bioelectromagnetics Association*, *18*(3), pp.215-222.

Ismail, A.H., 2015. Influence of Radiation Doses on the Ratio of Blast Cells, Lymphocytes and Neutrophils inside Blood Samples of Leukaemia Patients: In vitro. *ZANCO Journal of Pure and Applied Sciences*, 27(3), pp.65-74.

Kadhim, A.A., Seah, B.T. and Zubair, A.M., 2016. Influence of magnetic field on blood viscosity. *Advances in Environmental Biology*, *10*(1), pp.107-111.

Keating, F.K., Butenas, S., Fung, M.K. and Schneider, D.J., 2011. Platelet-white blood cell (WBC) interaction, WBC apoptosis, and procoagulant activity in stored red blood cells. *Transfusion*, *51*(5), pp.1086-1095.

Keating, F.K., Fung, M.K. and Schneider, D.J., 2008. Induction of platelet white blood cell (WBC) aggregate formation by platelets and WBCs in red blood cell units. *Transfusion*, *48*(6), pp.1099-1105.

Kenjereš, S., 2008. Numerical analysis of blood flow in realistic arteries subjected to strong non-uniform magnetic fields. *International Journal of Heat and Fluid Flow*, *29*(3), pp.752-764

Kizilova, N., Batyuk, L. and Baranets, V., 2018, September. Human Red Blood Cell Properties and Sedimentation Rate: A Biomechanical Study.

In *The International Conference of the Polish Society of Biomechanics* (pp. 3-22). Springer, Cham.

Lim, H.J., Nam, J.H., Lee, Y.J. and Shin, S., 2009. Measurement of the temperature-dependent threshold shear-stress of red blood cell aggregation. *Review of scientific instruments*, *80*(9), p.096101.

Marcinkowska-Gapinska, A. and Nawrocka-Bogusz, H., 2013. Analysis of the magnetic field influence on the rheological properties of healthy persons blood. *BioMed research international*, *2013*.

McCann, J., Dietrich, F. and Rafferty, C., 1998. The genotoxic potential of electric and magnetic fields: an update. *Mutation Research/Reviews in Mutation Research*, *411*(1), pp.45-86.

Milovanovich, I.D., Ćirković, S., De Luka, S.R., Djordjevich, D.M., Ilić, A.Ž., Popović, T., Arsić, A., Obradović, D.D., Oprić, D., Ristić-Djurović, J.L. and Trbovich, A.M., 2016. Homogeneous static magnetic field of different orientation induces biological changes in subacutely exposed mice. *Environmental Science and Pollution Research*, *23*(2), pp.1584-1597.

Mohammed, A., 2017. Effect of 50 Hz, 0.85 mT Magnetic Fields on hematological Parameters. *Journal of scientific and engineering research*, *4*(2), pp.85-92.

Mohaseb, M.A., Shahin, F.A., Ali, F.M. and Baieth, H.A., 2017, June. Effect of electromagnetic fields on some biomechanical and biochemical properties of rat's blood. In *Journal of Physics: Conference Series* (Vol. 869, No. 1, p. 012059). IOP Publishing.

Maulood, I.M. and Mahmud, A.M., 2016. Effects of Potassium and Magnesium on Some Hematological Profiles in Two Kidney, One Clip-Hypertensive and Normotensive Rats. *ZANCO Journal of Pure and Applied Sciences*, 28(5), pp.19-32.

Maulood, K.A., 2018. Assessment of some hematological, biochemical parameters and cardiac biomarker levels in patients with ischemic heart disease in Erbil city. *ZANCO Journal of Pure and Applied Sciences*, 30(2), pp.86-93.

Okano, H. and Ohkubo, C., 2001. Modulatory effects of static magnetic fields on blood pressure in rabbits. *Bioelectromagnetics: Journal of the Bioelectromagnetics Society, The Society for Physical Regulation in Biology and Medicine, The European Bioelectromagnetics Association*, *22*(6), pp.408-418.

Qader, V.A. and Hawezy, H.J.S., 2019. Effect of occupational exposure to chemicals on some biochemical parameters. *ZANCO Journal of Pure and Applied Sciences,* 31(1), pp.40-45.

Mustafa. B. *et al.* /ZJPAS: 2019, 31 (6): 40-50

50

Rampling, M.W., Meiselman, H.J., Neu, B. and Baskurt, O.K., 2004. Influence of cell-specific factors on red blood cell aggregation. *Biorheology*, *41*(2), pp.91-112.

Riberiro, P.C., Davidovich, M.A., Wajnberg, E., Bemski, G. and Kischinevsky, M., 1981. Rotation of sickle cells in homogeneous magnetic fields. *Biophysical journal*, *36*(2), pp.443-447.

Sağdilek, E., Sebik, O. and Çelebi, G., 2012. Investigation of the effects of 50 Hz magnetic fields on platelet aggregation using a modified aggregometer. *Electromagnetic biology and medicine*, *31*(4), pp.382-393.

Salem, A., Hafedh, A., Rached, A., Mohsen, S. and Khémais, B.R., 2005. Zinc prevents hematological and biochemical alterations induced by static magnetic field in rats. *Pharmacol Rep*, *57*(5), pp.616-22.

Schuhfried, O., Vacariu, G., Rochowanski, H., Serek, M. and Fialka-Moser, V., 2005. The effects of low-dosed and high-dosed low-frequency electromagnetic fields on microcirculation and skin temperature in healthy subjects. *International journal of sports medicine*, *26*(10), pp.886-890.

Selmaoui, B., Bogdan, A., Auzeby, A., Lambrozo, J. and Touitou, Y., 1996. Acute exposure to 50 Hz magnetic field does not affect hematologic or immunologic functions in healthy young men: a circadian study. *Bioelectromagnetics: Journal of the Bioelectromagnetics Society, The Society for Physical Regulation in Biology and Medicine, The European Bioelectromagnetics Association*, *17*(5), pp.364-372.

Sihem, C., Hafedh, A., Mohsen, S., Marc, P.J. and Khmais, B.R., 2006. Effects of sub-acute exposure to magnetic field on blood hematological and biochemical parameters in female rats. *Turk J Hematol*, *23*, pp.182-187.

Strieth, S., Strelczyk, D., Eichhorn, M.E., Dellian, M., Luedemann, S., Griebel, J., Bellemann, M., Berghaus, A. and Brix, G., 2008. Static magnetic fields induce blood flow decrease and platelet adherence in tumor microvessels. *Cancer biology & therapy*, *7*(6), pp.814-819.

Ueno, S., Lövsund, P. and Öberg, P.Å., 1986. Effects of alternating magnetic fields and low-frequency electric currents on human skin blood flow. *Medical and Biological Engineering and Computing*, *24*(1), pp.57-61.

Vergallo, C. and Dini, L., 2018. Comparative Analysis of Biological Effects Induced on Different Cell Types by Magnetic Fields with Magnetic Flux Densities in the Range of 1–60 mT and Frequencies up to 50 Hz. *Sustainability*, *10*(8), p.2776.

Wyszkowska, J., Jędrzejewski, T., Piotrowski, J., Wojciechowska, A., Stankiewicz, M. and Kozak, W., 2018. Evaluation of the influence of in vivo exposure to extremely low-frequency magnetic fields on the plasma levels of pro-inflammatory cytokines in rats. *International journal of radiation biology*, *94*(10), pp.909-917.

Xu, S., Okano, H. and Ohkubo, C., 2001. Acute effects of whole-body exposure to static magnetic fields and 50-Hz electromagnetic fields on muscle microcirculation in anesthetized mice. *Bioelectrochemistry*, *53*(1), pp.127-135.

Yamagishi, A., 1990. Biological systems in high magnetic field. *Journal of Magnetism and Magnetic Materials*, *90*, pp.43-46.

Yamamoto, T., Nagayama, Y. And Tamura, M., 2004. A blood-oxygenation-dependent increase in blood viscosity due to a static magnetic field. *Physics in Medicine & Biology*, *49*(14), p.3267.

Ye, T., Phan-Thien, N. and Lim, C.T., 2016. Particle-based simulations of red blood cells—A review. *Journal of biomechanics*, *49*(11), pp.2255-2266.

Zaghloul, M.S., 2011. Effects of Chronic Exposure to Static Electromagneti c Field on Certain Histological Aspects of the Spleen and Some Haematological Parameters in Albino Rats. *Journal of American Science*, *7*(8).

RESEARCH PAPER

Sustainability of Aquifer and Ground Water Condition in Erbil Basin/ Iraq

Dana Khider Mawlood

Department of Civil Engineering, College of Engineering, Salahaddin University-Erbil, Kurdistan Region, Iraq.

A B S T R A C T:

Groundwater is the main source of water in Erbil province, Iraq. The change in climate and the rapid development in the city, generally, increases the rate of GW depletion. The study aims to investigate the effects of the current exploitation of groundwater on the sustainability of the aquifer. Data like climate, soil, number of wells, and the hydrogeology of Erbil aquifer are compiled to recognize the current and future conditions of the aquifer. The results show that there is an irresponsible use of GW. The water table has been found to decrease around 1.24 meters annually. This comes due to excessive use, lack of awareness and absence of clear and strict policy towards GW sustainability in the region. The challenges facing the Department of Groundwater Resources, which is responsible for managing and developing GW sources are indicated. A set of recommendations are then presented for improving the GW management and sustainability.

INTRODUCTION:

The availability of groundwater is a major reason for its use as a vital source of water supply worldwide. Groundwater provided a low-cost water source available with a good considerable quality that requires less treatment. It is one of the most valuable renewable resources. Groundwater (GW) is being used for drinking water supply increasingly around the world (Zhou, 2009). The fresh water represents only 3% of all of Earth's water and 68.7% of the fresh water is stored in glaciers and icecaps while GW represents only 30.1%. surface water is 0.3%, and 0.9% is in other minor storage (Council, 2001). The continuous discharge of industrial wastewater, pesticides and the use of domestic sewage as fertilizers, waste dump and overexploitation of resource have an extremely negative impact on groundwater sustainability (Harter, 2003).

Groundwater sustainability is the development and use of groundwater in a manner that can be maintained for an infinite time without causing unacceptable environmental, economic, or social consequences (Alley et al., 1999). Depletion of the small part of the total volume of GW in storage can have a huge effect on surface water, water quality, or subsidence which can be a factor that limits development.

Although groundwater is mentioned as a renewable resource, it does not recycle rapidly. The recycling process of GW depends on the aquifer's characteristics like type, depth, connectivity, and location. Generally, the shallow GW renewal rate is around 15% less than the deep GW (Jones, 2014). The demand for freshwater increase day by day, majorly for irrigation purposes, and that rise in demand and the decreasing availability of water burden GW reservoirs and this ultimately deplete the GW quantity and quality. Overutilization, contamination and presumption contamination considered as the key factors for GW depletion. There are many examples of GW depletion, but the classic case is that the water levels in Borrego Valley, southern California, San Diego country

Mawlood. D /ZJPAS: 2019, 31 (6): 51-60

52

declined 0.6 meters per year (2 feet per year) in the past two decades where the extracted water was used for intensive agriculture along with irrigation (Ponce, 2006).

The loss of base flow is the most important impact of GW depletion. When the base flow decreases, there are many negative impacts occur. It causes a severe crisis of safe drinking and irrigated water, and other impacts are (Mitra, 2015):

- Increased flood's frequency and magnitude
- Loss of wetland and riparian plants
- Accelerate the erosion
- Changes in channel morphology
- Increase the drought frequency
- biodiversity Losses
- drying up of wells
- increase the cost well infrastructure and the cost of pumping
- intrusion of salt-water
- climate change etc.

There will always be tradeoffs between the use of groundwater and possible environmental influences, thus, a balanced approach to water utilization between environmental and developmental requirements must be supported. Understanding recharge is vital for managing most of GW systems. Managers need accurate data and information about the recharge (inputs) and the natural discharge and pumping (outputs) within each basin in order to manage the resource of GW properly. It is essential to estimate the recharge (inputs) in any groundwater systems analysis and the impact of water extraction (Mawlood et al., 2017). Without a good recharge estimation, the GW extraction impact cannot be assessed properly, and will also affect the estimation reliability of long-term behavior of an aquifer. Also, the accurate estimates of inputs and outputs are very important to assess GW contamination, mainly the diffuse agricultural contamination (such as pesticides and nitrates) (Sophocleous, 2005).

Groundwater is the main source of water in Erbil city, Iraq. However, this source is under the risk of depletion due to the major developments that have taken place over the past two decades at all levels in the city. The rapid developments, population growth,

industrialization, urbanization, and agriculture activities, in addition to that, Erbil province has welcomed around one million displaced people who have refugee to the city because of the wars that took place in 2014 and still going until today. In order to increase the aquifers efficiency and maintaining faster GW recharging, the Kurdish Government forbade drilling wells by pile equipment on 22nd of August 2010, there are still some illegal drillings that occur here and there (Majeed and Ahmad, 2002). All that increase the consumption and exploitation, reduce the availability and increases the contamination vulnerability of groundwater in the city.

In Erbil, GW facing the risk of Contamination by the disposal of industrial and urban wastes and agricultural chemicals. The disposal of wastewater in septic tanks, including human wastes, is a common practice in the urban areas in the city. In some parts of the city, the concentrations of the nitrate and alkalis are exceeding the Iraqi and WHO standards (Wali and Alwan, 2016). Groundwater sustainability represents a major problem in the region. However, there are very limited studies that consider water management and GW sustainability in Erbil (Mawlood et al., 2016).

This paper aims to investigate the approximate amount of GW discharge and estimate the annual recharge (Precipitation) over each sub-basin in Erbil. Calculate the change in the water table (decrease) of groundwater resulting due to exploitation and the change in the water table (increase) due to recharge considering the specific yield of the soils as well as to investigates the effects of the current exploitation of groundwater on the sustainability of the aquifer.

2. LITREATURE REVIEW

Wali and Alwan (2016) studied the quality of Groundwater through assessing vulnerability of aquifer to Contamination in the city of Erbil, Iraq. They aimed to evaluate the most vulnerable areas that are vulnerable to the exploitation and overall pollution due to the geological characteristics and other human factors. They attempt to create a map for groundwater vulnerability for the city through evaluating the vulnerability and discovering groundwater vulnerable zones to pollution of Erbil's aquifer. They used DRASTIC method within GIS environment to provide spatial examination of the conditions and parameters

Mawlood. D /ZJPAS: 2019, 31 (6): 51-60

53

under which groundwater may be polluted. Their results showed that most of the study areas have a moderate vulnerability level for contamination which can affect GW sustainability in the future.

Shi et al. (2012) from China, studied the Sustainable utilization and development of GW resources considering land subsidence. The city of Suzhou, as one of China's most developed regions, suffered severe land subsidence due to the extensive use of GW since the 1980s. They took this case to study the possibility of controlling land subsidence while developing the GW resources to satisfy the growing demands of water supply. The authorities banned GW exploration for several years in an attempt to control land subsidence. So, the researchers analyzed the relationship between GW levels and land deformation focusing on the deformation features after the ban period. They developed a 1-D deformation model and 3-D groundwater model to simulate GW levels and its deformation.

In his paper, Dizayee (2014), studied the Degradation and Sustainability of the groundwater in Erbil Province. He mentioned that there is uncertainty about the sustainable use of the groundwater in Erbil Basin and the stages of its development are poorly understood. This study identifies the importance of water sustainability by showing the rates of over-exploitation and the shortage of groundwater recharge supply through describing the hydrological conditions of the basin. To understand the condition of the basin, the researcher compiled the data about the aquifer's hydrogeology, soil, wells, and climate. The researcher used cross sections and subsurface mapping across the basin to determine the nature of hydrologic units, fluctuations of GW levels and the GW flow, also described the geometry, lithology, water level and thickness of the aquifer system of the basin. His results show unsustainable usage of GW of Erbil basin.

Qureshi et al. (2010) studied the prospects and the challenges of the sustainable management of groundwater in Pakistan. The researchers mentioned that in Pakistan, many direct and indirect strategies for managing the groundwater has been applied over the last four decades but these management strategies showed limited success. To solve the problems of the dropping of water tables, overdraft and degradation in GW quality they argued what they called, techno-

institutional approaches and the researchers also developed management tools and frameworks that work for the needs of Pakistan and mentioned that the demand and supply management approaches should be applied in the country, also noted several important points to be taken regarding demand and supply management as the use of alternate water resources should, revision of the patterns of the existing implants, adoption of new technologies for water preservation. The researchers highly recommended to adhere to instructions and the regulatory frameworks established by the local authorities and to improve coordination between the organizations that are responsible for GW resources management.

Zhou (2009) in his paper titled 'A critical review of groundwater budget myth, safe yield, and sustainability'. He mentioned the controversy caused by the application of water balance principle and the debate about the use of the equation of water balance to determine the sustainable yield and safe yield. Zhou used the water balance equation to clarify the controversy about water budget and to critically analyze sustainable yield and safe yield concepts. Also used a hypothetical numerical simulation to reveal the natural balance of the groundwater, the dynamic development, and influences of pumping on the capture. He concluded that natural recharge cannot determine the social, economic impact made by the dynamic development of the capture and cannot determine the safety yield. Also concluded that the concept of sustainability emphasizes more the maintenance of the social and the natural environment benefits. To simulate the impacts of groundwater development scenarios, Zhou represents that the groundwater numerical model is the best available tool to be used.

Gupta and Babel (2005) from Thailand studied the groundwater sustainable management challenges. They identified the impact of unplanned utilization of GW in their country and the long-term related consequences. They gathered the needed data from several related studies to assess and understand the multi-aquifer system for different pumping and storage conditions. They also put guidelines on operating this system in order to improve the existing condition. They pointed out the important role of the concerned authorities (the department of

Mawlood. D /ZJPAS: 2019, 31 (6): 51-60

54

groundwater resources) and how they must improve their performance and activities in the evaluation of the resources, effective planning, and management to reduce the risk of GW exhaustion and to move toward more sustainable GW utilization.

Sophocleous (2005) presented a paper studying the sustainability of GW recharge in Kansan, the united states of America. The researcher studied the characteristics of Kansas aquifer and estimated the approximate amounts of recharge and discharge in the area aiming to determine the aquifer's long-term behavior and reassess its sustainable yield, and to do so, he depends on previous studies regarding GW in the region at different scales. The results showed a severe imbalance between the recharge and discharge amounts. This was due to the excessive cultivation and irrigation which exceed the amounts precipitation as the predominant recharge source in many cases. However, to stabilize the system, the researcher pointed out the importance of reducing water use, using more efficient irrigation techniques and adopting more sustainable practices like water-saving land-use for instance. Moreover, he determined several necessary steps for more sustainable use of GW, which includes, improving the knowledge base and the public awareness; adopting more effective ecosystem management approaches for managing GW; effective reporting and providing easy information access and adopting a long-term sustainable use goal.

Kinzelbach et al. (2003) studied the problems related to the sustainable groundwater management and the use of some scientific tools. They discussed GW modeling, methods for GW recharge quantification, and the interfacing to the field of socio-economic. They concluded that water management can be highly improved using new available tools including differential GPS, automatic data collection, remote sensing, digital terrain models, modeling and the coupling of models from different disciplines.

3. INFORMATION and METHODS
3.1 STUDY AREA

Erbil province is the capital of Kurdistan region in the northern part of Iraq and covers an area of 15,074 km^2 which represent 3.5% of the total area of Iraq with a population of 2,113,391 people. It is one of the most important agricultural provinces in Iraq. It is the fourth largest province in Iraq after Baghdad (the Iraqi capital), Basra, and Mosul (Ninawa). It is bounded by Ninawa to the west, Salah al-Din to the southwest, Kirkuk to the south, Duhok to the northwest and Al-Sulaymaniyah to the east see Figure 1. The central town is Erbil city where over the half of the governorate's population lives in (NCCI, 2015).

Groundwater is the main source of agriculture, irrigation and drinking water in Erbil for the surface water is mostly unsuitable for human consumption due to various reasons. Drilled wells are used to extract the groundwater since its available all over the district. Thus, the groundwater has a vital role in all life aspects in the city. Groundwater contamination and sustainability represents a major problem in the region. However, there are limited studies investigate water management and groundwater sustainability in Erbil.

Figure (1): Location Maps of The Study Area.

3.2 ERBIL BASIN

Erbil Basin or Dashty Hawler Basin is the groundwater reservoir in Erbil Province, it covers an area of approximately 3,200 km^2 and an approximate depth of 800 meters. As determined by Ahmed (2009), Erbil basin considered as one of the most important basins in the region for its water quality, quantity and its proximity to the surface. It has an unconfined aquifer, this means that the precipitation infiltrates into the aquifer directly, but some parts in the area of study, the aquifer becomes semi-confined or confined because of some thick clay layers. In general, the Erbil Basin is divided into three sub-basins, the first one is the Northern sub-basin named Kapran, the second one is the Central sub-basin, and the third sub-basin is the Southern one named Bashtapa, as shown Figure 2 (Habib et al., 1990, Majeed and Ahmad, 2002).
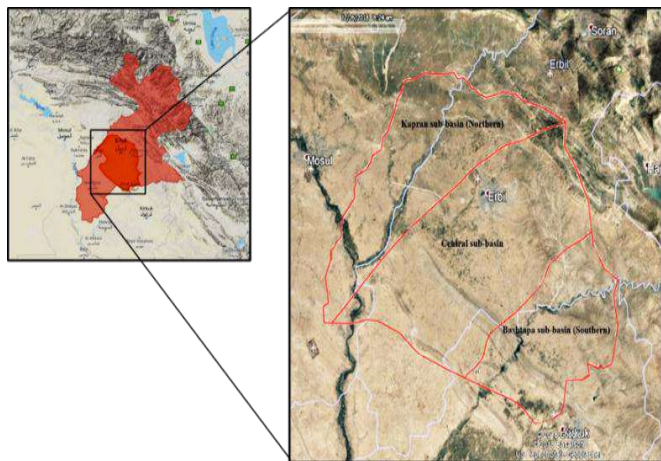
Mawlood. D /ZJPAS: 2019, 31 (6): 51-60

55

Figure (2): Erbil Basin Map

3.2.1 Kapran Sub-Basin (Northern)

As determined by Majeed and Ahmad (2002), the northern sub-basin covers an area of 915 km^2. According to records from deep wells, the geographical formations in this sub-basin consists of gravel, coarse and medium-grained sand, silt, conglomerate, and clay beds. The data shows that the specific yield of this layer is approximately equaled 0.26. The Ministry of Agriculture and Water Resources adopted a study made by the Al-Furat Centre. This study mentioned that the number of wells drilled must not exceed 225 wells in the whole sub-basin. Though, the results showed that there are 2554 wells drilled in this sub-basin.

3.2.2 Central Sub-Basin

Majeed and Ahmad (2002), mentioned that the central sub-basin covers an area of 1400 km^2. According to records, the geographical formations in this sub-basin consists of gravel, coarse sand, clay, and conglomerate strata. The data shows that the specific yield of this layer is approximately equaled 0.244. Most of the wells drilled in this basin are for agricultural purposes. Al-Furat Centre's study mentioned that the number of wells drilled must not exceed 738 wells in this sub-basin, but the actual number found of wells drilled in this area was 4257 wells.

3.2.3 Bashtapa Sub-Basin (Southern)

According to Majeed and Ahmad (2002), this sub-basin covers an area of 885 km^2. According to records, the geographical formations in this sub-basin consists of coarse and medium-grained sand, clay, with some silt or silty clay. The data shows that the specific yield of this layer is approximately equaled 0.225. Al-Furat Centre's study determined that 500 is the optimum number of wells allowed, but they found that there are 583 wells drilled in this area, this exceeds the optimum number by 83 wells.

3.3 RAINFALL

Rainfall considered as one of the most important climate phenomena, and It can change within a very short time period (Dizayee, 2014). The average annual rainfall varies from season to other and from year to other due to various factors and different climate conditions. Hameed (2013) described Erbil climate and its rainfall Condition as shown in Figure 3. Erbil Province climate, generally, varies between the steppes and the Mediterranean climate regions. Mostly, the wet season begins in the month of October and ends in May, while the dry season begins from the month of June to September. The average annual rainfall is around 590 (mm/year) as determined by Hameed (2013). As shown in the Figure below, the amount of precipitation decreases from the northeast toward the southwest of Erbil Province, this denotes that the northeastern parts take more precipitation quantities than the southwestern parts of the city. The quantity of rainfall varies from 200 (mm/year) in the southwestern parts to 1,200 (mm/year) in the northeastern parts, with around 700 (mm/year) of annual average rain (Dizayee, 2014, Hameed, 2013). According to the Erbil governorate profile (NCCI, 2015) and to a global climate statistics website (Climate-Data.Org, 2018), around 543 (mm/year) of average annual rainfall occurs in Erbil city, while another website mentioned that 437 (mm/year) is the annual average precipitation (meteoblue-weather, 2018). However, Zakaria (2012) mentioned that to grow an economical crop, the

Mawlood. D /ZJPAS: 2019, 31 (6): 51-60

56

amount of the average annual rainfall must not be less than 300 (mm/year). In this study the precipitation data presented by Hameed (2013) was taken into consideration, the researcher took the least average annual rainfall in the area of study. it is essential to study and analyze the data regarding the critical situation. Thus, the average annual rainfall will be 420, 400, and 390 (mm/year) over the northern, central and southern sub-basin respectively.
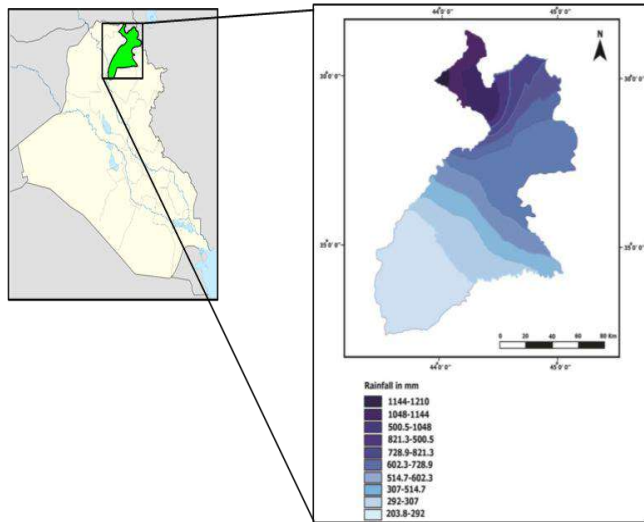

Figure (3): Spatial distribution of average annual rainfall in Erbil, Hameed (2013)

3.4 SOILS

Soils in Erbil Province varies in depth due to its unique geographical location. Soils depth is different from the northeastern parts, where the mountainous region lies, to southwestern parts, where the valley and plain lands of Erbil. By looking at Figure 4, the area of study (i.e. Erbil basin) lies under zone 3, 4 and 5. Zone 3 represents a brown soil with shallow and medium phase over a layer of gravel, lime-rich non-gravel and silt loam layers, same as zone 4 but it has gravel silt-clay layers with surface cracks under the brown soil layer. The area represented by zone 5 contains a lithocholic soils with sands and gypsum soils, varies from moderate to shallow depth over lime-rich silt-loam and gravelly to very gravelly varied layers (Hameed, 2013).
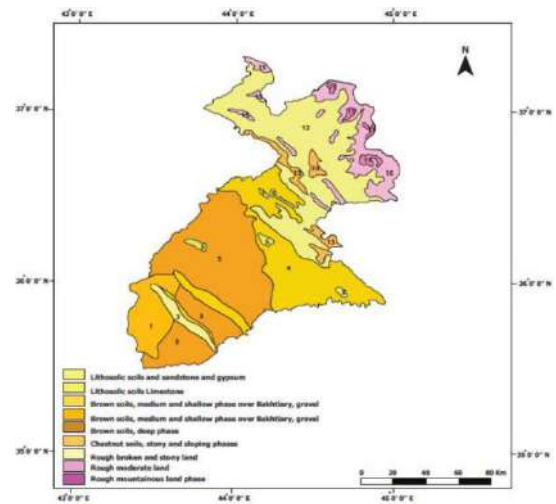
Figure (4): Erbil Province soil types, Hameed (2013)

3.5 RECHARGE and RENEWABLE of GW ACCORDING to the SPECIFIC YIELD of AQUIFER

The specific yield is known as the ratio of the water volume that a saturated soil or rock will yield by gravity to the total volume of the soil or rock. In order to estimate the available water supply during a period of recharge, the specific yield (Sy) of soil or rock materials must be determined. SY is usually expressed as a percentage and these values have been estimated, as shown in table (1), for the different types of soil materials that fill the fresh GW producing basins.

Table 1: Values of specific yield, Johnson (1967)

Soil	Specific Yield
Gravel	0.15 – 0.35
Coarse-grained sand	0.20 – 0.35
Medium-grained sand	0.15 – 0.30
Fine-grained sand	0.10 – 0.25
Silt	0.03 – 0.20
Clay	0.00 – 0.05

By having the values of the specific yield of each sub-basin of Erbil aquifer, which is 0.260 for the northern one, 0.244 for the central, and 0.225 for the southern sub-basin, the change in water table Δh due both recharge and discharge will be calculated accordingly as explained in the following derivation:

Specific yield, $Sy = (V\ drain)/(V\ total)$ .... (Eq. 1)

While: $V\ total = A * \Delta h$ .... (Eq. 2)

Mawlood. D /ZJPAS: 2019, 31 (6): 51-60

57

Where:

A is the recharge surface area, to be taken as the aquifer's geographical area.

Δh is the change in head (water table) due to discharge.

So: $Sy = (V\ drain)/(A * \Delta h)$ .... (Eq. 3)

For the change in water levels due to recharge, the specific yield equation will be as follow:

$Sy = (V\ added)/(A * \Delta h)$ .... (Eq. 4)

In this case, the volume of water added will represent the volume of precipitation on that area, and Δh will represent the rise of the water table due to the added water. So, the recharge R can be determined by the volume of the added water divided by the area of aquifer.

$R = (V\ added)/(A)$ .... (Eq. 5)

By substituting Eq.5 in Eq.4, the specific yield equation will be as follow:

$Sy = R/(\Delta h\ rise)$ .... (Eq. 6)

So: $\Delta h\ rise = R/(Sy)$ .... (Eq. 7)

From (Eq. 3), Δh, the change in head (water table) due to discharge can be calculated as:

$\Delta h\ drain = (V\ drain)/(A * Sy)$ .... (Eq. 8)

4. RESULTS and DISCUSSION

The data collected about Erbil basin, shown in table (2), giving the area, recharge, discharge and the specific yield for each sub-basin. It can be noticed that the central sub-basin covers the largest area with around 1400 km^2. On the other hand, it can be mentioned that the difference in the area covered by Kapran and Bashtapa sub-basin is very small compared to the recorded discharge in both sub-basins. This difference is related to the population distribution

and the number of wells drilled in each one of them.

Table 2: The Data Collected for Each Sub-Basin

sub-basin	Area (Km^2)	Recharge (mm/year)	Discharge (m^3/min)	Specific Yield (Sy)
Kapran sub-basin (Northern)	915	420	1250	0.260
Central sub-basin	1400	400	1450	0.244
Bashtapa sub-basin (Southern)	885	390	250	0.225

By performing (Eq. 7), the results of the change in the head (Δh) due to recharge are shown in the following table:

Table 3: The Change in Head (Δh) due to Recharge

sub-basin	Sy	R (m/year)	Δh (m)
Kapran sub-basin (Northern)	0.26	0.42	1.62
Central sub-basin	0.244	0.4	1.64
Bashtapa sub-basin (Southern)	0.225	0.39	1.73
		sum	4.99
		average	1.66

From table (3), the increase in the head (water table) for the northern and the central sub-basin are almost the same with 1.62 and 1.64 meters per year respectively, this is because the data gathered about both sub-basins show that they have almost the same soil characteristics and precipitation amounts. On the other hand, the water table in the southern sub-basin (Bashtapa) increases around 1.73 meters annually. The average increase in the water table in Erbil basin is around 1.66 meters annually.

By performing (Eq. 8), the results of the change in the head (Δh) due to discharge are shown in the following table:

Table 4: The Change in Head (Δh) due to Discharge

sub-basin	Sy	Area Meters*10^6 (m^2)	Discharge*10^6 (m^3/ year)	Δh (m)
Kapran sub-basin (Northern)	0.26	915	657	2.76
Central sub-basin	0.244	1400	762.12	2.23

Mawlood. D /ZJPAS: 2019, 31 (6): 51-60

58

Bashtapa sub-basin (Southern)	0.225	885	131.4	0.66
			Sum	5.65
			Average	1.9

From table (4) above, the results show that the decrease in the head (water table) for the northern sub-basin (Kapran) is around 2.76 meters annually while the central sub-basin records a drop of 2.23 meters per year. Bashtapa sub-basin has the lowest change with around 0.66 meters. The average decrease in the water table due water extraction is around 1.9 meters annually. These results depend on the parameters of (Eq. 8) which are the specific yield, area, and discharge. Although the central sub-basin has the largest rate of discharge yet is comes after Kapran sub-basin in term of the fall of the water table, this is mainly related to the large area that is covered by the central sub-basin.

The difference in the change of head (Δh) between the discharge and recharge for each Sub-basin is shown in the following table:

Table5: The Difference in Change of Head

sub-basin	Δh due Discharge (m)	Δh due Recharge (m)	$\Delta h_D - \Delta h_R$
Kapran sub-basin (Northern)	2.76	1.62	1.14
Central sub-basin	2.23	1.64	0.59
Bashtapa sub-basin (Southern)	0.66	1.73	-1.07
		Total	0.66
		average	0.22

This result given above lights the red alarm. It indicates an overall decrease in the water table in Erbil basin. The northern sub-basin shows a loss of water table with around 1.14 meters annually while the central one with around 0.59 meters per year. Only the southern sub-basin shows an opposite result, it increases with around one meter per year. These results are related to the number of wells drilled in each part, the overall agricultural activities, population distribution, etc. However, the overall decline in GW levels is around 0.22 meters per annum, which is alarming the risk of drought in the long term.

These results comes as a proof of the concernes mentioned by Dizayee in his study in 2014 as he warned of the danger of GW depletion due to lack of GW management as well as the increasing in the number of drilled wells relative to the total area of Erbil.

However, there are several points must be taken into consideration to pass disasters due to the expected depletion of the GW sources:

- Manage aquifer recharge

- Use of recycled or reclaimed water

- Conjunctive use of GW and surface water

- Set GW resource objectives and forecast water demand

- Incorporate the hydrologic cycle and natural processes in GW management

- Reassess GW management on a regular basis.

- Reduce water loss in storing and delivering GW

- Work toward laws, regulations, and incentives that encourage the sustainable use of GW.

- Raise awareness about maintaining GW as a reserve

- Monitoring water use and water levels are key components

- Recognition of managed aquifer recharge as a critical component

- Increase the funding for cooperative GW quantity data collection is the most useful action the government authorities can take, according to the GW professionals around the country.

- the government must support the cooperative data collection of water quality, aquifer mapping, and pertinent scientific research is also important

- Implement source water protection and remediation for private and public GW uses.

Mawlood. D /ZJPAS: 2019, 31 (6): 51-60

59

- Adjust codes, laws, and practices for cost-effective provision of safe sustainable water

- Using modern methods for water extracting and wells maintenance like using Use modern pumps, providing regular well maintenance and pumping equipment and the use of CO_2 cleaning technology which include pumping liquid carbon dioxide into the well that cleans the well and provide consistent well yield, improve efficiency and maximize wells' life.

5. CONCLUSION

Groundwater is considered as a strategic resource of water due to its usual high quality and continual availability. However, the sustainable management of GW represents a vital issue all over the world. Erbil province mainly depends on GW because it is the only source available for use and consumption. The rapid growth of the city and the excessive exploitation of GW burdens the water storage in the aquifer besides that there are over three thousand illegal drilled wells over the area of study. In general, the city consumes large quantities of water without a clear policy towards the use of water resources and water sustainability. Lack of awareness among people and institutions has a significant impact on the depletion of groundwater. The results show that there is a decrease in the groundwater level by 0.22 meters annually. The continued neglect and irresponsibility in the use of water resources, Erbil aquifer will face depletion and drought in the long-term which will create a disaster on the economic, agricultural and environmental levels.

REFERENCES

AHMED, M. R. 2009. Ground Water Quality of Selected Wells in Zaweta District, Northern Iraq. *Tikrit Journal of Eng. Sciences,* 17**,** 28-35.

ALLEY, W. M., REILLY, T. E. & FRANKE, O. L. 1999. *Sustainability of ground-water resources*, US Department of the Interior, US Geological Survey.

CLIMATE-DATA.ORG. 2018. *Climate of Erbil* [Online]. Available: https://en.climate-data.org/asia/iraq/erbil/erbil-4976/ [Accessed].

COUNCIL, N. R. 2001. *Investigating groundwater systems on regional and national scales*, National Academies Press.

DIZAYEE, R. H. 2014. Groundwater Degradation and Sustainability of the Erbil Basin, Erbil, Kurdistan Region, Iraq. *Texas Christian University, Fortworth, Texas. Student thesis.*

GUPTA, A. D. & BABEL, M. 2005. Challenges for sustainable management of groundwater use in Bangkok, Thailand. *International Journal of Water Resources Development,* 21**,** 453-464.

HABIB, H., AL-SAIGH, N. & HASSAN, Z. Geochemistry of undergroundwater in Erbil City, Iraq. conference of SDRC, Mosul, 1990.

HAMEED, H. 2013. Water harvesting in Erbil Governorate, Kurdistan region, Iraq: detection of suitable sites using geographic information system and remote sensing. *Student thesis series INES*.

Harter, T. (2003). Groundwater Quality and Groundwater Pollution. http://dx.doi.org/10.3733/ucanr.8084 Retrieved from https://escholarship.org/uc/item/0vw7400h.

JOHNSON, A. I. 1967. Specific yield: compilation of specific yields for various materials.

JONES, J. A. A. 2014. *Global hydrology: processes, resources and environmental management*, Routledge.

KINZELBACH, W., BAUER, P., SIEGFRIED, T. & BRUNNER, P. 2003. Sustainable groundwater management--Problems and scientific tool. *Episodes-Newsmagazine of the International Union of Geological Sciences,* 26**,** 279-284.

MAJEED, R. & AHMAD, M. 2002. Brief References on Hydrogeological Characters of Erbil Basin. *Unpublished Report, Erbil-Iraq.*

MAWLOOD, D., HUSSEIN, E. A. J. J. Z. J. O. P. & SCIENCES, A. 2016. Integrated Water Management in Mala Omer, Erbil, KRI. 28.

MAWLOOD, D. K., MUSTAFA, J. S. J. Z. J. O. P. & SCIENCES, A. 2017. Analyze the well losses and aquifer losses on the pumping test results. 29**,** 127-133.

METEOBLUE-WEATHER. 2018. *Climate of Erbil* [Online]. Available: https://www.meteoblue.com/en/weather/forecast/modelclimate/erbil_iraq_95446 [Accessed 25-Dec 2018].

MITRA, S. 2015. Groundwater Sustainability-A Brief Review. *International Journal of Ecosystem,* 5**,** 43-46.

NCCI 2015. Erbil Governorate Profile. Governmental Document Presented By NGO Coordination Committee for Iraq.

PONCE, V. M. 2006. Groundwater utilization and sustainability. *San Diego State University, College of Engineering. San Diego, Calif.[http://groundwater. sdsu. edu/].*

QURESHI, A. S., MCCORNICK, P. G., SARWAR, A. & SHARMA, B. R. 2010. Challenges and prospects of sustainable groundwater management in the Indus Basin, Pakistan. *Water resources management,* 24**,** 1551-1569.

SHI, X., FANG, R., WU, J., XU, H., SUN, Y. & YU, J. 2012. Sustainable development and utilization of groundwater resources considering land subsidence in Suzhou, China. *Engineering geology,* 124**,** 77-89.

Mawlood. D /ZJPAS: 2019, 31 (6): 51-60

60

SOPHOCLEOUS, M. 2005. Groundwater recharge and sustainability in the High Plains aquifer in Kansas, USA. *Hydrogeology Journal,* 13**,** 351-365.

WALI, K. I. & ALWAN, Z. M. 2016. Quality management for Ground water by Assessment of Aquifer Vulnerability to Contamination in Erbil City. *Engineering and Technology Journal,* 34**,** 698-714.

ZAKARIA, S. 2012. *Rain water harvesting and supplemental irrigation at Sinjar district in northwest Iraq.* Luleå tekniska universitet.

ZHOU, Y. 2009. A critical review of groundwater budget myth, safe yield and sustainability. *Journal of Hydrology,* 370**,** 207-213.

RESEARCH PAPER

Synthesis, Characterization, and Antibacterial Activity of Novel Mutual Non-Steroidal Anti-inflammatory Prodrugs

Banaz M. Hamadameen[1], Dana M. Hamad Ameen[1]

[1]Department of Pharmaceutical chemistry, College of Pharmacy, Hawler Medical University, Erbil, Kurdistan Region, Iraq

A B S T R A C T:
Non steroidal anti-inflammatory drugs (NSAIDs) are among the most used analgesic and anti-inflammatory drugs. However inhibition of cyclooxygenase1 and acidic groups such as carboxylic groups in most NSAIDs cause gastrointestinal (GI) side effects. Therefore masking the acidic groups till it pass through the GI tract will decrease the direct GI side effects and because *N*-(2,6-dimethylphenyl)-acetamide **1** also has anti-inflammatory activity so the synthesized ester prodrugs might act as mutual prodrugs. Moreover, because of emerging of new strains of bacteria and resistance of bacteria to the available antibacterial agents, new antibacterial agents are needed. The NSAIDs have antibacterial activity and *N*-(2,6-dimethylphenyl) acetamide **1** also has antibacterial activity so binding of these molecules with each other might give more potent antibacterial agent. 2-Chloro-*N*-(2,6-dimethyl phenyl) acetamide **1** was utilized to synthesize ester prodrug of various NSAIDs **2a-f**. The 2-Chloro-N-(2,6-dimethylphenyl)-acetamide **1** undergo substitution reaction at α position with various sodium carboxylate of NSAIDs **2a-f** in DMSO. The constitution of the newly synthesized ester prodrugs of NSAIDs **3a-f** had been confirmed on the basis of their IR, ¹H and ¹³C-NMR spectral data. All the synthesized ester prodrugs **3a-f** were screened for their *in vitro* antibacterial activities against *Staphylococcus aureus* ATCC 25923 and *Escherichia coli* ATCC 25922 however, their antibacterial activity decreased compared with their starting **1** and **2a-f**.

INTRODUCTION :

Non steroidal anti-inflammatory drugs (NSAIDs) constitute the first level of pain treatment in the world health organization (WHO) strategy (Galvez-Llompart *et al.*, 2010). NSAIDs exert their actions by inhibiting the synthesis of prostaglandins from arachidonic acid through non selective inhibition of cyclooxygenase 1 and 2 (COX 1 and COX 2) or selective inhibition of COX 2 (Laine, 2002). Like most other drugs, these molecules are not devoid of side effects. The most frequent side effects of NSAIDs are gastrointestinal side effects which include gastrointestinal irritation, ulcer and bleeding (Bjarnason *et al.*, 2018). Inhibition of COX 1 is responsible for these side effects, for this reason selective COX 2 inhibitors were synthesized but these medications instead cause cardiovascular side effects (Marnett, 2009, Bäck *et al.*, 2011).

In addition, the acidic groups in NSAIDs such as carboxylic group in mefenamic acid **2a,** flufenamic acid **2b,** tolfenamic acid **2c,** niflumic acid **2d,** diflunisal **2e** and diclofenac **2f** are responsible for gastric irritation which lead to

* **Corresponding Author:**
Dana M Hamad Ameen
E-mail: dameen@pha.hmu.edu.iq

ulcer and bleeding when administered orally (Laine, 2002). For this reason temporary masking of the acidic group will protects the gastric mucosa from local irritation and decrease mucosal injury (Abdulhadi *et al.*, 2013, Makhija *et al.*, 2013, Datar and Shendge, 2015, Ashraf *et al.*, 2016).

Moreover, recently particular attention was given to numerous derivatives of acetamides by the researchers as these molecules exhibit different biological activity such as antibacterial and antifungal (Ertan *et al.*, 2007, Jamkhandi and Disouza, 2012, Hamad *et al.*, 2017), anti-inflammatory (de Castro Barbosa *et al.*, 2009), antilieshmania (Pacheco *et al.*, 2013), antituberculosis (Yadav *et al.*, 2018), insecticide (Kalyanasundaram and Mathew, 2006), anthelmintic (Sawant and Kawade, 2011), antioxidant and anticancer (Özkay *et al.*, 2010, Chen *et al.*, 2013, Pawar *et al.*, 2017), anticonvulsant and antidepressant (Soyer *et al.*, 2004, Tarikogullari *et al.*, 2010, Guan *et al.*, 2016). In this study, various NSAIDs **2a-f** were attached to *N*-(2,6-dimethyl phenyl) acetamide **1** to decrease the gastric irritation by masking the acidic carboxylic group through ester linkage as shown in Scheme 1. The prodrugs **3a-f** might act as a mutual prodrug as both molecules poses anti-inflammatory activity (Galvez-Llompart *et al.,* 2010).

On the other hand, because of emerging of new strains of microorganisms and resistance of microbes to current antibacterial agents, new antibacterial agents needed to be synthesized . *N*-(2,6-dimethyl phenyl) acetamide **1** had antibacterial activity (Hamad *et al*., 2017) and NSAIDs had been reported to possess antibacterial activity and they are known as non-antibiotics (Al-janabi, 2010, Yin *et al.*, 2014, Ahmed *et al.*, 2017) and co-administration of NSAIDs with antibiotics showed synergistic effect (Chan *et al.*, 2017) and decrease the severity of colonic damage by counteracting the NSAID-induced fall in colonic microcirculation and bacterial translocation to extra-intestinal organs (Zwolinska-Wcislo *et al.*, 2011). The ester linkage in the newly synthesized prodrugs **3a-f** will be hydrolyzed by esterase enzyme to release the parent NSAID **2a-f** and *N*-(2,6-dimethyl phenyl) acetamide **1**.

1. MATERIALS AND METHODS

This experimental study was designed to synthesize new ester prodrugs of some NSAIDs and to evaluate the antibacterial activity of the synthesized compounds **3a-f**. All the synthetic procedures were done at Hawler Medical University, College of Pharmacy, Pharmaceutical Chemistry and Organic Chemistry Lab, between 1st of March 2018 to 15th of October 2018. The NSAIDs **2a-f** were purchased from (Sigma Aldrich, UK and Apollo Healthcare Resources, Singapore) the 2-Chloro-*N*-(2,6-dimethylphenyl)-acetamide **1** purchased from (Apollo Healthcare Resources, Singapore). All the chemicals used directly without further purification.

The melting points were determined on a Gallenkamp electro-thermal apparatus by open capillary method and are uncorrected. The purity of the compounds were checked using pre-coated TLC plates 60 F254 (Merck, Germany) using toluene: acetone (2:1) solvent system. The developed chromatographic plates were visualized under UV at 254 nm. IR spectra were recorded on a SCHIMADZU Spectrophotometer, as KBr disc (Chemistry Department, College of Education, Salahaddin University/Erbil). ^{1}H and ^{13}C-NMR spectra were measured using a Bruker Ultra shield 400 MHz with internal TMS (at University of Science and Technology/ Irbid- Jordan), chemical shifts are given in ppm. Then after, the synthesized compounds 3a-j and their starting 1 and 2a-f were screened for their *in vitro* antimicrobial activities against *Staphylococcus aureus* ATCC 25923 and *Escherichia coli* ATCC 25922 at Hawler Medical University, College of Pharmacy, Microbiology and virology Lab.

1.1. General procedure for the synthesis of ester prodrug of various NSAIDs:

To a mixture of NSAIDs **2a-f** (2.5 mmol) with sodium bicarbonate (2.5 mmol) in 20 of ml DMSO, 2-Chloro-*N*-(2,6-dimethylphenyl)-acetamide **1** (2.5 mmol) was added and stirred for 24 hours as shown in Scheme 1. All the reactions were monitored by TLC on pre-coated silica gel plates 60 F254 (Merck, Germany) visualizing with UV light (254 nm). After stopping the reaction, the reaction mixture was added to ice-water (100 ml) and the precipitate was vacuum filtered and left to dry. The solid residue after drying was re-crystallized from absolute ethanol (Hamad *et al*., 2017).

1.2. Procedure of antibacterial activity:

Staphylococcus aureus ATCC 25923 and *Escherichia coli* ATCC 25922 were inoculated in Muller Hinton agar and incubated at 37 °C for 24 hours. After incubation, a loop of each bacteria were inoculated into sterile test tubes containing sterile normal saline and adjusted to 0.5 McFarland standard. Then 96 well-flat micro titer plates were filled with 100 µl of the synthesized prodrugs **3a-f** and the starting compounds **1** and **2a-f** in concentration of 1mg/ml, 0.5mg/ml and 0.1mg/ml of each compound in addition to 10 µl of diluted cultures individually and tween 20%

used as a blank. The micro titer plates were incubated at 37 °C for 24 hours then by using ELISA reader the 96-flat wells were read at 600 nm (Chung *et al.*, 2011, Taye *et al.*, 2011, Molla *et al.*, 2016, Hamad *et al.*, 2016).

1.3. Statistical Analysis:

All data are expressed as Mean±SD of triplicate experiments.
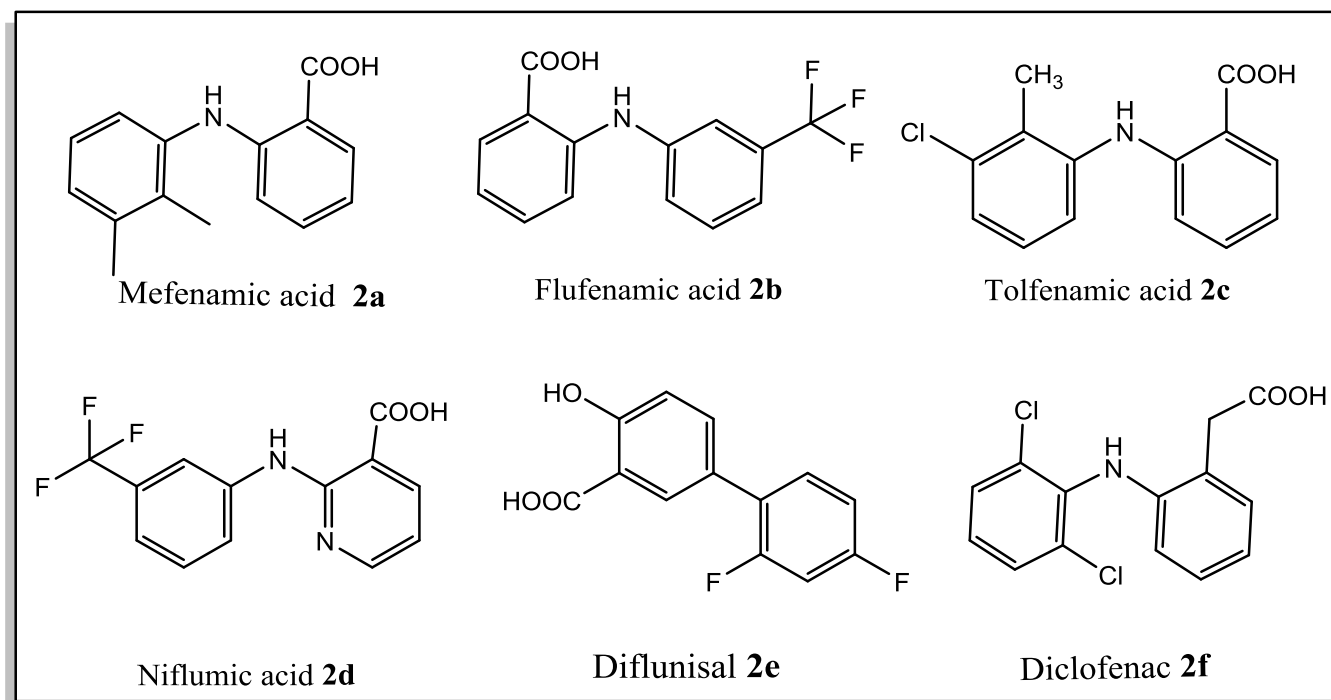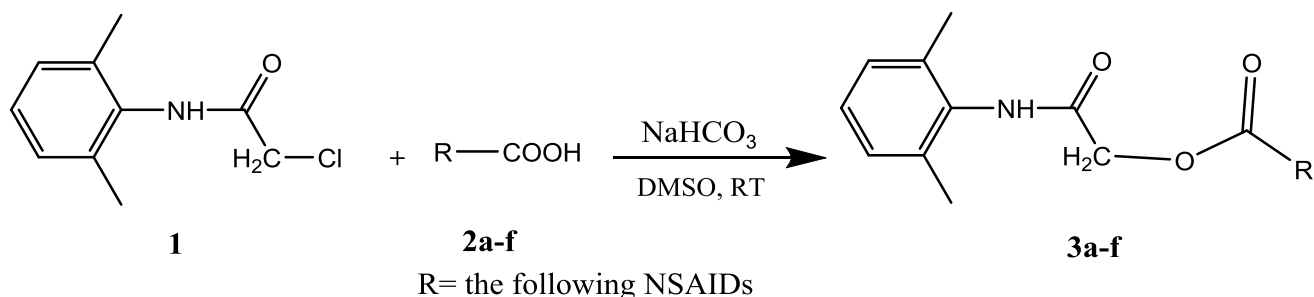
Scheme 1: synthesis of prodrugs of NSAIDS 3a-f.

2. RESULTS AND DISCUSSION

2.1 RESULTS

This study was aimed to synthesize, spectroscopic study and evaluation of biological activity of few novel NSAIDs prodrug **3a-f** attached through ester linkage to *N*-(2,6-dimethylphenyl) acetamide **1** to mask the acidic carboxylic group. The 2-Chloro-*N*-(2,6-dimethylphenyl)-acetamide **1** undergo substitution reaction at α position with various sodium carboxylate of NSAIDs **2a-f** (Scheme 1). The products were obtained in good yields and in high purity, in which a single spot appeared on the TLC plate and they have narrow melting points (Table 1). The IR and H¹ and C¹³-NMR spectral data support the substitution of the chloro group with various sodium carboxylate of NSAIDs. The IR and H¹ and C¹³-NMR spectral data are shown in Table 2. *In vitro* antibacterial activity of the startings **1** and **2a-f** and the synthesized prodrugs **3a-f** was performed against *Staphylococcus aureus* ATCC 25923 and *Escherichia coli* ATCC 25922. The antibacterial results are shown in Table 3 and Table 4. The starting **1** and **2a-f** showed antibacterial activity and inhibit the growth of both types of bacteria in all the three concentrations (1mg/ml, 0.5mg/ml and 0.1mg/ml), however, the synthesized prodrugs **3a-f** showed lower antibacterial activity or no bacterial growth inhibition. Additionally, most of the synthesized prodrugs **3a-f** were more active against *Escherichia coli than Staphylococcus aureus.*
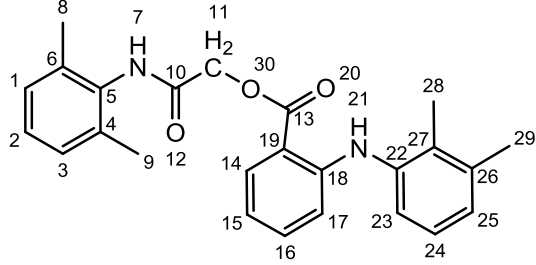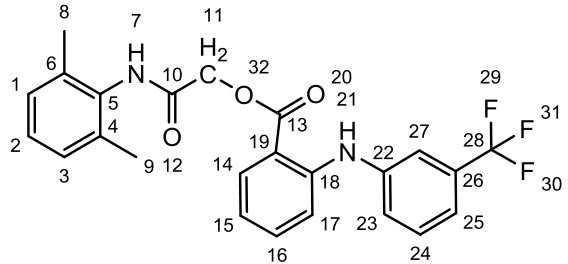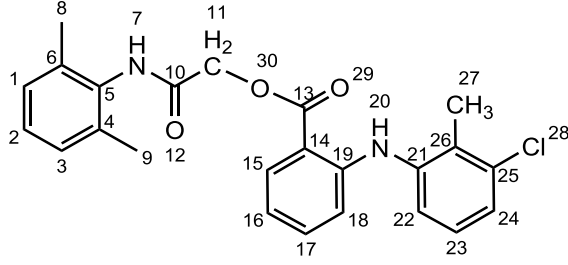
Table 1: Physical properties of synthesized compounds 3a-f:

Compounds	Physical appearance	Yield (%)	Melting point °C	Rf value *
3a	Colorless fluffy powder	67	217-219	0.82
3b	Colorless fluffy powder	82	159-161	0.81
3c	Colorless fluffy powder	66	205-207	0.81
3d	Colorless fluffy powder	74	215-216	0.78
3e	Colorless powder	66	223-225	0.78
3f	Pink powder	75	162-164	0.77

*Rf value, toluene: acetone (2:1) used as eluent.

Table 2: Spectroscopic data of the synthesized compounds (3a-f)

Compounds	Spectroscopic data
3a	**IR in cm^{-1}:** 3319, 3244 (NH str. amine and amide), 1689 (C=O ester), 1660 (C=O amide), 1222 (C-O ester). **¹HNMR** (400 MHz, DMSO- d_6): δ 1.24(s, 3H, $_{29}CH_3$),

1.31(s, 6H, $_8$CH$_3$, $_9$CH$_3$), 1.44 (s, 3H, $_{28}$CH$_3$), 4.13 (s, 2H, $_{11}$CH$_2$), ((6.68, d, 1H, J=8Hz), (6.75, t, 1H), (7.08,s, 4H), (7.13,s,2H),(7.36, t, 1H), (8.04, d, 1H, J=4Hz) 10Ar-H), 9.12(s, 1H, Ar-NH), 9.57(s, 1H, Ar-NHCO).

^{13}CNMR (101 MHz, DMSO-d$_6$): δ C$_{29}$-14.09, C$_8$, C$_9$-18.46, C$_{28}$-20.69, C$_{11}$-63.41, Ar (C)-110.69-149.16, C$_{10}$-166.00, C$_{13}$-167.98.

3b

IR in cm^{-1}: 3323, 3201 (NH str. amine and amide), 1685 (C=O ester), 1658 (C=O amide), 1228 (C-O ester).

^{1}HNMR (400 MHz, DMSO-d$_6$): δ 2.17 (s, 6H, $_8$CH$_3$, $_9$CH$_3$), 5.01 (s, 2H, $_{11}$CH$_2$), ((9.98, t, 1H) (7.08, s, 3H) (7.34, d, H, J = 8 Hz 2) (7.50, m, 4H) (8.06, d, 1 H, J = 8 Hz) 11Ar-H), 9.29 (s, 1H, Ar-NH), 9.60 (1H, s, Ar-NHCO).

^{13}CNMR (101 MHz, DMSO-d$_6$): δ C$_8$, C$_9$-17.80, C$_{11}$-62.76, C$_{28}$-114.16, Ar (C)-115.45-144.76, C$_{10}$-165.22, C$_{13}$-166.58.

3c

IR in cm^{-1}: 3313, 3246 (NH str. amine and amide), 1691 (C=O ester), 1666 (C=O amide), 1222 (C-O ester).

^{1}HNMR (400 MHz, DMSO- d_6): δ 2.18 (s, 6 H, $_8$CH$_3$, $_9$CH$_3$), 2.26 (s, 3 H, $_{27}$CH$_3$), 5.00 (s, 2 H, $_{11}$CH$_2$), ((6.84, t, 2 H) (7.09, s, 3 H) (7.25, m, 3 H) (7.43, t, 1 H) (8.06, d, 1 H, J = 8 Hz) 10Ar-H), 9.20 (s, 1 H, Ar-NH), 9.59 (1 H, s, Ar-NHCO).

^{13}CNMR (101 MHz, DMSO-d_6): δ C$_{27}$-14.46, C$_8$,C$_9$-

	17.80, C_{11}-62.84, Ar (C) -111.16-147.25, C_{10}-165.25, C_{11}-167.17.
3d 	**IR in cm^{-1}:** 3265 (NH str. amine and amide overlaped), 1697 (C=O ester), 1668 (C=O amide), 1116 (C-O ester). **^{1}HNMR** (400 MHz, DMSO- d_6): δ 2.18 (s, 6 H, $_8$CH$_3$, $_9$CH$_3$), 5.07 (s, 2 H, $_{11}$CH$_2$), ((7.02, d, 4 H, J = 20 Hz) (7.35, s, 1 H) (7.55, s, 1 H) (7.89, s, 1 H) (8.29, s, 1 H) (8.43, d, 2 H, J= 28 Hz) 10Ar-H), 9.63 (s, 1 H, Ar-NH), 10.15 (1 H, s, Ar-NHCO). **^{13}CNMR** (101 MHz, DMSO-d_6): δ C_8, C_9-17.89, C_{11}-63.30, C_{29}-107.85, Ar (C)-114.81-154.45, C_{10}-165.10, C_{14}-166.11.
3e 	**IR in cm^{-1}:** 3219 (NH str. amide), 1678 (C=O str. ester), 1662 (C=O str. amide), 1207 (C-O str. ester). **^{1}HNMR** (400 MHz, DMSO- d_6): δ 2.16 (s, 6 H, $_7$CH$_3$, $_8$CH$_3$, 5.02 (s, 2 H, $_{12}$CH$_2$), ((7.08, m, 5 H) (7.36, s, 1 H) (7.56, s, 1 H) (7.69, s, 1 H) (8.04, s, 1 H) 9Ar-H), 9.57 (s, 1 H, Ar-NHCO), 10.52 (1 H, s, Ar-OH). **^{13}CNMR** (101 MHz, DMSO- d_6): δ C_7, C_8-17.78, C_{12}-63.14 Ar (C)-104.32-159.16, C_{10}-164.90, C_{14}-167.24.
3f 	**IR in cm^{-1}:** 3315, 3250 (NH str. amine and amide), 1761 (C=O ester), 1730 (C=O amide), 1136 (C-O ester). **^{1}HNMR** (400 MHz, DMSO- d_6): δ 1.26(s, 6H, $_8$CH$_3$, $_9$CH$_3$), 3.12 (s, 2H, $_{14}$CH$_3$), 3.92 (s, 2H, $_{11}$CH$_2$), ((5.39, d, 1H, J=4Hz), (6.20, d, 5H, J=8Hz), (6.37,t, 1H),

	(6.41,d,1H, J=4Hz),(6.68, d, 2H, J=8Hz), (8.04, d, 1H, J=4Hz) 10Ar-H), 8.58(s, 1H, Ar-NH)
	^{13}CNMR (101 MHz, DMSO-d_6): δ C$_8$, C$_9$-18,39, C$_{14}$-37,29, C$_{11}$-63,32, Ar (C)-116.10-143.51, C$_{10}$-165.93, C$_{13}$-171.56.

Table 3: Minimum inhibitory concentrations of the synthesized prodrugs **3a-f** and their corresponding starting materials **1**and **2a-f** against *Staphylococcus aureus* ATCC 25923.

Compounds	Concentration		
	1mg/ml	0.5mg/ml	0.1mg/ml
1	0.0395 ± 0.002	0.0415 ± 0.002	0.055 ± 0.014
2a	0.0395 ± 0.039	0.047 ± 0.003	0.099 ± 0.012
3a	N	N	N
2b	0.0555 ± 0.115	0.054 ± 0.003	0.0615 ± 0.007
3b	N	N	0.0535
2c	0.048 ± 0.005	0.0555 ± 0.003	0.061 ± 0.008
3c	N	N	0.092
2d	0.0615 ± 0.016	0.061 ± 0.006	0.0565 ± 0.007
3d	N	N	N
2e	0.0395 ± 0.003	0.0635 ± 0.009	0.052 ± 0.002
3e	0.0475 ± 0.007	0.051 ± 0.007	0.0525 ± 0.015
2f	0.0645 ± 0.012	0.0695 ± 0.004	0.063 ± 0.006
3f	N	N	N

N= no bacterial inhibition

Table 4: Minimum inhibitory concentrations of the synthesized prodrugs **3a-f** and their corresponding starting materials **1**and **2a-f** against *Escherichia coli ATCC 25922.*

Compound	Concentration		
	1mg/ml	0.5mg/ml	0.1mg/ml
1	0.0420 ± 0.001	0.0515 ± 0.0005	0.058 ± 0.014
2a	0.0405 ± 0.0005	0.0465 ± 0.002	0.0495 ± 0.012
3a	0.0815 ± 0.0335	N	0.084 ± 0.023
2b	0.0490 ± 0.002	0.053 ± 0.002	0.056 ± 0.007
3b	0.0625 ± 0.0035	0.048 ± 0.005	0.0455 ± 0.007
2c	0.0455 ± 0.0015	0.0495 ± 0.025	0.054 ± 0.009
3c	N	0.0705 ± 0.021	0.056 ± 0.007
2d	0.046 ± 0.002	0.0535 ± 0.005	0.0545 ± 0.005
3d	N	0.059 ± 0.018	0.082 ± 0.007
2e	0.040 ± 0.002	0.050 ± 0.0005	0.0495 ± 0.005
3e	0.0365 ± 0.0005	0.0385 ± 0.001	0.050 ± 0.014
2f	0.0585 ± 0.0052	0.058 ± 0.003	0.0545 ± 0.004
3f	0.091 ± 0.0335	0.0435 ± 0.003	0.0625 ± 0.005

N= no bacterial inhibition

2.2. DISCUSSION

Prodrug approach is one of the most used approaches to decrease the gastrointestinal side effects. Many prodrugs have been synthesized to decrease the direct GI irritation through masking the acidic groups by either ester or amide linkage (Galanakis *et al.*, 2004, Huang *et al.*, 2011, Amir *et al.*, 2016, Ashraf *et al.*, 2016). In this study the acidic carboxylic groups of various NSAIDs **2a-f** have been masked with an acetamide derivative **1** through an ester linkage using nucleophilic substitution reaction as a simple strategy in polar aprotic solvent at room temperature (Scheme 1).

At room temperature condition, the nucleophilic substitution reactions progress smoothly (Hamad et al., 2017), most of the reactions need more than 24 hours to complete and products were obtained in good yields and in high purity. The infrared spectra of the formed NSAID prodrugs **3a-f** confirmed the substitution reaction at the alpha position in **1** by showing two strong absorption bands at carbonyl region due to carbonyl groups of the ester and amide moieties, respectively (Table 2) and it is in agreement with the obtained ^{1}H and ^{13}C -NMR spectrum (Table 2). For example, the infrared spectrum of

mefenamic ester prodrug **3a** has revealed several absorption bands at 1689 and 1660 cm⁻¹ due to carbonyl group stretching of ester and amide moieties, respectively and absorption bands at 3319 and 3244 cm⁻¹ due to NH stretching of amine and amide, while in the IR of **1** there is only one band in carbonyl region; and these spectral data are in agreement with the obtained ¹H-NMR spectrum, (Figure 1-3) which display four signals at 2.10, 2.17, 2.29, 4.98 ppm due to methyl and methylene hydrogen atoms and two singlet signals at 9.12 and 9.57 ppm of the NH group of amine and amide moieties while in the ¹H-NMR of starting **1** there is only one peak for NH group .

Moreover the data of ¹³C-NMR also support the substitution of the chloro group and the formation of ester prodrugs by showing signals at 14.09, 18.46, 20.69 and 63.41 ppm due to carbon atoms of methyl and methylene groups. Furthermore, there are two signals at 166 and 167.98 ppm due to carbonyl carbon atoms of amide and ester groups present in the structure of the mefenamic ester prodrug **3a** (Katke et al., 2011).

Importantly, NSAIDs had been found to have antibacterial activity (Al-janabi, 2010, Yin *et al*., 2014, Chan *et al*., 2017, Ahmed *et al*., 2017) and the attempted acetamide **1** had been evaluated and showed antibacterial activity (Hamad *et al*., 2017), therefore joining these two moieties might

kill two birds by one stone. Most of the synthesized prodrugs **3a-f** were effective against Gram negative bacteria (*E. coli*) because their cell walls contain a thin peptidoglycan layer (without techoic acids) that is surrounded by a thick plasma membrane, while most of them were inactive against Gram positive bacteria (*S. aureus*) because of their thick peptidoglycan cell wall.

Unfortunately, the antibacterial results showed that most of the synthesized prodrugs **3a-f** had less antibacterial activity as compared with their starting **1** and **2a-f,** this is might be due to the blockage of carboxylic group which form hydrogen bond with subsite I of the clamp-binding motifs (CBM)-Binding Pocket of bacterial Sliding Clamp resulting in inhibition of the bacterial DNA polymerase III b subunit, an essential interaction hub that acts as a mobile tether on DNA for many essential partner proteins in DNA replication and repair (Yin *et al*., 2014). In the synthesized prodrugs **3a-f,** the ester group cannot form hydrogen bond and inhibit DNA replication and repair as in NSAIDs.

The synthesized prodrugs **3a-f** might act as mutual prodrugs because this antibacterial study is an *in vitro* study, in *in vivo* there is an esterase enzyme which will hydrolyze the ester linkage and release back the parent NSAID **2a-f** and attempted acetamide **1** which both possess antibacterial and anti-inflammatory activities.
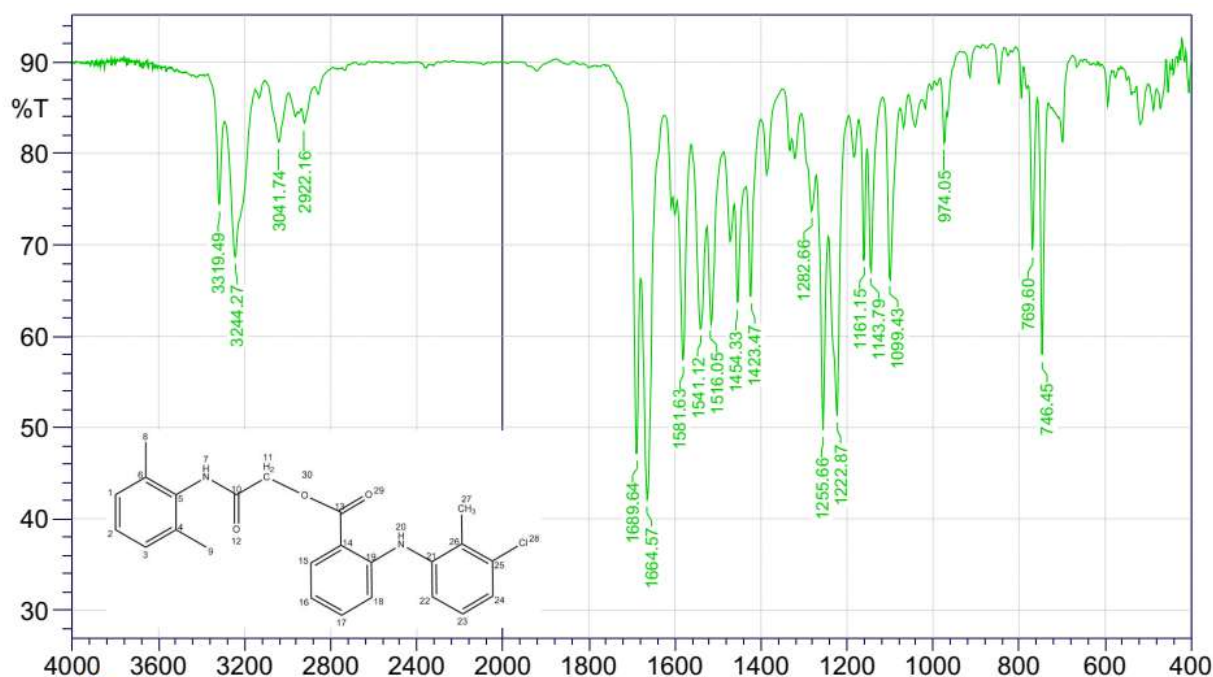

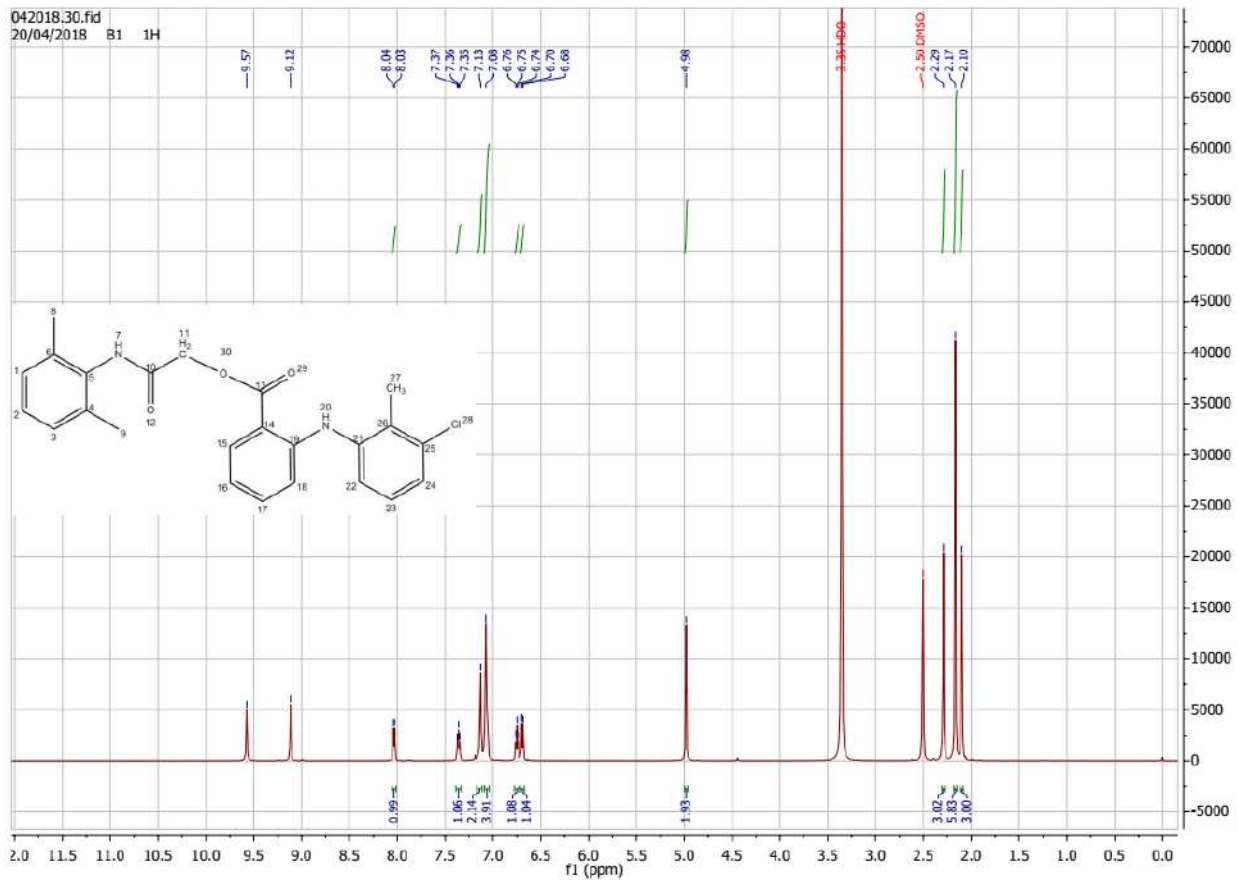**Figure 1: IR spectra of compound 3a.**
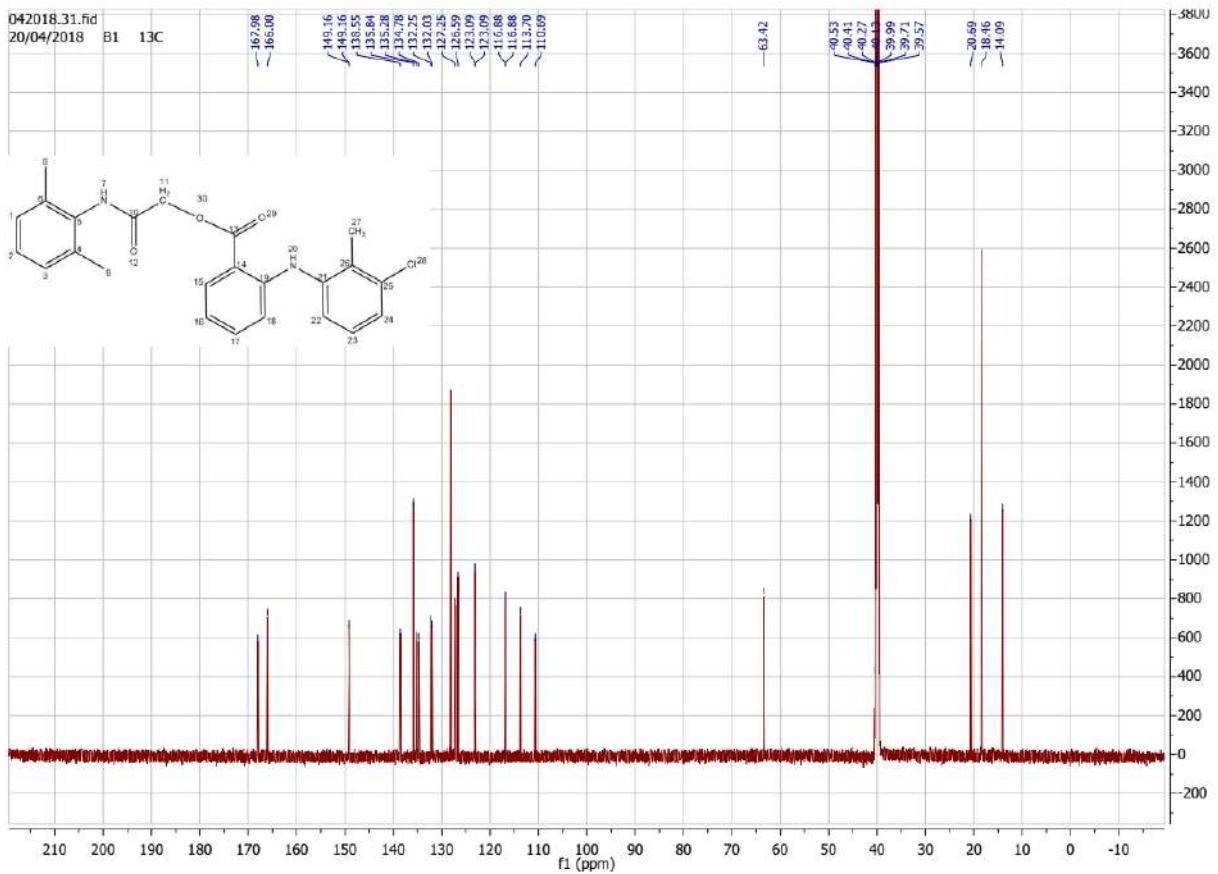
Figure 2: ¹H-NMR spectra of compound 3a.

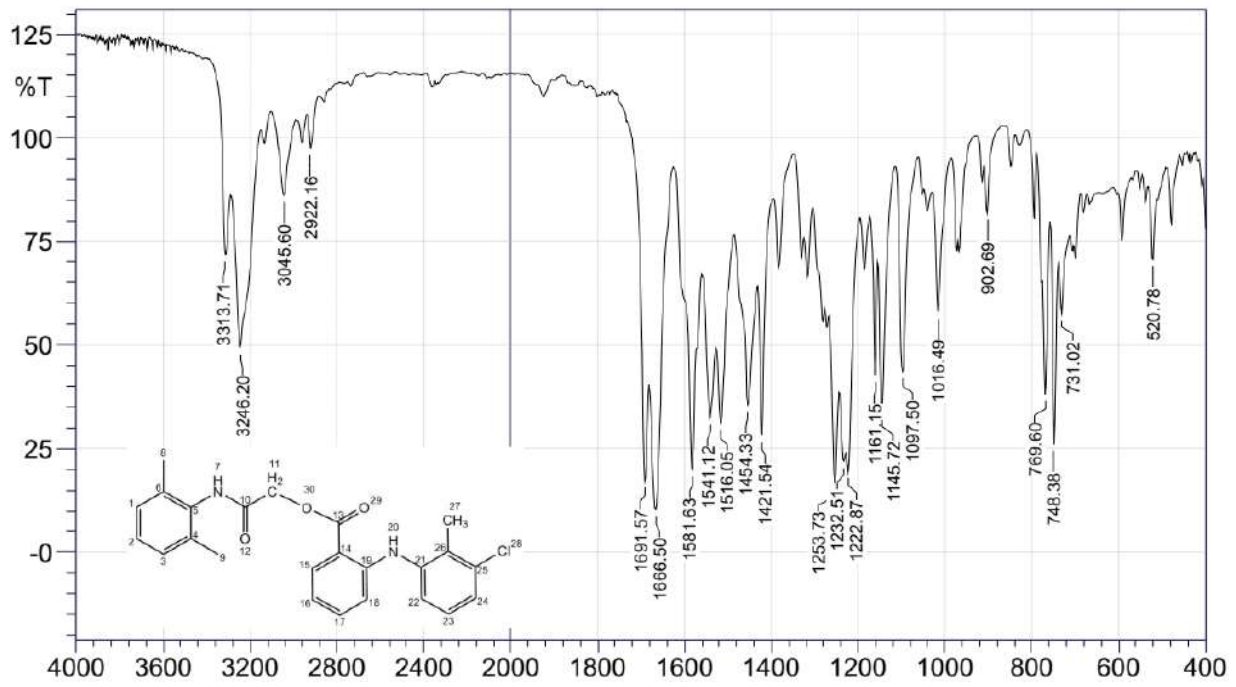**Figure 3: ¹³C-NMR spectra of compound 3a.**

Figure 4: IR spectra of compound 3c.
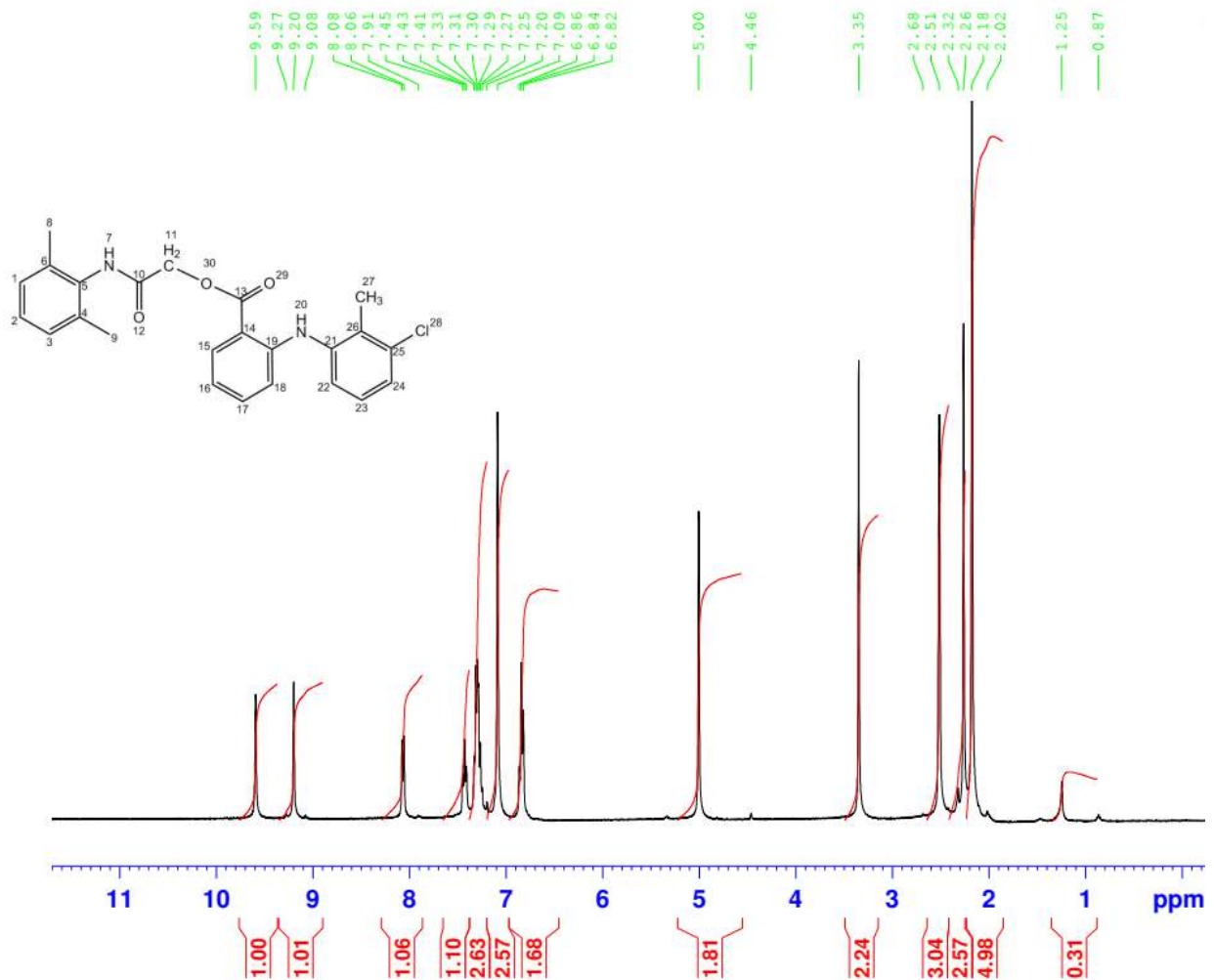
Figure 5: ¹H-NMR spectra of compound 3c.
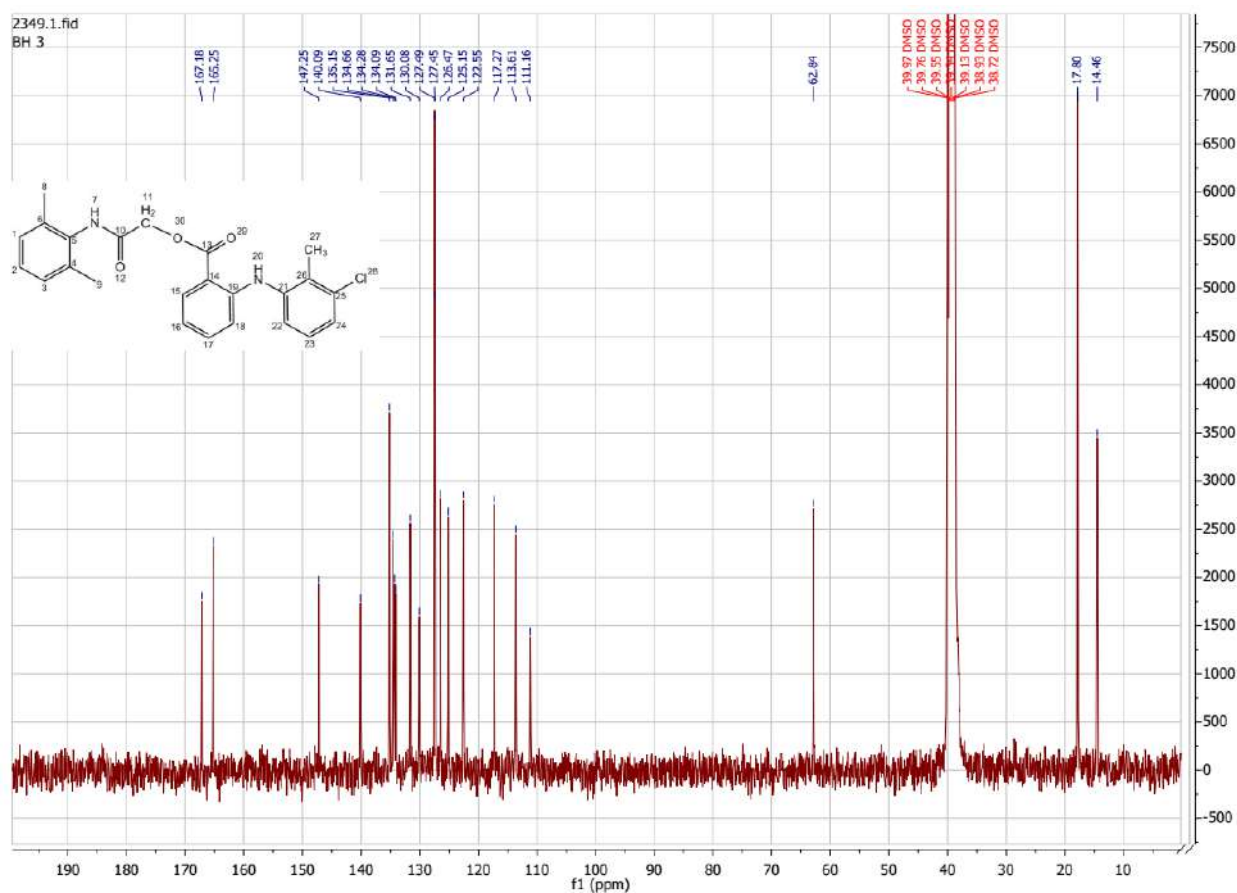
Figure 6: ¹³C-NMR spectra of compound 3c.

2. CONCLUSIONS

A simple, classic, efficient and convinient approach and easy work-up had been used for the synthesis of prodrugs of NSAIDS **3a-f** with a view to mask the irritating acidic carboxylic group, to have good antibacterial activity and to increase the anti-inflammatory activity of the NSAIDs **2a-f**. The chemical method, the reaction condition was mild; the products were obtained in good yields in suitable time. Another advantage is that the products can be separated conveniently from the reaction mixture (with a simple re-crystallization technique) in high purity and no chromatographic method needed for their purification. The antibacterial profile of all the synthesized prodrugs **3a-f** (Table 3 and Table 4) revealed that the synthesized prodrugs **3a-f** possessed lower or no antibacterial activity towards *Escherichia coli* and *staphylococcus aureus.* The synthesized prodrugs **3a-f** were more effective against Gram negative bacteria (*E. coli) than the* Gram positive bacteria (*S. aureus).*

Acknowledgements

Conflict of Interest

Authors have no conflict of interest.

.

References

ABDULHADI, S. L., QASIR, A. J. & RAZZAK, N. A. A. 2013. Synthesis of new conjugates of some NSAIDs with sulfonamide as possible mutual prodrugs using tyrosine spacer for colon targeted drug delivery. *Iraqi Journal of Pharmaceutical Sciences (P-ISSN: 1683-3597, E-ISSN: 2521-3512),* 22**,** 22-29.

AHMED, E. F., EL-BAKY, R. M. A., AHMED, A. B. F., WALY, N. G. & GAD, G. F. M. 2017. Antibacterial activity of some non-steroidal anti-inflammatory drugs against bacteria causing urinary tract infection. *Am. J. Infect. Dis. Microbiol,* 5**,** 66-73.

AL-JANABI, A. A. H. S. 2010. In vitro antibacterial activity of Ibuprofen and acetaminophen. *Journal of global infectious diseases,* 2**,** 105.

AMIR, M., AKHTER, M. & SOMAKALA, K. 2016. Synthesis, In Vitro and In Vivo Evaluation of the N-Ethoxycarbonylmorpholine Ester of Diclofenac as a Prodrug. *Indian J. Chem. B,* 55**,** 989-998.

ASHRAF, Z., ALAMGEER, M. K., HASSAN, M., ABDULLAH, S., WAHEED, M., AHSAN, H. & KIM, S. J. 2016. Flurbiprofen–antioxidant mutual prodrugs as safer nonsteroidal anti-inflammatory drugs: synthesis, pharmacological investigation, and computational molecular modeling. *Drug design, development and therapy,* 10**,** 2401.

BÄCK, M., YIN, L. & INGELSSON, E. 2011. Cyclooxygenase-2 inhibitors and cardiovascular risk in a nation-wide cohort study after the withdrawal of rofecoxib. *European heart journal,* 33**,** 1928-1933.

BJARNASON, I., SCARPIGNATO, C., HOLMGREN, E., OLSZEWSKI, M., RAINSFORD, K. D. & LANAS, A. 2018. Mechanisms of damage to the gastrointestinal tract from nonsteroidal anti-inflammatory drugs. *Gastroenterology,* 154**,** 500-514.

CHAN, E. W. L., YEE, Z. Y., RAJA, I. & YAP, J. K. Y. 2017. Synergistic effect of non-steroidal anti-inflammatory drugs (NSAIDs) on antibacterial activity of cefuroxime and chloramphenicol against methicillin-resistant Staphylococcus aureus. *Journal of global antimicrobial resistance,* 10**,** 70-74.

CHEN, I.-L., CHEN, J.-J., LIN, Y.-C., PENG, C.-T., JUANG, S.-H. & WANG, T.-C. 2013. Synthesis and antiproliferative activities of N-(naphthalen-2-yl) acetamide and N-(substituted phenyl) acetamide bearing quinolin-2 (1H)-one and 3, 4-dihydroquinolin-2 (1H)-one derivatives. *European journal of medicinal chemistry,* 59**,** 227-234.

CHUNG, P. Y., NAVARATNAM, P. & CHUNG, L. Y. 2011. Synergistic antimicrobial activity between pentacyclic triterpenoids and antibiotics against Staphylococcus aureus strains. *Annals of Clinical Microbiology and Antimicrobials,* 10**,** 25.

DATAR, P. & SHENDGE, T. 2015. Design, synthesis and stability studies of mutual prodrugs of NSAID's. *Chem Informatics,* 1**,** 1-7.

DE CASTRO BARBOSA, M. L., DE ALBUQUERQUE MELO, G. M., DA SILVA, Y. K. C., DE OLIVEIRA LOPES, R., DE SOUZA, E. T., DE QUEIROZ, A. C., SMANIOTTO, S., ALEXANDRE-MOREIRA, M. S., BARREIRO, E. J. & LIMA, L. M. 2009. Synthesis and pharmacological evaluation of N-phenyl-acetamide sulfonamides designed as novel non-hepatotoxic analgesic candidates. *European Journal of Medicinal Chemistry,* 44**,** 3612-3620.

ERTAN, T., YILDIZ, I., OZKAN, S., TEMIZ-ARPACI, O., KAYNAK, F., YALCIN, I., AKI-SENER, E. & ABBASOGLU, U. 2007. Synthesis and biological evaluation of new N-(2-hydroxy-4 (or 5)-nitro/aminophenyl) benzamides and phenylacetamides as antimicrobial agents. *Bioorganic & medicinal chemistry,* 15**,** 2032-2044.

GALANAKIS, D., KOUROUNAKIS, A. P., TSIAKITZIS, K. C., DOULGKERIS, C., REKKA, E. A., GAVALAS, A., KRAVARITOU, C., CHARITOS, C. & KOUROUNAKIS, P. N. 2004. Synthesis and pharmacological evaluation of amide conjugates of NSAIDs with L-cysteine ethyl ester, combining potent antiinflammatory and antioxidant properties with significantly reduced gastrointestinal toxicity. *Bioorganic & medicinal chemistry letters,* 14**,** 3639-3643.

GALVEZ-LLOMPART, M., M GINER, R., C RECIO, M., CANDELETTI, S. & GARCIA-DOMENECH, R. 2010. Application of molecular topology to the search of novel NSAIDs: Experimental validation of activity. *Lett Drug Des Discov,* 7**,** 438-445.

GUAN, L.-P., LIU, B.-Y., QUAN, Y.-C., YANG, L.-Y., ZHEN, X.-H. & WANG, S.-H. 2016. Synthesis and evaluation of phenyliminoindolin-containing phenylacetamide derivatives with the antidepressant and anticonvulsant effects. *Medicinal Chemistry,* 12**,** 786-794.

HAMAD, A. N., AHMED, S. M., JAWHAR, Z. H., HAMAD, D. H. & SALIH, K. M. 2017. Synthetic Approaches and Pharmacological Evaluation of Some New Acetamide Derivatives and 5-Benzylidene-2-(2, 6-dimethyl-phenylimino)-thiazolidin-4-ones. *ZANCO Journal of Pure and Applied Sciences,* 29**,** 13-24.

HAMAD, A. N., BRIEM, R. R. & NOORADDIN, S. M. 2016. Synthesis, structure elucidation and antibacterial screening of some new 1, 3-imidazolinone derivatives using micro broth dilution assay. *ZANCO Journal of Pure and Applied Sciences,* 27**,** 19-30.

HUANG, Z., VELÁZQUEZ, C. A., ABDELLATIF, K. R., CHOWDHURY, M. A., REISZ, J. A., DUMOND, J. F., KING, S. B. & KNAUS, E. E. 2011. Ethanesulfohydroxamic acid ester prodrugs of nonsteroidal anti-inflammatory drugs (NSAIDs): synthesis, nitric oxide and nitroxyl release, cyclooxygenase inhibition, anti-inflammatory, and ulcerogenicity index studies. *Journal of medicinal chemistry,* 54**,** 1356-1364.

JAMKHANDI, C. & DISOUZA, J. I. 2012. Synthesis and antimicrobial evaluation of 2-(1H-1, 2, 3-Benzotriazol-1-yl)-N-phenylacetamide derivatives. *Research J. Pharm. and Tech,* 5**,** 1072-75.

KALYANASUNDARAM, M. & MATHEW, N. 2006. N, N-diethyl phenylacetamide (DEPA): a safe and effective repellent for personal protection against hematophagous arthropods. *Journal of medical entomology,* 43**,** 518-525.

KATKE, S., AMRUTKAR, S., BHOR, R. & KHAIRNAR, M. 2011. Synthesis of biologically active 2-chloro-N-alkyl/aryl acetamide derivatives. *International Journal of Pharma Sciences and Research,* 2**,** 148-156.

LAINE, L. The gastrointestinal effects of nonselective NSAIDs and COX-2–selective inhibitors. Seminars in arthritis and rheumatism, 2002. Elsevier, 25-32.

MAKHIJA, D., SOMANI, R. & CHAVAN, A. 2013. Synthesis and pharmacological evaluation of antiinflammatory mutual amide prodrugs. *Indian journal of pharmaceutical sciences,* 75**,** 353.

MARNETT, L. J. 2009. Mechanisms of cyclooxygenase-2 inhibition and cardiovascular side effects—The plot thickens. *Cancer prevention research,* 2**,** 288-290.

MOLLA, Y., NEDI, T., TADESSE, G., ALEMAYEHU, H. & SHIBESHI, W. 2016. Evaluation of the in vitro antibacterial activity of the solvent fractions of the leaves of Rhamnus prinoides L'Herit (Rhamnaceae) against pathogenic bacteria. *BMC complementary and alternative medicine,* 16**,** 287.

ÖZKAY, Y., IŞıKDAĞ, İ., İNCESU, Z. & AKALıN, G. 2010. Synthesis of 2-substituted-N-[4-(1-methyl-4, 5-diphenyl-1H-imidazole-2-yl) phenyl] acetamide derivatives and evaluation of their anticancer activity. *European journal of medicinal chemistry,* 45**,** 3320-3328.

PACHECO, D. J., TRILLERAS, J., QUIROGA, J., GUTIÉRREZ, J., PRENT, L., COAVAS, T., MARÍN, J. C. & DELGADO, G. 2013. N-(4-((E)-3-Arylacryloyl) phenyl) acetamide Derivatives and their Antileishmanial Activity. *Journal of the Brazilian Chemical Society,* 24**,** 1685-1690.

PAWAR, C. D., SARKATE, A. P., KARNIK, K. S. & SHINDE, D. B. 2017. Synthesis and evaluation of [N-(Substituted phenyl)-2-(3-substituted) sulfamoyl) phenyl)] acetamide derivatives as anticancer agents. *Egyptian Journal of Basic and Applied Sciences,* 4**,** 310-314.

SAWANT, R. & KAWADE, D. 2011. Synthesis and biological evaluation of some novel 2-phenyl benzimidazole-1-acetamide derivatives as potential anthelmintic agents. *Acta Pharmaceutica,* 61**,** 353-361.

SOYER, Z., KıLıÇ, F. S., EROL, K. & PABUÇCUOĞLU, V. 2004. Synthesis and anticonvulsant activity of some ω-(1H-imidazol-1-yl)-N-phenylacetamide and propionamide derivatives. *Il Farmaco,* 59**,** 595-600.

TARIKOGULLARI, A. H., FATMA, S. K., EROL, K. & PABUCCUOGLU, V. 2010. Synthesis and anticonvulsant activity of some alkanamide derivatives. *Arzneimittelforschung,* 60**,** 593-598.

TAYE, B., GIDAY, M., ANIMUT, A. & SEID, J. 2011. Antibacterial activities of selected medicinal plants in traditional treatment of human wounds in Ethiopia. *Asian Pacific Journal of Tropical Biomedicine,* 1**,** 370-375.

YADAV, S., LIM, S. M., RAMASAMY, K., VASUDEVAN, M., SHAH, S. A. A., MATHUR, A. & NARASIMHAN, B. 2018. Synthesis and evaluation of antimicrobial, antitubercular and anticancer activities of 2-(1-benzoyl-1 H-benzo [d] imidazol-2-ylthio)-N-substituted acetamides. *Chemistry Central Journal,* 12**,** 66.

YIN, Z., WANG, Y., WHITTELL, L. R., JERGIC, S., LIU, M., HARRY, E., DIXON, N. E., KELSO, M. J., BECK, J. L. & OAKLEY, A. J. 2014. DNA replication is the target for the antibacterial effects of nonsteroidal anti-inflammatory drugs. *Chemistry & biology,* 21**,** 481-487.

ZWOLINSKA-WCISLO, M., KRZYSIEK-MACZKA, G., PTAK-BELOWSKA, A., KARCZEWSKA, E., PAJDO, R., SLIWOWSKI, Z., URBANCZYK, K., DROZDOWICZ, D., KONTUREK, S. & PAWLIK, W. 2011. Antibiotic treatment with ampicillin accelerates the healing of colonic damage impaired by aspirin and coxib in the experimental colitis. Importance of intestinal bacteria, colonic microcirculation and proinflammatory cytokines. *Journal of Physiology and Pharmacology,* 62**,** 357.

RESEARCH PAPER

Detection of *Toxoplasma gondii* among Healthy Populations by Different Techniques in Erbil Province

Ahmed Akil Khudhair Al-Daoody, Tara Srood Suad, Hiba Rizgar Hashim, Omer Dler Babasheikh, Helen Yousif Akram, Sarab Khairadin Ali

Department of Medical Microbiology, College of Health Sciences, Hawler Medical University, Erbil, Kurdistan Region, Iraq.

A B S T R A C T:

   Toxoplasma gondii causes the foremost widespread protozoan infection with a broad variety of host range. Toxoplasmosis in Immunocompetent person is usually asymptomatic but severe complications might occur in immunocompromised persons and life threatening congenital infections can develop during pregnancy. This study was conducted to investigate the prevalence and risk factors of *T. gondii* among healthy populations in Erbil City. A total of 167 healthy participants were examined for the detection of *T. gondii* in Erbil City from November 2017 to January 2018 by using Latex agglutination test and ELFA-IgM and IgG. For collecting full information about the participants, a special questionnaire sheet was prepared and data were analyzed using SPSS software version 21. Out of 167 samples examined 41(24.6%) were positive by LAT, 14(8.4%) were positive for IgG by Mini-Vidas and 26(15.6%) were positive for IgM by Mini-Vidas. The prevalence rate of toxoplasmosis among females was (25.6%) which was higher than that seen among males (23.5%) but statistically insignificant. High seropositivity (28.2%) was observed in age group 11-20. Those who had contact with cats showed high percentage (25.7%) of infection, also in rural residents seropositivity was higher (30.8%) than urban residents (22.7%). No significant differences were observed between those who consumed and non-consumed fast food. Our study concluded that to reduce risk of toxoplasma infection in our community, it should avoidance direct contact with cat and soil, or consumes fast food, poultry or ordinary farm meat without sufficient cooking.

1.INTRODUCTION :

   Toxoplasmosis is a zoonotic parasitic infection of humans and animals produced by *Toxoplasma gondii* (Al-Mossawei *et al*., 2016). It belongs to coccidian parasites, which having an alternating two-generation life cycle (Koyee and Faraj, 2015; Lorenzi et al., 2016). *T. gondii* can infecting any mammalian or avian cells and replicating within these nucleated cells, has two part of life cycle; divided to sexual replication in feline host and asexual replication in nonfeline host (Abd Al-Hussien et al., 2016).

   Toxoplasmosis causes a lots of disease syndromes in women, ranging from headache-like symptoms in healthy adults, severe symptoms in immuno-deficiency individuals, to birth damage in fetus when females are exposed during pregnancy (Rahi and Jasim, 2011). In normal individuals, extracellular Tachyoites in acute phase of infection are rapidly destroyed and controlled with the immunity, whereas intracellular Bradyzoites multiplication is hindered, and formed tissue cysts, which are commonly found in the skeletal muscle, heart, retina and brain, generally cause little or no tissue lesion (Champoux et al., 2004). Chronic phase of toxoplasma infection might cause myocarditis, developing to permanent heart defect and pneumonia (Bogitsh et al., 2013).

* **Corresponding Author:**
Ahmed Akil Khudhair Al-Daoody
E-mail: ahmed.akil@hmu.edu.krd or ahmed_akil2007@yahoo.com

Khudhair Al-Daoody. A. *et al.* /ZJPAS: 2019, 31 (6): 75-83

76

Oocysts shed only in feces of feline family especialy cats, in intermediate host species, the ingestion of mature oocysts from contaminated water, soil or contact with cat feces cause infection in exposed host (Esch and Petersen, 2013). Humans also become infected by eating tissue cysts in raw or inadequate cooked meat (Hill and Dubey, 2002; Al-Daoody, 2012).

In human and mammals hosts, *T. gondii* is so much related with congenital infection and abortment; this parasite can be transmitted by cross the hemato-placental transmission of the rapidly growing tachyzoite form mother to fetus during pregnancy (Halonen and Weiss, 2009).

In addition, in several hosts tachyzoites may also be transmitted in the milk from the mother to the baby (Dubey, 2010). Transmission of *T.gondii* can also occur through blood transfusion if the donor has recently acquired toxoplasmosis and is parasitemic at the time of blood sampling, transmission can also occur during organ transplantation (Hill and Dubey, 2002).

Aims of the study

1. Detection of toxoplasmosis among healthy individuals in Erbil City.
2. Assess the risk factors of toxoplasmosis such as (contact with cat, contact with soil, type of meat consumed and residency) within the same investigated group.

2.MATERIALS AND METHODS

2.1 Study Population
The samples were collected from (November 2017 to January 2018) at Rizgari Hospital and Hawler Teaching Hospital. The study was conducted on 167 people (the age ranged from 3.5 to 35 years old) and various information about the participants was collected through a special questionnaire sheet.

2.3.Samples Collection

This study was carried out on 167 samples (81 Males and 86 Females). Blood samples were collected from all participants, and then transported to each of Rizgary and Hawler Teaching Hospital microbiology labs. The collected blood were centrifuged at 3000 rpm for 10 minutes to separate the sera which were then divided to 2 parts and placed into Eppendorf tubes labeled with names and numbers then stored at -20 c° in the freezer to be tested later.

2.3 Serological techniques

Three serological tests were performed on the samples to detect *T. gondii* infection, which were LAT (Latex Agglutination Test) was provided from PLASMATEC (UK) and ELFA (Enzyme Linked Fluorescence Assay)-IgG/IgM provided from (bioMerieux SA) (France) (L21-TOX.V1) (2010-07).
 Statistical Analysis

The results obtained from the serological techniques and the questionnaire data submitted to statistical analysis by using statistical package social system (SPSS v: 21).

RESULTS

3.1 Frequency of anti-*Toxoplasma* antibodies in the sera by Latex agglutination test, IgG test by mini-vidas device and IgM test by mini-vidas device:
A total of 167 participants were tested for *Toxoplasma gondii* antibodies in the present study by LAT test technique then by ELFA-IgG and ELFA-IgM antibodies by mini-vidas device. The overall percentage of infection were 41(24.6%) by LAT, 14(8.4%) by Mini Vidas – IgG and 26(15.6%) by Mini Vidas – IgM as seen in (**Table 1).**

Khudhair Al-Daoody. A. *et al.* /ZJPAS: 2019, 31 (6): 75-83

77

Table 1: Frequency of anti-*Toxoplasma* antibodies in the sera by three techniques.

Techniques	Participants		Total
	No. +ve (%)	No. -ve (%)	
Latex agglutination test	41(24.6)	126(75.4)	167
ELFA - IgG	14(8.4)	153(91.6)	167
ELFA - IgM	26(15.6)	141(84.4)	167

3.2 Sero-prevalence of anti-*Toxoplasma* antibodies in relation to gender by LAT:

As shown in **(Table 2),** in 167 samples (81) samples were taken from males and (86) from females. A higher sero-positivity was observed among females (25.6%) than males (23.5%), but the difference was statistically insignificant (P.value = 0.752).

Table 2: Sero prevalence of anti-*Toxoplasma* antibodies in relation to gender by LAT.

Gender	Latex agglutination test		Total	P.value
	No. +ve (%)	No. -ve (%)		
Male	19(23.5)	62(76.5)	81(48.5)	
Female	22(25.6)	64(74.4)	86(51.5)	0.752
Total	41(24.6)	126(75.4)	167(100)	

3.3 Distribution of anti-*Toxoplasma* antibodies among the surveyed population according to different age groups by LAT:

Seropositivity for anti-*Toxoplasma* antibodies appeared to be highest among the ages ranging from 11-20 years that had a seropositive result of 28.2% and close to that was among the ages of ≤10 years which had a result of 25 % followed by those among the age range 21-30 years which had a seropositivity of 22.5% and lowest results were

among the age group of ≥ 31 years that had a seropositivity of 10%. The differences were not statistically significant (P.value=0.602) as shown in **(Figure 1).**

Figure 1: Prevalence of anti-*Toxoplasma* antibodies according to age group by LAT.

3.4 Seropositivity of *Toxoplasma gondii* antibodies according to contact with cats by LAT:

In a total of 167 sample participants who had contact with cats had seropositivity of 9/35 (25.7%) while those who had no contact with cats had a seropositivity of 32/132 (24.2%). As presented in **(Table 3)** and have shown no statistical significance (P.value =0.857).

Table 3: Prevalence of anti-*Toxoplasma* antibodies according to the contact with cats by LAT.

Contact with cats	Latex agglutination test		Total	P.value
	No. +ve %)	No. -ve (%)		
Yes	9(25.7)	26(74.3)	35(21.0)	
No	32(24.2)	100(75.8)	132(79.0)	0.857
Total	41(24.6)	126(75.4)	167(100)	

3.5 Prevalence of *Toxoplasma gondii* antibodies according to residency by LAT:

Statistically no significant differences (P.value=0.303) were recorded in infection according to residency, after exam a total of 167 samples **(Figure 2).** Although higher seropositive results were recorded among rural residents 12/39(30.8%), while lower results were among urban residents 29/128 (22.7%).

Khudhair Al-Daoody. A. *et al.* /ZJPAS: 2019, 31 (6): 75-83

79
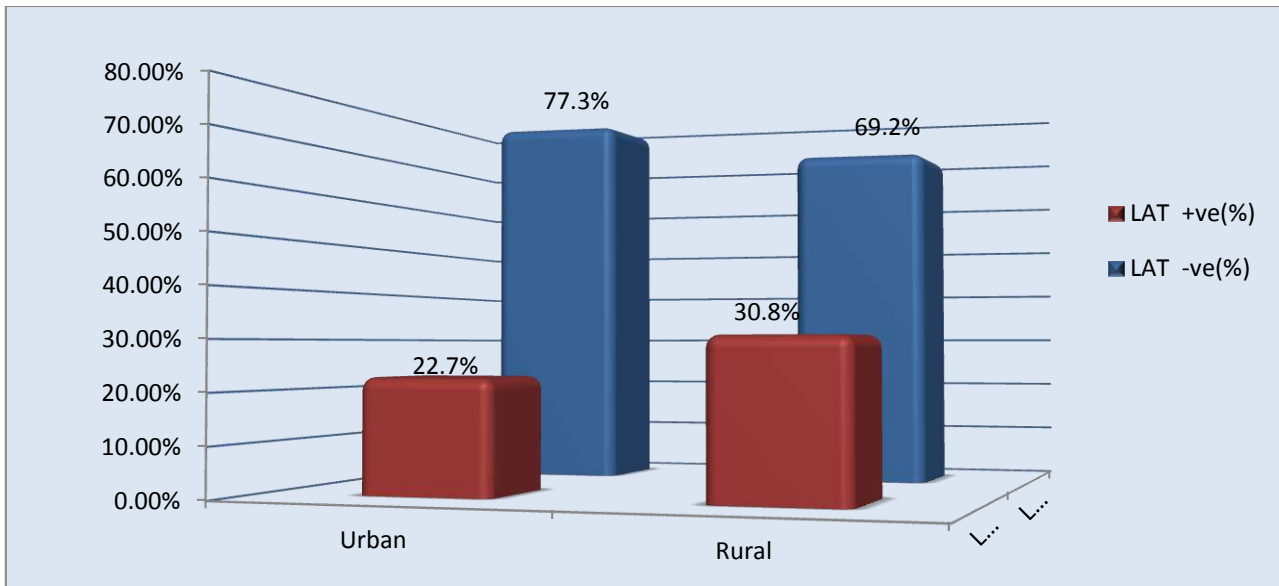
Figure 2: Prevalence of anti-*Toxoplasma* antibodies in a healthy population according to the residence area by LAT.

3.6 Seroprevalence of *Toxoplasma gondii* antibodies according to Fast-Food consumption by LAT:

As shown in **(Figure 3)** highest seropositivity was among those who consumed fast food, which was (25.4 %) while it was (22.0%) among those that didn't consume fast food but the difference was not statistically significant (P.value=0.656).
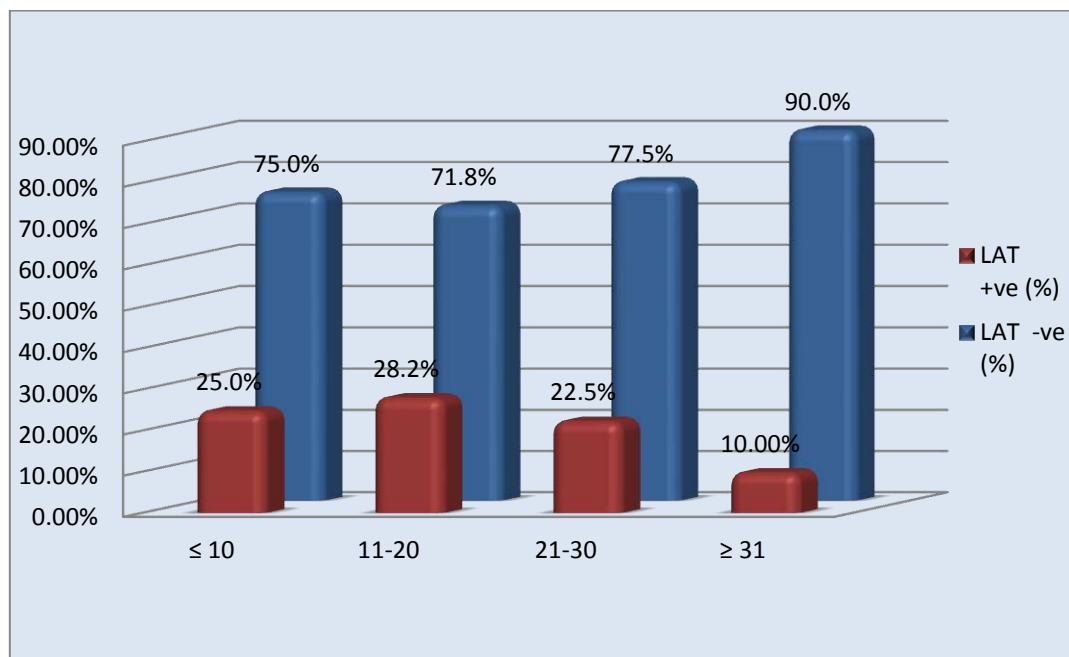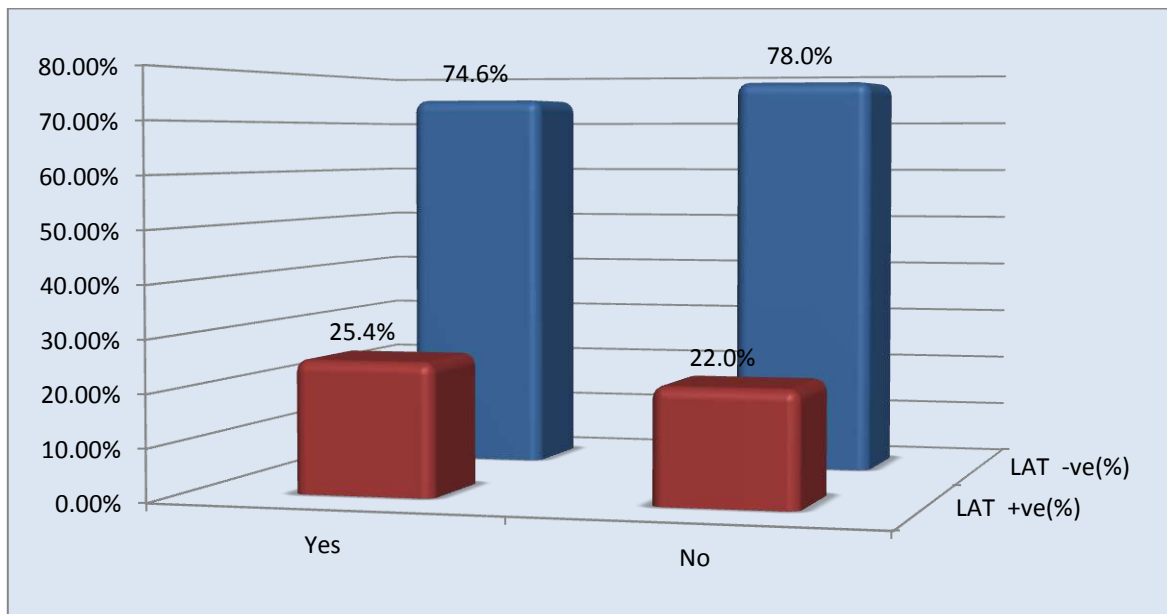

Figure 3: Prevalence of anti-*Toxoplasma* antibodies according to Fast-Food consumption by LAT.

3.7 Seropositivity of *Toxoplasma gondii* antibodies according to contact with soil by LAT:

As shown in **(Table 4).** The high rate of seropositivity was observed among those who had contact with soil (25.8%), while it was (23.8%)

Khudhair Al-Daoody. A. *et al.* /ZJPAS: 2019, 31 (6): 75-83

80

among those who had no contact with soil, although this difference statistically was not significant (P.value=0.77).

Table 4: Seroprevalence of anti-*Toxoplasma* according to contact with soil by LAT.

Contact with soil	Latex agglutination test		Total	P. value
	No. +ve (%)	No. -ve (%)		
Yes	17(25.8)	49(74.2)	66(39.5)	
No	24(23.8)	77(76.2)	101(60.5)	0.77
Total	41(24.6)	126(75.4)	167(100)	

3.8 Distribution of *Toxoplasma gondii* antibodies according to Type of meat consumed by LAT:

In a total of 167 samples highest seropositivity was among those who ate ordinary farm meat (27.5%) followed by those who ate both ordinary farm meat and poultry meat (23.7 %) While lowest seropositivity was observed among those who ate only poultry meat (23.5%) as seen in **(Figure 4),** but the difference was not statistically significant (P.value=0.884).
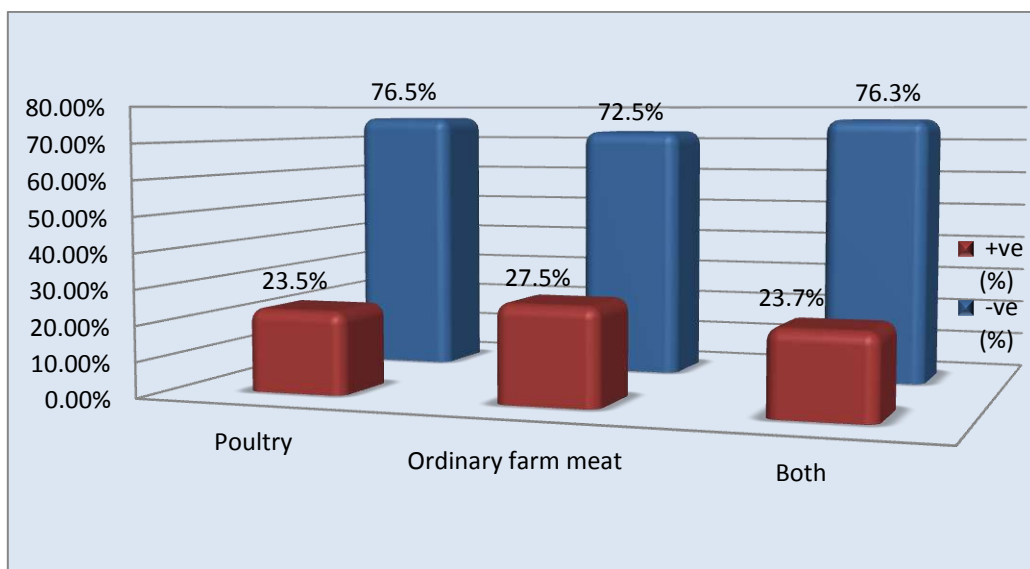
Figure 4: Prevalence of anti-*Toxoplasma* antibodies in relation to the type of meat consumed by the participants by LAT

4. DISCUSSION

The present study evaluates the prevalence of toxoplasmosis in healthy participants in Erbil city. The overall prevalence of anti-*Toxoplasma* antibody **(Table 1)** was (24.6%) by Latex agglutination test, this result is similar to other studies, which were done in Thi-qar (21.94%) by (Al-Mosawi *et al*., 2005), in Kirkuk (21.5%) by (Obaid, 2017), and in Kerbala (25.6%) by (Hasan,

2011). While disagree with (Shin *et al*., 2009) in Korea who recoded (6.6%), and in Mexico (4.6%) by (Galván-Ramírez *et al.,* 2010). Whereas higher results were recorded in Erbil (45.2%) by (Al-Daoody and Khoshnaw, 2012), in Baghdad (38%) by (Al-Mossawei *et al.,* 2016).

These differences in results might be due to differences in the environment, climate factors socio-demographic and habit differences in these populations, or could be due to used different methods to diagnose toxoplasma infection. Certain characteristics of the Korean population might contribute to the low prevalence. For example, in Korea, the range of meats that are eaten undercooked or raw is narrow; the frequency of raising a cat is low (Shin *et al*., 2009).

In our study no significant difference was observed between males and females although a higher seropositivity was observed among females (25.6%) than males (23.5%) **(Table 2).** Similar results were obtained by (Marques *et al.,* 2008) in Brazil. While other studies like that of Thi-qar by (Al-Mosawi *et al*., 2005) and Kirkuk by (Obaid, 2017), have shown a significant difference between male and female positive rates for anti-*Toxoplasma* antibodies. Higher seropositivity among females might be due to the fact that femlaes spend more time in the kitchen cooking handling meat and taste uncooked meat.

The highest occurrence of *T.gondii* antibody (28.2%) was among the age group (11-20) **(Figure 1)** this result was consistent to a study done in Mexico by (Galván-Ramírez *et al.,* 2010). The high prevalence among these age groups might be due to the possibility that most of them are students, which increases their contact with risk factors such as contact with soil or outdoor eating, and disagree with other studies in Erbil by (Al-Daoody, 2012) and in Kerbala by (Hasan, 2011), Which they stated that seroprevalence of toxoplasmosis increases with age.

Our results showed no significant difference among age groups, which is in agreement with results reported by (Obaid, 2017) in Kirkuk and (Sero-Prevalence of TORCH, 2017) in Erbil, but disagree with results reported by a study done in Kerbala by (Hasan, 2011).

Although cats are the definitive hosts that shed oocysts, statistically no significant difference was detected between persons who had contact with cats and those who had no contact with cats, in spite of high rate of infection was seen in persons that had contact with cats (25.7%) than those who had no contact with cats (24.2%) **(Table 3),** which might be due to the presence of many stray cats around the neighborhoods, this result is similar to studies done in Kirkuk by (Obaid, 2017), in Brazil by (Marques *et al.,* 2008) and in Ethiopia by (Gelaye *et al.,* 2015). In disagreement with our results was a study done by (Alrashada *et al.,* 2016) in Saudi Arabia that detected a lower seropositivity in those who had contact with cats, and studies done by (Galván-Ramírez *et al*., 2010) in Mexico and by (Rahi and Jasim, 2011) in Kut city, that showed there was a relationship between the prevalence of the disease and contact with cats. These differences might be due to the fact that pets are more common in Mexico than in Erbil or Kirkuk and also differences in basic personal hygiene among the surveyed populations of Kut and Erbil city.

In spite of no significant difference was observed between participants of urban and rural, but higher seropositivity was observed among rural residences (30.8%) **(Figure 2).** Similar results were obtained by a study in Iran by (Fallah *et al.,* 2014**).** In contrast to our result another study was done in Erbil by (Al-Daoody, 2012) that showed higher results among urban residences. Other studies like that of Kerbala by (Hasan, 2011) reported a significant statistical difference. The high infection rate in rural areas can be explained by the differences in life style, type of feeding, overcrowding, contact with animals and water source (Koyee and Faraj, 2015). In addition to the fact that urban residences might be have a general awareness about the disease and less contact with soil and animals, than rural residences, and water service facilities are well established in cities.

Our study showed no statistical significant difference between seropositivity and fast food consumption although the highest seropositivity was among those who consumed fast food, which was (25.4 %) while it was (22.0%) among those that didn't consume fast food **(Figure 3).** This might be due to the possibility of eating undercooked or uncooked meat containing *T. gondii* tissue cysts in restaurants and fast food facilities.

The prevalence of anti-*Toxoplasma* antibodies in our study according to the contact with soil was (25.8%) and (23.8%) in those who had no contact

Khudhair Al-Daoody. A. *et al.* /ZJPAS: 2019, 31 (6): 75-83

82

with soil **(Table 4),** but the differences were statistically insignificant. Other studies like that of Kerbala by (Hasan, 2011) had similar results.

The prevalence of anti-*Toxoplasma* antibodies was highest among those that ate ordinary farm meat (27.5%) followed by those who ate both ordinary farm meat and poultry meat (23.7 %) While lowest seropositivity was observed among those who ate only poultry meat (23.5%) but the differences were statistically insignificant **(Figure 4).** Similar results were reported by (Marques *et al.*, 2008) in Brazil that showed no significant difference between seropositivity and type of meat consumed. Ingesting tissue cyst containing undercooked or uncooked meat can infect humans (Al-Daoody and Khoshnaw, 2012).

5. CONCLUSIONS

In our research we concluded that. The rate of infected females was higher than the rate of infected males, there was no significant effect of contact of individual with cat or soil on prevalence of toxoplasmosis, and the people who consume fast food, poultry or ordinary farm meat are more likely to have toxoplasmosis, Finally in order to reduce the infection, we should avoidance contact with cat and soil, or eating these types of food without sufficient cooking.

ACKNOWLEDGEMENT

REFERENCES:

Abd Al-Hussien, E.F.; Nassir, N.F. and Kadhim, A. (2016). Study of prevalence and some immunological characteristics of *Toxoplasma gondii* infections in pregnant women. Journal of Babylon University/ pure and applied sciences; 24(2): 526-533.

Al-Daoody, A.A.Kh. (2012). Detection of *Toxoplasma gondii* antibodies in Persons Referred to Maamon-Dabbagh Health Center for Medical Examination before Marriage, Erbil, North of Iraq. Tikrit Medical Journal; 18(1): 11-25.

Al-Daoody, A.A.Kh. and Khoshnaw, K.J.S. (2012). Sero-prevalence and sensitivity patterns of anti-Toxoplasma IgM and IgG antibodies in pregnant women. Wassit Journal for Science and Medicine; 5(2):31-42.

Al-Mosawi, R.A.; AL-Aboody, B.A. and AL-Temimi, M.B. (2005). Diagnostic study of *Toxoplasma gondii* in students of Thi-Qar university-Iraq by Real- Time PCR. Iraqi Academic Scientific Journals; 5(2): 9-15.

Al-Mossawei, M.T.; AL-Mossawei, H.M. and AL-Dujaily, Kh.Y. (2016). Serological study of toxoplasmosis spread among unmarried female university students using LAT, ELISA and IgG avidity. Baghdad Science Journal; 13(4): 714-720.

Alrashada, N.; Alqarash, Z.; Alshehri, F.; Al-Khamees, L. and Alshqaqeeq, A. (2016). Toxoplasmosis among Saudi Female Students in Al-Ahssa, Kingdom of Saudi Arabia: Awareness and Risk Factors. Open Journal of Preventive Medicine; 6(8): 187-195.

Bogitsh, B.J.; Carter, C.E. and Oeltmann, T.N. (2013). Blood and Tissue Protozoa III: Other Protists. Human Parasitology. 4th edition. Netherlands. Elsevier; 3(6): 139-144.

Champoux, J.J.; Drew, W.L.; Neidheart, F.C.; Plorde, J.J.; Sporozoa, R.K.J. and Ray, C.G. (2004). Sheeris Medical Microbiology. 4th edition. New York City, U.S.A. McGraw-Hill; pp:722-727.

Dubey, J.P. (2010). Toxoplasmosis of Animals and Humans, 2nd edition. Taylor and Francis Group, U.K.; pp: 5-73.

Esch, K.J. and Petersen, Ch.A. (2013). Transmission and Epidemiology of Zoonotic Protozoal Diseases of Companion Animals. Clinical Microbiology Review; 26(1): 58-85.

Fallah, E.; Rasuli, A.; Shahbazi, A.; Ghojazadeh, M.; Khanmohammadi, M.; Hamzavi, F. and Roshanaei, R. (2014). Seroprevalence of *Toxoplasma gondii* Infection among High School Girls Ajabshir from East Azarbaijan Province, Iran. J caring Sci; 3 (3): 205-210.

Galván-Ramírez, M.D.; Pérez, L.R.; Agraz, S.Y.; Avila, L.S.; Armenta, A.S.; Corella, D.B.; Fernandez, J.R. and Sanroman, R.T. (2010). Seroepidemiology of toxoplasmosis in high-school students in the metropolitan area of Guadalajara, Jalisco, Mexico. Scientia Medica (Porto Alegre); 20(1): 59-63

Gelaye, W.; Kebede, T. and Hailu, A. (2015). High prevalence of anti-toxoplasma antibodies and absence of *Toxoplasma gondii* infection risk factors among pregnant women attending routine antenatal care in two Hospitals of Addis Ababa, Ethiopia. International Journal of Infectious Diseases; 34(1): 41–45.

Halonen, S.A. and Weiss, L.M. (2009). *Toxoplasma gondii* Presentations at the 10th International Workshops on Opportunistic Protists: 100 Years and Counting. American society for Microbiology; 8(4): 437-440.

Hasan, S.F. (2011). Seroprevalence of Toxoplasmosis Among comers to marriage in Kerbala governorate. Kerbala Journal of Pharmaceutical Sciences; 2. (7): 90-97.

Hill, D. and Dubey, J.P. (2002). *Toxoplasma gondii*: transmission, diagnosis and prevention. Maryland, USA. Clinical microbiology and infections; 8(10): 634-640.

Koyee, Q.M. and Faraj, A.M. (2015). Prevalence of Cryptosporidium Spp. With Other Intestinal

Khudhair Al-Daoody. A. *et al.* /ZJPAS: 2019, 31 (6): 75-83

83

Microorganisms among Regular Visitors of Raparin Pediatric Hospital in Erbil City-Kurdistan Region, Iraq. Zanco Journal of Pure and Applied Sciences; 27(4): 57-64.

Lorenzi, H.; Khan, A.; Behnke, M.S.; Namasivayam, S.; Swapna, L.S.; Hadjithomas, M.; *et al*.,. (2016). Local admixture of amplified and diversified secreted pathogenesis determinants shapes mosaic *Toxoplasma gondii* genomes. Nature communications; 7(11): 10133-47.

Marques, J.M.; Da Silva, D.V.; Correia, N.A.B.; Velasquez, L.G.; Da Silva, R.C.; Langoni, H. and Da Silva, A.V. (2008). Prevalence and Risk Factors for Human Toxoplasmosis in a Rural Community. J. Venom. Anim. Toxins incl. Trop. Dis; 14(4): 674-684.

Obaid, H.M. (2017). Survey study on toxoplasmosis among Kirkuk university students. Iraqi Academic Scientific Journals; 5(1): 253-259.

Rahi, A.A. and Jasim, S.E. (2011). Diagnosis of *Toxoplasma gondii* in Women by Dipstick Dye Immunoassay (DDIA). Wasit Journal for Science and Medicine; 4(2): 58-61.

Sero-Prevalence of TORCH Infections Among Pregnant and Non-Pregnant Women Using Different Immunological Techniques in Erbil City, Kurdistan Region / Iraq. ZANCO Journal of Pure and Applied Sciences, Vol. 29, no. 2, June (2017), https://zancojournals.su.edu.krd/index.php/JPAS/article/view/776.

Shin, D.; Cha, D.; Hua, Q.J.; Cha, G. and Lee, Y. (2009). Seroprevalence of *Toxoplasma gondii* Infection and Characteristics of Seropositive Patients in General Hospitals in Daejeon, Korea. Korean J Parasitol; 47(2):125-130.

RESEARCH PAPER

Polymorphism of miRNA and its Impact on IVF Failure

Rande Khasro Dizay[1], Suhad Asaad Mustafa[2]

1Department of Biology, College of Sciences, Salahaddin University-Erbil, Kurdistan Region, Iraq.

2Scientific Research Center, Salhaddin Univesity-Erbil, Erbil, Kurdistan Region, Iraq.

A B S T R A C T:

In vitro fertilization (IVF) failure is not only the cause of despair among couples and individuals undergoing the treatment, it´s also been contributing to the impediment of assistive reproductive technologies (ART) development, miRNAs have been linked to significant events in the reproduction course and the identification of miRNA polymorphisms may provide a good lead for the potential of diagnosis and treatment of unidentified IVF failure causes, the aim of the present study was to explore the association between the miRNA polymorphism (*mir-125a* T>Crs12975333) and IVF failure. Our case-control study consisted of 100 Kurdish women in total, 50 belong to the case group that underwent IVF failure and the other 50 belong to the control group who have had at least two successful pregnancies and no history of pregnancy loss, we used tetra amplification refractory mutation system to identify the polymorphisms within the groups, the TT genotype was found more frequently in IVF failure patients when compared to the healthy women (OR: 5.268, CI: 1.07-25.7, *P*=0.025) and T allele was more present in the case group (OR:1.9, CI:1.06-3.41, *P*=0.028). The difference in genotype and allele frequencies of *mir-125a* of the two groups may indicate that it has an effect on the target mRNAs and alter the implantation of embryo during IVF cycles.

1. INTRODUCTION :

MicroRNAs (miRNAs) are a class of small, single stranded, non-coding RNAs, first discovered in 1993 in *c. Elegans (*Lee *et al., 1993)*, miRNA´s main function is regulation of gene expression at the post-transcriptional level, they do so by degrading or blocking the translation of mRNA (messenger RNA) mostly by interacting with the 3´ untranslated region of the mRNA(Pogribny, 2018, O'Brien *et al*., 2018). MiRNAs are widely conserved across many species thus making them a sought after topic of research. Since each miRNA usually targets

hundreds of different mRNAs thus they act as the main controller of gene expression, the bulk of mammalian protein coding genes seem to be regulated under miRNA control(Bitetti *et al*., 2018), and the key biological processes; cell differentiation, proliferation, apoptosis, embryo implantation and its development are regulated by these molecules(Kim *et al*., 2019). MiRNAs have been associated with many female related disorders including ovarian cancer (Nakamura *et al*., 2016) breast cancer (Wang and Luo, 2015) endometriosis (Nothnick *et al*., 2015) and polycystic ovarian syndrome(Sørensen *et al*., 2014). The possibility of miRNAs affecting implantation in animal model was suggested by chakrabarty *et al* where they showed the effect of miRNA on certain genes that are involved in implantation(Chakrabarty *et al*., 2007). Another

study that was also based on animal model showed the differences in miRNA levels in IVF and *in vivo* embryos of porcine, where the changes were related to different stages of development and culture conditions(Stowe *et al*., 2012). Li *et al* showed that alterations in miRNA subsets affect the expression of certain genes that are crucial for implantation and hence decrease the embryo receptivity in women undergoing IVF treatment(Li *et al*., 2011). The relationship between *mmu-mir-367a* and its mRNA target (pcna) was the first example of miRNA regulating primordial follicle assembly in mice (Zhang *et al*., 2014).

Louise Brown was the first child born using *in vitro* fertilization back in July 15th 1978. This event became a beacon of hope for couples suffering from long or short term infertility. IVF has since then undergone many modifications and advancements and in 2014 it was reported that more than 5 million babies had been born with the aid of IVF (Kovacs, 2014), however like most other procedures it is yet to be perfected and the success rates are still relatively low. In humans, about 40% of unsuccessful IVF treatments are due to implantation failure(Dentillo *et al*., 2007), this failure can be related to the embryo transfer technique, embryo quality and endometrial receptivity (O'Flynn, 2014), the latter two are regulated by a cascade of events including miRNAs effect on different genes (Kropp and Khatib, 2015, Shi *et al*., 2017).

There are approximately 240 Single nucleotide polymorphisms (SNP) and rare mutations have been reported in miRNAs and their association with IVF outcome has been established (Kroliczewski *et al*., 2018, Lee *et al*., 2019, Cho *et al*., 2016).The appearance of a SNP in a miRNA's mature sequence may have different but certain consequences on the miRNA either by loss of binding, change in the binding efficacy or recognizing different mRNA targets than their own (Brennecke *et al*., 2005, Agarwal *et al*., 2015). Changes can also happen to miRNA biogenesis if the SNPs were introduced at the pre- or pri-miRNA sequences (Sood *et al*., 2006).

Even though the particular SNP has been studied to evaluate their relationship with other disease such as gastric cardia adenocarcinoma(Singh *et al*., 2017), Breast cancer (Peterlongo *et al*., 2011) autoimmune thyroid disease (Latini *et al*., 2017).

To our knowledge there is no previous publications to study the relation of rs12975333 to IVF failure, however *mir-125a* has been known to be a factor in many reproductive disorders in females such as primary ovarian failure in mice (Wang *et al*., 2016),Placenta Accreta (Gu *et al*., 2019), repeated pregnancy loss (Hu *et al*., 2014) unexplained recurrent spontaneous abortions (Li and Li, 2016) early pregnancy loss (Hosseini *et al*., 2018). In this present study we used Tetra ARMS (Amplification Refractory Mutation System) to detect SNPs of *mir-125a* G>T (rs12975333) in Kurdish women to evaluate their relation with IVF failure.

2. MATERIALS AND METHODS

2.1 Study Design

In total, 100 subjects were recruited for this study with ages ranging from (17-40) years, 50 female patients who have undergone failed IVF cycles were recruited from Hawler Maternal Hospital, Iraqi Kurdistan Region. The patients who had partners that were infertile (male factor infertility) and/or had any successful pregnancies were excluded. The control group also consisted of 50 subjects that were recruited in an outpatient clinic; these were healthy women who have had at least two successful pregnancies and had no history of miscarriages or any form of implantation failure. All subjects from both groups had their height and weight measured. Smokers and women above the age of 40 were excluded in this case-control study, the practical part of this study was conducted at the Scientific Research Center, Erbil, Iraq.

2.2Biochemical Analysis and Genotyping

Venous blood (5mL) was drawn from all subjects, 3mL of which was placed into a vacuumed EDTA tube for DNA extraction, while the rest was placed into a vacuumed Gel tube, they were then spun for 15 minutes at 10,000 rpm, the separated serum was then transferred to an Eppendorf tube for Biochemical analysis, all the tubes were frozen at -20° C for further analysis.

The hormonal assays were analyzed using cobas e411 (Roche Ltd, Switzerland).

DNA was extracted using GeNet Bio DNA extraction kit for whole blood and then tested for concentration and purity using Nanodrop (Thermo Scientific, UK), the samples appeared to have a concentration range between (22.13- 91.68 ng/µL) and were all within the normal range of purity. After optimization all samples were prepared for the PCR, In 0.2 mL PCR tubes containing 10µ of Master mix (Primer Taq Premix 2X, GeNet Bio) and the tetra primers each of 25 pmol concentration were added along with DNA and RNA free distilled water and DNA (50 ng). Then the PCR tubes were placed into the PCR wells (Techne TC-512, UK). DNA was visualized post PCR using a Gel Electrophoresis system (Cleaver, UK), the gel had a 2% agarose concentration and was stained with Safe Dye (Prime safe Dye, Genet Bio) prior to casting onto the tray. The DNA bands were then visualized using a Gel documentation system (Proxima 2500, India). Finally, the results were statistically analyzed using IBM SPSS Statistics v22.

2.3 Primer Design

The primers used in this research were designed by a web-based primer designing tool (Primer1) available at http://primer1.soton.ac.uk/primer1.html(Collins and Ke, 2012). For checking the primer specificity we used another web-based tool (PrimerBLAST) available at https://blast.ncbi.nlm.nih.gov/Blast.cgi, the designed primers are shown in **Table.1.**

Table 1. List of Primers used

Gene	Primer	Sequence 5´-3´	length	T_m[1]	T_a[2]	Expected amplicon size
mir-125a **rs12975333**	FO	CTATACGGCCTCCTAGCTTTCCCCAG	26	71.0	58.9	673 (Non-Specific)
	RO	CCAGGGGAGAAGCTAGTAACCTTTATGA	28	68.7		
	FI (T)	CATGTTGCCAGTCTCTAGGTCCCTAAT	27	68.3		263 (T-allele)
	RI (G)	TGGATGTCCTCACAGGTTAAAGGATC	30	66.3		463 (G-allele)

1: melting temperature, 2: annealing temperature, both measured in Celsius.

2.4 Tetra ARMS PCR Optimization

Optimization for *mir-125a* started by testing the primers at different concentrations (10, 25, 35 and 50 pmol) at an estimated annealing temperature, the optimum primer concentration was set at 25 pmol. Later we tested different annealing temperatures using Gradient PCR for each of the Forward Outer (FO) & Reverse Inner (RI), Forward Inner (FI) & Reverse Outer (RO), and FO & RO.

3. RESULTS

The first allele to be optimized was T-allele shown in **Figure (1)** which is an agarose gel image of a Gradient PCR for T-allele (FI & RO) at temperatures (57.1°-58.0°-58.9°-59.6°-61.3°-62.1°) we see the T-allele whose expected band size is at 263 bp shows up at all the temperatures with the thickest band at 58.9, as for G-allele whose expected band is at 463 bp and Non-specific whose expected band is at 673 bp are shown in **Figures (2** and **3) ,** respectively, they

both seem to demonstrate extra undesirable bands at temperatures lower than 59.6, as for all the tetra primers together we tested at the temperature range (57.1°-58.0°-58.9°-59.6°-61.3°-62.1°-63.0°) shown in **Figure (4).** The three expected bands show clearly at 58.9 however it fades in the following higher temperatures and doesn't show at lower temperatures, based on the information shown in these figures and other trials we concluded that the optimum PCR conditions for Tetra ARMS for *mir-125a* is 25 pmol primer concentration at 58.9° annealing temperature.

The subjects´ clinical and anthropometric characteristics including; Luteinizing hormone (LH), Estradiol, Progesterone, Prolactin, Thyroid Stimulating Hormone (TSH), Anti-Mullerian Hormone (AMH), Follicle Stimulating Hormone (FSH) and Body Mass Index (BMI), the data is presented in **Table (2**) in the form of mean± Standard deviation and *P*-value. There was no significant difference between the groups in all the criteria except for (Age) where women of the Case group had higher age mean (*P*=0.008) and (Family History) with regards to sibling history of infertility there was a significant difference (*P*=0.027) when the Case group was compared to the Control group, the genotypes for both case and control groups were detected using Tetra ARMS PCR analysis, the genotypes are as follows TT, GG and TG and they are shown in **Figure 5**. The statistical analysis of the genotype and allele frequencies is shown in **Table 3.** the genotype frequencies for the case group were 27, 14 and 9 for TG, GG and TT genotypes , respectively, while for the control group it were 26, 22 and 2 for TG, GG and TT genotypes , respectively, the TT Genotype was significantly higher in the IVF failure women (OR: 5.26, CI:1.07-25.7, *P*=0.025) as for the alleles GG and TG no significant difference was found between the two groups, Also T-allele was found more in the patient group with a significant difference(OR:1.9, CI:1.06-3.14, *P*=0.028).
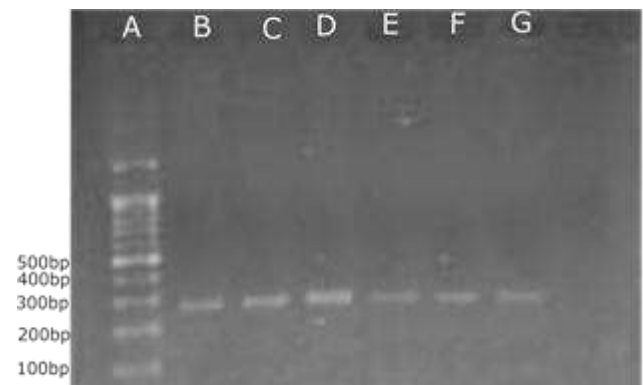
Figure 1. Image of T-allele optimization A: DNA marker, B:57.1°, C: 58.0°, D:58.9°, E:59.6°, F:61.3°, G:62.1°. 2% Gel.
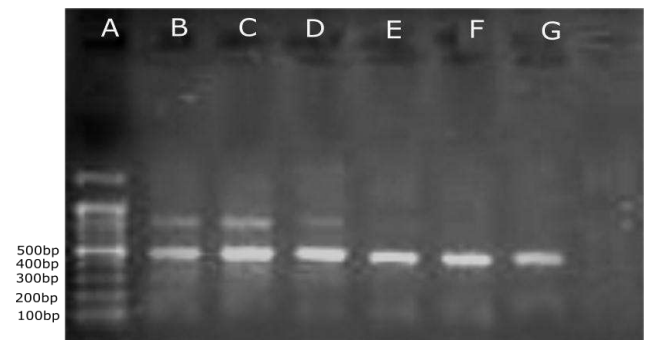
Figure 2. Image of G-allele optimization A: DNA marker, B:57.1°, C: 58.0°, D:58.9°, E:59.6°, F:61.3°, G:62.1°. 2% Gel.
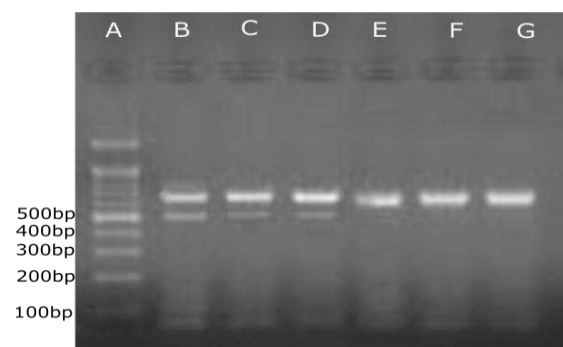
Figure 3. Image of non-specific band optimization A: DNA marker, B:57.1°, C: 58.0°, D:58.9°, E:59.6°, F:61.3°, G:62.1°, 2% Gel.
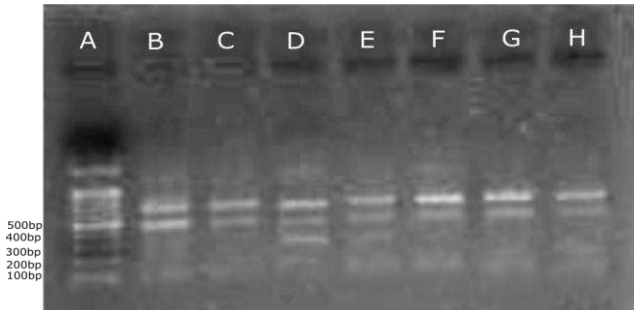
Figure 4. Image of tetra ARMS optimization A: DNA marker, B:57.1°, C: 58.0°, D:58.9°, E:59.6°, F:61.3°, G:62.1°, H: 63°. 2% Gel.
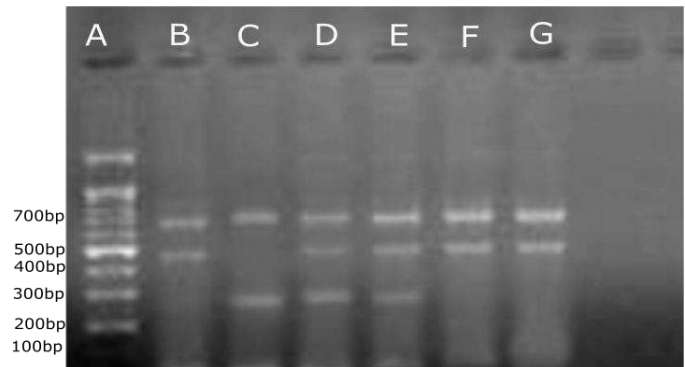
Figure 5. Image of gel showing all three genotypes A: DNA marker, B:GG, C: TT, D:TG, E:TG, F:GG, G:GG. 2% Gel.

Table 2. Clinical and Antrhopometric Characteristics of both case and control groups

Characteristic	Case (n.50)	Control (n.50)	*P* value
Luteinizing hormone	6.617[a]±3.652[b]	7.045[a]±4.552[b]	0.602
Estradiol	190.2±626.5	34.89±19.83	0.083
Progesterone	0.644±0.483	0.792±0.577	0.167
Prolactin	21.07±9.44	17.59±17.61	0.221
Thyroid Stimulating Hormone	2.505±1.523	2.227±1.833	0.310
Anti-Mullerian Hormone	2.883±2.07	2.503±1.042	0.249
Follicle Stimulating Hormone	6.951±2.952	6.579±1.822	0.450
Body Mass Index	29.0± 5.1	27.8±4.33	0.230
Age	33.6± 4.19	31.3± 4.57	0.008
Family History (Siblings) (n)% YES	7 (14)	1(2)	0.027
Family History (Relatives) (n)% YES	10 (20)	8(16)	0.62

a: Mean value, b: Standard deviation

Table 3. Genotype and Allele frequencies in Case and Control groups

Gene/SNP	Genotype	Allele	Case	Control	*P* value	OR (95% CI)
mir-125 T>G rs12975333	TT	NA	27	26	0.025	5.26(1.07-25.7)
	GG	NA	14	22	0.096	0.49(0.21-1.13)
	TG	NA	9	2	0.841	1.08(0.49-2.37)
	NA	T	45	30	0.028	1.90(1.06-3.41)
	NA	G	55	70		

NA: not applicable, OR: odds ratio, CI: Confidence interval.

4. DISCUSSION

In vitro fertilization has been marked by several milestones and accomplishments that are also accompanied by some obstacles that linger in regards to success rates. Our results show no significant difference between the clinical characteristics of IVF failure patients and the control group which means that we can omit the possibility of hormonal changes as a factor in this analysis, one interesting thing was that sibling family history was significantly higher in the case group when compared to the control group which suggests that there is definitely a genetic link between direct family history of infertility and IVF failure. the association between *mir-125a* G>T seems clear in our study as the TT genotype was found significantly more frequent in the case group which shows it is 5 times more likely to undergo failed IVF if the genotype TT is present, the main factor for IVF failure is implantation failure and Hu *et al* found that *miR-125a* was differentially detected in rats during the pre-implantation vs. implantation period (Hu *et al*., 2011)**,** a probable reason as to why mutations in *mir-125a* cause IVF failure is the change in expression of the two genes LIFR and ERB2, the former has been related to trophoblast growth and placental differentiation while the latter has been found to play a role in differentiation of trophoblast cells and stromal proliferation, which has been elucidated when a study was conducted on two variants of *mir-125a* in women with recurrent pregnancy loss (Hu *et al*., 2011). Another possibility is the effect of the miRNA on embryo development, however when Borges *et al* studied miRNAs in culture media of in vitro embryos they eliminated that possibility since among other of *mir-125a* exhibited no difference in expression levels (Borges *et al*.), bioinformatics study shows that *mir-125a* a member of the *mir-125* family is involved in preimplantation embryo development by control *sebox* maternal effect gene which is known to pay role in very early embryonic development (Kim *et al*., 2016) the expression levels of miR-125a in mural and cumulus granulosa cells which are involved in folliculogenesis in healthy women who are undergoing IVF treatment (Andrei *et al*., 2019)*lin-28,* a controller of pluripotency of embryonic stem cells has been shown to be downregulated by *mir-125a* which further demonstrate the effect of this miRNA on embryonic development in mice (Potenza and Russo, 2013, Kim *et al*., 2016) Hu *et al* also studied mutations in the pri-region of *mir-125a* genes affect functions endometrium including cell proliferation, migration, proliferation and embryonic development in women with repeated pregnancy loss(Hu *et al*., 2014) the above mentioned research further validate our results.

5. CONCLUSIONS

In conclusion our study found a significant association the TT genotype of *mir-125a* G>T polymorphism and IVF failure. Although the exact roles of the genotype require further exploratory experiments, their discovery may lead to an insight into understanding the complex reasoning behind IVF failure. We recommend other researchers to go into expressional studies and the genotypes effect on its target genes.

Conflict of Interest

The authors declare no conflict of interest.

REFERENCES

AGARWAL, V., BELL, G. W., NAM, J. W. & BARTEL, D. P. 2015. Predicting effective microRNA target sites in mammalian mRNAs. *Elife,* 4.

ANDREI, D., NAGY, R. A., VAN MONTFOORT, A., TIETGE, U., TERPSTRA, M., KOK, K., VAN DEN BERG, A., HOEK, A., KLUIVER, J. & DONKER, R. 2019. Differential miRNA Expression Profiles in Cumulus and Mural Granulosa Cells from Human Pre-ovulatory Follicles. *Microrna,* 8**,** 61-67.

BITETTI, A., MALLORY, A. C., GOLINI, E., CARRIERI, C., CARREÑO GUTIÉRREZ, H., PERLAS, E., PÉREZ-RICO, Y. A., TOCCHINI-VALENTINI, G. P., ENRIGHT, A. J., NORTON, W. H. J., MANDILLO, S., O'CARROLL, D. & SHKUMATAVA, A. 2018. MicroRNA degradation by a conserved target RNA regulates animal behavior. *Nature Structural & Molecular Biology,* 25**,** 244-251.

BORGES, E., JR., SETTI, A. S., BRAGA, D. P. A. F., GERALDO, M. V., FIGUEIRA, R. D. C. S. & IACONELLI, A., JR. miR-142-3p as a biomarker of blastocyst implantation failure - A pilot study. *JBRA assisted reproduction,* 20**,** 200-205.

BRENNECKE, J., STARK, A., RUSSELL, R. B. & COHEN, S. M. 2005. Principles of MicroRNA–Target Recognition. *PLOS Biology,* 3**,** e85.

CHAKRABARTY, A., TRANGUCH, S., DAIKOKU, T., JENSEN, K., FURNEAUX, H. & DEY, S. K. 2007. MicroRNA regulation of cyclooxygenase-2 during embryo implantation. *Proc Natl Acad Sci U S A,* 104**,** 15144-9.

CHO, S. H., CHUNG, K. W., KIM, J. O., JANG, H., YOO, J. K., CHOI, Y., KO, J. J., KIM, J. H., NISHI, Y., YANASE, T., LEE, W. S. & KIM, N. K. 2016. Association of miR-146aC>G, miR-149C>T, miR-196a2T>C, and miR-499A>G polymorphisms with risk of recurrent implantation failure in Korean women. *Eur J Obstet Gynecol Reprod Biol,* 202**,** 14-9.

COLLINS, A. & KE, X. 2012. Primer1: primer design web service for tetra-primer ARMS-PCR. *The Open Bioinformatics Journal,* 6.

DENTILLO, D. B., SOUZA, F. R., MEOLA, J., VIEIRA, G. S., YAZLLE, M. E., GOULART, L. R. & MARTELLI, L. 2007. No evidence of association of MUC-1 genetic polymorphism with embryo implantation failure. *Braz J Med Biol Res,* 40**,** 793-7.

GU, Y., MENG, J., ZUO, C., WANG, S., LI, H., ZHAO, S., HUANG, T., WANG, X. & YAN, J. 2019. Downregulation of MicroRNA-125a in Placenta Accreta Spectrum Disorders Contributes Antiapoptosis of Implantation Site Intermediate Trophoblasts by Targeting MCL1. *Reproductive Sciences***,** 1933719119828040.

HOSSEINI, M. K., GUNEL, T., GUMUSOGLU, E., BENIAN, A. & AYDINLI, K. 2018. MicroRNA expression profiling in placenta and maternal plasma in early pregnancy loss. *Mol Med Rep,* 17**,** 4941-4952.

HU, Y., HUO, Z.-H., LIU, C.-M., LIU, S.-G., ZHANG, N., YIN, K.-L., QI, L., MA, X. & XIA, H.-F. 2014. Functional study of one nucleotide mutation in pri-miR-125a coding region which related to recurrent pregnancy loss. *PloS one,* 9**,** e114781-e114781.

HU, Y., LIU, C.-M., QI, L., HE, T.-Z., SHI-GUO, L., HAO, C.-J., CUI, Y., ZHANG, N., XIA, H.-F. & MA, X. 2011. Two common SNPs in pri-miR-125a alter the mature miRNA expression and associate with recurrent pregnancy loss in a Han-Chinese population. *RNA biology,* 8**,** 861-872.

KIM, J., LEE, J. & JUN, J. H. 2019. Identification of differentially expressed microRNAs in outgrowth embryos compared with blastocysts and non-outgrowth embryos in mice. *Reprod Fertil Dev,* 31**,** 645-657.

KIM, K.-H., SEO, Y.-M., KIM, E.-Y., LEE, S.-Y., KWON, J., KO, J.-J. & LEE, K.-A. 2016. The miR-125 family is an important regulator of the expression and maintenance of maternal effect genes during preimplantational embryo development. *Open biology,* 6**,** 160181.

KOVACS, P. 2014. Embryo selection: the role of time-lapse monitoring. *Reprod Biol Endocrinol,* 12**,** 124.

KROLICZEWSKI, J., SOBOLEWSKA, A., LEJNOWSKI, D., COLLAWN, J. F. & BARTOSZEWSKI, R. 2018. microRNA single polynucleotide polymorphism influences on microRNA biogenesis and mRNA target specificity. *Gene,* 640**,** 66-72.

KROPP, J. & KHATIB, H. 2015. Characterization of microRNA in bovine in vitro culture media associated with embryo quality and development. *J Dairy Sci,* 98**,** 6552-63.

LATINI, A., CICCACCI, C., NOVELLI, G. & BORGIANI, P. 2017. Polymorphisms in miRNA genes and their involvement in autoimmune diseases susceptibility. *Immunologic research,* 65**,** 811-827.

LEE, H. A., AHN, E. H., JANG, H. G., KIM, J. O., KIM, J. H., LEE, Y. B., LEE, W. S. & KIM, N. K. 2019. Association Between miR-605A>G, miR-608G>C, miR-631I>D, miR-938C>T, and miR-1302-3C>T Polymorphisms and Risk of Recurrent Implantation Failure. *Reprod Sci,* 26**,** 469-475.

LEE, R. C., FEINBAUM, R. L. & AMBROS, V. 1993. The C. elegans heterochronic gene lin-4 encodes small RNAs with antisense complementarity to lin-14. *Cell,* 75**,** 843-54.

LI, D. & LI, J. 2016. Association of miR-34a-3p/5p, miR-141-3p/5p, and miR-24 in decidual natural killer cells with unexplained recurrent spontaneous abortion. *Medical science monitor: international medical journal of experimental and clinical research,* 22**,** 922.

LI, R., QIAO, J., WANG, L., LI, L., ZHEN, X., LIU, P. & ZHENG, X. 2011. MicroRNA array and microarray evaluation of endometrial receptivity in patients with high serum progesterone levels on the day of hCG administration. *Reproductive biology and endocrinology : RB&E,* 9**,** 29-29.

NAKAMURA, K., SAWADA, K., YOSHIMURA, A., KINOSE, Y., NAKATSUKA, E. & KIMURA, T. 2016. Clinical relevance of circulating cell-free

microRNAs in ovarian cancer. *Molecular cancer,* 15**,** 48-48.

NOTHNICK, W. B., AL-HENDY, A. & LUE, J. R. 2015. Circulating Micro-RNAs as Diagnostic Biomarkers for Endometriosis: Privation and Promise. *Journal of minimally invasive gynecology,* 22**,** 719-726.

O'BRIEN, J., HAYDER, H., ZAYED, Y. & PENG, C. 2018. Overview of MicroRNA Biogenesis, Mechanisms of Actions, and Circulation. *Frontiers in Endocrinology,* 9.

O'FLYNN, N. 2014. Assessment and treatment for people with fertility problems: NICE guideline. *Br J Gen Pract,* 64**,** 50-51.

PETERLONGO, P., CALECA, L., CATTANEO, E., RAVAGNANI, F., BIANCHI, T., GALASTRI, L., BERNARD, L., FICARAZZI, F., DALL'OLIO, V. & MARME, F. 2011. The rs12975333 variant in the miR-125a and breast cancer risk in Germany, Italy, Australia and Spain. *Journal of medical genetics,* 48**,** 703-704.

POGRIBNY, I. P. 2018. MicroRNAs as biomarkers for clinical studies. *Exp Biol Med (Maywood),* 243**,** 283-290.

POTENZA, N. & RUSSO, A. 2013. Biogenesis, evolution and functional targets of microRNA-125a. *Molecular genetics and genomics,* 288**,** 381-389.

SHI, C., SHEN, H., FAN, L.-J., GUAN, J., ZHENG, X.-B., CHEN, X., LIANG, R., ZHANG, X.-W., CUI, Q.-H., SUN, K.-K., ZHAO, Z.-R. & HAN, H.-J. 2017. Endometrial MicroRNA Signature during the Window of Implantation Changed in Patients with Repeated Implantation Failure. *Chinese medical journal,* 130**,** 566-573.

SINGH, D. K., ZHANG, W., XU, Y., YIN, J., GU, H. & JIANG, P. 2017. Hsa-miR-34b/c rs4938723 T> C, pri-miR-124-1 rs531564 C> G, pre-miR-125a rs12975333 G> T and hsa-miR-423 rs6505162 C> A polymorphisms and the risk of gastric cardia adenocarcinoma. *Int J Clin Exp Med,* 10**,** 14919-14926.

SOOD, P., KREK, A., ZAVOLAN, M., MACINO, G. & RAJEWSKY, N. 2006. Cell-type-specific signatures of microRNAs on target mRNA expression. *Proc Natl Acad Sci U S A,* 103**,** 2746-51.

SØRENSEN, A., WISSING, M., SALÖ, S., ENGLUND, A. & DALGAARD, L. 2014. MicroRNAs related to polycystic ovary syndrome (PCOS). *Genes,* 5**,** 684-708.

STOWE, H. M., CURRY, E., CALCATERA, S. M., KRISHER, R. L., PACZKOWSKI, M. & PRATT, S. L. 2012. Cloning and expression of porcine Dicer and the impact of developmental stage and culture conditions on MicroRNA expression in porcine embryos. *Gene,* 501**,** 198-205.

WANG, C., LI, D., ZHANG, S., XING, Y., GAO, Y. & WU, J. 2016. MicroRNA-125a-5p induces mouse granulosa cell apoptosis by targeting signal transducer and activator of transcription 3. *Menopause,* 23**,** 100-107.

WANG, W. & LUO, Y.-P. 2015. MicroRNAs in breast cancer: oncogene and tumor suppressors with clinical potential. *Journal of Zhejiang University. Science. B,* 16**,** 18-31.

ZHANG, H., JIANG, X., ZHANG, Y., XU, B., HUA, J., MA, T., ZHENG, W., SUN, R., SHEN, W., COOKE, H. J., HAO, Q., QIAO, J. & SHI, Q. 2014. microRNA 376a regulates follicle assembly by targeting Pcna in fetal and neonatal mouse ovaries. *Reproduction,* 148**,** 43-54.

RESEARCH PAPER

Synthesis, Spectroscopic study and Biological activity of some New Heterocyclic compounds derived from Sulfadiazine

Sangar A. Hassan[1], Media N. Abdullah[2]

[1]Department of Chemistry, College of Science, University of Raparin, Sulaimanyah, Kurdistan Region, Iraq
[2]Department of Chemistry, College of Science, Salahaddin University-Erbil, Kurdistan Region, Iraq

A B S T R A C T:

This study illustrates the synthesis and spectroscopic study of new β-lactam and novel Pyrrolone derivatives with the study of their antioxidant and antibacterial activities. This study included two major steps, the first step involved the synthesis of imine derivatives (**3a-j**) from sulfadiazine. The second step contained the synthesis of 2-Azetidinone (**4a-j**) and Pyrrolone (**5a-j**) heterocyclic compounds that have been generated through the reaction between synthesized imine derivatives with chloroacetyl chloride and fumaryl chloride in the presence of triethylamine, respectively. The structures of the synthesized compounds were confirmed on the basis of their spectral data such as FT-IR, ^{1}H-NMR and ^{13}C-NMR spectra, which provided the expected frequencies and signals. Lastly, all products were screened for the antioxidant activity and against two kinds of bacteria *Staphylococcus aureus G (+ve)* and *Escherichia coli G (-ve)* microorganisms. The products showed lower to high antioxidant activity as compared to standard ascorbic acid. Some of the products evaluated inactive and others slight to high activity against both kinds of bacteria.

1. INTRODUCTION

Heterocyclic compounds are ring compounds that contain one hereto atom or more in addition to carbon. Heterocyclic compounds are very important due to their wide applications in industrial drug designs (Taylor et al., 2016), especially those heterocycles that contain nitrogen atoms (Gupta and Halve, 2015) , biological fields (Al-Mulla, 2017), and medicinal chemistry (Arya et al., 2014).

Sulfadiazine is one of the pyrimidinyl sulfonamide derivatives (Shahid et al., 2018). The large numbers of synthetic antibacterial sulfonamides with their different modifications have allowed to examine the effect of structural alteration on the antibacterial activity (Mohammed abd al-khaliq, 2015).

The first synthesis of Schiff base has been reported in the 19th century by Schiff (1864), then a various methods for the synthesis of azomethines have been described (Adam, 2018), (Zheng et al., 2009). Imine compounds are broadly applied in the medicinal and the pharmaceutical fields because they have antibacterial, antifungal and antitumor activity (Sinha et al., 2008). And they are used as polymer stabilizers, pigments, dyes, catalysts, and intermediate in organic synthesis (Da Silva et al., 2011).

* **Corresponding Authors:**
Sangar Ali Hassan and Media Noori Abdullah
E-mail: sangar.ali@uor.edu.krd or media.abdullah@su.edu.krd

Hassan. S. *and* Abdullah .M/ZJPAS: 2019, 31 (6): 92-109

93

2-Azetidinones, commonly known as *β*-lactams which is a four membered cyclic amide in which the nitrogen atom is attached to the *β*-carbon relative to the carbonyl. The first synthetic *β*-lactam has been prepared by Hermann Staudinger in 1907 from the reaction of the imine of aniline and benzaldehyde with diphenylketene in a [2+2] cycloaddition (Salunkhe and Piste, 2014). Azetidine-2-ones are part of antibiotics structure are known to exhibit interesting biological activities (Abdulsada et al., 2018).

Pyrrolones (pyrrolin-2-ones) are the five-membered heterocyclic ring and can be synthesized by different methods using Schiff bases (Kumar et al., 2014). It have the wide spectrum of biological activities (Nunna et al., 2014) such as anti-inflammatory, analgesic, antibacterial (El-Shehry et al., 2013) cardiotonic (Böhm et al., 1991) and antitumor activities (Ali et al., 2014).

Because of the importance and interesting class of four and five membered heterocyclic ring system and their wide spectrum of biological activities. We have synthesized the series of new azetidine-2-one and novel series of pyrrolone derivatives, from synthesized Sulfadiazine Schiff bases by using Ultrasound assisted technique and studied their antioxidant and antibacterial activities.

2. MATERIAL AND METHODS

Open capillary tubes were used to measure the melting points. Reactions have been examined by thin layer chromatography via silica gel-G as adsorbent using n-hexane: methanol: chloroform (6:2:2) as eluent. Sonication was implemented in an ultrasonic cleaner (DIGITAL PRO$^+$, 40 KHz and a normal power 180 W, in Raparin University). FT-IR ranges have been documented on spectrometer (Thermo Fisher FT-IR Model: Nicolet iS 10, in Raparin University), Spectrophotometer (JENWAY Model: 6705, in Raparin University). ^{1}H-NMR and ^{13}C-NMR spectra recorded on a Bruckner (400 MH$_Z$, in Zanjan University/ Iran) using TMS as internal standard and (DMSO-d6), chemical shift are assessed in parts per million (δ ppm), and the abbreviations used were s=singlet, d=doublet, t=triplet, m=multiplet, br=broad.

2.1. General Procedure for the synthesis of sulfadiazine Schiff bases (3a-j)

An equimolar quantity of sulfadiazine (0.01 mole) and different substituted aromatic aldehydes (0.01 mole) were dissolved in a 15 ml of methanol, then a catalytic amount of glacial acetic acid was added. The solution irradiated in the ultrasonic bath at 60 ^{o}C for (30-60 minutes). The complete of the reaction was controlled by a thin-layer chromatography. The volume of the solvent minimized to half, chilled, the achieved precipitate was filtered, dried and recrystallized by the mixture of absolute ethanol and n-hexane (70:30). All of the produced compounds were shown in the (**Table 1**).

Table 1: Physical data for the sulfadiazine Schiff base derivatives (**3a-j**)

Comp.	-R	Chemical Formula	color	Yield %	m.p. ^{o}C
3a	2-OH	$C_{17}H_{14}N_4O_3S$	yellow-orang	93	246-248
3b	2-Cl	$C_{17}H_{13}ClN_4O_2S$	white	91	205-207
3c	4-OCH$_3$	$C_{18}H_{16}N_4O_3S$	white	88	225-229
3d	4-NO$_2$	$C_{17}H_{13}N_5O_4S$	milky	90	265-269
3e	3-NO$_2$	$C_{17}H_{13}N_5O_4S$	light yellow	87	250-253
3f	-H	$C_{17}H_{14}N_4O_2S$	white-yellow	85	207-210
3g	4-F	$C_{17}H_{13}FN_4O_2S$	light yellow	83	225-228
3h	2-OH,3-OCH$_3$	$C_{18}H_{16}N_4O_4S$	orange	89	230-234
3i	Cinnamaldehyde	$C_{19}H_{16}N_4O_2S$	yellow	91	211-214
3j	4-N(CH$_3$)$_2$	$C_{19}H_{19}N_5O_2S$	dark-yellowish	88	245-248

Hassan. S. *and* Abdullah .M/ZJPAS: 2019, 31 (6): 92-109

94

2.2. General Procedure for the synthesis of 2-azetidinones (4a-j)

The synthetized Schiff base (**3a-j**), (0.01 mole) and triethylamine (0.02 mole) were dissolved in a dry 1,4-dioxane (25 ml), chloroacetyl chloride (0.02 mole) added to the mixture in portion wise with vigorous stirring for 30 minutes at (0–5 ^{o}C). The resulted mixture was treated in ultrasonic bath 2 hours. The triethylamine hydrochloride formed during the reaction was filtered off and the filtrated stand at room temperature for 48 hours, the organic phase extracted with (25 mL) of ethyl acetate, splashed with water (2x50 mL) to remove the excess chloroacetyl chloride and dried up with MgSO$_4$. Under reduced pressure the solvent was eliminated and the products were collected (**Table 2**).

Table 2: Physical data for 2-azetidinone derivatives (**4a-j**)

Comp.	R	Chemical formula	color	Yield %	M.p. ^{o}C
4a	2-OH	$C_{19}H_{15}ClN_4O_4S$	milky	85	173-176
4b	2-Cl	$C_{19}H_{14}Cl_2N_4O_3S$	white-yellow	83	190-193
4c	4-OCH$_3$	$C_{20}H_{17}ClN_4O_4S$	yellow	81	207-211
4d	4-NO$_2$	$C_{19}H_{14}ClN_5O_5S$	white-yellow	82	177-180
4e	3-NO$_2$	$C_{19}H_{14}ClN_5O_5S$	orange	83	187-191
4f	H	$C_{19}H_{15}ClN_4O_3S$	light yellow	82	198-202
4g	4-F	$C_{19}H_{14}ClFN_4O_3S$	milky	80	229-232
4h	2-OH,3-OCH$_3$	$C_{20}H_{17}ClN_4O_5S$	white	85	235-238
4i	Cinnamaldehyde	$C_{21}H_{17}ClN_4O_3S$	yellow	84	163-166
4j	4-N(CH$_3$)$_2$	$C_{21}H_{20}ClN_5O_3S$	yellow-orange	82	210-214

2.3. General Procedure for synthesis of 2*H*-pyrrole-2-ones or Pyrrolones (5a-j)

The synthesized Schiff base (0.01 moles) (**3a-j**) and triethyl amine (0.02 moles) were dissolved in dry 1,4-dioxane (25 ml), to this mixture, fumaryl chloride solution (0.02 moles) was added in corresponding portion with strong stirring at (0–5 ^{o}C) for an hour. The resulted mixture was irradiated for 3 hours by ultrasonic at room temperature. Triethylamine hydrochloride that formed during the reaction was filtrated off and the filtrated stand at room temperature for 24 hours. The residual was poured into crushed-ice water the excess fumaryl chlorid was converted to fumaric acid which dissolve in the water. The precipitate was recrystallized by the mixture of absolute ethanol and n-hexane (70:30), to offer the preferred product (**Table 3**).

Table 3: Physical data for pyrrolone derivatives (**5a-j**)

Comp.	R	Chemical Formula	Color	Yield %	M.p. ^{o}C
5a	2-OH	$C_{21}H_{16}N_4O_6S$	light brown	92	178-180
5b	2-Cl	$C_{21}H_{15}ClN_4O_5S$	brown	86	158-161
5c	4-OCH$_3$	$C_{22}H_{18}N_4O_6S$	rusty	88	170-174
5d	4-NO$_2$	$C_{21}H_{15}N_5O_7S$	brown	89	195 dec.
5e	3-NO$_2$	$C_{21}H_{15}N_5O_7S$	light yellow	90	230-234
5f	H	$C_{21}H_{16}N_4O_5S$	yellow	85	240 dec.
5g	4-F	$C_{21}H_{15}FN_4O_5S$	yellow	85	210-213
5h	2-OH,3-OCH$_3$	$C_{22}H_{18}N_4O_7S$	brown	86	220 dec.
5i	Cinnamaldehyde	$C_{23}H_{18}N_4O_5S$	light brown	91	188-191
5j	4-N-(CH$_3$)$_2$	$C_{21}H_{16}N_4O_6S$	dark brown	87	246-250

Dec= decomposition

Hassan. S. *and* Abdullah .M/ZJPAS: 2019, 31 (6): 92-109

95

2.4. General procedure for antioxidant activity

Three different concentrated solutions have been prepared (1, 25 and 50 µg/ml) from the synthesized compounds. An equal amount of sample solution was added to an equal amount of 0.1 mM ethanolic DPPH (2, 2-diphenyl-1-picrylhydrazyl) solution, vortexes and allowed to stand at the dark place at 25°C for 30 min for the reaction to occur. After 30 min of incubation period, the absorbance was read against a blank at 517 nm with UV/Visible spectrophotometer.

$$DPPH \text{ scavenged } (\%) = \frac{Ac - As}{Ac} * 100$$

Ac - is control reaction's absorbance.
As - is synthesized compound's absorbance.

2.5. General procedure for antibacterial activity

The Agar diffusion method was used. The well of the Agar was made by sterile cork borer, which is equal to (6mm in diameter). 100 µl of each (500 ppm and 1000 ppm) synthesized compound solutions was added to the bacteria plates. DMSO are used as solvent to dissolve our synthesized compounds because it has not inhibition activity, also it can be used as a control negative. For 24 hours the plated have been incubated, and at 37 °C.

3. RESULTS AND DISCUSSION

3.1. Schiff base derivatives (3a-j)

The Schiff base derivatives are made via condensation reaction of amine with diverse aromatic aldehydes by using methanol as solvent and glacial acetic acid as a catalyst (**Scheme 1**)

R= 2-OH, 2-Cl, 3-OCH₃, 4-NO₂, 3-NO₂, H, 4-F, 2-OH-3-OCH₃ and 4-N(CH₃)₂
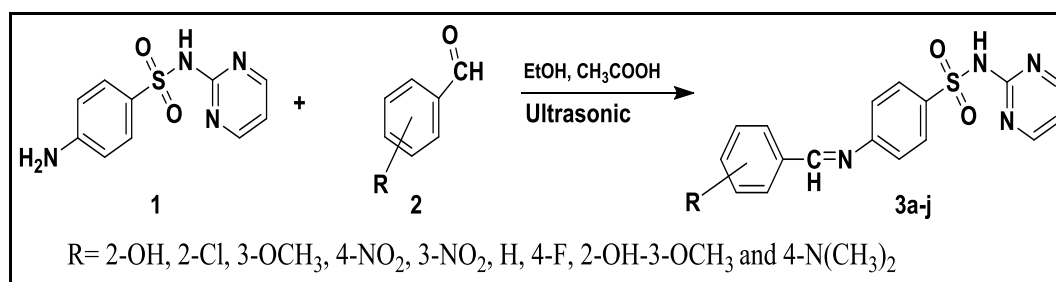
Scheme 1: Synthesis of Schiff base derivatives (**3a-j**)

The FT-IR of Schiff base derivatives have been illustrated in the (**Table 4**) that showed different bands, the important bands region (1594-1630 cm^{-1}) that refer to the (C=N) imine extending vibration, and the disappearance of (NH₂) and (C=O) bands in sulfadiazine and aromatic aldehydes respectively, these changes are proved that the Schiff base derivatives are formed.

Table 4: FT-IR Absorption bands for the Schiff base derivatives (**3a-j**)

Comp.	N-H str.	C-H Ar. str.	CH=N	C=C str.
3a	3350	3029	1619	1579
3b	3294	3029	1629	1577
3c	3287	3026	1625	1578
3d	3332	3040	1594	1578
3e	3301	3039	1626	1579
3f	3302	3040	1623	1579
3g	3281	3045	1630	1579
3h	3297	3040	1615	1578
3i	3298	3027	1625	1577
3j	3267	3042	1603	1573

Hassan. S. *and* Abdullah .M/ZJPAS: 2019, 31 (6): 92-109

96

The ^{1}H-NMR data for imine derivatives (**3a-j**) in (**Table 5**) are shown a signal for the proton of (C$\underline{\text{H}}$=N) groups at (9.00–8.40) ppm; while the aromatic protons are appeared at the region (8.80 – 6.80) ppm.

Table 5: ^{1}H-NMR Chemical shifts data for the Schiff base compounds (**3a-j**)

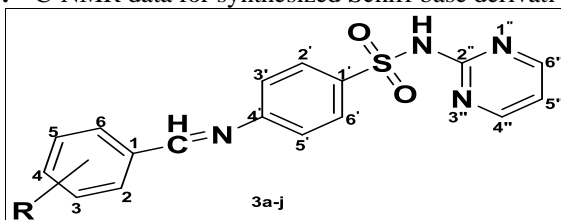| Comp.	br, s SO$_2$N$\underline{\text{H}}$	s C$\underline{\text{H}}$=N	m (H $_{Ar.}$)	Other Different group protons
3a	11.92	8.98	8.55-7.03	12.55 (s, O$\underline{\text{H}}$)
3b	11.81	8.85	8.52-7.10	
3c	11.82	8.51	8.54-7.10	3.850 (s, OC$\underline{\text{H}}_3$)
3d	11.55	8.53	8.51-7.03	
3e	11.22	8.84	8.80-7.09	
3f	11.86	8.63	8.54-7.07	
3g	11.85	8.63	8.52-7.08	
3h	11.94	9.00	8.54-6.92	12.66 (s, O$\underline{\text{H}}$), 3.86 (s, OC$\underline{\text{H}}_3$)
3i	11.85	8.40	8.52-7.10	7.34 (d, J=8.4 Hz, ph-C$\underline{\text{H}}$ aldehyde) 7.07 (t, J=4.8 Hz, J=9.6 Hz, C=C$\underline{\text{H}}$ aldehyde).
3j	11.78	8.42	8.54-6.80	3.06 (s, N-(C$\underline{\text{H}}_3$)$_2$)

In ^{13}C-NMR data of the Schiff base derivatives (**3a-j**), (**Table 6**) the signals for the carbon of (C$\underline{\text{}}$=N) group of compounds appeared at (160.73 – 157.36) ppm, also these data confirm the formation of the sulfadiazine Schiff base.

**Table 6:** ^{13}C-NMR data for synthesized Schiff base derivatives (**3a-j**)

Comp.	^{13}C-NMR
3a	165.86 (C̲ 2"), 162.87 (C̲ 2), 160.73 (C̲=N), 158.89 (C̲ 4"), 157.34 (C̲ 6"), 152.72 (C̲ 4'), 138.44 (C̲ 1'), 134.51 (C̲ 4), 133.05 (C̲ 6), 129.57 (C̲ 2', C̲ 6'), 122.23 (C̲ 3', C̲ 5'), 119.86 (C̲ 5), 119.79 (C̲ 1, 117.20 (C̲ 3), 116.32 (C̲ 5").
3b	159.25 (C̲ 2"), 158.88 (C̲ 6"), 158.80 (C̲ 4"), 157.38 (C̲=N), 155.40 (C̲ 4'), 138.16 (C̲ 1'), 135.89 (C̲ 1), 134.01 (C̲ 2), 132.65 (C̲ 4), 130.64 (C̲ 3), 129.56 (C̲ 2', C̲ 6'), 129.11 (C̲ 6), 128.20 (C̲ 5), 121.73 (C̲ 3', C̲ 5'), 116.31 (C̲ 5").
3c	162.72 (C̲ 2"), 158.88 (C̲ 4), 158.73 (C̲=N), 157.70 (C̲ 6"), 157.41 (C̲ 4"), 156.18 (C̲ 4'), 137.14 (C̲ 1'), 132.31 (C̲ 2), 131.43 (C̲ 6), 130.11 (C̲ 2'), 129.47 (C̲ 6'), 128.94 (C̲ 1), 121.6 (C̲ 3', C̲ 5'), 116.32 (C̲ 5"), 114.99 (C̲ 3), 114.85 (C̲ 5), 55.94 (OC̲H$_3$).
3d	162.09 (C̲ 2"), 158.80 (C̲=N), 157.62 (C̲ 6"), 157.41 (C̲ 4"), 147.84 (C̲ 4'), 146.95 (C̲ 4), 141.40 (C̲ 1), 138.46 (C̲ 1'), 130.33 (C̲ 2'), 129.97 (C̲ 6'), 128.58 (C̲ 2), 128.17 (C̲ 6), 124.55 (C̲ 3), 124.10 (C̲ 5), 116.13 (C̲ 5"), 112.99 (C̲ 3'), 112.62 (C̲ 5').
3e	161.98 (C̲ 2"), 158.91 (C̲=N), 157.70 (C̲ 6"), 157.62 (C̲ 4"), 153.53 (C̲ 4'), 148.67 (C̲ 3), 137.51 (C̲ 1'), 135.35 (C̲ 1), 131.43 (C̲ 6), 131.11 (C̲ 5), 129.51 (C̲ 2'), 129.04 (C̲ 6'), 126.72 (C̲ 2), 123.63 (C̲ 4), 121.83 (C̲ 3', C̲ 5'), 116.00 (C̲ 5").
3f	163.64 (C̲ 2"), 158.88 (C̲=N), 157.66 (C̲ 6"), 157.41 (C̲ 4"), 155.86 (C̲ 4'), 137.60 (C̲ 1'), 136.00 (C̲ 1), 132.58 (C̲ 4), 130.36 (C̲ 6), 129.51 (C̲ 2), 125.34 (C̲ 3, C̲ 5), 121.64 (C̲ 2', C̲ 6'), 116.32 (C̲ 3'), 115.99 (C̲ 5'), 112.64 (C̲ 5").
3g	166.06 (C̲ 2"), 162.36 (C̲ 4), 158.87 (C̲=N), 157.71 (C̲ 4"), 157.41 (C̲ 6"), 155.69 (C̲ 4'), 137.65 (C̲ 1'), 131.87 (C̲ 1), 130.33 (C̲ 6, C̲ 2), 129.98 (C̲ 2'), 129.48 (C̲ 6'), 121.64 (C̲ 3', C̲ 5'), 116.65 (C̲ 3), 116.43 (C̲ 5), 115.99 (C̲ 5").
3h	166.01 (C̲ 2"), 158.88 (C̲ 4"), 158.73 (C̲ 6"), 157.36 (C̲=N), 153.55 (C̲ 4'), 152.51 (C̲ 2), 148.40 (C̲ 3), 138.48 (C̲ 1'), 130.36 (C̲ 6, C̲ 2'), 129.61 (C̲ 6'), 124.29 (C̲ 6), 122.21 (C̲ 3"), 119.69 (C̲ 1), 117.97 (C̲ 5), 116.31 (C̲ 5"), 115.99 (C̲ 4), 58.94 (OC̲H$_3$).
3i	165.01 (C̲ 2"), 158.88 (C̲=N), 158.73 (C̲ 4"), 157.41 (C̲ 6"), 155.87 (C̲ 4'), 146.48 (C̲ 1'), 137.49 (C̲ 1), 135.66 (ph-C̲ aldehyde), 129.56 (C̲ 3, C̲ 5, C̲ 2', C̲ 6'), 124.29 (C̲ 4), 129.48 (C̲ 2, C̲ 6), 129.00 (C̲ 3', C̲ 5'), 121.52 (C=C̲ aldehyde), 115.99(C̲ 5").
3j	162.58 (C̲ 2"), 158.88 (C̲ 4"), 158.74 (C̲ 6"), 157.43 (C̲=N), 156.76 (C̲ 4'), 153.24 (C̲ 4), 136.38 (C̲ 1'), 131.29 (C̲ 2', C̲ 6'), 129.44 (C̲ 2, C̲ 6), 123.71 (C̲ 1), 121.53 (C̲ 3', C̲ 5'), 116.31 (C̲ 5"), 111.89 (C̲ 3, C̲ 5), 58.94 (N-(C̲H$_3$)$_2$).

3.2. 2-Azetidinone derivatives (4a-j)

Hassan. S. *and* Abdullah .M/ZJPAS: 2019, 31 (6): 92-109

97

4-membered heterocyclic compounds are known as 2-azetidinone or (β-lactam) were synthesized from the reaction of azomethine derivatives (**3a-j**) with chloroacetyl chloride in the present triethylamine as illustrated in (**Scheme 2**).

R= 2-OH, 2-Cl, 3-OCH$_3$, 4-NO$_2$, 3-NO$_2$, H, 4-F, 2-OH-3-OCH$_3$ and 4-N(CH$_3$)$_2$
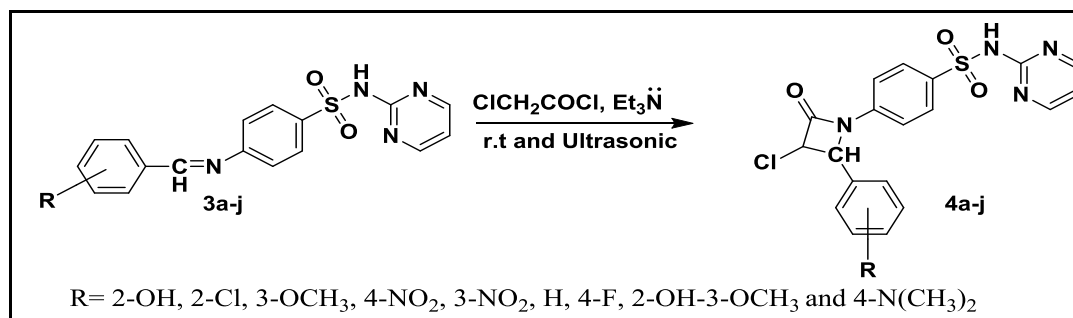
Scheme 2: Synthesis of 2-azetidinone derivatives (**4a-j**)

The general feature of the FT-IR absorption bands of 2-azetidinones derivatives (**4a-j**) which has been shown in (**Table 7**) consists of the presence of bands at (1765– 1701) cm^{-1} which belong to carbonyl groups in 2-azetidinones structure, this evidence confirmed the formation of the described products.

Table 7: FT-IR Absorption band of 2-azetidinone derivatives (**4a-j**)

Comp.	N-H str.	C-H Ar. str.	C=O str.	C=C str.
4a	3343	3036	1733	1580
4b	3303	3035	1721	1580
4c	3269	3036	1736	1573
4d	3312	3036	1701	1576
4e	3303	3035	1721	1581
4f	3313	3035	1748	1580
4g	3269	3036	1736	1573
4h	3324	3081	1723	1580
4i	3298	3036	1704	1581
4j	3314	3036	1765	1585

Table (8) has shown the ^{1}H–NMR chemical shift for 2-Azetidinones (**4a-j**). The proton of (CH=N) group of imines were appeared as a singlet in the region (9.00–8.40 ppm) and converted to doublet and appeared in the region (5.68-4.53) ppm as (CH-N $_{lactam}$) group of 2-azetidinones. Other difference when 2-azetidinone derivatives are formed a doublet was appeared in the region (6.08-4.74) ppm which belongs to (CH-Cl $_{lactam}$), which are a good evidence for obtaining the desired β-lactam products.

Table 8: ^{1}H–NMR data for the prepared 2-Azetidinone compounds (**4a-j**)

Comp	br, s (SO$_2$NH)	m (H $_{Ar.}$)	CH-Cl $_{lactam}$	CH-N $_{lactam}$	Other different group protons
4a	11.85	8.55-6.64	5.16 (d, J=13.2 Hz)	5.06 (d, J=12 Hz)	10.001 (s, OH)
4b	11.80	8.63-7.08	5.35 (d, J=12 Hz)	5.27 (d, J=12 Hz)	
4c	11.19	8.51-7.12	5.35 (d, J=12 Hz)	5.31 (d, J=12 Hz)	3.41(s, OCH$_3$)
4d	11.94	8.96-6.93	5.62 (d, J=29.2Hz)	5.52 (d, J=30.4Hz)	
4e	10.90	8.44-7.25	5.92 (d, J=33.2 Hz)	5.48 (d, J=32.8Hz)	
4f	11.26	8.43-7.26	5.06 (d, J=30.4 Hz)	4.94 (d, J=28 Hz)	
4g	11.81	8.52-7.06	6.08 (d, J=12.4 Hz)	5.68 (d, J=11.6 Hz)	
4h	12.70	8.76-7.07	5.53 (d, J=22.4 Hz)	5.43 (d, J=22 Hz)	10.99 (s, OH), 4.022 (s, OCH$_3$)

Hassan. S. *and* Abdullah .M/ZJPAS: 2019, 31 (6): 92-109

98

4i	11.86	8.76-7.27	4.74 (d, J=11.2 Hz)	4.53 (t, J=11.6Hz, J=23.6Hz)	7.15 (d, J=8 Hz, ph-C$\underline{H}$), 6.88 (t, J=7.2 Hz, J=16 Hz,-C=C$\underline{H}$)
4j	11.78	8.52-7.05	5.34 (d, J=22.4 Hz)	5.17 (d, J=18.4 Hz)	3.05 (s, N-(C$\underline{H}_3$)$_2$)

In the (**Table 9**) the ^{13}C–NMR data for the synthesized compounds **(4a-e)** shows that the carbon of carbonyl groups appears at (166.09–154.31) ppm, in addition to a signal for ($\underline{C}$–N $_{lactam}$) and ($\underline{C}$-Cl $_{lactam}$) carbon groups that appeared at (70.89–57.41) ppm, which are the strong evidence for the formation of the anticipated products.

Table 9: ^{13}C-NMR data for the 2-Azetidinone derivatives **(4a-j)**
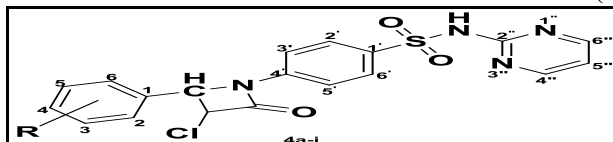
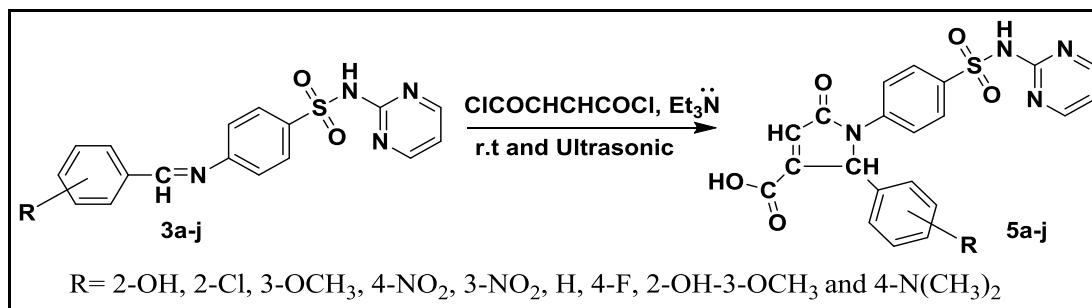| Comp.	^{13}C-NMR
4a	168.31 ($\underline{C}$ 2"), 166.09 ($\underline{C}$=O $_{lactam}$), 161.84 ($\underline{C}$ 4", $\underline{C}$ 6"), 158.73 ($\underline{C}$ 2), 157.70 ($\underline{C}$ 4'), 152.86 ($\underline{C}$ 1'), 138.46 ($\underline{C}$ 1), 135.50 ($\underline{C}$ 2', $\underline{C}$ 6'), 129.97 ($\underline{C}$ 4), 129.51 ($\underline{C}$ 6), 122.57 ($\underline{C}$ 5), 121.84 ($\underline{C}$ 3'), 121.73 ($\underline{C}$ 5'), 116.31 ($\underline{C}$ 3), 116.09 ($\underline{C}$ 5"), 68.39 ($\underline{C}$-Cl $_{lactam}$), 65.98 ($\underline{C}$-N $_{lactam}$).
4b	162.87 ($\underline{C}$ 2"), 162.72 ($\underline{C}$=O $_{lactam}$), 158.88 ($\underline{C}$ 4"), 158.73 ($\underline{C}$ 6"), 157.70 ($\underline{C}$ 1), 156.18 ($\underline{C}$ 4'), 137.14 ($\underline{C}$ 1'), 132.31 ($\underline{C}$ 2), 130.33 ($\underline{C}$ 2'), 130.11 ($\underline{C}$ 6'), 129.97 ($\underline{C}$ 3, $\underline{C}$ 6), 128.94 ($\underline{C}$ 4), 125.31 ($\underline{C}$ 5),121.60 ($\underline{C}$ 3', $\underline{C}$ 5'), 116.32 ($\underline{C}$ 5"), 63.70 ($\underline{C}$-N $_{lactam}$), 59.43 ($\underline{C}$-Cl $_{lactam}$).
4c	163.64 ($\underline{C}$ 2"), 158.88 ($\underline{C}$=O $_{lactam}$), 157.66 ($\underline{C}$ 4"), 157.41 ($\underline{C}$ 6"), 155.86 ($\underline{C}$ 4'), 153.55 ($\underline{C}$ 1', $\underline{C}$ 4), 137.60 ($\underline{C}$ 1), 136.65 ($\underline{C}$ 2'), 136.00 ($\underline{C}$ 6'), 132.58 ($\underline{C}$ 6, $\underline{C}$ 2), 129.38 ($\underline{C}$ 3' ,$\underline{C}$ 5'), 121.64 ($\underline{C}$ 3, $\underline{C}$ 5), 116.32 ($\underline{C}$ 5"), 63.90 ($\underline{C}$-N $_{lactam}$), 58.85 ($\underline{C}$-Cl $_{lactam}$), 57.35 (O$\underline{C}$H$_3$).
4d	169.81 ($\underline{C}$ 2"), 154.31 ($\underline{C}$=O $_{lactam}$), 142.86 ($\underline{C}$ 4", $\underline{C}$ 6"), 137.63 ($\underline{C}$ 1), 132.23 ($\underline{C}$ 4), 130.12 ($\underline{C}$ 4'), 129.76 ($\underline{C}$ 1'), 128.79 ($\underline{C}$ 2), 128.56 ($\underline{C}$ 6), 128.20 ($\underline{C}$ 3), 128.5 ($\underline{C}$ 5), 126.98 ($\underline{C}$ 2'), 126.62 ($\underline{C}$ 6'), 123.89 ($\underline{C}$ 3'), 123.07 ($\underline{C}$ 5'), 115.95 ($\underline{C}$ 5"), 70.89 ($\underline{C}$-N $_{lactam}$), 63.86 ($\underline{C}$-Cl $_{lactam}$).
4e	164.69 ($\underline{C}$ 2"), 162.72 ($\underline{C}$=O $_{lactam}$), 158.88 ($\underline{C}$ 4"), 158.73 ($\underline{C}$ 6"), 137.14 ($\underline{C}$ 3), 132.31 ($\underline{C}$ 1), 131.43 ($\underline{C}$ 4'), 130.33 ($\underline{C}$ 1'), 130.11 ($\underline{C}$ 6), 129.47 ($\underline{C}$ 2'), 128.94 ($\underline{C}$ 6'), 121.60 ($\underline{C}$ 3', $\underline{C}$ 5', $\underline{C}$ 4), 116.32 ($\underline{C}$ 2), 114.99 ($\underline{C}$ 5"), 70.83 ($\underline{C}$-N $_{lactam}$), 64.99 ($\underline{C}$H-Cl $_{lactam}$).
4f	169.82 ($\underline{C}$ 2"), 154.33 ($\underline{C}$=O $_{lactam}$), 142.87 ($\underline{C}$ 4", $\underline{C}$ 6"), 137.63 ($\underline{C}$ 1), 130.13 ($\underline{C}$ 4'), 129.77 ($\underline{C}$ 1'), 128.79 ($\underline{C}$ 2'), 128.56 ($\underline{C}$ 6'), 128.19 ($\underline{C}$ 3), 128.05 ($\underline{C}$ 5), 126.62 ($\underline{C}$ 2), 126.37 ($\underline{C}$ 6), 124.54 ($\underline{C}$ 4), 123.89 ($\underline{C}$ 3'), 123.09 ($\underline{C}$ 5'), 115.95 ($\underline{C}$ 5"), 70.33 ($\underline{C}$-N $_{lactam}$), 66.87 ($\underline{C}$-Cl $_{lactam}$).
4g	164.69 ($\underline{C}$ 2"), 162.87 ($\underline{C}$=O $_{lactam}$), 162.72 ($\underline{C}$ 4), 158.88 ($\underline{C}$ 4"), 157.70 ($\underline{C}$ 6"), 137.14 ($\underline{C}$ 4'), 132.31 ($\underline{C}$ 1), 131.43 ($\underline{C}$ 1'), 130.33 ($\underline{C}$ 2'), 130.11 ($\underline{C}$ 6'), 129.47 ($\underline{C}$ 2), 128.94 ($\underline{C}$ 6), 121.60 ($\underline{C}$ 3', $\underline{C}$ 5'), 114.99 ($\underline{C}$ 5"), 114.85 ($\underline{C}$ 3), 112.61 ($\underline{C}$ 5), 73.65 ($\underline{C}$-N $_{lactam}$), 65.88 ($\underline{C}$-Cl $_{lactam}$).
4h	169.09 ($\underline{C}$ 2"), 161.35 ($\underline{C}$=O $_{lactam}$), 160.11 ($\underline{C}$ 4", $\underline{C}$ 6"), 136.92 ($\underline{C}$ 3), 128.13 ($\underline{C}$ 2), 128.08 ($\underline{C}$ 4'), 125.04 ($\underline{C}$ 1'), 124.85 ($\underline{C}$ 2', $\underline{C}$ 6'), 123.19 ($\underline{C}$ 1), 122.79 ($\underline{C}$ 5), 121.99 ($\underline{C}$ 3'), 121.66 ($\underline{C}$ 5'), 116.55 ($\underline{C}$ 6), 116.48 ($\underline{C}$ 5"), 114.50 ($\underline{C}$ 4), 57.41 ($\underline{C}$-N $_{lactam}$), 55.94 ($\underline{C}$-Cl $_{lactam}$), 52.64 (O$\underline{C}$H$_3$).
4i	166.69 ($\underline{C}$ 2"), 162.93 ($\underline{C}$=O $_{lactam}$), 158.83 ($\underline{C}$ 4", $\underline{C}$ 6"), 143.02 ($\underline{C}$ 4'), 142.91 ($\underline{C}$ 1', $\underline{C}$ 1), 137.08 (ph-$\underline{C}$ $_{aldehyde}$), 135.35 ($\underline{C}$ 2'), 135.29 ($\underline{C}$ 6'), 134.77 ($\underline{C}$ 3), 134.48 ($\underline{C}$ 5), 131.99 (C=$\underline{C}$ $_{aldehyde}$), 129.46 ($\underline{C}$ 2, $\underline{C}$ 6), 126.48 ($\underline{C}$ 4),119.43 ($\underline{C}$ 3', $\underline{C}$ 5') 118.96 ($\underline{C}$ 5"), 69.46 ($\underline{C}$-N $_{lactam}$), 62.93 ($\underline{C}$-Cl $_{lactam}$).
4j	166.79 ($\underline{C}$ 2"), 165.90 ($\underline{C}$=O $_{lactam}$), 162.92 ($\underline{C}$ 4"), 162.14 ($\underline{C}$ 6"), 144.18 ($\underline{C}$ 4), 138.32 ($\underline{C}$ 4'), 137.62 ($\underline{C}$ 1'), 131.28 ($\underline{C}$ 1), 129.65 ($\underline{C}$ 2', $\underline{C}$ 6'), 129.10($\underline{C}$ 2, $\underline{C}$ 6), 126.78 ($\underline{C}$ 3', $\underline{C}$ 5'), 120.09 ($\underline{C}$ 5"), 118.97 ($\underline{C}$ 3, $\underline{C}$ 5), 63.54 ($\underline{C}$-N $_{lactam}$), 54.93 ($\underline{C}$-Cl $_{lactam}$), 49.07 (N-(C$\underline{H}_3$)$_2$).

3.3. 2*H*-pyrrole-2-ones derivatives (5a-j)

Five membered nitrogen heterocyclic compounds 2*H*-pyrrole-2-one or (pyrrolone) derivatives **(5a-j)** are synthesized from the reaction of imines **(3a-j)** with fumaryl chloride in the present triethylamine as illustrated in **(Scheme 3)**.

Hassan. S. *and* Abdullah .M/ZJPAS: 2019, 31 (6): 92-109

99

R= 2-OH, 2-Cl, 3-OCH$_3$, 4-NO$_2$, 3-NO$_2$, H, 4-F, 2-OH-3-OCH$_3$ and 4-N(CH$_3$)$_2$

Scheme 3: Synthesis of pyrrolone derivatives (**5a-j**)

The general feature of the FT-IR absorption bands of synthesized pyrrolone derivatives (**5a-j**) which has been shown in (**Table 10**) consists of bands at (1676 –1660) cm^{-1} which belong to carbonyl groups in pyrrolone structure. The (N-H$_{str}$) peak was disappeared due to the broad peak of (OH$_{str}$) at the region (3500-2500) cm^{-1} (**Figure 9**).

Table 10: FT-IR Absorption band of 2*H*-pyrrole-2-ones derivatives (5a-j)

Comp.	N-H and OH str.	C-H Ar. str.	C=O str.	C=C str.
5a	3500-2500	3082	1662	1587
5b	3500-2500	3082	1666	1590
5c	3500-2500	3082	1661	1526
5d	3500-2500	3085	1664	1527
5e	3500-2500	3083	1659	1592
5f	3500-2500	3082	1660	1591
5g	3500-2500	3082	1666	1583
5h	3500-2500	3082	1661	1586
5i	3500-2500	3083	1666	1586
5j	3500-2500	3034	1676	1589

Table (**11**) shows the ^{1}H–NMR chemical shifts for 2*H*-pyrrole-2-one derivatives (**5a-j**) the protons of (C$\under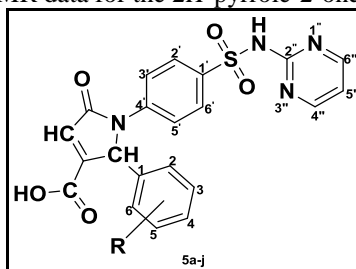line{H}$-N $_{pyrrolone}$) appeared as a singlet in the region (5.97-5.10) ppm. The proton of carboxylic acid (COO$\underline{H}$) appeared in the region (13.20- 12.26) ppm.

Table 11: ^{1}H-NMR data for 2*H*-pyrrole-2-one derivative compounds (**5a-j**)

Comp	s COO$\underline{H}$	br, s SO$_2$N$\underline{H}$	m, (H $_{Ar.}$)	S C$\underline{H}$-C=O pyrrolone	S C$\underline{H}$-N pyrrolone	Other different group protons
5a	13.06	11.56	8.57-6.67	7.244	5.20	10.15 (s, O$\underline{H}$)
5b	13.20	11.75	7.99-6.70	with H$_{Ar}$	5.15	
5c	13.12	11.00	8.51-6.66	with H$_{Ar}$	5.97	3.87 (s, (OC$\underline{H}_3$)
5d	12.90	11.09	8.53-6.91	7.10	5.10	
5e	12.26	10.95	8.52-6.65	6.73	5.16	
5f	12.73	10.90	8.52-7.04	7.25	5.24	
5g	13.09	10.96	8.53-6.73	7.04	5.19	
5h	13.11	11.73	8.75-6.61	7.38	5.89	10.21 (s, O$\underline{H}$), 4.097 (s, OC$\underline{H}_3$)
5i	13.15	11.41	8.75-7.15	7.96	4.61 (d, J=7.6Hz)	7.05 (d,J=6.4Hz,ph-C$\underline{H}$) 6.615 (t,J=7.2Hz,J=15.2 Hz, C=C$\underline{H}$)
5j	13.11	11.52	8.52-6.71	7.30	5.48	3.04 (s, N(C$\underline{H}_3$)$_2$)

Table (**12**) include the ^{13}C–NMR data for the 2*H*-pyrrole-2-one derivative**s** (**5a-j**), the carbonyl carbon of pyrrolone appeared at (163.11–151.31) ppm, while the signal for COOH carbon appeared at (175.07-166.19) ppm and the signal for the carbon of ($\underline{C}$-N $_{pyrrolone}$) appeared at (66.46-52.70) ppm. These evidence confirmed the formation of the described products.

Hassan. S. *and* Abdullah .M/ZJPAS: 2019, 31 (6): 92-109

100

Table 12: ^{13}C-NMR data for the 2*H*-pyrrole-2-one derivatives **(5a-j)**

Comp.	^{13}C-NMR
5a	166.47 (COOH), 162.90 (C 2"), 162.68 (C=O pyrrolone), 158.85 (C 4", C 6", C 2), 157.36 (C 4', (HC=C pyrrolone), 143.00 (C-COOH pyrrolone), 137.08 (C 1'), 135.36 (C 2'), 135.29 (C 6'), 134.76 (C 6), 134.47 (C 4), 131.97 (C 1), 129.45 (C 3', C 5'), 126.79 (C 5), 119.36 (C 3), 118.93 (C 5"), 52.70 (C-N pyrrolone).
5b	169.62 (COOH), 166.79 (C 2"), 165.90 (C=O pyrrolone), 162.92 (C 4"), 162.14 (C 6"), 144.04 (HC=C pyrrolone), 139.26 (C 1), 139.18 (C 4'), 137.62 (C-COOH pyrrolone), 136.92 (C 1'), 132.23 (C 2), 131.28 (C 2'), 130.57 (C 6'), 129.65 (C 3), 129.10 (C 4), 129.06 (C 6) , 126.78 (C 5), 120.09 (C 3', C 5'), 118.97 (C 5"), 57.41 (C-N pyrrolone).
5c	168.72 (COOH), 163.57 (C 2"), 162.36 (C=O pyrrolone), 158.87 (C 4), 157.71 (C 4"), 157.41 (C 6"), 155.69 (HC=C pyrrolone), 153.53 (C 4'), 137.65 (C-COOH pyrrolone), 132.91 (C 1'), 132.81 (C 1), 132.74 (C 2'), 132.71 (C 6'), 131.97 (C 2),131.87 (C 6), 129.98 (C 3'), 129.48 (C 5'), 121.64 (C 5"),116.97 (C 3), 116.75 (C 5), 57.91 (C-N pyrrolone), 55.75 (OCH$_3$).
5d	170.24 (COOH, C 2"), 154.50 (C=O pyrrolone), 148.18 (C 4", C 6"), 145.69 (C 4), 137.25 (HC=C pyrrolone), 133.02 (C 1), 132.18 (C 4'), 130.80 (CH-COOH pyrrolone), 130.08 (C 1'), 129.59 (C 2'), 129.25 (C 6'), 128.25 (C 3), 128.01 (C 5), 124.11(C 1), 123.77(C 6), 121.73 (C 3"), 120.61 (C 5'),115.75 (C 5"), 66.45 (C-N pyrrolone).
5e	172.67 (COOH), 169.70 (C 2"), 166.69 (C 4"), 166.49 (C 6"), 165.47 (C=O pyrrolone), 162.67 (C 3), 158.62 (HC=C pyrrolone), 157.26 (C 1),142.93 (C 4'), 136.93 (C-COOH pyrrolone), 135.10 (C 1'), 134.98 (C 6), 134.35 (C 5), 132.70 (C 2', C 6'), 129.70 (C 3'), 129.35 (C 5'), 128.77 (C 4), 119.35 (C 2), 116.12 (C 5"), 60.67 (C-N pyrrolone).
5f	175.07 (COOH), 166.48 (C 2"), 162.69 (C=O pyrrolone), 158.84 (C 4"), 158.73 (C 6"), 157.68 (HC=C pyrrolone), 153.32 (C 4'), 142.90 (C 1, C-COOH pyrrolone), 137.07 (C 1'), 134.47 (C 2', C 6'), 130.31 (C 6), 129.46 (C 5), 125.47 (C 4, C 6), 119.40 (C 3', C 5'), 116.00 (C 5"), 66.46 (C-N pyrrolone).
5g	166.69 (COOH), 166.49 (C 2"), 163.11 (C=O pyrrolone), 162.93 (C 4), 158.83 (C 4"), 157.35 (C 6"), 143.02 (HC=C pyrrolone), 142.91 (C 4'), 137.08 (C-COOH pyrrolone), 135.35 (C 1'), 134.48 (C 1), 131.99 (C 2', C 6'), 129.46 (C 2, C 6), 119.43 (C 3'), 119.01 (C 5'), 118.96 (C 3, C 5), 116.26 (C 5"), 65.89 (C-N pyrrolone).
5h	169.56 (COOH), 153.80 (C 2"), 151.31 (C=O pyrrolone), 143.95 (C 4", C 6"), 142.78 (C 3), 137.19 (HC=C pyrrolone), 130.11 (C 2), 129.06 (C 4'), 128.96 (C-COOH pyrrolone), 128.80 (C 1'), 126.91 (C 1),121.64 (C 2'), 121.44 (C 6'), 119.70 (C 3'), 119.48 (C 5'), 119.14 (C 5), 118.90 (C 6), 118.67 (C 5"), 112.06 (C 4), 62.50 (C-N pyrrolone), 56.56 (OCH$_3$).
5i	166.19 (COOH), 158.84 (C 2"), 157.13 (C=O pyrrolone), 153.73 (C 4", C 6"), 138.92 (HC=C pyrrolone), 135.18 (C 4'), 134.52 (C-COOH pyrrolone), 133.48 (C 1), 132.80 (C 1'), 129.56 (C 2'), 129.42 (C 6'), 129.22 (ph-C aldehyde), 128.96 (C 2, C 6), 128.73 (C 3, C 5), 127.55 (C 4), 122.76 (C 3'), 122.65 (C 5'), 121.60 (C-CH aldehyde), 116.27 (C 5"), 58.31 (C-N pyrrolone).
5j	169.37 (COOH), 162.68 (C 2"), 162.55 (C=O pyrrolone), 154.79 (C 4"), 154.56 (C 6"), 152.74 (C 4), 140.30 (HC=C pyrrolone), 140.10 (C 4'), 138.86 (C-COOH pyrrolone), 138.56 (C 1'), 130.49 (C 2'), 130.39 (C 6'), 129.98 (C 2), 129.87 (C 6), 125.01 (C 1), 121.94 (C 3', C 5'), 112.92 (C 3, C 5), 112.45 (C 5"), 67.61 (C-N pyrrolone), 56.94 (N-(CH$_3$)$_2$).

3.4. Antioxidant activity

The antioxidant activity of synthesized compounds are illustrated in the (**Table 13, Table 14 and Table 15**) for azomethines (**3a-j**), 2-azetidinones (**4a-j**) and 2*H*-pyrrole-2-ones (**5a-j**), correspondingly in contrast to the standard ascorbic acid. The antioxidant activity of the synthesized compounds were changed according to the ability of compounds to act as free radical scavengers or hydrogen donors and to evaluate antioxidant activity.

The synthesized Schiff base derivatives possess the antioxidant activity as compared to standard ascorbic acid. The antioxidant activity of imine derivatives are weaker than the standard ascorbic acid except for compound (**3i**), and the Antioxidant activity of compound (**3i**) is greater than the standard **ascorbic acid › 3e › 3f › 3b› 3a› 3g› 3d, 3h ›3c.**

Hassan. S. *and* Abdullah .M/ZJPAS: 2019, 31 (6): 92-109

101

Table 13: Antioxidant (DPPH test) for the Schiff basederivatives **(3a-j)**

Comp.	Concentration µg/ml	Absorbance	%SCV	IC$_{50}$ (µg/ml)
3a	1	0.029	3.33	
	25	0.022	26.66	49.83
	50	0.015	50	
3b	1	0.028	6.66	
	25	0.021	30	49.22
	50	0.015	50	
3c	1	0.026	13.33	
	25	0.023	23.33	78.97
	50	0.019	36.66	
3d	1	0.027	10	
	25	0.021	30	53.57
	50	0.016	46.66	
3e	1	0.029	3.33	
	25	0.023	46.66	33.95
	50	0.018	66.66	
3f	1	0.027	10	
	25	0.019	36.66	39.49
	50	0.012	60	
3g	1	0.028	6.66	
	25	0.022	26.66	50.45
	50	0.015	50	
3h	1	0.027	10	
	25	0.021	30	53.57
	50	0.016	46.66	
3i	1	0.026	13.33	
	25	0.016	46.66	32.49
	50	0.01	66.66	
3j	1	0.027	10	
	25	0.021	30	53.57
	50	0.016	46.66	

Table14: Antioxidant (DPPH test) for 2-Azetidinone derivative **(4a-j)**

Comp.	Concentration µg/ml	Absorbance	% SCV	IC$_{50}$ (µg/ml)
4a	1	0.023	23.33	
	25	0.02	33.33	57.98
	50	0.016	46.66	
4b	1	0.027	10	
	25	0.019	36.66	39.49
	50	0.012	60	
4c	1	0.023	23.33	
	25	0.019	36.66	55.71
	50	0.016	46.66	
4d	1	0.026	13.33	
	25	0.018	40	36.23
	50	0.011	63.33	
4e	1	0.029	3.33	71.02
	25	0.025	16.66	
	50	0.019	36.66	

Hassan. S. *and* Abdullah .M/ZJPAS: 2019, 31 (6): 92-109

102

4f	1	0.028	6.66	72.49
	25	0.024	20	
	50	0.019	36.66	
4g	1	0.027	10	34.94
	25	0.018	40	
	50	0.01	66.66	
4h	1	0.023	23.33	80.79
	25	0.021	30	
	50	0.018	40	
4i	1	0.025	16.66	30.44
	25	0.016	46.66	
	50	0.009	70	
4j	1	0.027	10	45.45
	25	0.020	33.33	
	50	0.014	53.33	

Table 15: Antioxidant (DPPH test) for 2*H*-pyrrole-2-one derivatives **(5a-j)**

Comp.	Concentration µg/ml	Absorbance	%SCV	IC_{50}(µg/ml)
5a	1	0.028	6.66	92.93
	25	0.025	16.66	
	50	0.021	30	
5b	1	0.027	10	59.64
	25	0.022	26.66	
	50	0.017	43.33	
5c	1	0.025	16.66	79.91
	25	0.021	30	
	50	0.019	36.66	
5d	1	0.026	13.33	41.68
	25	0.019	36.66	
	50	0.013	56.66	
5e	1	0.021	30	101.4
	25	0.02	33.33	
	50	0.018	40	
5f	1	0.023	23.33	80.79
	25	0.021	30	
	50	0.018	40	
5g	1	0.018	40	23.3
	25	0.016	46.66	
	50	0.01	66.66	
5h	1	0.025	16.66	46.11
	25	0.02	33.33	
	50	0.014	53.33	
5i	1	0.025	16.66	34.68
	25	0.017	43.33	
	50	0.011	63.33	
5j	1	0.028	6.66	47.98
	25	0.02	33.33	
	50	0.015	50	

In our study we have seen that the antioxidant activity of azomethine derivatives close to the antioxidant activity of 2-azetidinone, but the antioxidant activity of 2*H*-pyrrole-2-one are lower.

Hassan. S. *and* Abdullah .M/ZJPAS: 2019, 31 (6): 92-109

103

Ascorbic Acid (Vitamin C) is a significant antioxidant that has an essential part in preventing free radicals as demonstrates in (**Table 16**).

Table 16: Antioxidant (DPPH) for Ascorbic acid as standard

Ascorbic acid	Concentration µg/ml	Abs.	% SCV	IC$_{50}$ (µg/ml)
	1	0.025	16.66	
	25	0.017	43.33	32.96
	50	0.01	66.66	

3.5. Antibacterial activity

The antibacterial activity for azomethine derivative (**3e**, **3d, 3h and 3j**) had high activity for gram positive (**Figure 1**) and (**3e**) had high activity for gram negative (**Figure 2**). Compound of (**3a, 3c, 3g** and **3j**) were inactive for gram positive but for gram negative only (**3i**) was inactive while it was dissolved 500 µg/ml (500ppm) in DMSO. According to the our results the antibacterial activity of the synthesized Schiff bases are changed depending on the functional groups, as in the presence of Nitro-groups, it have

the extreme antibacterial activity such as compound (**3d**) that shown in the (**Figure 1**).
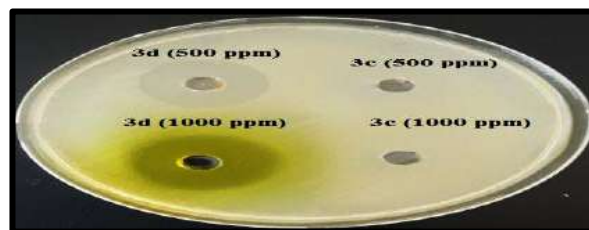

Figure 1: Gram positive for 4-((4-methoxybenzylidene) amino)-N-(pyrimidin-2-yl) benzenesulfonamide **(3c)** and ((4-nitrobenzylidene) amino)-N-(pyrimidin-2-yl) benzenesulfonamide **(3d)**
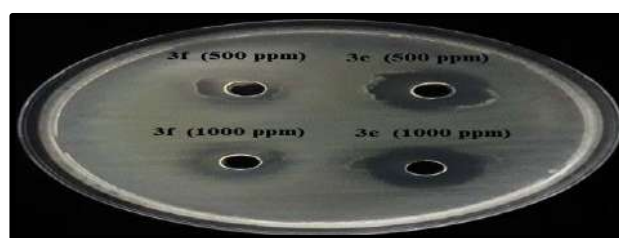

Figure 2: Gram negative for 4-((3-nitrobenzylidene) amino)-N-(pyrimidin-2-yl) benzenesulfonamide **(3e)** and 4-(benzylideneamino)-N-(pyrimidin-2-yl) benzenesulfonamide **(3f)**

As shown in (**Table17, 18 and 19**) the antibacterial activity of azomethine derivatives greater than the antibacterial activity 2*H*-pyrrole-2-one derivatives, but lower than the antibacterial activity of 2-azetidinone derivatives.

Table 17: Antibacterial activity for azomethine derivatives **(3a-j)**

Comp.	Gram positive (*staphylococcus aureus*)		Gram negative(*Escherichia coli*)	
	500 µg/ml(500ppm)	1000 µg/ml(1000ppm)	500 µg/ml(500ppm)	1000 µg/ml(1000ppm)
3a	-	-	+	+
3b	-	+	+	+
3c	-	-	+	+
3d	++	+++	++	++
3e	++	+++	+++	+++
3f	-	+	+	+
3g	-	-	+	+
3h	++	+++	++	++
3i	-	-	-	+
3j	++	+++	+	+

Table 18: Antibacterial activity for 2-Azetidinone derivatives **(4a-j)**

Comp.	Gram positive (*staphylococcus aureus*)		Gram negative(*Escherichia coli*)	
	500 µg/ml(500ppm)	1000 µg/ml(1000ppm)	500 µg/ml(500ppm)	1000 µg/ml(1000ppm)
4a	+	+++	+	+
4b	-	-	+	+
4c	++	++	+	+
4d	+	++	-	+
4e	++	++	+	+

Hassan. S. *and* Abdullah .M/ZJPAS: 2019, 31 (6): 92-109

104

4f	++	++	+	+
4g	++	++	+	-
4h	++	++	+	-
4i	++	++	+	+
4j	++	++	+	+

Table 19: Antibacterial activity for 2*H*-pyrrole-2-one derivatives (**5a-j**)

Comp.	Gram positive(*staphylococcus aureus*)		Gram negative(*Escherichia coli*)	
	500 μg/ml(500ppm)	1000 μg/ml(1000ppm)	500 μg/ml(500ppm)	1000 μg/ml(1000ppm)
5a	++	+++	-	+
5b	++	++	-	-
5c	-	-	-	+
5d	-	+	+	++
5e	-	+	+	+
5f	+	++	+	+
5g	-	-	-	-
5h	+	+	+	+
5i	-	+	-	+
5j	++	++	+	+

High active = +++ (inhibition zone = 16-20 mm), moderately active = ++ (Inhibition zone = 10-15 mm), slightly active = + (inhibition zone = 3-9 mm), Inactive = - (inhibition zone < 3).

4. CONCLUSIONS

In this work, a new series of 2-Azetidinone and a novel series Pyrrolone derivatives are synthesized by a suitable and practical methods and the products can separated easily from the reaction mixture with high purity, by using ultrasound assisted technique. During the purification processes, it was found that a mixture of absolute ethanol and n-hexane in ratio (70:30) is a favorable solvent for recrystallization of Imine and Pyrrol-2-one derivatives and washed the organic phase of the ethyl acetate solution that contain the impure 2-Azetidinone with water. The evaluated results of all the products afforded the important antibacterial activities against *staphylococcus aureus G (+ve), Escherichia coli G (-ve)* and antioxidant activity as compared to standard ascorbic acid.
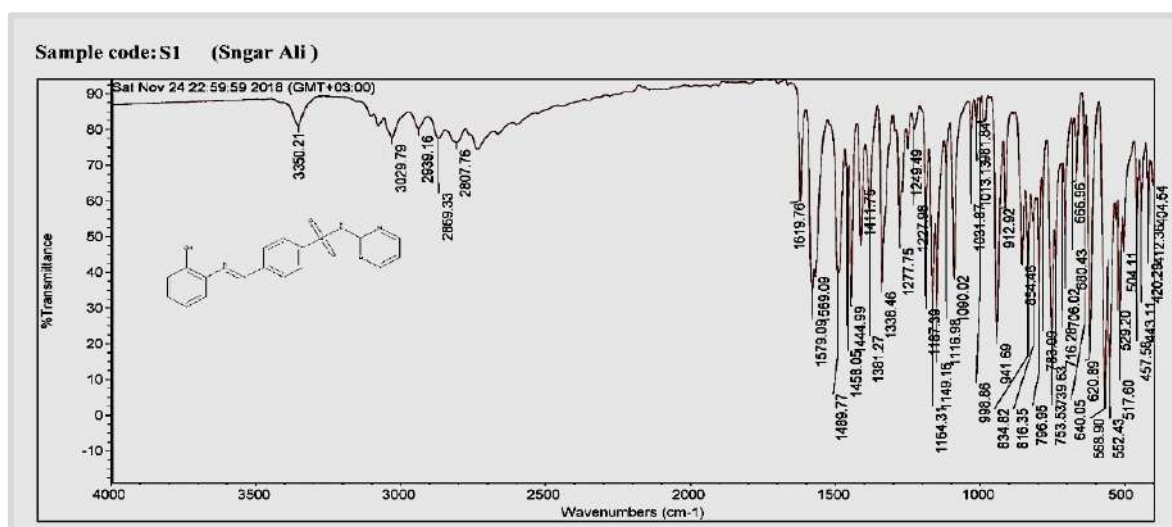
Figure 3: FT-IR Spectrum for 4-((2-hydroxybenzylidene) amino)-N-(pyrimidin-2-yl) benzenesulfonamide (**3a**)

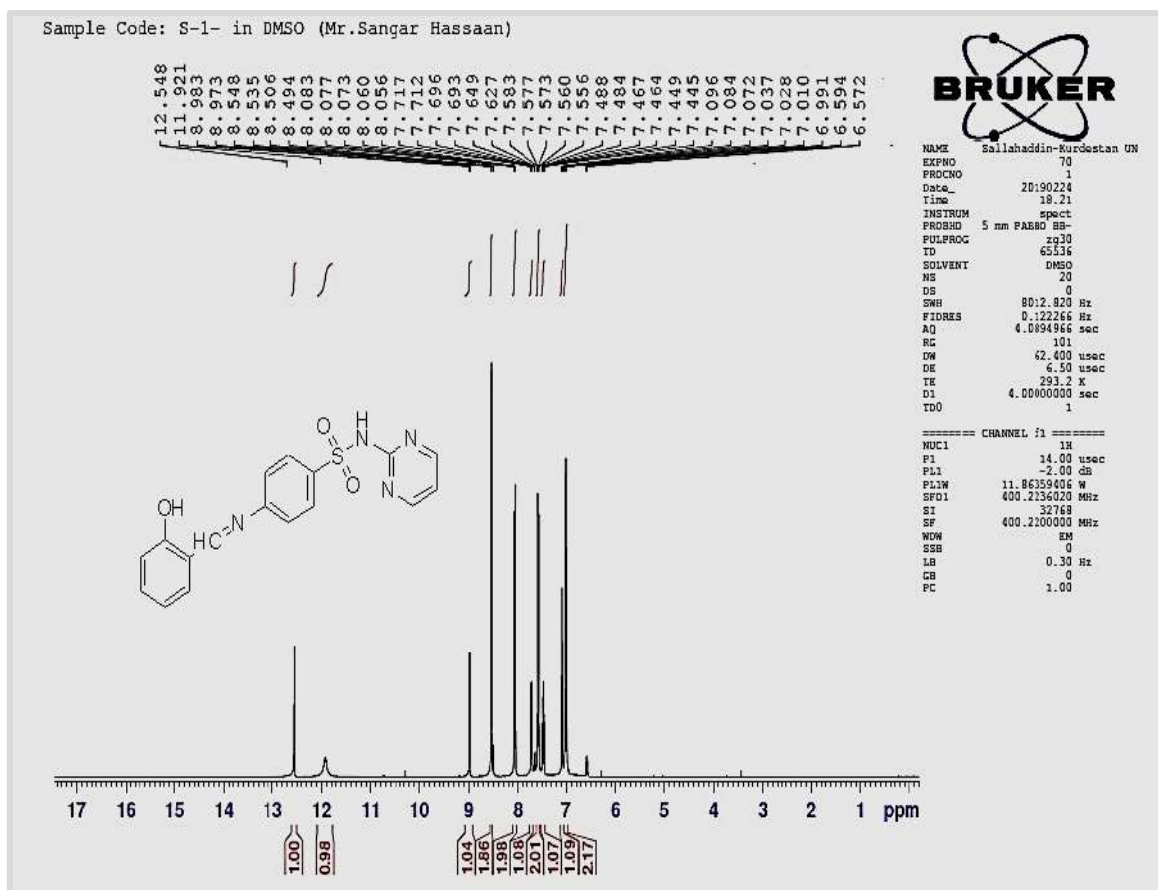Hassan. S. *and* Abdullah .M/ZJPAS: 2019, 31 (6): 92-109

105

Figure 4: ^{1}H-NMR Spectrum for 4-((2-hydroxybenzylidene) amino)-N-(pyrimidin-2-yl) benzenesulfonamide **(3a)**

Figure 5: ^{13}C-NMR Spectrum for 4-((2-hydroxybenzylidene) amino)-N-(pyrimidin-2-yl) benzenesulfonamide **(3a)**
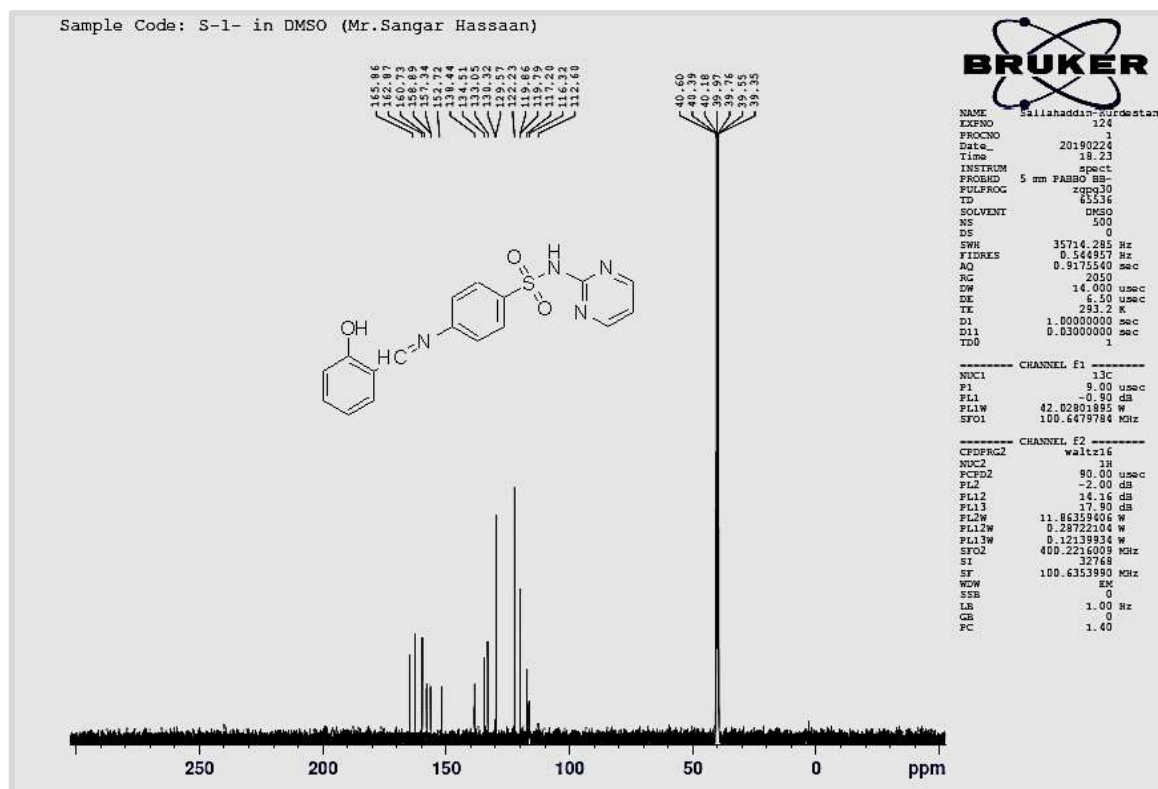
Hassan. S. *and* Abdullah .M/ZJPAS: 2019, 31 (6): 92-109

106

Figure 6: FT-IR Spectrum for 4-(3-chloro-2-(2-hydroxyphenyl)-4-oxoazetidin-1-yl)-N-(pyrimidin-2-yl) \ benzenesulfonamide **(4a)**

Figure 7: ¹HNMR Spectrum for 4-(3-chloro-2-(2-hydroxyphenyl)-4-oxoazetidin-1-yl)-N-(pyrimidin-2-yl) benzenesulfonamide **(4a)**

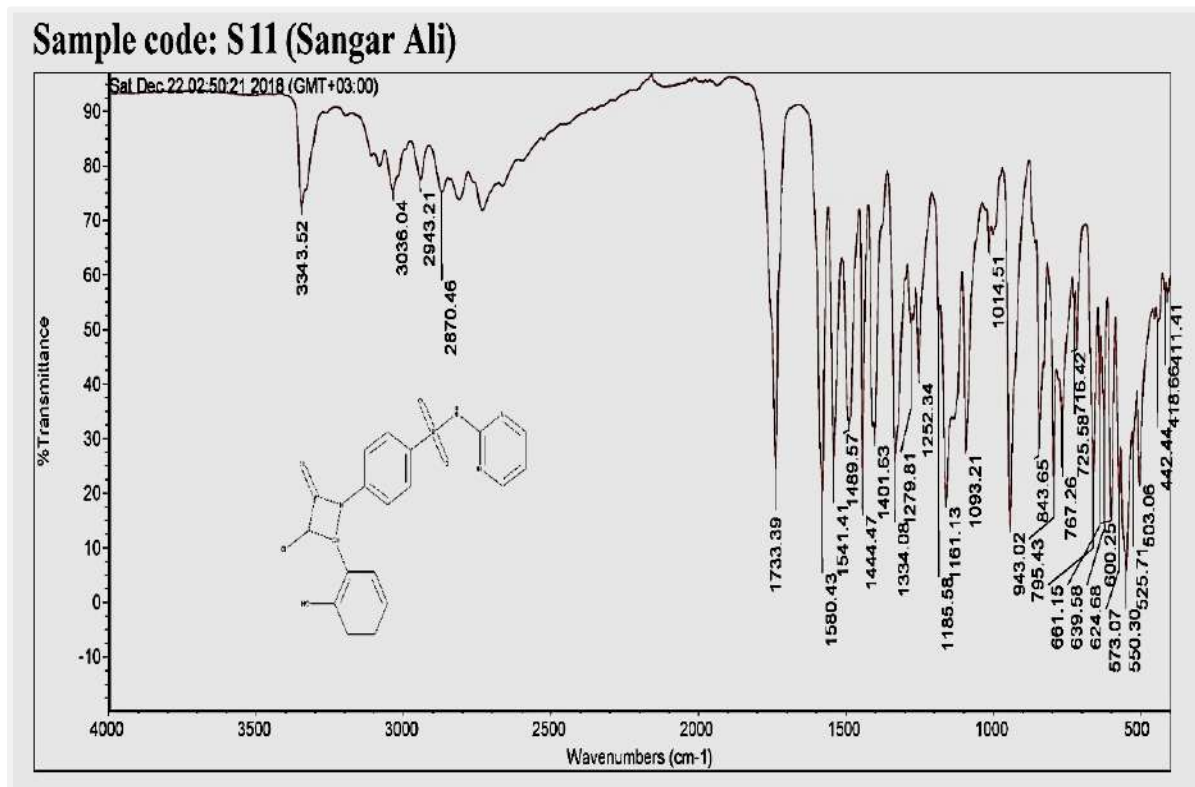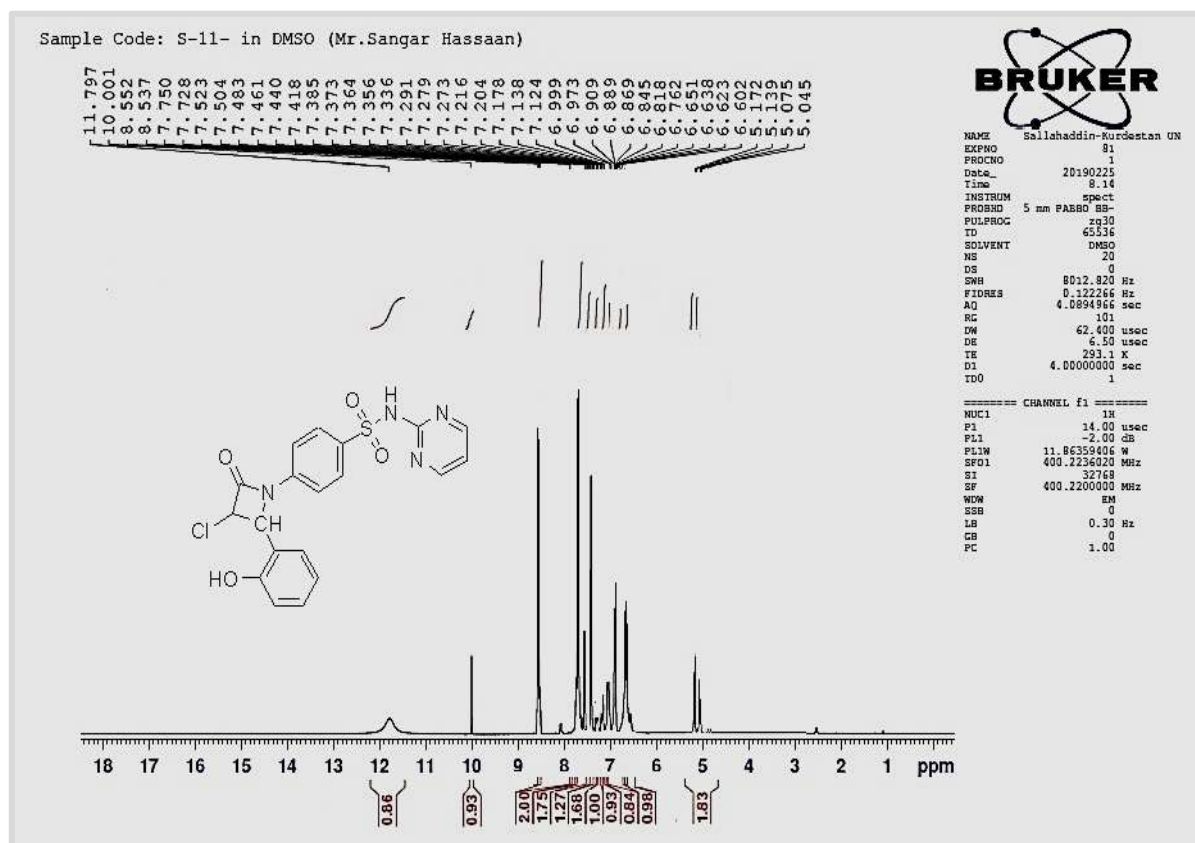Hassan. S. *and* Abdullah .M/ZJPAS: 2019, 31 (6): 92-109

107
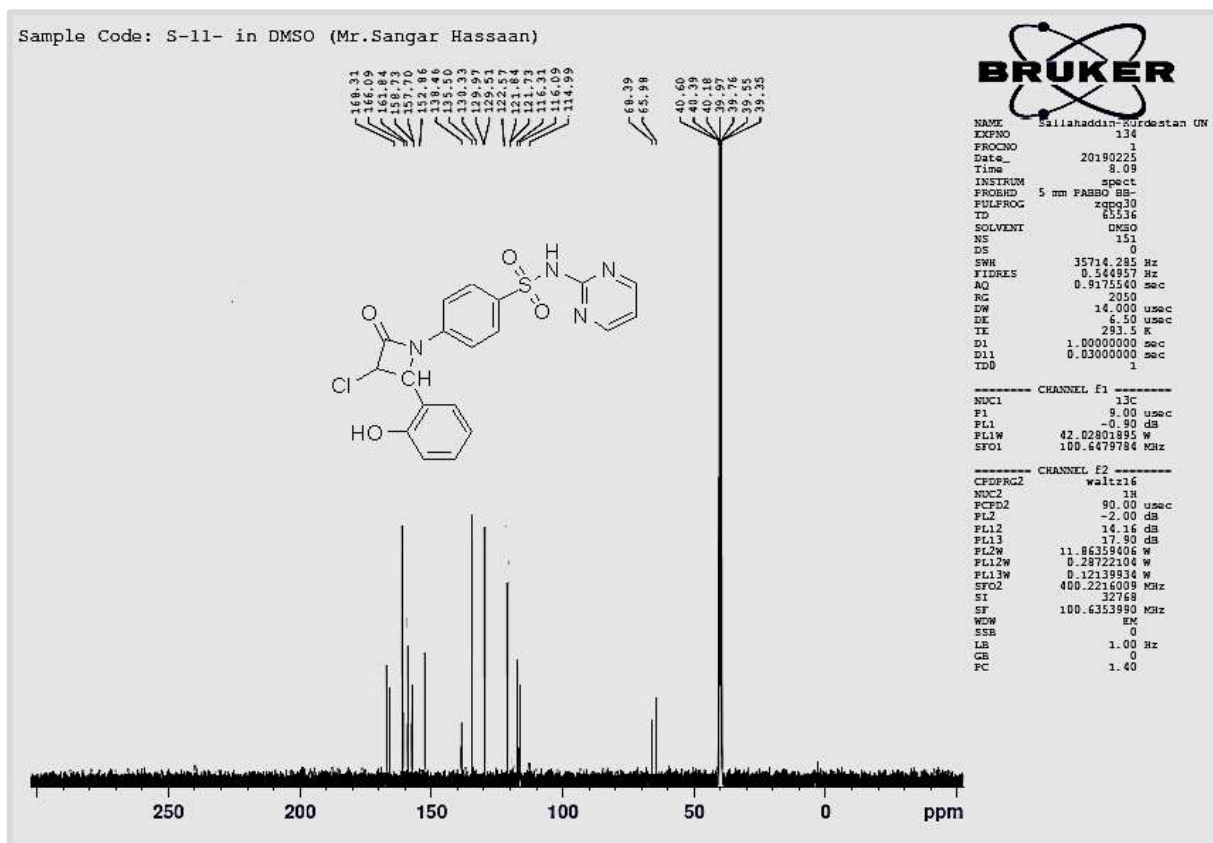
Figure 8: ^{13}C-NMR Spectrum for 4-(3-chloro-2-(2-hydroxyphenyl)-4-oxoazetidin-1-yl)-N-(pyrimidin-2-yl) benzenesulfonamide (**4a**)

Figure 9: FT-IR Spectrum for 2-(2-hydroxyphenyl)-5-oxo-1-(4-(N-(pyrimidin-2-yl) sulfamoyl) phenyl)-2, 5-dihydro-1*H*-pyrrole-3-caboxylic acid (**5a**)

Hassan. S. *and* Abdullah .M/ZJPAS: 2019, 31 (6): 92-109

108

Figure 10: ^{1}H-NMR Spectrum for 2-(2-hydroxyphenyl)-5-oxo-1-(4-(N-(pyrimidin-2-yl) sulfamoyl) phenyl)-2, 5-dihydro-1*H*-pyrrole-3-caboxylic acid **(5a)**

Figure 11: ^{13}C-NMR Spectrum for 2-(2-hydroxyphenyl)-5-oxo-1-(4-(N-(pyrimidin-2-yl) sulfamoyl) phenyl)-2, 5-dihydro-1*H*-pyrrole-3-caboxylic acid **(5a)**

Hassan. S. *and* Abdullah .M/ZJPAS: 2019, 31 (6): 92-109
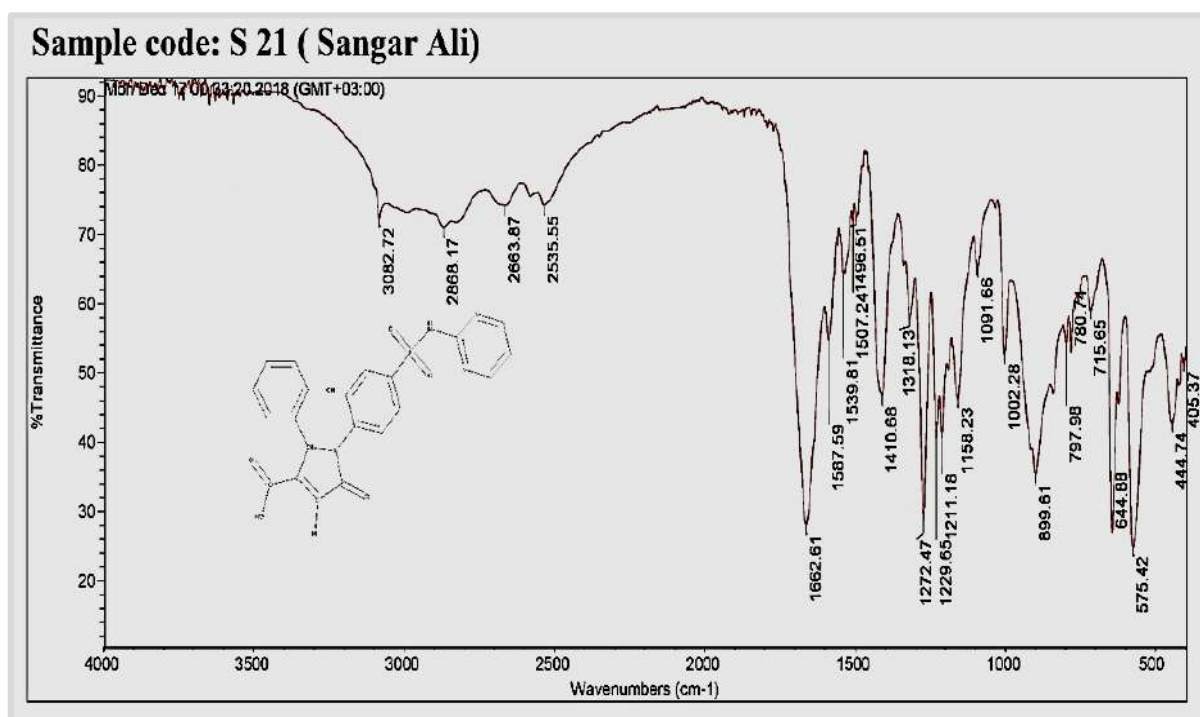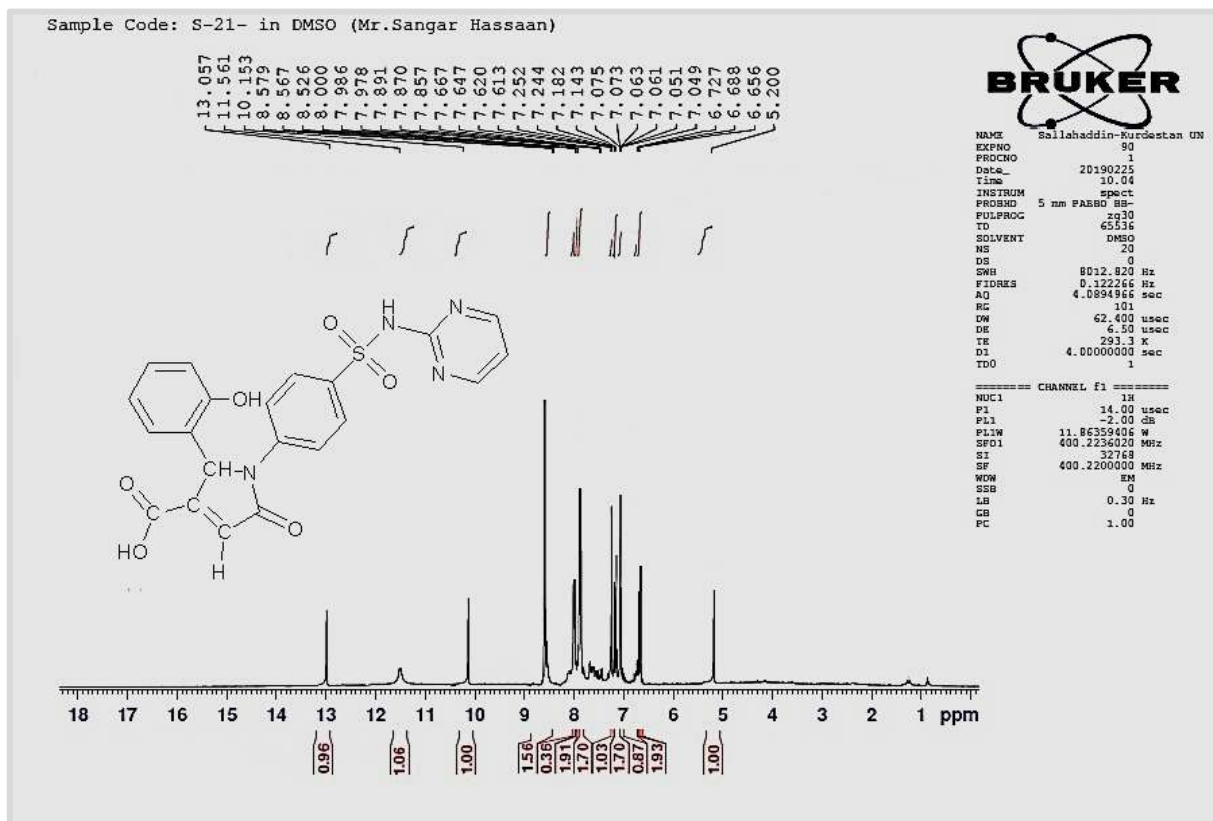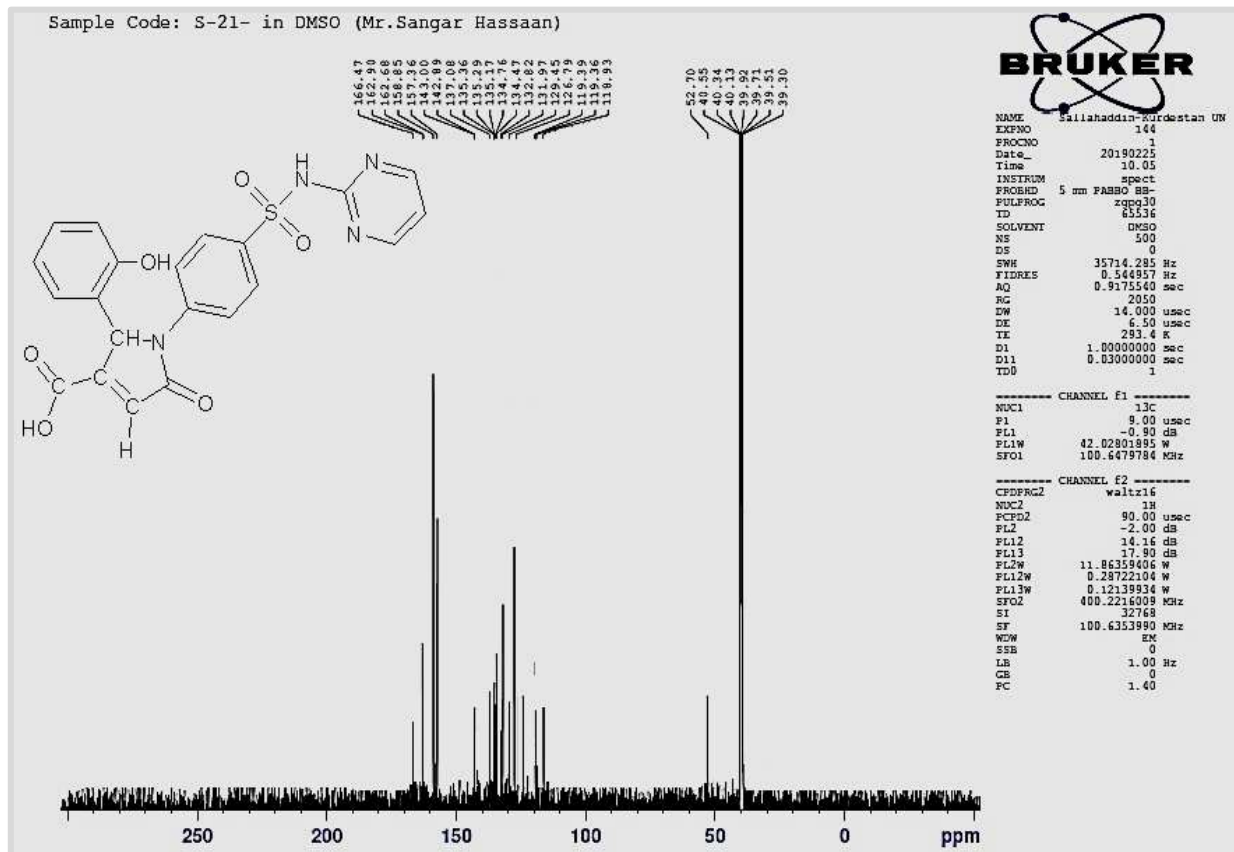
109

References

ABDULSADA, A. H., NASSER, N. H. & HUSSEIN, A. K. 2018. Synthesis and Preliminary Antibacterial Evaluation of Schiff Base Metal Complexes of Ampicillin and Cephalexin. *Acta Chimica and Pharmaceutica Indica*, 8, 123

ADAM, R. W. 2018. Synthesis and Characterization of some New synthesis of N-(pyrimidin-2-yl) benzenesulfonamide derivatives combined with oxaimidizolidine. *Journal of Pharmaceutical Sciences and Research,* 10, 3103.

AL-MULLA, A. 2017. A review: biological importance of heterocyclic compounds. *Der Pharma Chemica,* 9**,** 141-1472.

ALI, Y., ALAMA, M. S., HAMIDA, H. & HUSSAIN, A. 2014. 2 (3h) pyrrolone–a biologically active scaffold (a review). *Oriental Journal of Chemistry,* 30**,** 01-16.

ARYA, N., JAGDALE, A. Y., PATIL, T. A., YERAMWAR, S. S., HOLIKATTI, S. S., DWIVEDI, J., SHISHOO, C. J. & JAIN, K. S. 2014. The chemistry and biological potential of azetidin-2-ones. *European journal of medicinal chemistry,* 74**,** 619-656.

BÖHM, M., MORANO, I., PIESKE, B., RÜEGG, J., WANKERL, M., ZIMMERMANN, R. & ERDMANN, E. 1991. Contribution of cAMP-phosphodiesterase inhibition and sensitization of the contractile proteins for calcium to the inotropic effect of pimobendan in the failing human myocardium. *Circulation research,* 68**,** 689-701.

DA SILVA, C. M., DA SILVA, D. L., MODOLO, L. V., ALVES, R. B., DE RESENDE, M. A., MARTINS, C. V. & DE FÁTIMA, Â. 2011. Schiff bases: A short review of their antimicrobial activities. *Journal of Advanced research,* 2**,** 1-8.

EL-SHEHRY, M. F., ABU-ZIED, K. M., EWIES, E. F., AWAD, S. M. & MOHRAM, M. E. 2013. Synthesis of some novel azaheterocycles utilizing 3-(4-nitrobenzylidene)-5-phenylfuran-2 (3H)-one with expected antimicrobial activity. *Der pharma chem,* 5**,** 318-326.

GUPTA, A. & HALVE, A. 2015. [Beta]-LACTAMS: A MINI REVIEW OF THEIR BIOLOGICAL ACTIVITY. *International Journal of Pharmaceutical Sciences and Research,* 6**,** 978.

KUMAR, D., SINGH, A. & WALIA, Y. K. 2014. Synthesis and Characterization of 2H-Pyrrole-2-Ones of (5-Benzoyl-benzoimidazol-1-yl)-acetic acid hydrazide derivatives. *Asian J. of Adv. Basic Sci,* 2**,** 40-46.

MOHAMMED ABD AL-KHALIQ, Z. 2015. *Synthesis, characterization and antibacterial activity of new series of sulfamethoxazole derivatives.* Ministry of Higher Education.

NUNNA, R., RAMACHANDRAN, D., MODI, V. B. & GOSWAMI, K. J. 2014. Synthesis, Characterization and Anti Microbial Activity of Some Novel Heterocyclic Compounds Having Sulphamido Moiety. *Chemical Science,* 2**,** 00-00.

SALUNKHE, D. & PISTE, P. 2014. A brief review on recent synthesis of 2-azetidinone derivatives. *Int J Pharm Life Sci,* 5**,** 666-689.

SHAHID, M., SALIM, M., KHALID, M., TAHIR, M. N., KHAN, M. U. & BRAGA, A. A. C. 2018. Synthetic, XRD, non-covalent interactions and solvent dependent nonlinear optical studies of Sulfadiazine-Ortho-Vanillin Schiff base:(E)-4-((2-hydroxy-3-methoxy-benzylidene) amino)-N-(pyrimidin-2-yl) benzene-sulfonamide. *Journal of Molecular Structure,* 1161**,** 66-75.

SINHA, D., TIWARI, A. K., SINGH, S., SHUKLA, G., MISHRA, P., CHANDRA, H. & MISHRA, A. K. 2008. Synthesis, characterization and biological activity of Schiff base analogues of indole-3-carboxaldehyde. *European journal of medicinal chemistry,* 43**,** 160-165.

TAYLOR, A. P., ROBINSON, R. P., FOBIAN, Y. M., BLAKEMORE, D. C., JONES, L. H. & FADEYI, O. 2016. Modern advances in heterocyclic chemistry in drug discovery. *Organic & biomolecular chemistry,* 14**,** 6611-6637.

ZHENG, Y., MA, K., LI, H., LI, J., HE, J., SUN, X., LI, R. & MA, J. 2009. One pot synthesis of imines from aromatic nitro compounds with a novel Ni/SiO 2 magnetic catalyst. *Catalysis letters,* 128**,** 465-474.

RESEARCH PAPER

Effect of Different Foliar Herbicides on Weed Control, Yield and Its Component of Simeto (*Triticum durum L.*)

Dara M.A Jaff[1], Ismail A. Said[2]

[1]Department of Biology, College of Education, Salahaddin University-Erbil, Kurdistan Region, Iraq
[2]Department of Plant Production, Khabat Technical Institute, Erbil Polytechnic University, Erbil, Kurdistan Region, Iraq

A B S T R A C T:

A field experiment was conducted at the Technical Institute Research Station of Khabat to study the efficiency of three herbicides on the control of weeds in *Triticum durum L.* (Simeto variety). The herbicides were Pallas (for broadleaves and grasses), Traxos (for grasses) and 2, 4-D amine salt (for broadleaves). Three doses of each of the herbicides were applied at the five leaf stage of the crop. Characteristics studied were growth index, yield component and quality of the wheat variety. In addition, weed control and reduction percentages were calculated. The data show the significant efficiency of the treatments. However, the crop was severely affected by the Pallas doses application, although it was more effective than any others herbicides applied in this work to decrease number of weeds in a meter square.

INTRODUCTION:

Wheat (*Triticum aestivum L.*) is considered the staple food for more than one third of world population (Kaur et al., 2017). The yield of this crop is markedly affected by weeds density, as their losses to wheat yield approximately account between 35% to 57% (Petrova et al., 2015). However, there are several methods that can be used to control weeds in cereal crops, vis; prevention, mechanical, cultural, physical, biological as well as chemicals. Each method may be used alone or together, as an integrated weed management for a successful weed control program (Qasem, J. R., 2011).

However, using of herbicides in the past two decade has been tested to increase markedly crop yield by reducing the effect of weed problems in cereal fields. Due to different weed types (grasses and broadleaves); many herbicides have been developed to use in crop fields (Kumar and Singh, 2010). Furthermore, incorrect using of herbicides might be hazardous to the health of the farmers and their crops; as well as to the environment. Thus, the farmers should consider several factors that affect the herbicides efficiency, including the choice of using the correct product to certain weed, timing of the treatment, equipment inspection and maintenance, calculation of the dose applied, application techniques and safety (Wopereis et al., 2009). Accordingly, this experiment was conducted to study the effective of three different herbicides as foliage application for the control of weeds in wheat variety Simeto.

* **Corresponding Author:**
Ismail A. Said
E-mail: ismail.said@epu.edu.iq or ias1981@hotmail.com

Jaff. D. *and* Said .I. /ZJPAS: 2019, 31 (6): 110-116

111

MATERIALS AND METHODS

An experiment was carried out at the Technical Institute Research Station of Khabat's district, 40 km west of Erbil. The land was prepared by plowing with moldboard plow, and then rotavator was used for harrowing; then the area for this experiment was designed as randomized complete block with three replications, each block was divided to 10 experimental units (12 m^2). Seeds of *Triticum durum L.* (Simeto variety) were sown at 30 kg/donum. The three herbicides used were Pallas (for broadleaves and grasses), Traxos (for grasses) and 2, 4-D amine salt (for broadleaves) (Table-2).

Three doses of each of the herbicides were applied as recommended dose, plus 25% of the recommended dose and minus 25% of the recommended doses. The spray was performed at five leaf stage of the crop according to the Zadock scale for wheat growth stages (DPI-NSW, n.d).

Data collection:

After five weeks of the treatments application, the number of weeds was counted in a meter square (Table-1) and then the control percentage of the weeds by the herbicides was calculated and analyzed statistically. In addition, data were taken for the growth rate of the crop by measuring the main stem length and number of tillers for ten plants which were taken in the middle rows of the experiments unit. Also, the ten main stem and spikes were placed in oven at 70°C for 48 hours to dry, and the dry matters were weighed.

The percentage of weeds control was calculated by the following formula (Jassim and Rudhan, 2011):

$$C.W = \frac{A - B}{A} \times 100$$

Where:

C.W= Weed control percentage
A= Number of weeds in Control plots
B= Number of Weeds In treated Plots

Table-1: Scientific names and families of observed weeds in the experimental area.

No.	Scientific name	Family
1.	*Hordeum gluacum L.*	Poaceae
2.	*Lolium rigidum L.*	Poaceae
3.	*Bromus sp. L.*	Poaceae
4.	*Vulpia octoflora L.*	Poaceae
5.	*Malva parviflora L.*	Malvaceae
6.	*Matricaria anthemis L.*	Asteraceae
7.	*Fumaria officinalis L.*	Fumariaceae
8.	*Brassica napus L.*	Brassicaceae
9.	*Plantago lanceolate L.*	Plantaginaceae

Reduction Percentage:

Reduction percent was calculated by taking weeds samples in every plot through quadrat meter square, and the weeds plant were weighted freshly then put in oven at 70°C for 48 hours to

Jaff. D. *and* Said .I. /ZJPAS: 2019, 31 (6): 110-116

112

obtain the dry matter. The following formula was used to calculate Reduction%.

Reduction %= (fresh wt of weeds-dried wt of weeds)/fresh wt * 100

Table-2: Common, trade and chemical names of the herbicides.

No.	Common Name	Trade Name	Chemical Name	Recommended dose
1	2,4-D	2,4-D amine salt	2,4-dichlorophenoxy acetic acid amine salt	1 L/ha
2	Pallas	Pyroxsulam	N-(5,7-dimethoxy[1,2,4]triazolo[1,5-a]pyrimidin-2-yl)-2-methoxy-4-(trifluoromethyl) pyridine-3-sulonamide	0.5 L/ha
3	Traxos	Pinoxaden and clodinafop propargyl	2,2-dimethyl-propionic acid 8-(2,6-diethyl-4-methylphenyl)-1,2,3,4-tetrahydro-7-oxo7H-Pyrazolo[1,2-d][1,2,5]oxadi-azepin9-ylester (Pinoxaden) (R)-2-[4-[(5-chloro-3-fluoro-2-pyridinyl)oxy]phenoxy]-propionicacid propynyl ester (clodinafoppropargyl) [(5-chloro-8-quinolinyl)oxy]-aceticacid1-methylhexyl ester	1 L/ha

(Grain Protein) appears as rotated text in left margin of table

n Content:

Protein percent of the grains was determined by Kjeldahl method at Agriculture College – University of Duhok.

Yield Production:

Yield was calculated according to spike/m^2, grains per spike and weight of 1000 grains.

RESULTS

There were significant variations of herbicides application on stem and spike dry matter of wheat (Figure 1&2). Pallas doses had markedly negative on stem dry matter of the crop particularly the recommended concentration. In addition, all doses of traxos as well as 2, 4-D (R+25%) treatments had negative on stem dry matter and reduces the stem dry matter of the plant (figure-1). Similarly, the spike dry matter of the crop was also affected by the treatments. Generally, pallas doses, in particular the recommended-pallas treatment, and traxos (R-25%) were effective to diminish the spike dry matter of wheat (figure-2)

Jaff. D. *and* Said .I. /ZJPAS: 2019, 31 (6): 110-116

113
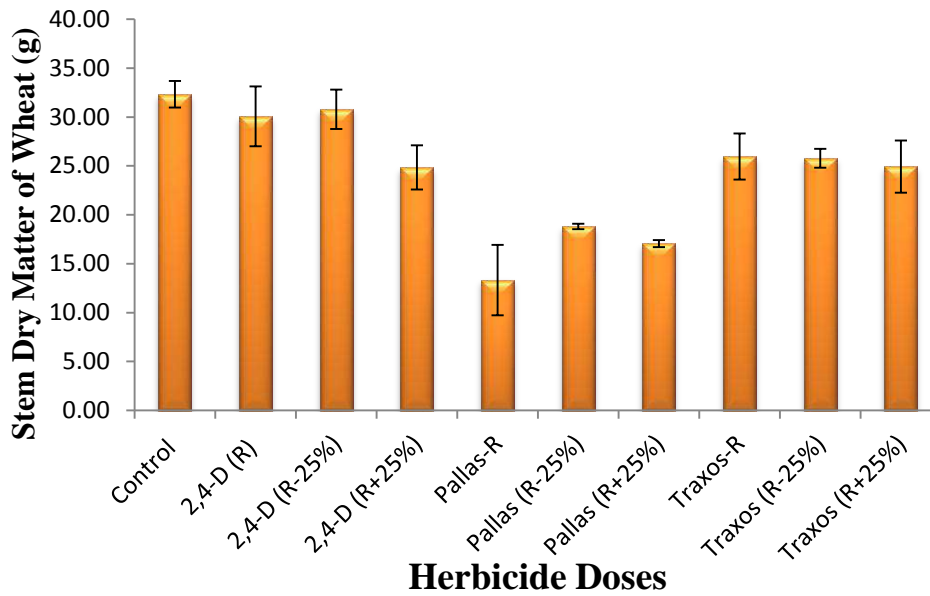
Figure-1: Effect of different rates of herbicides on stem dry matter of wheat (R refers to recommended rate)

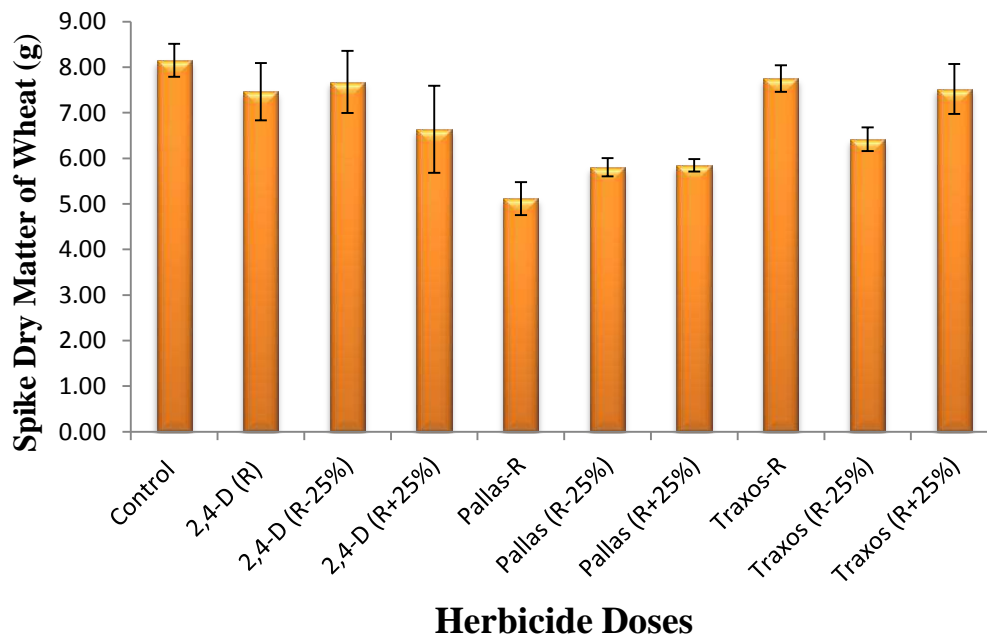**Figure-2:** Effect of different rates of herbicides on spike dry matter of wheat (R refers to recommended rate)

Furthermore, Pallas treatments especially the R and (R+25%) were effectively decreased stem length of the crop. In addition, the traxos concentrations reduced the stem length but were better than the pallas doses (figure-3).

Jaff. D. *and* Said .I. /ZJPAS: 2019, 31 (6): 110-116

114
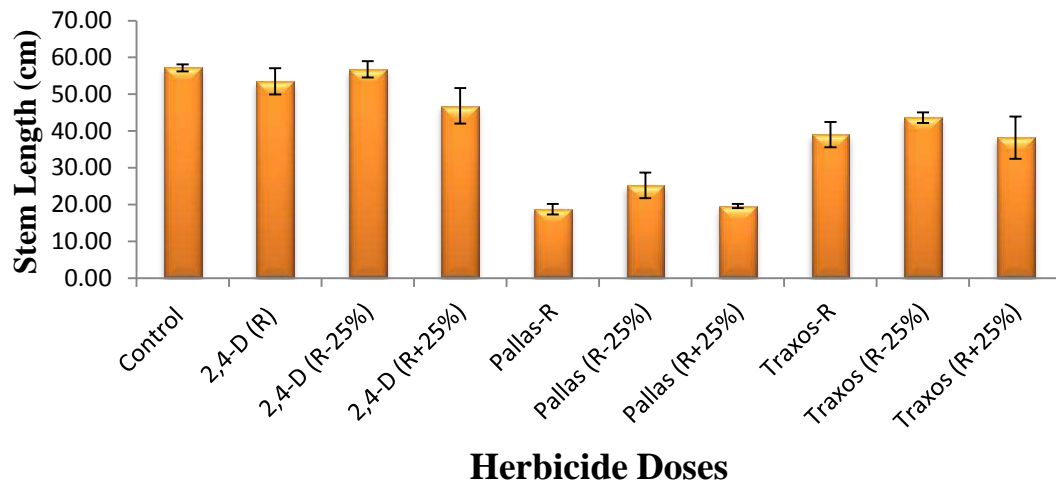
Figure-3: Effect of different rates of herbicides on stem length of wheat (R refers to recommended rate)

However the pallas treatments had negative effects on growth index of the crop, the herbicide (pallas) at all doses were more effective than the other treatments in weed control; as the calculation of weed control percentage explains more in (Table-3).

Table-3: Weed control and reduction percentage of grasses and broadleaves) in wheat field by different

Herbicides (Treatments)	Weed Control Percentage		Reduction %	
	Grasses	Broadleaves	Grasses	Broadleaves
2, 4-D(R-25%)	0.0	55.56 b	0	79.46a
2, 4-D (R)	0.0	59.26ab	0	74.89a
2, 4-D (R+25%)	0.0	85.19 ab	0	77.15a
Pallas (R-25%)	94.29a	92.59a	81.13a	79.40 a
Pallas (R)	95.71a	100 a	100a	92.22a
Pallas (R+25%)	94.29 a	92.59 a	100a	100a
Traxos (R-25%)	75.71b	0.0	33.22b	0
Traxos (R)	77.14 b	0.0	41.37 b	0
Traxos (R+25%)	64.29 b	0.0	43.56 b	0
Mean	83.57	80.86		

herbicide rates:

Jaff. D. *and* Said .I. /ZJPAS: 2019, 31 (6): 110-116

115

DISCUSSION:

Hordeum glaucum was the main infesting weed in the experiment area, as well as, *Fumaria officinalis* and *Matricaria anthemis*, and some other species which have been shown in table-1. Generally, the herbicides applications were effective to reduce weeds population; in particular, the pallas treatment at all doses. Dalga, et al. 2014 reported that Pyroxsulam is a very good herbicide to control broadleaves as well as grassy weeds. However, the concentration of the herbicide greatly affected the crop growth index such as stem dry matter and spike dry matter; also the stem height of the crop. The negative impact on the crops growth rate was due to delay the growth of the plant. In addition, the Traxos treatment showed different effect on both weeds and the crop. The higher dose of the herbicide was relatively more effective than the recommended and R- 25% dose. Chhokar, et al. (2015) in their investigation concluded that 50 and 60 g active ingredient of Pinoxaden 2.53% + Clodinafoppropargyl 2.53% (the two main components of Traxos) were more effective to reduce weeds population than 40 g. Also, this herbicide influenced had detrimental impact on parameters such as stem length and stem dry matter but wasR less than Pallas (Figure 1 and2). Furthermore, the 2,4-D + 25% was effective to diminish broadleaf weeds population and did not injury the crop compared to Pallas then Traxos. Based on this investigation, further study is needed to explain precise application of Pallas as well as the dose, as the herbicide was more efficient to diminish the weeds population despite the crop was affected.

Furthermore, the herbicides had different impact on protein percentage. The three concentrations of 2, 4-D herbicide had no effect on protein content similarly to Traxos. Shaw et al. (1955) in their test of 2, 4-D on wheat grain protein included that Protein content was a more precise index of the effect of 2, 4-D on wheat than yield. In addition, the doses of traxos herbicide showed no impact on protein percent of the grain. Tagour et al. 2011 confirmed in their work that differnet rate of traxos did not affect the protein percent of wheat grain. Furthermore, all pallas concentrations reduced the protein percentage; particularly the (pallas R+25%) dose (table-4).

Table-4: Effect of herbicides doses on yield and yield components of Wheat:

Treatments	Spike no./m2	Grains / Spike	1000 grains weightt. (g)	Yield (t/ha)	Grain Protein %
Control	217.33 a	25.73 ab	38.10 ab	2.08 a	13.45 ab
2,4-D (R-25%)	192 a	24.39 ab	40.13 ab	1.84 ab	12.8 b
2,4-D (R)	186.66 a	23.91 ab	36.13 ab	1.51 ab	13.70 ab
2,4-D (R+25%)	194.66 a	24.69 ab	39.03 ab	1.86 ab	13.05 ab
Pallas (R-25%)	174.66 a	16.86 bc	27.03 b	0.77 b	13.03 ab
Pallas (R)	184 a	14.88 c	32.20 ab	1.03 ab	12.94 ab
Pallas (R+25%)	250 a	10.59 c	35.50 ab	0.92 b	12.82 b
Traxos (R-25%)	186.66 a	23.62 ab	42.70 a	1.80 ab	13.08 ab
Traxos (R)	174.66 a	24.63 ab	41.80 a	1.77 ab	13.32 ab
Traxos (R+25%)	153.33 b	26.81 a	36.53 ab	1.52 ab	13.16 ab

Conclusion

However, the herbicide can be effective to reduce the weeds problem in wheat fields, it might influence growth parameters of the crop. The pallas was the most effective to reduce weeds biomass but affected the crop growth index. So, the pallas herbicide needs more research to be its

Jaff. D. *and* Said .I. /ZJPAS: 2019, 31 (6): 110-116

116

impacts explained then recommended to the farmers.

References:

Chhokar, R.S., Sharma, R.K., Singh,R.K., Gill, S.G. and Meena, R.P. 2015, " Ready mix combination of pinoxaden and clodinafop for efficient control of grass weeds in wheat", Journal of Wheat Research, Vol. 7, Issue. 1, pp 55-58.

Dalga, D., Sharma, JJ. and Tana, T. 2014," Evaluation of Herbicides and Their Combinations for Weed Management in Bread Wheat (*Triticum astivum L.*) In Southern Ethiopia", International Journal of Novel Research in Life Sciences, Vol. 1, Issue 1, Pp 31-47. Department of Primary Industry (DPI) , n.d. "Zadoks decimal code", New South Wasles, Australia. From http://www.dpi.nsw.gov.au/__data/assets/pdf_file/0008/188 684/zadocs-decimal-   code.pdf

Jassim, A. A. and Rudhan, S. A. 2011," Evaluation an Inject Seed Weed Control Herbicide Equipment Performance Under Soil Surface Using TREFLAN", Diyala Agricultural Science Journal, Vol. 3, Issue 2, pp 373-382.

Kaur, A., Chand, A., Singh, A.N. 2017, "Little seed canary grass (*Phalaris minor Retz.*) promoting own growth functional traits but suppressing of wheat crop (*Triticum aestivum L.*) at vegetative stage: An ecological assessment", Annals of Plant Sciences, Vol.6, no.11.

Kumar, S. and Singh, A.K. 2010," A review on herbicide 2, 4-D damage reports in wheat (*Triticum aestivum L.*)", Journal of Chemical and Pharmaceutical Research, Vol. 2, Issue 6, pp. 118-124.

Qasem, J. R. 2011," Herbicides Applications: Problems and Considerations", *University of Jordan, Jordan*.

Petrova, S.T., Valcheva, E.G., Valcheva, I.G. 2015, "A Case Study of Allelopathic Effect on Weeds in Wheat*",* Ecologia Balakanica, Vol.7, no.1.

Shaw, W.C., Willard, C.J., Bernard, R.L. 1955, "The Effect of 2,4-Dichlorophenoxyacetic Acid (2,4-D) on Wheat, Oats and Barley", Research Bulletin 761, Ohio Agricultural Experiment Station, Wooster, Ohio.

Tagour, R. M. H., Abd El-Hamad, G. H., El-Metwally, I.M. 2011, "Improving Herbicides Efficacy of Topik and Traxos on Wheat Plants and Associated Weeds by Adjuvants Arkopal", Nature and Science, Vol. 9, no. (11).

Wopereis, M.C.S., Defoer, T., Idinoba, P., Diak, S. and Dugue, M. 2009," Safe and correct use of herbicides", Curriculum for Participatory Learning and Action Research (PLAR) for Integrated Rice Management (IRM), Africa Rice Center (WARDA).

RESEARCH PAPER

Preparation and Characterization of Neodymium(III) arginine complex.

Ary Bahman Faiq

Department of Medical Laboratory, Technical College of Health, Sulaimani Polytechnic University, Sulaimani, Kurdistan Region, Iraq

A B S T R A C T:
A new complex of neodymium(III) arginine was prepared from $Nd(NO_3)_3.6H_2O$ and arginine. The preparation involves mixing the metal-ligand by the ratio 1:2 dissolving both in H_2O and then purifying by ethanol/diethyl ether. The primary analyses showed that the mole ratio of the metal−ligand complex is 1:1. The ^{1}H-NMR spectrum of the complex observed a broadness attributed to the coordination of the paramagnetic metal with the ligand. In addition to, the comparison of vibrational spectra of free and coordinated arginine in the region of carbonyl, imine, and amino groups all indicated the occurrence of the complex. The Uv-vis spectra were also inspected where a new band appeared in the range of 240–270 nm assigned to the ligand metal charge transfer.

1. INTRODUCTION:

Arginine has three functional groups (carboxyl, amine, and imine) each one can donate electrons to form hydrogen bonding or to metals having empty orbitals as shown in figure 1.

Arginine exists in the structure of many enzymes. Arginine in one subunit has the ability of binding with another one and with substrates through hydrogen bonding (Wang et al. 2004; and Karsten and Cook 1993). In erythrocytes glycolysis pathway the enzyme bisphosphoglycerate mutase converts 1,3-biphosphoglycerate (1,3-BPG) to 2,3-biphosphoglycerate (2,3-BPG). This substrate 1,3-BPG binds with the enzyme at different amino acids in which arginine is one of them specially at the guanidinium site studied by (Garel et al. 1993),

also quoted that "mutation in arginine89 resulted in significant perturbation in the enzyme's catalytic activity". A study made by Fairlie et al. (1997) on arginine complexes, the X-ray and NMR spectra showed that the guanidine group of arginine had contributed in the coordination with Co(III) and Pt (II) ions.

The spectroscopic studies are quit helpful for interpreting the occurrence of the complex (Aiyelabola et al. 2012; and Martins et.al 2003). The arginine infrared spectrum shows bands of C=O stretching in the regions 1700 to 1660 cm^{-1} and N−H deformation from 1650 to 1610 cm^{-1} (Kumar and Rai 2010; Muley et al. 2009; and Wang et al. 2014).

Some of previous investigations of arginine complexes focused on bands shifting of carbonyl stretching around 1700cm^{-1} and of imine stretching around 1550cm^{-1} (Kong and Yu 2007; Ozturk et al. 2014; Wu et al. 2010; and Sunatkari et al. 2015) due to their interactions with metals.

Furthermore, shifting in N−H deformation band around 1630cm^{-1} of the arginine is another indicator taken for assessing the occurrence of the

---

* **Corresponding Author:**
Ary Bahman Faiq
E-mail: ary.faiq@spu.edu.iq

complex (Kong and Yu 2007; and Aruna 2007). Therefore, an arginine molecule that contains six donating sites can very likely create a coordination bond with neodymium(III) ion from more than one site. The scope of this study is the synthesis of Nd(III)arginine complex investigating it by techniques of elemental analyses, ^{1}H–NMR, infrared, and Uv-visible spectroscopies to observe any significant changes that may occur.
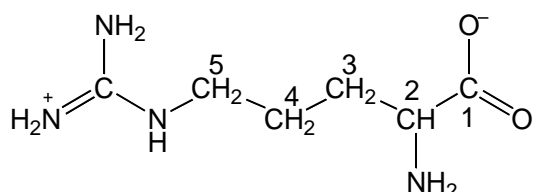

Figure 1. the zwitterion structure of arginine

2. MATERIALS AND METHODS

2.1 Complex Preparation

L-Arginine monohydrate was purchased from Scharlau supplier and neodymium(III) nitrate hexahydrate from Santa Cruz Biotechnology. The synthesis of Nd(III) arginine complex is as the followings; 1mmole $Nd(NO_3)_3.6H_2O$ was dissolved in 10mL H_2O and mixed with 2mmole of arginine also dissolved in 10mL H_2O at temperature 70°C for 2hours. The solution started appearing emulsified, the heating continued until the volume reduced to 10mL. After cooling the solution, 15mL ethanol was added followed by diethyl ether till the complex precipitated. The complex dried at 60°C for one day.

2.2 Analyses

The elemental analysis was performed to estimate the percentage of each element in the free and complexed arginine. The Nd^{3+} ion in the complex was determined through the following steps; first the metal turned into oxides at 550°C for 2 hours, dissolved in 3M HCl, and finally titrated with EDTA at pH 5.5 acetate buffer using murexide indicator (a pilot titration was previously made). Conductivity measurements were performed in DMF solvent purchased from Bruck.

The molar conductivity was experimentally estimated using Friedrich Kohlrausch equation by preparing a series of 10^{-3} molar of the complex at 25°C. The pH of L-

arginine solution was also checked at 25°C to see the scale of its protonation using pH-meter Hanna 211. The ^{1}H–NMR spectra were obtained in D_2O solvent by instrument Bruker 500MHz Avance III. The NMR and elemental analyses were accomplished at Department of chemistry/Jordan University/Jordan. The infrared spectra were performed in solid KBr using instrument model Perkin Elmer/ spectrum one FTIR at Department of chemistry/University of Sulaimani. The ultraviolet-visible spectra were obtained by preparing the solutions in distilled water using EMC-LAB UV-6100PC double beam spectrophotometer working at 2nm slit-width.

3. RESULTS

3.1 Elemental analysis

Arginine has four protonation constants. The measured pH is 11.2 so it is expected to be in a zwitterionic form (Fitch et al. 2015) figure 1. The complex synthesis involved mixing 1millimoles of $Nd(NO_3)_3$ with 2millimoles of arginine (Arg) but the results of the elemental analysis showed that the most probable mole ratio of Nd^{3+} arginine matching with the theoretical calculations is 1:1 table 1. The results also showed that one nitrate anion expelled. Therefore, it can be concluded that the Nd^{3+} ion interacted with the ionic oxygen of the carboxylate ion and substituted for the expelled nitrate ion. Hence the chemical formula of the complex becomes $NdArg(NO_3)_2$. The limiting molar conductivity (Λ_o) is 138 $S.cm^2.mol^{-1}$ suggesting 1:2 electrolyte solution (Geary 1971).

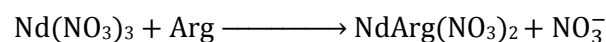$$Nd(NO_3)_3 + Arg \longrightarrow NdArg(NO_3)_2 + NO_3^-$$

Table 1. the elemental analyses of $NdArg(NO_3)_2$ complex.

Elements	Theoretical%	Found%
Nd^{3+}	32.3	30.7
N	19.1	18.1
C	16.4	17.4
H	3	4

3.2 ^{1}H-NMR spectra

The ^{1}H–NMR spectra of zwitterion arginine and its complex were scanned to 20ppm. The free L-arginine shows three peaks; one at 1.55ppm assigned to the hydrogen atoms at C3 and C4 (overlapped) meanwhile the others hydrogen NMR C2 and C5 appear at 3.2 and 3.1 ppm respectively (Wishart et al 2009; and Yanagisawa and Yamamoto 2013) figure 2a.
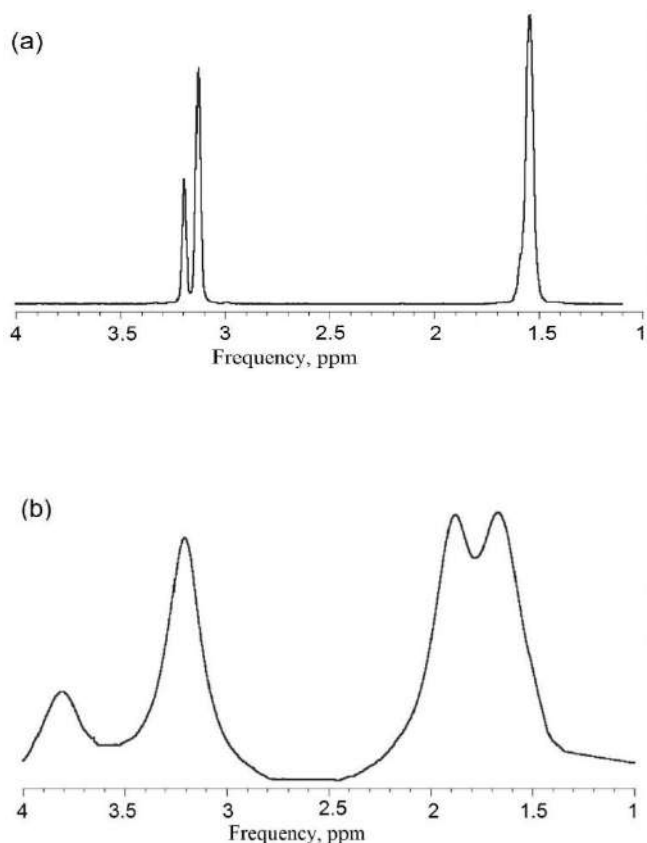

Figure 2. ^{1}H-NMR spectra of (a) Arg and (b) NdArg(NO$_3$)$_2$ in D$_2$O

3.3 IR spectra

The IR spectrum of arginine was compared with that of complexed arginine table 2. The high intensity carbonyl stretching band of free arginine that appears at 1679cm^{-1} shifted to 1664cm^{-1} in the spectrum of the arginine complex figure 3.

The stretching band of guanidine-imine group also shows a significant shift but to higher energy from 1555 to 1580 cm^{-1} assigned to the coordination of Nd(III) with imine group (Bush et al. 2008; Forbes et al. 2007; Govani et al. 2009; and Rosu et al. 2005). The broad band 1633–1614 cm^{-1} is expected to be for N–H deformations but does not showed any shift figure 3. In the same

time C–NH stretching band at 1138 cm^{-1} shifted to 1115 cm^{-1} after complexation (Govani et al. 2009; Barth 2000; and Petrosyan and Sukiasyan 2008).

Table 2. The infrared spectral data of arginine and its complex

Band		υ / cm^{-1}	
		Arg	NdArg(NO$_3$)$_2$
C=O str		1679	1664
C=N$_{str}$		1555	1582
C–N$_{str}$		1138	1115
	υ_o asym		1384
NO$_3^-$	υ_1		1500
	υ_3		825

Notes: str stretching; def deformation; asym asymmetric stretching.

Furthermore, the complex IR spectrum shows four bands at 825, 1500 (shoulder), and 1384 cm^{-1} assigned to $\upsilon_3, \upsilon_1, \upsilon_o$ NO$_3^-$ vibrations respectively (Petrosyan and Sukiasyan 2008; Gupta and Sirvastava 2014; Tahaa et al. 2011; and Miller and Wilkins 1952). A band appearing at 1763cm^{-1} assigned to be for the nitrate ion and another one occurred at 551cm^{-1} assigned to Nd–O (Tahaa et al. 2011 and Arif et al. 2001).
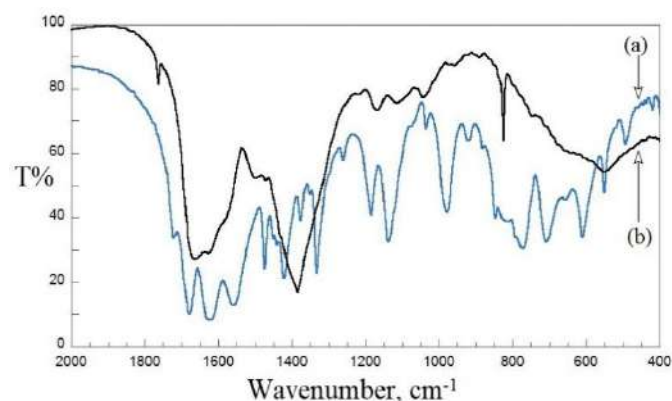

Figure 3. Fourier transform−infrared spectra of (a) L-arginine and (b) NdArg(NO$_3$)$_2$

3.4 UV–vis spectra

Scanning neodymium nitrate in the Uv-vis region reveals three bands at 348, 302, and 215nm (not shown) figure 4. The complex spectrum shows a new absorption region 240 to 270 nm

neither the free $Nd(NO_3)_3$ ion nor the free arginine showed this band (Otten et al. 2007).

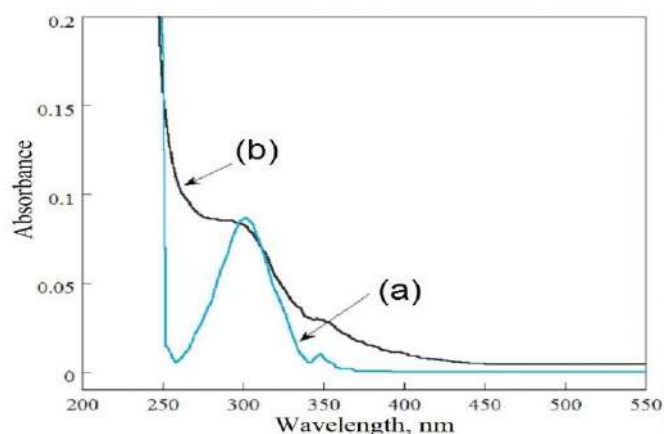**Figure 4.** UV-vis spectra of (a) $Nd(NO_3)_3$ and (b) $NdArg(NO_3)_2$ both at $1.88*10^{-3}$ molar in H_2O

4. DISCUSSION

4.1 ^{1}H–NMR

The ^{1}H-NMR spectrum at C2 of the complexed arginine shows a significant broadness and shifting at frequency 3.8ppm which is different from the free arginine (Arg) 3.21ppm figure 2. This broadness and shifting to the low shield field is due to the interaction of paramagnetic Nd(III) with the amino group mostly that is at C2 as quoted by Cotton (2006) "the magnitude of the proton shifts depends upon the distance of the proton from the site of coordination to the lanthanide ion". The complexed arginine spectrum at C3 also shifted from 1.54 to 1.90ppm which shows a greater shift than that of C4 to 1.67ppm.

Overall, these shifting and broadness prove the contribution of amino group at C2 in the coordination bond. It is noteworthy that H-NMR spectrum of arginine could give different frequencies for different optical activities dextro, levo, or mixture also the pH could cause a shift therefore it is recommended to compare the obtained H-NMR with the correct reference which is L-arginine in the current study.

4.2 IR and Uv-vis spectra

This IR shifting of the complexed carbonyl group to low energy resulted from interaction and charge transfer of carboxyl group to the metal ion disrupting the electronic resonance in COO^-

letting lesser electronic cloud on the carbonyl group and lower vibrational energy.

As arginine contains three amino groups it is difficult from IR interpretation to conclude which one interacted with the metal ion. Altogether shiftings in energy of COO^-, C=NH, and C–NH bands are interpreted as evidence for their interactions with Nd(III) Barth 2000.

Comparison of the electronic absorption spectra of arginine and its complex resulted in appearance of a new band in 240 – 270 nm assigned to ligand-metal charge transfer, this band was also observed in a previous study on lanthanides by Tahaa et al. (2011).

5. CONCLUSIONS

The analyses revealed that the zwitterion arginine can coordinate with $Nd(NO_3)_3$ through three sites (carboxylate ion, imine, and amino) groups with liberation of one nitrate ion forming $NdArg(NO_3)_2$. The evidences for complex occurrence are based on low energy shifting in IR spectra of carbonyl stretching by 15cm^{-1} and high C=N shifting by 27cm^{-1} and of the amino groups from 1138 to 1115 cm^{-1}.

Furthermore, the broadness in the H-NMR spectrum for all carbon atoms resulted from surrounding the Nd(III) ion by the carboxylate and guanidine terminuses of the ligand arginine and the amino group at C2 as well. Finally, the polydentate arginine can take the role of a chelating ligand where the Nd(III) encapsulated by the three mentioned groups.

References

Aiyelabola, T.O. Ojo, I.A. Adebajo, A.C. Ogunlusi, G.O. Oyetunji, O. Akinkunmi, E.O. and Adeoye, A.O. 2012. Synthesis, characterization, and antimicrobial activities of some metal(II) amino acids' complexes. Advances in Biological Chemistry. http://dx.doi.org/10.4236/abc.2012.23034

Arif, M. Rehman, S. Arshad, M. Masud, K. and Arshad, N. 2001. Studies on the thermal decomposition of copper (II) flouride complexes with various amino Acids in nitrogen atmosphere. Turk J. Chem 25:73−79.

Aruna, A. Anurhada A. Tomas, P.C. Mohamed, M.G. Rajasekar, S.A. Vimalan, M., Mani, G. and Sagayaraj, P. 2007. Growth Optical, and thermal studies of L-arginine perchlorate. Indian J. Pure Appl. Phys. 45:524–528.

Barth, A. 2000. The infrared absorption of amino acid side chains, Prog. Chem. Org. Nat. Prod. https://doi.org/10.1016/S0079-6107(00)00021-3

Bush, M.F. Oomens, J. Saykally, R.J. and Williams, E.W. 2008. Effects of alkaline earth metal ion complexation on amino acid zwitterion stability. J. Am. Chem. Soc. https://doi.org/10.1021/ja711343q

Cotton, S. 2006. Lanthanides and Actinides. In: NMR applications, first edn, Wiley, England. PP 77. https://doi.org/10.1002/0470010088

Fairlie, D.P. Jackson, W.G. Skelton, B.W. Wen, H. White, A.H. Wickramasinghe, W.A. Woon, T.C. and Taube, H. 1997. Models for Arginine−Metal Binding. Synthesis of Guanidine and Urea Ligands through Amination and Hydration of a Cyanamide Ligand Bound to Platinum(II), Osmium(III), and Cobalt(III). *Inorg. Chem.* https://doi.org/10.1021/ic961138e

Fitch, C.A. Platzer, G. Okon, M. Moreno, B.G. and McIntosh, L.P. 2015. Arginine: Its pKa value revisited. Protein Sci. https://doi.org/10.1002/pro.2647

Forbes, M.F. Bush, M.F. Polfer, N.C. Oomens, J. Dunbar, R.C. Williams, E.R. and Jockusch, R.A. 2007. Infrared spectroscopy of arginine cation complexes: direct observation of gas-phase zwitterions. J. Phys. Chem. https://doi.org/10.1021/jp074859f

Garel, MC. Lemarchandel, V. Calvin, MC. Arous, N. Craescu, C.T. Prehu, MO. Rosa, J. and Rosa, R. 1993. Amino acid residues involved in the catalytic site of human erythrocyte bisphosphoglycerate mutase. Functional consequences of substitutions of His10, His187 and Arg89. Eur. J Biochem. https://doi.org/10.1111/j.1432-1033.1993.tb17786.x

Geary, W.J. 1971. The use of conductivity measurement in organic solvents for the characterization of coordination compounds. Coord. Chem Rev. https://doi.org/10.1016/S0010-8545(00)80009-0

Govani, J.R. Durrer, W.G. Manciu, M. Botez, C. and Manciua, F.S. 2009. Spectroscopic study of L-arginine interaction with potassium dihydrogen phosphate crystals. J. Mater. Res. https://doi.org/10.1557/JMR.2009.0290

Gupta, S.K. and Srivastava, A. 2014. Magneto, Spectral and Thermal Studies of Lanthanum and Lanthanides (III) Nitrate and Perchlorate Complexes of 2-Benzoylaminopyridine N-Oxide. JCBPSc 4:1945–1951.

Karsten, W.E. and Cook, P.F. 2007. Multiple roles of arginine 181 in binding and catalysis in the NAD-malic enzyme from Ascaris suum. Biochemistry. https://doi.org/10.1021/bi701524z

Kong, J. and Yu, S. 2007. Fourier transform Infrared spectroscopic analysis of protein secondary structures. Acta Biochimica et Biophysica Sinica. https://doi.org/10.1111/j.1745-7270.2007.00320.x

Kumar, S. and Rai, S.B. 2010. Spectroscopic studies of L-arginine molecule. I.J.P.A.P 48:251–255.

Martins, T.S. Araújo, A.AS. Da Silva, S.M. Matos, J.R. Isolani, P.C. and Vicentini, G. 2003. Synthesis, characterization, spectroscopic study and thermal analysis of rare-earth picrate complexes with L-arginine. J. Solid State Chem. https://doi.org/10.1016/S0022-4596(02)00153-6

Miller, F.A. and Wilkins, C.H. 1952. Infrared Spectra and Characteristic Frequencies of Inorganic Ions. Anal Chem. https://doi.org/10.1021/ac60068a007

Muley, G.G. Rode, M.N. and Pawar, B.H. 2009. FT-IR, thermal, and NLO studies on amino Acid (L-arginine and L-alanine) doped KDP crystals. Acta physica polonica 116:1033 – 1038.

Otten, D.E. Petersen, P.B. and Saykally, R.J. 2007. Observation of nitrate ions at the air/water interface by UV-second harmonic generation. Chem. Phys. Lett. https://doi.org/10.1016/j.cplett.2007.10.081

Ozturk, Z. Kose, D.A. Asan, A. and Ozkan, G. 2014. Porous metal-organic Cu(II) complex of L-arginine; synthesis, characterization, hydrogen storage properties, and molecular simulation calculations. Hittite Sci. Eng. https://doi.org/10.17350/HJSE19030000001

Petrosyan, A.M. and Sukiasyan, R.P. 2008. Vibrational spectra of L-arginine nitrates. J. of Mol Struct. https://doi.org/10.1016/j.molstruc.2007.03.032

Rosu, T. Negoiu, M. and Circu, V. 2005. Complex combination of Cu(II) with mixed ligands. Analele UniversităŃii din Bucuresti – Chimie I-II: 153–159.

Sunatkari, L. Talwatkar, S.S., Tamgadge, Y.S. and Muley, G.G. 2015. Synthesis, Characterization, and optical properties of L-arginine stabilized gold nanocolloids. JNN. https://doi.org/:10.5923/j.nn.20150502.02

Tahaa, Z.A. Ajlouni, A.M. Al-Hassan, K.A. Hijazi, A.K. and Faiq, A.B. 2011. Syntheses, characterization, biological activity, and fluorescence properties of bis-(salicylaldehyde)-1,3-propylenediimine Schiff base ligand and its lanthanide Complexes. Spectrochimica acta Part A. https://doi.org/10.1016/j.saa.2011.06.018

Wang, T. Wang, L. Wu, D. Xia, W. Zhao, H. and Jia, D. 2014. Hydrothermal synthesis of nitrogen-doped graphene hydrogels using amino acids with different acidities as doping agents. J. mater. Chem. A. https://doi.org/10.1039/C4TA00170B

Wang, Y. Wei, Z. Bian, Q. Cheng, Z. Wan, M. Liu, L. and Gong, W. 2004. Crystal structure of human bisphosphoglycerate mutase. JBC. https://doi.org/10.1074/jbc.M405982200

Wishart, DS. Knox, C., Guo, AC. Eisner, R. Young, N. Gautam, B. Hau, DD. Psychogios, N. Dong, E. Bouatra, S. Mandal, R. Sinelnikov, I. Xia, J Jia L. Cruz, JA. Lim, E. Sobsey, CA. Shrivastava, S. Huang, P. Liu, P. Fang, L. Peng, J. Fradette, R. Cheng, D. Tzur , D. Clements, M. Lewis, A. De Souza, A. Zuniga, A. Dawe, M. Xiong, Y. Clive, D. Greiner, R. Nazyrova, A. Shaykhutdinov, R. Li, L. Vogel, HJ. Forsythe Yamaji T. Saito, T. and Hayamizu, K. 2009. HMDB: a knowledgebase for the human metabolome. NAR. https://doi.org/10.1093/nar/gkn810

Yanagisawa M. and Yamamoto O., 2013. Spectral database of organic compounds, SDBS No. 1143, L-arginine. http://sdbs.db.aist.go.jp/sdbs/cgi-bin/direct_frame_disp.cgi?sdbsno=1143

Wu, Z. Fernandez-Lima, F.A. and Russell, D.H. 2010. Amino acid influence on copper binding to peptides: cysteine versus arginine. J. Am. Soc. Mass Spectrom. https://doi.org/10.1016/j.jasms.2009.12.020

RESEARCH PAPER

Present status of *Salmonella* Typhi in different age groups hospitalized patients in Duhok City, Iraq.

Muslim Abbas Allu[1], Mahde Saleh Assafi[2],*, Reem Fouad Polse[3], Mohammad Ismail Al-Berfkani[1]

1- Department of Medical Laboratory Technology, Duhok Polytechnic University, Duhok, Kurdistan Region, Iraq
2- Department of Biology, School of Sciences, University of Duhok, Duhok, Kurdistan Region, Iraq.
3-Department of Biology, Faculty of Sciences, University of Zakho, Zakho, Kurdistan Region, Iraq,

A B S T R A C T:

Typhoid fever is still recognized as one of the most important global health problem. *Salmonella* species are the main cause of typhoid fever that causes health threat in developing countries. The purpose of this study was to find out the prevalence and the risk factors of *Salmonella* Typhi from people presenting with fever to Azadi general hospital, Duhok, Iraq. A total of 2323 patient blood samples (992 males and 1331 females) were collected through the period January 2017 to December 2017. Serologic-proved typhoid fever for *Salmonell*a Typhi was diagnosed by Widal test. Out of 2323 blood samples, 824 (35.47%) were diagnosed as serologic-proved typhoid fever. The highest percentage (37.3%) of typhoid fever was recorded at age group 21–30 years and the less prevalence was at age group more than 51 years (29%) (p=0.4036). No significant differences was found in frequency of typhoid fever in males (35.4%) and females (35.5%) (p=0.9387). The incidence of typhoid fever in June (39%) was significantly higher than the incidence rate in other months of the year (p=0.0086). Typhoid fever has a considerable challenge to public health. The age group 21-30 years is the vulnerable group for typhoid fever. The typhoid fever is independent of sex and it is a seasonal disease with the majority of cases occurring is the June. Awareness should be created in young generation related to polluted water and hygienic food to eradicate this particular infection. Hence, health education classes play an important role in to reduce the infection rate.

1.INTRODUCTION :

Enteric fever is a serious bacterial infection caused by *Salmonella enterica* serovars Typhi. It is predicted that morbidity rate of typhoid fever is over than 21 million cases per year worldwide and some of this cases lead to death (Ochiai *et al.*, 2008; Buckle *et al.*, 2012).

Salmonella enterica serovars Typhi is transmitted through contaminated food or water. Human are the only reservoir for *Salmonella* Typhi and there are no known environmental hosts (Painter *et al.*, 2013). Typhoid fever is a systemic disease mainly characterized by a prolonged fever, poor appetite, vomiting, severe headache, malaise and weight loss (Ogoina, 2011). Untreated fever may persist for several weeks and the disease will be fatal in about 15% of the affected people (Heymann, 2004). Typhoid fever is caused primarily by *Salmonella enterica*

* **Corresponding Author:**
Mahde S Assafi
E-mail:mahde.assafi@uod.ac

Allu. M. *et al.* /ZJPAS: 2019, 31 (6): 123-129

124

serovar Typhi and to a lesser extent related serovars Paratyphi A, B, and C (Amicizia *et al.*, 2017). Enteric fever is endemic in many regions of the Asian and African continents also in countries such as Europe, Middle East and the South and Central America (Lee *et al.*, 2016). The incidence and mortality rate of enteric fever vary from region to region (Molbak *et al.*, 2002). Although the Widal test has been used for over a century, it is still widely used in developing countries because of its low cost, easy, relatively non-invasive and adequate substitute for blood, stool, or bone marrow culture (Lalremruata *et al*., 2014; Andualem *et al*., 2014). Typhoid fever is still one of the major health problems in developing countries. Egypt, Pakistan, Syria and Iraq are known as high-risk areas for developing this disease (Crump *et al*., 2003; Sharara and Kanj, 2014; Rasul *et al*., 2017). In Iraq, high rates of typhoid fever reported in different cities such as 67.1% in Sulaimani (Mohammed et al., 2013) 57% in Salahaldin (Al-Khushali, 2008) and 54.9% in Baghdad (Al-Khushali *et al.*, 2007). No similar study was achieved in Duhok city. Therefore, the aims of this study were to assess the prevalence of serologic-proved typhoid fever among patient populations admitted to Azadi general hospital, Duhok, Iraq and to investigate the effect of some factors such as gender, age, and seasonal variation on distribution of cases of typhoid fever among patients.

2. PATIENTS AND METHODS

2.1. Study design and sample collection

A total of 2323 blood samples were collected through the period January 2017 to December 2017 from people at different age groups attending Azadi general hospital, Duhok, Iraq. Of these, 992 (42.7%) were male patients and 1331 (57.3%) were from females. The inclusion criteria for the participants were: (a) Patients from all age groups (b) Not using antibiotics for two weeks before enrollment (c) Having both fever and diarrhea (d) Willing to participate in the study. The study was conducted with the approval of ethics committee of the Duhok Polytechnic University, Duhok, Iraq.

2.2. Widal agglutination test

Widal test for *Salmonella* Typhi was achieved using Somatic (O) and Flagellar (H) antigens Plasmatic Laboratory Products Limited (U.K).

Widal test was used to detect the antibody titers in sera. About 3 ml of blood samples were collected from each patient by venipuncture and transferred into sterile test tubes. Tubes were centrifuged for 5 minutes at 3000rpm. The serum was collected into clean container for each sample using micropipette. Two drops of each serum sample were carefully transferred separately on microscopic slide using a sterile micropipette. The *Salmonella* antigens (O) and (H) reagents were also dropped into the slide. Both were thoroughly mixed with the help of an applicator stick and the tile gently swirled for one minute for observable agglutination. Reacting antigens were classified as positive (+++)=1/320 during (0-15) seconds, (++)=1/160 during (15-45) seconds, and (+)=1/80 during 1 minute, while non-reactive antigens were classified as negative (-) (more than one minute). Reactive titers greater than or equal to 1:80 were classified as positive, while titers less than 1:80 were classified as negative (Itah and Akpan, 2004; Itah and Uweh, 2005).

2.4. Data analysis

All statistical analysis was performed using the SPSS 18 software. Chi-squared test was used to assess the associations between variables. P value of <0.05 were considered as significant.

3. RESULTS AND DISCUSSION

3.1. Serologic-proved typhoid fever (Slide agglutination Widal test)

Salmonella enterica serovar Typhi is the main causative agent of enteric fever and it is the most important pathogen cause typhoid fever in Iraq and other developing countries (Aljanaby and Medhat, 2017; Gibani *et al.*, 2018). In this study, a total of 2323 blood samples were collected from people who fulfilled the inclusion criteria. All collected blood samples were screened by Widal test. Overall prevalence of serologic-proved typhoid fever (positive results in Widal test) in blood samples was 35.47% (824/2323) (Table 1).

Salmonella have increased significantly, both in terms of the incidence and severity of cases of human Salmonellosis (Edelstein *et al.*, 2004). Our results showed higher rate of enteric fever compared to other studies in the country. A hospital based study conducted in AL-Musaib district, Babylon governorate, Iraq showed that 26.5% of the tested blood samples were serologic-

Allu. M. *et al.* /ZJPAS: 2019, 31 (6): 123-129

125

proved typhoid fever (AL-Khafaji *et al.*, 2006). But, results from another study performed in Baghdad, Iraq showed that the Widal test was positive in 78.65% of screened blood samples (Al-Roubaea *et al.*, 2008). In Ethiopia, 74.9% (376/502) of febrile outpatients have a reactive slide agglutination Widal test (Wasihun *et al.*, 2015).

The variation in the incidence rate could be contributed by different factors. For example, the high false positive rate may be due to cross reacting antibodies of other bacterial infections such as *S. Enteritidis* or other non-enteric *Salmonella* infection (Khoharo *et al.*, 2010; Ajibola *et al.*, 2018). Additionally, the antibodies (agglutinins) usually appear during the second week (Brooks *et al.*, 2004). Studies have reported false-positive Widal test results for patients with non-enteric fever *Salmonella* infections, malaria, typhus, meningitis, immunological disorders and chronic liver disease (Sharma *et al.*, 1993; Harries *et al.*, 1995).

Table 1: Age distribution of *Salmonella* Typhi.

Age group (Years)	No. of samples	No. of positive samples	% of positive samples
≤ 10	202	64	31.7
11 - 20	430	158	36.7
21 - 30	549	205	37.3
31 - 40	587	215	36.6
41 - 50	369	128	34.7
> 51	186	54	29
Total	232	842	35.47

3.2 Age distribution of typhoid fever

Different age groups showed varying number of positive samples of typhoid fever (Table 1). The highest rate was recorded in age group between 21–30 years (37.3%). The elderly patients (older than 50 years) showed less prevalence of typhoid fever (29%). The different distribution of *Salmonella* Typhi among these two age groups was statistically significant (p=0.4036).

These observations were consistent with various studies (Kumar *et al.*, 2013; Rasul *et al.*, 2017). Al-Roubaea *et al.* (2008) found that most infections were between age groups 21-30 years (30%) and the lowest rate (7%) was in age group 60-70 years. Furthermore, a study performed in Pakistan showed that the age group 21-30 years was highly affected by typhoid infection (Rasul *et al.*, 2017). Also, our finding was almost in accordance, with the study of Afroz *et al.*, (2014) who found that the highest rate (29.19%) of enteric fever in Dhaka, Bangladesh was in the 20-35 year age group which is very similar to this study age group (20-30 year). The high numbers of infections at this age group may be due to the fact that this is the working age group who are exposed to infection early in the community. Other possible causes include their consumption of unhygienic food and water in working places, and colleges along with increased number of social gatherings (Luby *et al.*, 1998).

3.3. Gender difference of typhoid fever

In the present study, the frequency ratio of typhoid fever in males (351; 35.4%) to females (473; 35.5%) was 1:1 and the differences was statistically not significant (p=0.9387) (Table 2). This finding was in accordance to the reports of other studies worldwide (Jaafar *et al.*, 2013; Rasul *et al.*, 2017). This suggests that typhoid fever is independent of sex. However, some population-based data from different areas of the country have shown a marked variation in frequency of typhoid cases of between males and females.

Allu. M. *et al.* /ZJPAS: 2019, 31 (6): 123-129

126

Table 2. Sex distribution of *Salmonella* Typhi

Age group (Years)	Male		Female	
	No. of samples	No. of positive (%)	No. of samples	No. of positive (%)
≤10	89	28 (31%)	113	36 (46.8%)
11-20	186	69 (37%)	244	89 (57.4%)
21-30	226	83 (37%)	323	122 (60.7%)
31-40	258	98 (38%)	329	117 (55.2%)
41-50	155	51(33%)	214	77 (56.2%)
>51	78	22 (28%)	108	32 (42.1%)
Total	992	351(35.4%)	1331	473 (35.5%)

The highest percentage of infected women was at age 21-30 years (60.7%) and the lowest (42.1%) was at age >51 years. However no significant difference was found between these two age groups (p=0.1264). In males, the age group 31-40 years showed highest infection rate (38%) and the lowest infection rate was at age group >51 years. But the differences between these two age groups was statistically not significant (p=0.1142). According to study in 2006, the typhoid fever rate was highest in female (60.4%) than males (39.5%) (AL-Khafaji *et al.*, 2006). Nevertheless, previous investigations have shown that the infection rate between males and females can vary geographically (Butler *et al.*, 1991; Bergh *et al.*, 1999).

3.4. Seasonal distribution of typhoid fever

Seasonal variations have marked epidemiological interest in typhoid fever.

Table 3. Seasonal distribution of *Salmonella* Typhi

Months	No. of samples	No. of positive	% of positive samples
January	139	48	34.53
February	195	75	38.46
March	199	77	38.69
April	133	50	37.59
May	198	75	37.88
June	192	76	39.58%
July	115	41	35.65
August	267	100	37.45
September	225	82	36.44
October	262	92	35.11
November	206	56	27.18
December	182	52	28.57
Total	2323	824	35.47

In this study, the rate of typhoid fever was varied during the year time. It was ranged from 27% in November to 39% in June (p= 0.0086) (Table 3). This varying is expected as the typhoid fever in Iraqi is a seasonal disease, with the majority of cases occurring in the summer months. The average temperature in Iraq ranges from higher than 48°C in July and August to below freezing in January. This finding is in accordance to other studies in Iraq and worldwide (Prajapati *et al.*, 2008; Rasul *et al.*, 2017). Studies showed that the highest number of patients with typhoid fever in Iraq and worldwide was in summer months, and less commonly in other months of the year (AL-Khafaji *et al.*, 2006; Prajapati *et al.*, 2008; Rasul *et al.*, 2017).

The high temperature in summer season could play a role in distribution the typhoid fever. The infection is transmitted by ingestion of food or

Allu. M. *et al.* /ZJPAS: 2019, 31 (6): 123-129

127

water contaminated with faeces (Parry *et al.*, 2002). Ice cream, raw fruit and vegetables fertilized with sewage are recognized as a significant risk factor for the transmission of typhoid fever (Kothari *et al.*, 2008). Epidemiological data suggest that waterborne transmission of *Salmonella* Typhi usually involves small inocula, whereas foodborne transmission is associated with large inocula and high attack rates over short periods. The major associated risk factors for typhoid fever in summer may include: eating locally prepared ice cream, more consuming of water and the domestic source of water is more likely to be contaminated with sewage, debris and garbage (Dewan *et al.*, 2013).

Because the test has serious cross-reactivity with many other infectious agents, Widal test may produce false-positive results (Su *et al.*, 2004). The test detects agglutinating antibodies to the O and H antigens of *Salmonella enterica* serotype Typhi. But unfortunately, *Salmonella enterica* serotype Typhi shares these antigens with other *Salmonella* serotypes such as *S.* Typhimurium and *S.* Enteritidis and other Non-Typhoidal Salmonella and shares cross-reacting epitopes with other Enterobacteriaceae (Parry *et al.*, 2002). The resulting Widal result may lack sensitivity and specificity, particularly in a community with endemic typhoid fever (Al-Roubaea *et al.*, 2008). The incidence of enteric fever decrease with proper food and water sanitation, pasteurization of milk and other dairy products and elimination of the use of human feces in food production and the use of typhoid vaccines (Lin *et al.*, 2001).

4. CONCLUSIONS

In conclusion, we demonstrate that typhoid fever have a considerable challenge to public health. All age group are affected by typhoid fever with high rate in age group 21-30 years. The typhoid fever is independent of sex. Typhoid fever in Iraq is a seasonal disease with the majority of cases occurring is the summer months. Awareness should be created in young generation related to polluted water and hygienic food to eradicate this particular infection. Hence, health education classes play an important role in to reduce the infection rate. The illiteracy and low educational status is associated with ignorance, poverty and poor personal hygiene.

REFERENCES

AFROZ, H.; HOSSAIN, M. AND FAKRUDDIN, M. 2014. A 6-year retrospective study of bloodstream Salmonella infection and antibiotic susceptibility of *Salmonella enterica* serovar Typhi and Paratyphi in a tertiary care hospital in Dhaka, Bangladesh. *Tzu Chi Medical Journal*, 26: 73-78.

AJIBOLA, O.; MSHELIA, M.B.; GULUMBE, B.H. AND EZE, A.A. 2018. Typhoid Fever Diagnosis in Endemic Countries: A Clog in the Wheel of Progress? *Medicina (Kaunas)*, 54.

AL-KHAFAJI, J.K.T.; AL-YASARI, H.F. AND AL-TAEI, M.H. 2006. Prevalence of Typhoid Fever among Pediatric Patients at AL-Musaib District. *Medical Journal of Babylon*, 6.

AL-KHUSHALI, M.N. 2008. Typhoid & paratyphoid fevers in Salahaldin governorate. *Tikrit Medical Journal*, 14: 107- 111.

AL-KHUSHALI, M.N.; AL-KHAFAJI, A.N. AND AL-AZZAWE, Z.K. 2007. Typhoid and paratyphoid fever in children in Kadhimiya Hospital. *Iraqi J. Comm. Med.*, 20.

AL-ROUBAEA, D.A.; AL-ANI, A.A. AND AL-SHAKER, N.M.M. 2008. Value of widal test in diagnosis of typhoid fever. *Iraqi J. Comm. Med.*, 21: 13-18.

ALJANABY, A.A.J. AND MEDHAT, A.R. 2017. Prevalence of Some Antimicrobials Resistance Associated-genes in *Salmonella* Typhi Isolated from Patients Infected with Typhoid Fever. *Journal of Biological Sciences*, 17: 171-184.

AMICIZIA, D.; ARATA, L.; ZANGRILLO, F.; PANATTO, D. AND GASPARINI, R. 2017. Overview of the impact of Typhoid and Paratyphoid fever. Utility of Ty21a vaccine (Vivotif(R)). *J Prev Med Hyg*, 58: E1-E8.

ANDUALEM, G.; ABEBE, T.; KEBEDE, N.; GEBRE-SELASSIE, S.; MIHRET, A. AND ALEMAYEHU, H. 2014. A comparative study of Widal test with blood culture in the diagnosis of typhoid fever in febrile patients. *BMC Res Notes*, 7: 653.

AFROZ, H.; HOSSAIN, M. AND FAKRUDDIN, M. 2014. A 6-year retrospective study of bloodstream Salmonella infection and antibiotic susceptibility of *Salmonella enterica* serovar Typhi and Paratyphi in a tertiary care hospital in Dhaka, Bangladesh. *Tzu Chi Medical Journal*, 26: 73-78.

AJIBOLA, O.; MSHELIA, M.B.; GULUMBE, B.H. AND EZE, A.A. 2018. Typhoid Fever Diagnosis in Endemic Countries: A Clog in the Wheel of Progress? *Medicina (Kaunas)*, 54.

AL-KHAFAJI, J.K.T.; AL-YASARI, H.F. AND AL-TAEI, M.H. 2006. Prevalence of Typhoid Fever among Pediatric Patients at AL-Musaib District. *Medical Journal of Babylon*, 6.

Allu. M. *et al.* /ZJPAS: 2019, 31 (6): 123-129

128

AL-KHUSHALI, M.N. 2008. Typhoid & paratyphoid fevers in Salahaldin governorate. *Tikrit Medical Journal*, 14: 107- 111.

AL-KHUSHALI, M.N.; AL-KHAFAJI, A.N. AND AL-AZZAWE, Z.K. 2007. Typhoid and paratyphoid fever in children in Kadhimiya Hospital. *Iraqi J. Comm. Med.*, 20.

AL-ROUBAEA, D.A.; AL-ANI, A.A. AND AL-SHAKER, N.M.M. 2008. Value of widal test in diagnosis of typhoid fever. *Iraqi J. Comm. Med.*, 21: 13-18.

ALJANABY, A.A.J. AND MEDHAT, A.R. 2017. Prevalence of Some Antimicrobials Resistance Associated-genes in *Salmonella* Typhi Isolated from Patients Infected with Typhoid Fever. *Journal of Biological Sciences*, 17: 171-184.

AMICIZIA, D.; ARATA, L.; ZANGRILLO, F.; PANATTO, D. AND GASPARINI, R. 2017. Overview of the impact of Typhoid and Paratyphoid fever. Utility of Ty21a vaccine (Vivotif(R)). *J Prev Med Hyg*, 58: E1-E8.

ANDUALEM, G.; ABEBE, T.; KEBEDE, N.; GEBRE-SELASSIE, S.; MIHRET, A. AND ALEMAYEHU, H. 2014. A comparative study of Widal test with blood culture in the diagnosis of typhoid fever in febrile patients. *BMC Res Notes*, 7: 653.

BERGH, V.E.T.A.M.; GASEM, M.H.; KEUTER, M. AND DOLMANS, M.V. 1999. Outcome in three groups of patients with typhoid fever in Indonesia between 1948 and 1990. *Trop Med Int Health*, 14: 211–215.

BROOKS, G.F.; BUTEL, J.S. AND MORE, S.A. 2004. Jawetz, Melnick and Adelberg's medical microbiology , McGraw-Hill companies ,Inc. , Appleton and Lange, 23rd edition.

BUCKLE, G.C.; WALKER, C.L. AND BLACK, R.E. 2012. Typhoid fever and paratyphoid fever: Systematic review to estimate global morbidity and mortality for 2010. *J Glob Health*, 2: 010401.

BUTLER, T.; ISLAM, A.; KABIR, I. AND JONES, P.K. 1991. Patterns of morbidity and mortality in typhoid fever dependent on age and gender: review of 552 hospitalised patients with diarrhoea. *Rev Infect Dis*, 14: 85–90.

CRUMP, J.A.; YOUSSEF, F.G.; LUBY, S.P.; WASFY, M.O.; RANGEL, J.M.; TAALAT, M.,MAHONEY, F.J. 2003. Estimating the incidence of typhoid fever and other febrile illnesses in developing countries. *Emerg Infect Dis*, 9: 539-544.

DEWAN, A.M.; CORNER, R.; HASHIZUME, M. AND ONGEE, E.T. 2013. Typhoid Fever and its association with environmental factors in the Dhaka Metropolitan Area of Bangladesh: a spatial and time-series approach. *PLoS Negl Trop Dis*, 7: e1998.

EDELSTEIN, M.; PIMKIN, M.; DMITRACHENKO, T.; SEMENOV, V.; KOZLOVA, N.; GLADIN, D.,STRATCHOUNSKI, L. 2004. Multiple outbreaks of nosocomial salmonellosis in Russia and Belarus caused by a single clone of Salmonella enterica serovar Typhimurium producing an extended-spectrum beta-lactamase. *Antimicrob Agents Chemother*, 48: 2808-2815.

GIBANI, M.M.; BRITTO, C. AND POLLARD, A.J. 2018. Typhoid and paratyphoid fever: a call to action. *Curr Opin Infect Dis*, 31: 440-448.

HARRIES, A.D.; KAMOTO, O.; MAHER, D.; MUKIBII, J. AND KHOROMANA, C. 1995. Specificity of Widal test in healthy blood donors and patients with meningitis. *J Infect*, 31: 149-150.

HEYMANN, D.L. 2004. Control of Communicable Diseases Manual. 18th ed.: American Public Health Association.

ITAH, A.Y. AND AKPAN, C.J. 2004. Correlation studies on Widal agglutination reaction and diagnosis of typhoid fever. *Southeast Asian J Trop Med Public Health*, 35: 88-91.

ITAH, A.Y. AND UWEH, E.E. 2005. Bacteria isolated from blood, stool and urine of typhoid patients in a developing country. *Southeast Asian J Trop Med Public Health*, 36: 673-677.

JAAFAR, N.J.; YUAN, X.G.; NUR, F.M.Z.; HENG, C.L.; HANI, M.H.; WAN, M.H.,KIA, K.P. 2013. Epidemiological analysis of typhoid fever in Kelantan from a retrieved registry. *Malay J Microbiol* 9: 147-151.

KHOHARO, H.K.; ANSARI, S. AND QURESHI, F. 2010. Evaluating single acute-phase Widal test for the diagnosis of typhoid fever. *Med Channel*, 16: 42-44.

KOTHARI, A.; PRUTHI, A. AND CHUGH, T.D. 2008. The burden of enteric fever. *J Infect Dev Ctries*, 2: 253-259.

KUMAR, M.S.; G, S.V.; R, P.; H, V.P.; P, M.R. AND E, R.N. 2013. Comparison of Salmonella typhi and Paratyphi A Occurrence in a Tertiary Care Hospital. *J Clin Diagn Res*, 7: 2724-2726.

LALREMRUATA, R.; CHADHA, S. AND BHALLA, P. 2014. Retrospective audit of the widal test for diagnosis of typhoid Fever in pediatric patients in an endemic region. *J Clin Diagn Res*, 8: DC22-25.

LEE, J.S.; MOGASALE, V.V.; MOGASALE, V. AND LEE, K. 2016. Geographical distribution of typhoid risk factors in low and middle income countries. *BMC Infect Dis*, 16: 732.

LIN, F.Y.; HO, V.A.; KHIEM, H.B.; TRACH, D.D.; BAY, P.V.; THANH, T.C.,SZU, S.C. 2001. The efficacy of a Salmonella typhi Vi conjugate vaccine in two-to-five-year-old children. *N Engl J Med*, 344: 1263-1269.

LUBY, S.P.; FAIZAN, K.; FISHER-HOCH, S.P.; SYED, A. AND MINTZ, E.D. 1998. Risk factors for typhoid fever in an endemic setting, Karachi, Pakistan. . *Epidemiol Infect* 120: 129-138.

MOHAMMED, M.O.; MUSTAFA, H.M. AND ALSHEIKHANI, M.A. 2013. The epidemiological clinical and laboratory characterisrics of typhoid fever outbreak in Sulaimani governorate during 2007-2008. *Duhok Medical Journal*, 7: 37-48

MOLBAK, K.; GERNER-SMIDT, P. AND WEGENER, H.C. 2002. Increasing quinolone resistance in Salmonella enterica serotype Enteritidis. *Emerg Infect Dis*, 8: 514-515.

OCHIAI, R.L.; ACOSTA, C.J.; DANOVARO-HOLLIDAY, M.C.; BAIQING, D.; BHATTACHARYA, S.K.; AGTINI, M.D.,CLEMENS, J.D. 2008. A study of

Allu. M. *et al.* /ZJPAS: 2019, 31 (6): 123-129

129

typhoid fever in five Asian countries: disease burden and implications for controls. *Bull World Health Organ*, 86: 260-268.

OGOINA, D. 2011. Fever, fever patterns and diseases called 'fever'--a review. *J Infect Public Health*, 4: 108-124.

PAINTER, J.A.; HOEKSTRA, R.M.; AYERS, T.; TAUXE, R.V.; BRADEN, C.R.; ANGULO, F.J. AND GRIFFIN, P.M. 2013. Attribution of foodborne illnesses, hospitalizations, and deaths to food commodities by using outbreak data, United States, 1998-2008. *Emerg Infect Dis*, 19: 407-415.

PARRY, C.M.; HIEN, T.T.; DOUGAN, G.; WHITE, N.J. AND FARRAR, J.J. 2002. Typhoid fever. *New England Journal of Medicine*, 347: 1770-1782.

PRAJAPATI, B.; RAI, G.K.; RAI, S.K.; UPRETI, H.C.; THAPA, M.; SINGH, G. AND SHRESTHA, R.M. 2008. Prevalence of Salmonella typhi and paratyphi infection in children: a hospital based study. *Nepal Med Coll J*, 10: 238-241.

RASUL, F.; SUGHRA, K.; MUSHTAQ, A.; ZEESHAN, N.; MEHMOOD, S. AND RASHID, U. 2017. Surveillance report on typhoid fever epidemiology and risk factor assessment in district Gujrat, Punjab, Pakistan. *Biomedical Research*, 28: 6921-6926.

SHARARA, S.L. AND KANJ, S.S. 2014. War and infectious diseases: challenges of the Syrian civil war. *PLoS Pathog*, 10: e1004438.

SHARMA, J.R.; PARMAR, I.B.; SHARMA, S.J. AND KESAVAN, A. 1993. False positive Widal reaction in malaria. *Indian Pediatr*, 30: 1343-1347.

SU, C.P.; CHEN, Y.C. AND CHANG, S.C. 2004. Changing characteristics of typhoid fever in Taiwa. *J Microbiol Immunol Infect*, 37: 109-114.

WASIHUN, A.G.; WLEKIDAN, L.N.; GEBREMARIAM, S.A.; WELDERUFAEL, A.L.; MUTHUPANDIAN, S.; HAILE, T.D. AND DEJENE, T.A. 2015. Diagnosis and Treatment of Typhoid Fever and Associated Prevailing Drug Resistance in Northern Ethiopia. *Int J Infect Dis*, 35: 96-102.

RESEARCH PAPER

Evaluation of *p53* expression among Colorectal Cancer patients

[1,2] Harmand Ali*, [3] Abdulkarim Y. Karim

1Department of Biology, Collage of Science, Salahaddin University-Erbil, Kurdistan Region, Iraq
2Department of Biology, Faculty of Education, Tishk International University, Erbil, Kurdistan Region, Iraq
3Department of Biology, Collage of Science, Salahaddin University-Erbil, Kurdistan Region, Iraq

A B S T R A C T:

Background and purpose: Colorectal cancer (CRC) is counted as a third most common cancer among men and the second most common among women. Besides that, among cancer-related mortality, the 3rd most common cause of death is due to the CRC worldwide. A tumor suppressor gene *p53* has the main role in regulating cell apoptosis, cell cycle arrest, and cell proliferation. Thus, abnormality in *p53* such as mutation or overexpression has a significant association with human cancer, in which alteration in this gene can be found in more than 50% of different cancer cases. Therefore, our aim in this study is to evaluate the expression level of *p53* gene focusing on its mRNA expression among colorectal cancer patients in Erbil, Kurdistan Region-Iraq.

Material and method: Forty-four pairs colorectal cancer tissues along with their corresponding non-cancerous tissues that were grouped based on the CRC types and patients' clinical features. The expression of the *p53* gene of the samples were evaluated by RT-PCR technique.

Result: results showed that expression of the *p53* gene in colorectal cancer samples was significantly increased (overexpressed) compared to the expression of normal samples (control) (n=44, p=0, 0001).

Conclusion: It might be possible to consider the overexpression of the *p53* gene as a molecular marker for colorectal cancer diagnosis in both men and women. However, for better understanding and confirming our opening findings further analysis are required.

1.INTRODUCTION :

Colorectal cancer, also called bowel cance, is a sort of cancer which develops in the parts of the large intestine. Both genders are able to develop colorectal cancer. However, the incedences rate is distinct from gender to others. Incedences of CRC in women booked for 9.4% among all cancers which make it the second most common right after breast cancer, while it is considered as the third most common among men by 10.0% globally.

Besides , among cancer-related mortality, the third most common cause of death was due to the CRC (Inamura, 2018). According to the statics of 2008, the estimation regarding the incidence and mortality of CRC showed that, approximately 50,000 death among the whole of 150,000 diagnosed cases (László, 2010). While the death rate was higher in the year of 2012, about 700,000 of the patients faced death due to CRC from a total number of about 1.3 million of newly diagnosed cases. However, the incidences of CRC were expected to be increased by 2030 that can reach the range of 2.2 million or even more within

* **Corresponding Author:**
Harmand Ali Hama
E-mail: harmand.ali@ishik.edu.iqor harmand.bio@gmail.com

a mortality rate in half number of the incidents about 1.1 million (Arnold et al., 2016).

The *p53* gene which is placed at chromosome 17q13.1 encodes the tumor suppressor p53 protein (Huang et al., 2014). When this gene gets mutated, which happens in more than 50% of cancer cases including CRC, it would express a mutant form of p53 (MTp53) which is highly associated with human cancer prognosis (Murata et al., 2013). The role of p53 protein in controlling cell proliferation and apoptosis is well known (Huang et al., 2014). Mutation in *p53* gene leads to loss of controlled cell death ability, which results in unregulated cell growth, accordingly, promoting tumorigenesis (Di Agostino et al., 2013).

This study aims to shed a light on, the expression rate of *p53* among CRC patient tissues, which was examined via RT-PCR. Moreover, to find out whether or not *p53* expression level has a correlation with the progression of tumor and its prognosis among colorectal cancer.

2.MATERIALS AND METHODS

2.1. *Patients and samples:* Overall 44 paired tissue samples (44 tumor tissue and 44 control) were obtained from CRC patients from the Rizgary Hospital in Erbil, Kurdistan Region-Iraq between October 2018 and April 2019. The obtained tissue samples (biopsies) of the CRC were preserved in RNALater in -20℃ until RNA analysis.

2.2. *RNA extraction:* RNA was extracted from the obtained colorectal tissue samples using the *ExiPrep*^{TM} Tissue total RNA kit (Bioneer, Korea) following the instruction of its manufacture. Biophotometer (Eppendorf, Germany, model: Biophotometer Plus 6132) was used to determine the quantification and qualification of total extracted RNA.

2.3. *Complementary DNA synthesis:* In order to measure the *p53* gene expression level, the mRNA converted to cDNA using Ipsogen RT Kit (Qiagen, GmbH, Hilden, Germany) following the manufacturer's instructions. Thermal cycling processes Master-cycler pro PCR System (Eppendorf, German) was used to regulate the required condition for the cDNA. Then, the cDNA was amplified by RT-PCR employing the expression primers described in table 1.

2.4. *Expression analysis of p53 gene*: RT-PCR was performed using Master-cycler pro PCR System (Eppendorf, German) with RT^2 SYBR Green ROX FAST Mastermix (Qiagen GmbH, Hilden, Germany) for *p53* expression. The housekeeping gene Glyceraldehyde-3- phosphate dehydrogenase (GAPDH) was used as internal control for normalization (Liu et al., 2014). Moreover, cDNA for *p53* was subjected to RT-PCR using a set of primers designed based on exon–exon junction using online tool primer-BLAST. However, for the GAPDH we used a set of primers which previously described by (Liu et al., 2014) as indicated in Table 1.

MJ Research, AB Applied Biosystem thermal cycler was used to optimize the primer. We have prepared 50μL reaction mixture in PCR tubes containing 2.5 μL cDNA template, 25 μL OnePCR^{TM} master mix (GeneDirex, Korea), 1 μL forward primer, 1 μL reverse primer and 20.5 μL ddH2O. The cycling conditions were set in which initial denaturation at 95℃ for 10 min, 35 cycles of denaturation at 95 ℃ for 45 sec, annealing temperatures mentioned in Table 1 for 30 sec and extension at 72℃ for 45 sec, and final extension at 72℃ for 4 min.

Table 1. The utilized primer sequences, PCR product and optimum annealing temperature.

Primer	Sequence 5'- 3'	PCR product	Annealing temperature	References
p53 gene	F- CTGTCATCTTCTGTCCCTTC	222	57.3	(NCBI, 2018)
	R- TGGAATCAACCCACAGCTGCA			
GAPDH gene	F- GGGTGATGCTGGTGCTGAGTATGT	700	68.1	(Liu et al., 2014)
	R- AAGAATGGGAGTTGCTGTTGAAGTC			

2.5. *Statistical analysis:* Graphpad prism 7 was used to statistically analyze the obtained data. Relative quantification RT-PCR was performed in triplicate. The values of threshold cycle (Lao and Grady) were obtained for *p53* and the Ct of housekeeping gene (GAPDH) was used to normalized the values. ΔCt method was performed in order to calculate relative changes (gene expression with respect to the housekeeping gene) in *p53* expression for both tumor and control samples separately.

In order to evaluate the data of present study, we have used the student's t-test to compare colon and rectum cancerous tissue with normal adjacent tissue of mRNA expression level of P53 gene with considering the normal distribution parameters of our data. The assumed significance value was considered at p ≤ 0.05. Beside of that descriptive statistical methods (mean, standard deviation, median, minimum, maximum rate and frequency) were considerable.

3.RESULTS

In this study, the expression of the *p53* gene for 44 pair of samples was studied. In order to investigate the expression profiles of *p53* in CRC patients, we have used qRT-PCR to evaluate the *p53* expressions. Moreover, Results revealed that *p53* expression was significantly higher (over-expressed) in tumor tissues than the normal tissue (Figure 1). The level of *p53* gene expression was counted from 44 obtained pairs. It was found out that mRNA expression rate from tumor samples was increased compared with its expression level in control samples (non-cancerous) and it was statistically significant (p=0,0001) based on (T-test; p ≤ 0,05). The level of mRNA expression is shown in Figure 2. for both control and tumor tissues.

4.DISCUSSION

For the last decades, *p53* gene and its encoded protein have been the most studied diagnostic and prognostic molecular marker among various types of cancer including CRC (van Houten et al., 2002, Yamashita et al., 2003). The *p53* gene which locates on chromosome 17q13.1 encodes the tumor suppressor p53 protein or named as wild type p53 (WTp53) (Huang et al., 2014). The *p53* gene is considered as a key part in mediating cell response for several sorts of stresses via inducing or suppressing those genes which are involved in apoptosis, DNA repair, cell cycle arrest, senescence and angiogenesis (Khailany et al., 2017). Numerous studies have reported *p53* overexpression among CRC cases. El-Mahdani et al. (1997) stated that over-expression of *p53* gene occurs frequently in colorectal tumors. Moreover, the *p53* gene mutation as well as the accumulation of p53 protein which is resulted in overexpression of its gene are common genetic feature in CRC (Akshatha et al., 2016). The mutation or loss of the *p53* gene can be identified in more than 50% of all different human cancers (Lee et al., 2013). The expression of mutated *p53* is results in MTp53 and it causes problems in cell cycle which leads to uncontrolled cell growth that promotes tumorigenesis. We intended to determine possible relationship of mRNA expression level and *p53* gene in CRC patients.

Several experiences that are new in cancer biology is depending on the investigation of gene expression examination (Huang et al., 2014, Khailany et al., 2017). This is because of examination of mRNA expression can be considered as an extremely valuable tool in the detection of cancer malignancy, as well as the classification of cancer as a prediction of disease resultant. In our study, the level of mRNA expression of *p53* gene was significantly increased (Up-regulated) as indicated in Figure 1 and 2. Similar results have been founded by (Akshatha et al., 2016, Smith et al., 1996) who also reported the *p53* overexpression in CRC.

Losing functionality of tumor suppressor genes which they normally inhibit tumor development, such as *p53* is well known event (Huang et al., 2014). Furthermore, in the case of *p53* gene the event not only stops with losing its function but also it works oppositely by stimulating tumorgenicity process (Theodoropoulos et al., 2009). For instance, the tumorigenicity osteosarcomas and pre-B cells fibroblasts has increased due to up-regulation of MTp53 (Huang et al., 2014). Additionally, in the case of human T-cell acute lymphoblastic leukemia with mutant p53 alleles which naturally occurs with stable expression have been found, in which increases tissue invasiveness and tumor formation (Theodoropoulos et al., 2009).

In the recent cancer-related studies, the main focus is on the alterations in the gene expression regulation that is not related to the DNA sequence changes and are known as the epigenetic alterations such as DNA methylation and alteration of microRNA expression that have main effect on mRNA expression (Goel and Boland, 2012). However, the effect of epigenetic modification cannot be considered as changes only in gene expressions that happen through modified interactions between the mRNAs or DNA regulator portions (Goel and Boland, 2012). This usually occurs through modifications in gene promoters, in splicing of transcripts or in the stability of transcripts. Although epigenetic alteration has been extremely useful as a diagnostic marker of colorectal cancer, it will not be enough and only marker to be depend on in diagnosis of CRC (Goel and Boland, 2012).
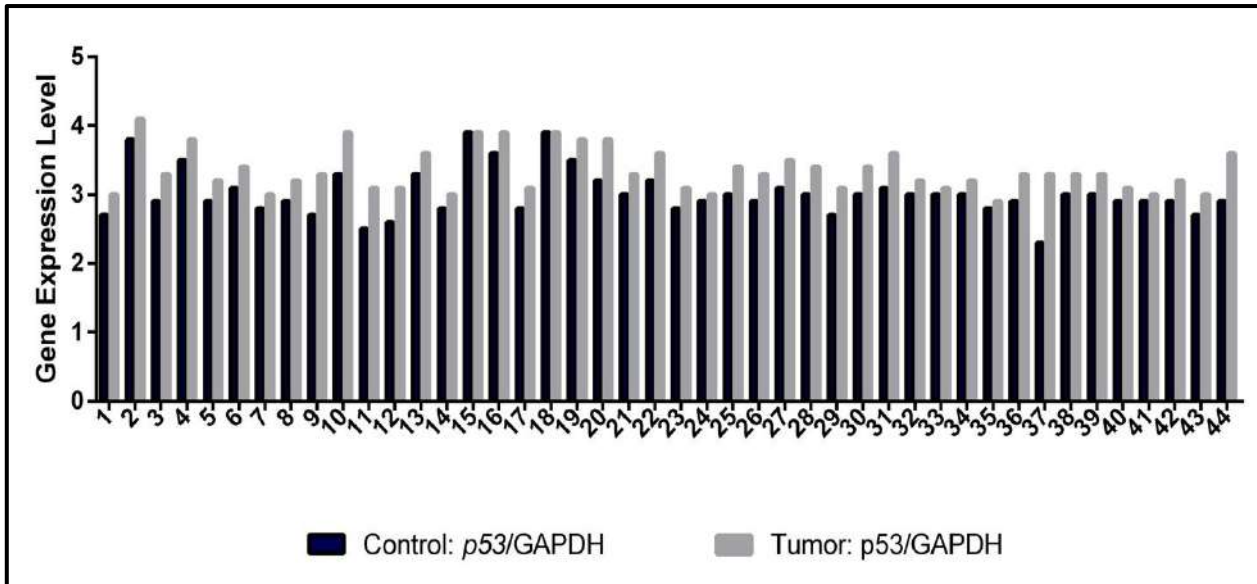

Figure 1. The level of mRNA expression of both normal and tumor tissue among CRC according to *p53*/GAPDH. The level of mRNA expression in 43 samples in tumor tissues increased compared with normal tissues.
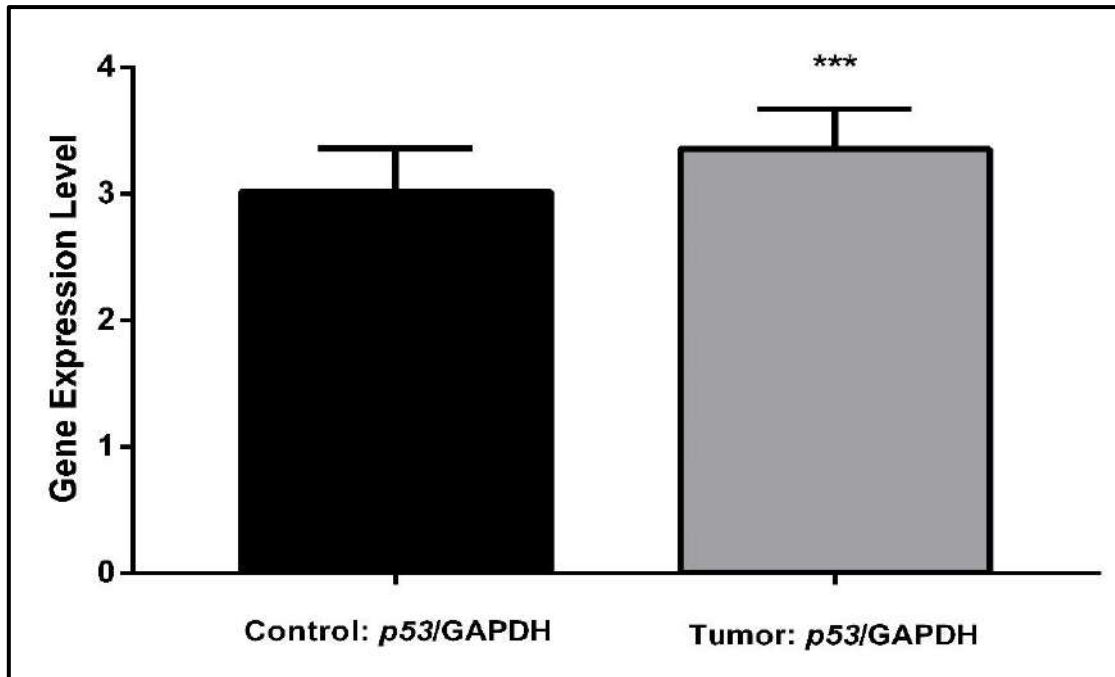

Figure 2. The statistical result of mRNA expression level of *p53*/GAPDH in both normal and tumor tissue samples among CRC patients.

5.CONCLUSIONS

All in all, it can be concluded that there was a significant relationship between overexpression of *p53* gene in tumor tissue and CRC occurrence which evaluated by RT-PCR. Thus, it can be stated that increased mRNA expression of *p53* gene could be a risk factor for colorectal cancer development. Despite of having evidences about relationship between CRC and *p53* gene further molecular investigations are essential including epigenetics and MicroRNA analysis in order to fully understand the correlation between colorectal cancer and molecular biomarkers.

References

AKSHATHA, C., MYSOREKAR, V., ARUNDHATHI, S., ARUL, P., RAJ, A. & SHETTY, S. 2016. Correlation of p53 overexpression with the clinicopathological prognostic factors in colorectal adenocarcinoma. *Journal of clinical and diagnostic research: JCDR,* 10**,** EC05.

ARNOLD, M., SIERRA, M. S., LAVERSANNE, M., SOERJOMATARAM, I., JEMAL, A. & BRAY, F. 2016. Global patterns and trends in colorectal cancer incidence and mortality. *Gut***,** gutjnl-2015-310912.

DI AGOSTINO, S., STRANO, S. & BLANDINO, G. 2013. Gender, mutant p53 and PML: a growing "affaire" in tumor suppression and oncogenesis. *Cell Cycle,* 12**,** 1824-1825.

EL-MAHDANI, N., VAILLANT, J., GUIGUET, M., PREVOT, S., BERTRAND, V., BERNARD, C., PARC, R., BEREZIAT, G. & HERMELIN, B. 1997. Overexpression of p53 mRNA in colorectal cancer and its relationship to p53 gene mutation. *British journal of cancer,* 75**,** 528.

GOEL, A. & BOLAND, C. R. 2012. Epigenetics of colorectal cancer. *Gastroenterology,* 143**,** 1442-1460. e1.

HUANG, K., CHEN, L., ZHANG, J., WU, Z., LAN, L., WANG, L., LU, B. & LIU, Y. 2014. Elevated p53 expression levels correlate with tumor progression and poor prognosis in patients exhibiting esophageal squamous cell carcinoma. *Oncology letters,* 8**,** 1441-1446.

INAMURA, K. 2018. Colorectal Cancers: An Update on Their Molecular Pathology. *Cancers,* 10**,** 26.

KHAILANY, R. A., AL-ATTAR, M. S. & HASAN, A. A. 2017. Association of P53 gene expression alteration among breast cancer patients in Erbil province. *Cukurova Medical Journal,* 42**,** 205-209.

LAO, V. V. & GRADY, W. M. 2011. Epigenetics and colorectal cancer. *Nature Reviews Gastroenterology and Hepatology,* 8**,** 686.

LÁSZLÓ, L. 2010. Predictive and prognostic factors in the complex treatment of patients with colorectal cancer. *Magyar onkologia,* 54**,** 383-394.

LEE, J. Y., KIM, H. J., YOON, N. A., LEE, W. H., MIN, Y. J., KO, B. K., LEE, B. J., LEE, A., CHA, H. J. & CHO, W. J. 2013. Tumor suppressor p53 plays a key role in induction of both tristetraprolin and let-7 in human cancer cells. *Nucleic acids research,* 41**,** 5614-5625.

LIU, Z.-C., YANG, Z.-X., ZHOU, J.-S., ZHANG, H.-T., HUANG, Q.-K., DANG, L.-L., LIU, G.-X. & TAO, K.-S. 2014. Curcumin regulates hepatoma cell proliferation and apoptosis through the Notch signaling pathway. *International journal of clinical and experimental medicine,* 7**,** 714.

MURATA, A., BABA, Y., WATANABE, M., SHIGAKI, H., MIYAKE, K., KARASHIMA, R., IMAMURA, Y., IDA, S., ISHIMOTO, T. & IWAGAMI, S. 2013. p53 immunohistochemical expression and patient prognosis in esophageal squamous cell carcinoma. *Medical Oncology,* 30**,** 728.

NCBI. 2018. *Homo sapiens p53 (p53) gene* [Online]. Available: https://www.ncbi.nlm.nih.gov/tools/primer-blast/index.cgi?ORGANISM=9606&INPUT_SEQUENCE=JF923572.1&LINK_LOC=nuccore [Accessed].

SMITH, D., JI, C. & GOH, H. 1996. Prognostic significance of p53 overexpression and mutation in colorectal adenocarcinomas. *British journal of cancer,* 74**,** 216.

THEODOROPOULOS, G. E., KARAFOKA, E., PAPAILIOU, J. G., STAMOPOULOS, P., ZAMBIRINIS, C. P., BRAMIS, K., PANOUSSOPOULOS, S.-G., LEANDROS, E. & BRAMIS, J. 2009. P53 and EGFR expression in colorectal cancer: a reappraisal of 'old'tissue markers in patients with long follow-up. *Anticancer research,* 29**,** 785-791.

VAN HOUTEN, V. M., TABOR, M. P., VAN DEN BREKEL, M. W., ALAIN KUMMER, J., DENKERS, F., DIJKSTRA, J., LEEMANS, R., VAN DER WAAL, I., SNOW, G. B. & BRAKENHOFF, R. H. 2002. Mutated p53 as a molecular marker for the diagnosis of head and neck cancer. *The Journal of Pathology: A Journal of the Pathological Society of Great Britain and Ireland,* 198**,** 476-486.

YAMASHITA, H., NISHIO, M., TOYAMA, T., SUGIURA, H., ZHANG, Z., KOBAYASHI, S. & IWASE, H. 2003. Coexistence of HER2 over-expression and p53 protein accumulation is a strong prognostic molecular marker in breast cancer. *Breast Cancer Research,* 6**,** R24.

RESEARCH PAPER

Cydia pomonella (L.) (Lepidoptera: Tortricidae) Larvae Infestation on Apple Trees According to Canopy Aspects

[1]Gona Sirwan Sharif , [2]Juhina Idrees Mohamad Ali

1 Department of Plant Protection, College of Agriculture, Salahaddin University-Erbil, Kurdistan Region, Iraq
2 Department of Plant Protection ,College of Agricultural and Forestry, Mosul University, Mosul, Iraq

A B S T R A C T:

The codling moth (*Cydia pomonella* L.) is one of the most important pests existing in the apple orchards of the Hiran-Iraq northern part, according to the climate of Iraq Codling moth has 2–3 generations per year. This study conducted to calculate the relation between distribution of codling moth and canopy aspects and also to estimate the relationship between diameter and height of trees with fallen fruits. The results revealed that the highest infestation recorded by second generation of codling moth which was 0.952, the highest mean values of the fallen fruit were 38.600, regarding canopy aspects the highest infestations were recorded in the South followed East and North side compare to West or Middle side, and also this investigation confirmed that there is a significant influence of tree height and rate of infestations by codling moth. This study concluded, that canopy aspects, height and diameter of trees, with climate condition such as temperature and humidity effect apple orchards infestation by codling moth.

1.   INTRODUCTION :

Cydia pomonella (Lepidoptera: Tortricidae), is considered one of the most significant pests of apples, pears and walnuts across the world, including the Western Cape, South Africa (Grigg- McGuffin et al., 2015 and Reyes et al., 2015). Codling moth hibernaculum overwinters from November to April, pupal stage keeps codling moth from winter climate and they emerge as adults during spring. Adult females will lay eggs on the surface of fruit after mating thus neonate larvae bore into the fruit calyx upon and develop internally leaving fruit damaged from feeding, final instars larvae exit the fruit and finally becomes adult and the cycle will repeat (Arthurs et al., 2006).

Weather conditions determine the rate/duration of these developmental processes (Lacey et al., 2008). The climate in northern Iraq is highly suitable for codling moth, resulting in 2–3 generations per year, from 2007 to 2016 annual local apple production decreased from 22% to 3% as a result of this pest (Ali, 2010).

Generally, fruits influenced by many factors (qader, 2019) and climate condition of Iraq has a role on plant productions (Salih, 2019). Apple fruit infestation patterns are influenced by many environmental variables such as temperature, humidity, light interception, wind, fruit phenology and canopy aspect (north, east, south, west) and tree height which influenced on the population dynamics of codling moth larvae in various varieties of apple trees (Stoeckli et al., 2008 and Mahzoum et al., 2017) and (Kappel and Quamme, 1993, Kührt et al., 2006, Stoeckli et al., 2008 and Wearing, 2016) .

Apple odor has a wide range of effects on adult codling moth behavior as enhanced virgin female

* **Corresponding Author:**
Gona Sirwan Sharif
E-mail: gonasirwansharif@gmail.com or gonasirwan@yahoo.com

Sharif. G. *and*.Ali.J /ZJPAS: 2019, 31 (6): 135-142

136

pheromone production, promoting upwind orientation of larvae and adults to the source of odor and the oviposition is stimulated by apple (Yan et al., 1999) and (Reed and Landolt, 2002). However, male codling moth was discovered to be attracted to a combination of volatile fruit such as (E, E) farnesol and a combination of (E)-β-farnesene and (E, E)-α-farnesene , Apple fruit infested with codling moth larvae boosted the output of (E)-β-ocimene and (E, E) -α-farnesene, which also enhanced the attractiveness of adult women (Reed and Landolt, 2002) .

The present study aimed to estimate the distribution of codling moth within a tree and its distribution in the North, East, South, West and Middle of the canopy and the relationship between tree height and the diameter of the fallen fruits.

2. Materials and Methods

2.1 Plant material

The research regarding ecological aspects of the *Cydia pomonella* L. pest was conducted in apple orchards filed, with surface 13,181 m^2 located in Heran northern part of Iraq (36°16'58.0"N 44°29'54.7"E; 850- m altitude), during the vegetative season of (May 2016 - May 2017). Apple orchard was uniform and untreated with pesticide. 30 apple trees were chosen randomly, they were 2 - 7.5m height and 3- 14 cm diameter (Mahzoum et al., 2017). The evolution of climate condition was recorded during entire study from general direction of agriculture and Irrigation, Erbil governorate.

2.2 Codling moth survey

A total of 750 fruits monitored and only 25 fruits were randomly observed from each tree. The infested fruits were noted frequently every 14 days during vegetative seasons on the north, east, south, and west side of the tree, as well as on the middle side of the apple tree (Mahzoum et al., 2017). For all two generations, infestations and physiological fruit disorder were reported regularly, from May until harvest covering the fruiting period (Dyhia and Ferroudja, 2016).

2.3 Statistical analysis

Statistical analysis performed on the percentage of apple fruits damaged by codling moth larvae depending on canopy aspect, canopy height and diameter of the apple trees. All statistical analyses were performed with SPSS version (25).

Significance levels for the Duncan post hoc test were set at $P < 0.05$, and mean ± standard error (SE).

3.The Results

3.1 The climatic characterization of the area

The climatic data and humidity for the present study were observed and presented in (Table 1). The highest recorded temperature for the present study was 35°C in August 2016, and the highest recorded humidity for the present study was 64.5% in May 2016.

Table 1. Average temperature and relative humidity/ Meteorological station in Shaqlawa - Erbil during May 2016 – May, 2017.

sampling date	Average of	
	Temperature 0C	Relative humidity %
28.5.2016	24.0	64.5
11.6.2016	25.0	47.5
26.6.2016	30.0	37.5
11.7.2016	29.0	36.0
24.7.2016	33.0	31.0
6.8.2016	35.0	29.0
20.8.2016	34.0	29.5
2.9.2016	31.5	27.0
16.9.2016	25.0	29.5
29.9.2016	21.0	27.5
13.5.2017	24.0	48.0
27.5.2017	24.0	41.5

3.2 Larvae infestation regarding canopy aspects

The first three data collection represent the first generation of the *Cydia pomonella* and the second generation was found in the next data collection of July and August 2016, after Harvesting fruits, in between August and September 2016, the infestation was lower down decreased to the zero (Table 2).

In the north side, the highest infestation of the codling moth larvae on apple fruit was recorded during May (2016) and the lowest infestation was recorded in September (Table 2, column 2) while infestation was appeared in the north site during the last week of May and reached the average

Sharif. G. *and*.Ali.J /ZJPAS: 2019, 31 (6): 135-142

137

range of (0-3). In the East side, the highest infestation of the codling moth larvae on apple fruit was recorded during mid of June and July and the lowest recorded during September (Table 2, column 3) while the infestation was appeared during end of May and reached the average range of 0.467 (0-3). In the South side, the highest mean values of codling moth larval infestation was 2.500 recorded in the last week of May and the lowest infestation was 0.200 occurred in the third week of August and September (Table 2, column 4) while the infestation was occurred during the last week of May and reached the average range of 1.000 (0-3). In the West side, the highest values for codling moth larval infestation was 1.533 during the fourth week of May and the lowest in the second and fourth week of September (Table 2, column 5) while for 2017 the infestation was appeared again during the last week of May and intensity was reached in average 0.900 and range (0-3). In the Middle side, the

highest mean values for codling moth larval infestation was 1.333, which was appeared during the fourth week of May and the lowest infestation during the second and fourth week of September (Table 2, column 6) while the infestation was 0.483 which was not statistically different when compare with the first year infestation during August and September.

In generally, during the period of study 2016-2017, the highest mean values of Codling moth larvae infections on apple trees were recorded in the South followed East and North side, however, there was no significant difference in between the South with North and East side. The lowest mean values for codling moth larval infestation were recorded in the Middle and West side respectively. In the last week of May (2017) were recorded the highest mean values of larvae infestation, the lowest mean values were recorded in September (2016) (Table 3, column AB, column aa).

Table 2. Influence sampling date on infested fruit by *Cydia pomonella* larvae in five aspects (North, East, South, West and Middle) throughout fruiting (2016 - 2017)

Sampling date	North		East		South		West		Middle	
	Range	Mean ± S.E.	Range	Mean ± S.E.	Range	Mean ± S.E.	Range	Mean ± S.E.	Range	Mean ± S.E.
28.5.20116	0-5	2.100 ± 0.264 a	0-5	1.633 ± 0.269 a	0-5	2.500 ± 0.310 a	0-4	1.533 ± 0.202 a	0-5	1.333 ± 0.289 a
11.6.2016	0-5	1.500 ± 0.243 b	0-5	1.800 ± 0.316 a	0-5	1.733 ± 0.303 b	0-5	1.300 ± 0.259 ab	0-4	1.200 ± 0.227 a
26.6.2016	0-5	0.900 ± 0.237 c	0-5	0.867 ± 0.224 bc	0-3	0.467 ± 0.150 ef	0-5	0.600 ± 0.212 cd	0-5	0.833 ± 0.235 ab
11.7.2016	0-4	0.967 ± 0.217 c	0-4	1.800 ± 0.281 a	0-4	1.633 ± 0.260 bc	0-5	1.500 ± 0.274 a	0-5	1.267 ± 0.225 a
24.7.2016	0-5	0.633 ± 0.237 cd	0-5	1.400 ± 0.294 ab	0-4	1.133 ± 0.218 cd	0-4	0.800 ± 0.211 c	0-4	0.833 ± 0.180 ab
6.8.2016	0-1	0.200 ± 0.074 de	0-2	0.300 ± 0.119 c	0-2	0.300 ± 0.119 f	0-2	0.133 ± 0.079 de	0-5	0.533 ± 0.218 bc
20.8.2016	0-3	0.233 ± 0.114 de	0-5	0.367 ± 0.195 c	0-2	0.200 ± 0.088 f	0-2	0.100 ± 0.074 de	0-2	0.267 ± 0.095 c
2.9.2016	0-1	0.067 ± 0.046 e	0-3	0.200 ± 0.139 c	0-3	0.200 ± 0.121 f	0-2	0.100 ± 0.074 de	0-2	0.200 ± 0.088 c
16.9.2016	0	0.000 ± 0.000 e	0-3	0.200 ± 0.139 c	0-3	0.200 ± 0.139 f	0-1	0.033 ± 0.033 e	0-1	0.100 ± 0.056 c
29.9.2016	0	0.000 ± 0.000 e	0-3	0.200 ± 0.139 c	0-3	0.200 ± 0.139 f	0-1	0.033 ± 0.033 e	0-1	0.100 ± 0.056 c
13.5.2017	0-1	0.222 ± 0.082 de	0-3	0.250 ± 0.132 c	0-5	0.519 ± 0.241 ef	0-2	0.241 ± 0.107 de	0-2	0.200 ± 0.088 c
27.5.2017	0-3	1.148 ± 0.225 bc	0-3	0.467 ± 0.157 c	0-3	1.000 ± 0.186 de	0-3	0.900 ± 0.188 bc	0-3	0.483 ± 0.154 bc

The data represent Mean ±S. E, n=30. The different letters with the same column indicate significant difference in fruit infestation according to Duncan Multiple range test, $p < 0.05$.

Sharif. G. and.Ali.J /ZJPAS: 2019, 31 (6): 135-142

138

Table 3. Means of interaction between five aspect (North, East, South, West and Middle) and sampling date of fruit on trees infested by *Cydia pomonella* throughout fruiting (2016 - 2017).

Sampling date	North Range	North Mean ± S.E.	East Range	East Mean ± SE.	South Range	South Mean ± S.E.	West Range	West Mean ± S.E.	Middle Range	Middle Mean ± S.E.	a a Range	a a Mean ± S.E.
28.5.20116	0-5	2.200 ± 0.281 ab	0-5	1.567 ± 0.257 c-f	0-5	2.500 ± 0.310 a	0-4	1.500 ± 0.202 c-g	0-5	1.233 ± 0.261 c-i	0-5	1.800 ± 0.123 a
11.6.2016	0-5	1.500 ± 0.243 c-g	0-5	1.800 ± 0.316 b-d	0-5	1.733 ± 0.303 b-e	0-5	1.300 ± 0.259 c-h	0-4	1.200 ± 0.227 d-g	0-5	1.507 ± 0.121 b
26.6.2016	0-5	0.967 ± 0.237 f-m	0-5	1.833 ± 0.280 bc	0-3	1.667 ± 0.260 b-e	0-5	1.567 ± 0.270 c-f	0-5	1.267 ± 0.225 c-h	0-5	1.460 ± 0.115 b
11.7.2016	0-4	0.967 ± 0.217 f-m	0-4	1.400 ± 0.294 c-h	0-4	1.133 ± 0.218 e-k	0-5	0.800 ± 0.211 h-q	0-5	0.833 ± 0.986 h-p	0-5	1.027 ± 0.102 c
24.7.2016	0-5	0.633 ± 0.237 i-r	0-5	0.867 ± 0.224 h-0	0-4	0.467 ± 0.150 l-r	0-4	0.600 ± 0.212 i-r	0-4	0.833 ± 0.235 h-p	0-5	0.680 ± 0.095d
6.8.2016	0-1	0.200 ± 0.074 p-r	0-2	0.300 ± 0.119 n-r	0-2	0.300 ± 0.119 n-r	0-2	0.133 ± 0.079 r	0-5	0.533 ± 0.218 k-r	0-5	0.293 ± 0.059 e
20.8.2016	0-3	0.233 ± 0.114 o-r	0-5	0.367 ± 0.195 m-r	0-2	0.200 ± 0.088 p-r	0-2	0.100 ± 0.074 r	0-2	0.267 ± 0.095 h-r	0-5	0.233 ± 0.054 e
2.9.2016	0-1	0.067 ± 0.046 r	0-3	0.200 ± 0.139 p-r	0-3	0.200 ± 0.121 p-r	0-2	0.100 ± 0.074 r	0-2	0.200 ± 0.088 p-r	0-3	0.153 ± 0.044 e
16.9.2016	0	0.000 ± 0.000 r	0-3	0.200 ± 0.139 p-r	0-3	0.200 ± 0.139 p-r	0-1	0.033 ± 0.033 r	0-1	0.100 ± 0.056 r	0-3	0.107 ± 0.041 e
29.9.2016	0	0.000 ± 0.000 r	0-3	0.200 ± 0.139 p-r	0-3	0.200 ± 0.139 p-r	0-1	0.033 ± 0.033 r	0-1	0.100 ± 0.056 r	0-3	0.107 ± 0.041 e
13.5.2017	0-1	0.167 ± 0.069 qr	0-3	0.233 ± 0.124 o-r	0-5	0.467 ± 0.218 l-r	0-2	0.267 ± 0.106 n-r	0-2	0.200 ± 0.088 p-r	0-5	0.267 ± 0.059 e
27.5.2017	0-3	1.033 ± 0.212 f-l	0-3	0.467 ± 0.157 l-r	0-3	1.000 ± 0.186 f-m	0-3	0.900 ± 0.188 g-n	0-3	0.467 ± 0.150 l-r	0-3	0.773 ± 0.082 d
AB	0-5	0.664 ± 0.061 ab	0-5	0.786 ± 0.069 ab	0-5	0.839 ± 0.069 a	0-5	0.611 ± 0.056 b	0-5	0.603 ± 0.054 b		

The data represent Mean ±S.E. n=30 the different letters indicate significant difference in fruit infestation according to Duncan Multiple range test, $p < 0.05$.

3.3 Infestation regarding generations of Codling moth

Codling moth recorded the highest infestation in the second-generation during July, August and September of (2016) was 0.952 in the Middle site while recorded the lowest mean values of infestation 0.300 in the North site. Infested fruits have the same distribution in apple trees during either the first or second generation of codling moth (Table 4).

Table 4. Mean of fruit infestation by first generation larvae and second-generation larvae of *Cydia pomonella* in five aspects (North, East, South, West and Middle) upon tree throughout fruiting (2016 - 2017).

Five aspects	First generation Range	First generation Mean ± S.E.	Second generation Range	Second generation Mean ± S.E.
North	0-5	1.479 ± 0.177 a	0-5	0.300 ± 0.069 c
East	0-5	1.433 ± 0.207 a	0-5	0.638 ± 0.136 b
South	0-5	1.567 ± 0.176 a	0-5	0.490 ± 0.071bc
West	0-5	1.133 ± 0.144 a	0-4	0.371 ± 0.069 c
Middle	0-5	1.122 ± 0.169 a	0-5	0.952 ± 0.220 a

The data represent Mean ±S.E. n=30 the different letters with the same column indicate significant difference in fruit infestation according to Duncan Multiple range test, $p < 0.05$.

3.4 Estimation of fallen fruits

The fallen fruits of orchard apple trees were recorded during the period of study and evaluation infestation between physiological disorder and attacked by codling moth larvae.

the highest mean values of the fallen fruit were 38.600 and the lowest (0.000) occurred in the fourth week of May and last week of September, 2016 .the highest mean value of fallen fruit by physiological disorder was 3.200 and 3.700, which occurred in the fourth week of May, 2016, and mid of May, 2017 the lowest mean values infestation (0.000) appeared at last week of September, 2016 while the highest mean values for fruits which attacked by codling moth was 35.400 occurred in the end of May (2016). The lowest mean values infestation (0.000) appeared in the third week of August (2016), end of September. (Table 5).

Sharif. G. and.Ali.J /ZJPAS: 2019, 31 (6): 135-142

139

Table 5. Influence of the sampling date on the fallen fruit as (physiological disorder or attacked by *Cydia pomonella*) throughout fruiting (2016 - 2017).

Sampling date	Fallen fruit			Physiological disorder			Attacked by codling		
	Range	Mean ±	S.E.	Range	Mean ±	S.E.	Range	Mean ±	S.E.
28.5.2016	8-97	38.600 ±	8.870 a	0-8	3.200 ±	0.892 a	90-7	35.400 ±	8.175 a
11.6.2016	8-50	23.200 ±	5.099 bc	0-2	0.400 ±	0.221bc	8-50	22.800 ±	5.048 b
26.6.2016	0-10	3.100 ±	1.069 de	0-1	0.200 ±	0.133 bc	0-9	2.900 ±	0.948 c
11.7.2016	1-11	6.200 ±	1.143 de	0-1	0.100 ±	0.100 c	1-11	6.100 ±	1.187 c
24.7.2016	0-3	1.100 ±	0.348 e	0-1	0.200 ±	0.133bc	0-3	0.900 ±	0.379 c
6.8.2016	0-2	0.400 ±	0.221 e	0-1	0.200 ±	0.133bc	0-2	0.200 ±	0.200 c
20.8.2016	0-1	0.100 ±	0.100 e	0-1	0.100 ±	0.100 c	0	0.000 ±	0.000 c
2.9.2016	0	0.000 ±	0.000 e	0	0.000 ±	0.000 c	0	0.000 ±	0.000 c
16.9.2016	0	0.000 ±	0.000 e	0	0.000 ±	0.000 c	0	0.000 ±	0.000 c
29.9.2016	0	0.000 ±	0.000 e	0	0.000 ±	0.000 c	0	0.000 ±	0.000 c
13.5.2017	0-55	13.500 ±	5.227 cd	0-10	3.700 ±	1.212 a	0-45	9.900 ±	4.239 c
27.5.2017	5-48	27.400 ±	4.300 b	0-4	1.600 ±	0.400 b	5-44	25.800 ±	4.090 b

The data represent Mean ±S.E. n=10 the different letters with the same column indicate significant difference in fruit infestation according to Duncan Multiple range test, $p < 0.05$.

3.5 Relationship between trees diameters and fallen fruits

(Table 6) represent the following data, the highest mean values of fallen fruits which attacked by codling moth, was 7.438 occurred on the tree with a diameter range between (7-9CM.), the lowest mean values (2.848) appeared in the tree diameters which range between (3-5 CM.). The highest mean values of fruit with physiology disorder, was 0.795, which occurred on the tree with a diameter range between (5-7 CM.), and the lowest mean values (0.199) appeared on tree with a diameter range between (9-11CM.) While for attacked by codling moth, the highest mean values were (6.960) occurred on tree diameter range between (7-9 CM.), the lowest mean values (2.485) appeared on tree diameter range between (3-5 CM.).

Table 6. Influence of the trees diameter on the fallen fruit as (physiological disorder or attacked by *Cydia pomonella*) throughout fruiting (2016 - 2017).

Tree diameters Range CM.	Fallen fruit Mean ± S.E.	Physiological disorder Mean ± S.E.	Attacked by codling moth Mean ± S.E.
3-5	2.848 ± 0.588 b	0.361 ± 0.122 ab	2.485 ± 0.481 b
5-7	7.408 ± 1.382 a	0.795 ± 0.189 a	6.593 ± 1.474 ab
7-9	7.438 ± 2.031 a	0.548 ± 0.212 ab	6.960 ± 1.811 a
9-11	4.118 ± 0.892 ab	0.199 ± 0.060 b	3.954 ± 0.876 ab
11-14	6.743 ± 1.858 ab	0.390 ± 0.154 ab	6.355 ± 1.748 ab

The data represent Mean ±S.E. n=10 the different letters with the same column indicate significant difference in fruit infestation according to Duncan Multiple range test, $p < 0.05$.

Sharif. G. *and*.Ali.J /ZJPAS: 2019, 31 (6): 135-142

140

3.6 Relationship between Canopy height and fallen fruits

The highest mean value of fallen fruit were 7.850 occurred on trees range between 6-8 m high and the lowest mean values 2.781 appeared on trees range between 2-4 m high. The highest mean

values of infestation were 7.300 occurred in the tree range between 6-8 m high and the lowest mean values was 2.416 appeared on trees height range between 2 and 4 m high (Table 7).

Table 7. Influence of the tree height on the fallen fruit as (physiological disorder or attacked by *Cydia pomonella*) throughout fruiting (2016 - 2017).

Tree height Range M.	Fallen fruit Mean ± S.E.		Physiological disorder Mean ± S.E.		Attacked by codling moth Mean ± S.E.	
2-4	2.781 ±	0.502 b	0.364 ±	0.103 a	2.416 ±	0.412 b
4-6	6.234 ±	0.828 ab	0.463 ±	0.099 a	5.799 ±	0.776 ab
6-8	7.850 ±	2.550 a	0.550 ±	0.150 a	7.300 ±	2.400 a

The data represent Mean ±S.E. n=10 the different letters with the same column indicate significant difference in fruit infestation according to Duncan Multiple range test, p < 0.05.

4. Discussion

There are many factors which enhance apple fruit infestation and it is fallen, for example, temperature, humidity, light interception, wind, fruit phenology and canopy aspect (north, east, south, west) and tree height (Stoeckli et al., 2008 and Mahzoum et al., 2017) and (Kappel and Quamme, 1993, Kührt et al., 2006, Stoeckli et al., 2008 and Wearing, 2016) .

4.1 Larvae infestation regarding canopy aspects

Data analysis from the present study indicated that there was no significant difference in between the South with North and East side. The lowest mean values for codling moth larval infestation were recorded in the Middle and West side respectively. The findings in this study were similar to the previous studies (MacLellan, 1962 and Blomefield et al., 1997) and (Kappel and Quamme, 1993, Kührt et al., 2006, Stoeckli et al., 2008 and Wearing, 2016) . The codling moth females oviposition behavior was influenced by the canopy aspects of apple trees. In addition, codling moth females avoid to lay eggs at low temperature areas under lab conditions (Kührt et al., 2006), and the less infestation was happened in the North site of apple trees by the first generation codling moth larvae, where because of low

temperature, as was recorded in this side (Stoeckli et al., 2008). (Wei et al., 2012 and Stoeckli et al., 2008) discovered that both of the codling moth oviposition and infestation, was increased in the South- and East-facing sides compared with that in the North-facing side of apple tree. While (Wearing, 2016) was recorded oviposition that increased and was greater in the North and East of the trees which in some seasons was greater fruit load. (Blomefield et al., 1997 and Wood, 1965) also found that the larval infestation was greater on the North- and East-facing aspect when compared with the South- and West-facing aspect of the apple trees, may be westerly winds play importance role to make greater of oviposition on the eastern side of the trees In Nelson (Sutherland et al., 1977) and on the pear trees was recorded a greater damage on the eastern side (Du et al., 2012). However, (Blago and Dickler, 1990 and Wei et al., 2015) showed that there were no relationship between oviposition and aspect within apple trees while its more commonly recorded in the Southern hemisphere.

The lowest mean values infestation (0.000) appeared in the second weeks of September 2016 in the north site. It is suggested that the disappearing infestation due to absence of fruits

Sharif. G. and.Ali.J /ZJPAS: 2019, 31 (6): 135-142

141

on the tree and the period of diapause larvae last flight (second generation). The present results disagree with the findings by (Dyhia and Ferroudja, 2016) in Algeria, it was observed that the fallen fruits began in early June and first of falls were recorded in the 13 July and increase lose with percentage of 7.51% to 44.37% due to infestation by the third generation of codling moth of red delicious variety.

Statistical analysis from present study confirmed significant influence of the tree height on the attacked by codling moth, however, there were no significant influence of the tree height on the fruit physiological disorder. Regarding canopy height the present study is similar to that recorded by (De Waal et al., 2011) while disagree (Stoeckli et al., 2008, Mahzoum et al., 2017) mentioned that first and second generation codling moth larvae infestation was influenced by canopy height of apple trees of different varieties and the middle part of the trees was higher attacked by codling moth larvae.

5.Conclusion
1. Canopy aspect and the side of tree enhance the infestation by Codling moth, as the lowest mean values for codling moth larval infestation were recorded in the Middle and West side
2. Disappear of infestation due to absence of fruits on tree.
3. According to the climate condition the number of generations change from specific location to other.
4. There are significant relations between tree diameter and tree height with infestation by codling moth.

References

ALI, H. N. (2010). Annual report fruit and vegetables (Local and Imported) p. 4

In: Ministry of Agriculture and water resource

ARTHURS, S., LACEY, L. & BEHLE, R. (2006). Evaluation of spray-dried lignin-based formulations and adjuvants as solar protectants for the granulovirus of the codling moth, *Cydia pomonella* (L). *Journal of Invertebrate pathology,* 93**,** 88-95.

BLAGO, N. & DICKLER, E. (1990). Neue Methode zur Untersuchung der Ei-Phänologie des Apfelwicklers, *Cydia pomonella* L.(Lep., Tortricidae). *Journal of Applied Entomology,* 109**,** 98-104.

BLOMEFIELD, T., PRINGLE, K. & SADIE, A. (1997). Field observations on oviposition of codling moth, *Cydia pomonella* (Linnaeus)(Lepidoptera: Olethreutidae), in an unsprayed apple orchard in South Africa. *African Entomology,* 5**,** 319-336.

DE WAAL, J. Y., MALAN, A. P. & ADDISON, M. F. (2011). Efficacy of entomopathogenic nematodes (Rhabditida: Heterorhabditidae and Steinernematidae) against codling moth, *Cydia pomonella* (Lepidoptera: Tortricidae) in temperate regions. *Biocontrol Science Technology* 21**,** 1161-1176.

DU, L., CHAI, S., GUO, J., LU, T. & ZHANG, R. (2012). Egg-laying features of *Cydia pomonella* adults. *Chin J Appl Entomol* 49**,** 70-79.

DYHIA, G. & FERROUDJA, M.-B. (2016). Monitoring of the codling moth Cydia pomonella up on ecological plot (untreated) red delicious variety in Algeria *Journal of Zoology and Research* 2**,** 1-6.

GRIGG-MCGUFFIN, K., SCOTT, I. M., BELLEROSE, S., CHOUINARD, G., CORMIER, D. & SCOTT-DUPREE, C. J. (2015). Susceptibility in field populations of codling moth, *Cydia pomonella* (L.)(Lepidoptera: Tortricidae), in Ontario and Quebec apple orchards to a selection of insecticides. *Pest management science* 71**,** 234-242.

KAPPEL, F. & QUAMME, H. A. (1993). Orchard training systems influence early canopy development and light microclimate within apple tree canopies. *Canadian Journal of Plant Science,* 73**,** 237-248.

KÜHRT, U., SAMIETZ, J. & DORN, S. (2006). Effect of plant architecture and hail nets on temperature of codling moth habitats in apple orchards. *Entomologia experimentalis et applicata*

118**,** 245-259.

LACEY, L. A., HEADRICK, H. L. & ARTHURS, S. P. (2008). Effect of temperature on long-term storage of codling moth granulovirus formulations. *Journal of economic entomology,* 101**,** 288-294.

MACLELLAN, C. (1962). Mortality of codling moth eggs and young larvae in an integrated control orchard. *The Canadian Entomologist* 94**,** 655-666.

MAHZOUM, A. M., LOUAHLIA, S., EL GHADRAOUI, L., ROCHDI, M. & LAZRAQ, A. (2017). Dynamics of codling moth larvae (*Cydia pomonella* L.) in three varieties of apple (Malus domestica Borkh.) in the region of Aït Sbaa

Sharif. G. *and*.Ali.J /ZJPAS: 2019, 31 (6): 135-142

142

(Morocco). *Journal of Materials and Environmental Sciences,* 9**,** 1512-1517.

QADER, H. (2019). Influence combination of Fruits Peel and Fertilizer Methods on growth and yield of Chickpea (*Cicer areitinum*) L. Plants. *ZANCO Journal of Pure and Applied Sciences.,* 31, 3, 45-51. .

REED, H. & LANDOLT, P. J. (2002). Attraction of mated female codling moths (Lepidoptera: Tortricidae) to apples and apple odor in a flight tunnel. *Florida Entomologist***,** 324-329.

REYES, M., BARROS-PARADA, W., RAMÍREZ, C. C. & FUENTES-CONTRERAS, E. J. J. O. E. E. (2015). Organophosphate resistance and its main mechanism in populations of codling moth (Lepidoptera: Tortricidae) from Central Chile. *Journal of Economic Entomology,* 108**,** 277-285.

SALIH, R. (2019). Effect of Sowing Dates and Varieties of Cotton (*Gossypium Hirsutum* L.) on Growth and Yield Parameters. *ZANCO Journal of Pure and Applied Sciences.,* Vol. 31, no. 3.

STOECKLI, S., MODY, K. & DORN, S. (2008). Influence of canopy aspect and height on codling moth (Lepidoptera: Tortricidae) larval infestation in apple, and relationship between infestation and fruit size. *Journal of economic entomology,* 101**,** 81-89.

SUTHERLAND, O., WEARING, C. & HUTCHINS, R. (1977). Production of α-farnesene, an attractant and oviposition stimulant for codling moth, by developing fruit of ten varieties of apple. *Journal of Chemical Ecology* 3**,** 625-631.

WEARING, C. H. (2016). Distribution characteristics of eggs and neonate larvae of codling moth, *Cydia pomonella* (L.)(Lepidoptera: Tortricidae). *International journal of insect science* 8**,** IJIS. S38587.

WEI, J., XU, J. & ZHANG, R. (2015). Oviposition site selection of the codling moth (Lepidoptera: Tortricidae) and its consequences for egg and neonate performance. *Journal of economic entomology* 108**,** 1915-1922.

WEI, Y., LUO, J., ZHOU, Z. & LIU, Y. (2012). The spatial distribution of *Cydia pomonella* eggs in apple orchards in Gansu Province. *Chin J Appl Entomol* 49**,** 49-53.

WOOD, T. (1965). Field observations on flight and oviposition of codling moth (Carpocapsa pomonella (L.)) and mortality of eggs and first-instar larvae in an integrated control orchard. *New Zealand Journal of Agricultural Research,* 8**,** 1043-1059.

YAN, F., BENGTSSON, M. & WITZGALL, P. J. (1999). Behavioral response of female codling moths, *Cydia pomonella*, to apple volatiles. *Journal of Chemical Ecology,* 25**,** 1343-1351.

RESEARCH PAPER

Compost quality assessment for the household solid wastes of Erbil city

Sayran.Y. Jalal and Yahya. A. Shekha

Department of Environmental Sciences, College of Science, Salahaddin University-Erbil- Kurdistan Region, Iraq

A B S T R A C T:

Fifty households were selected for collecting wastes from the houses in different quarters of Erbil city for seven days (from 2-October to 8-October 2015). The average rate of solid waste generation in Erbil City was 0.632 kg/capita/day, 732.18 tons/day for all inhabitants of Erbil city. A degradable portion of refuse estimated by 0.377 kg/capita/day which represent 60% of the solid waste composition. Four different procedures were applied to degradation organic waste for compost production: Aerobic, anaerobic, pit and vermicomposting. For compost quality assessment some indices were used as compost quality index (CQI), fertilizing index (FI) and clean index (CI). The value of compost quality index was ranged from (54.73 to 321.12). The compost quality status for all composts types falls under the extremely good category. Fertilizing index value ranged from (3.3 to 4.06 %), while the clean index value for studied composts was 5%. Based on FI and CI values aerobic and anaerobic composts falls under the best quality category, but pit and worm composts fall within the very good quality category. The physicochemical analysis includes: pH, EC, TOC, TP, TN, NO_3, CEC, Ash content, and K^+ was measured during the study.

INTRODUCTION :

Solid Waste Management (SWM) is the most important and essential problem facing humankind today. The large and growing quantities of solid waste (SW) have become a threat to people and the environment due to the increase in population and urbanization, as well as the toxic components of this waste, and industrial development has become a threat to human beings and the environment (Soufan, 2012).

Composting is an aerobic exothermic process for use as a soil conditioner and fertilizer due to the succession of various microbial communities used in biodegradable waste treatment (Shyamala and Belagali, 2015).

Compost prepared from different organic wastes differing in quality and stability, which also depends on the raw material composition used to produce compost.

Successful composting generally depends on some factors that influence the activities of the microorganism directly and indirectly. These including the type of composted raw material, the composition of nutrients, humidity, temperature, alkalinity and aeration (Shyamala and Belagali, 2012).

To classify the various types of compost, four specific quality parameters (which were the combination of one or more properties that regulate the nutrient mineralization from compost, as well as, its post soil application effectivity), were taken up to formulate (CQI) the Compost Quality Index. CQI has been formulated (using four specific parameters of compost quality: total nutrient content, C / N ratio, microbial potential and percent germination) to classify the quality of different compost types as good, moderate, poor, etc. for easy user understanding. By CQI, it could judge the compost quality that is best used (Bera *et al.,* 2013).

The objective of this investigation was to convert household solid waste into compost and reuse it as the soil fertilizer using four procedures

* **Corresponding Author:**
Yahya A. Shekha
E-mail: yahya.shekha@su.edu.krd or yahyanian@gmail.com

for compost production: aerobic, anaerobic, pit and vermicomposting, in order to know which method is more convenient.

2.MATERIALS AND METHODS

2.1. Study area:

Erbil is the largest city in Iraqi Kurdistan region and the state capital. The area of Erbil governorate is about 15075 km^2, with a population of 1542421, while Erbil city population of 885586 inhabitants (as at 2007), (Erbil Statistic Directorate, 2009). Then the Erbil city population well estimated as 1158520 inhabitants for 2015. According to data obtained from Erbil directorate municipality service and environment, the MSW collected from Erbil city and transported to Kani Kerzhala landfill reached to 2000 tons/day for 2015, while it was more than 2500 tons/day for 2014 and return this reduction in MSW generation to the economic crisis.

2.2. Sample collection and analysis

This study was conducted during the autumn months of the year 2015. Fifty urban houses were selected randomly from different quarters of Erbil city. To reliable estimation quantity of domestic solid waste and generation rate, each family supplied by nylon bags and requested to separated their waste to degradable waste (food scraps, papers of the yard trimmings) and non-degradable waste (plastic, nylon, cans, glass, metals, etc.). Daily samples collected for seven days of consequences from each house (350 samples), brought back to the college of science. The process of waste weighing for each nylon bags was done in glass houses of college, and degradable waste (non-cooked, free fat waste) were separated for composting.

2.3. Generation rate:

The generation rate (capita/day) of domestic solid was estimated waste based on the weight-volume analysis; the following equation was used (Aziz *et al.,* 2011).

$$\text{GR} = \frac{\text{Weight of solid waste(g)}}{\text{Population} * \text{Duration(d)}}$$

2.4. Production of Compost types:

Aerobic composting is composting that depends on bacteria thriving in an environment rich with oxygen. Erbil household organic waste, newspaper and triticale straw were used for aerobic composting. The experiment was conducted in a glass house of science college. The aerobic composting was conducted in aerobic condition, the temperature reaches 55°C during composting, and it requires 21 days for maturation (Preda *et al.,* 2013).

Anaerobic digestion involves the breakdown of organic matter in biomass such as animal dung, human excreta, green plant materials, household organic waste, food and so on by microorganisms in the absence of biogas oxygen, a mixture of methane and carbon dioxide with hydrogen sulphide traces. The process needs about two months for maturation and releasing ammonia (Rajeshwari and Balakrishnan, 2000).

While vermicompost is a process by which food materials, cooking waste, including vegetables and fruit peelings, and so on, can be transformed into compost by earthworms. In this study, *Eisenia foetida* as a species of the earthworm to produce compost was used which adapted to decaying organic material (Misra and Roy, 2002).

The last procedure is pit composting, which is recommended when the compost is prepared with soil and refuse. The method is appropriate for areas with low rainfall. Organic residues and light soil are placed in alternating layers, and a 15 - 20 cm thick layer of refuse covers the pit after filling. The materials can remain in the pit for three months without turning and watering. This process required about six months to reach maturation phase. (Misra and Roy, 2002).

After forming or preparing the different types of composts three samples were taken from each type of compost for physicochemical analysis.

2.5. Compost Indices:

The studied indices included: Compost quality index, fertilizing index, and clean index. The compost quality index (CQI) is a numerical expression used to transform large numbers of variables into a single number representing the compost quality level (Table 1), that had been classified according to Bera *et al.,* (2013) which is represented by the following equation:

$$CQI= \frac{NVNPK*MP*GI}{\frac{C}{N}ratio},$$

Where:

NVNPK = Total nutrient value in terms of total $(N+P_2O_5+ K_2O)$ percent.

MP = log10 value of total microbial population in terms of total bacteria,

total fungi and total actinomycetes.

GI = Germination Index percent.

Table (1). Compost Quality classification according to compost quality index as described by Bera *et al.,* (2013).

Classification of compost as per compost quality Index	
Compost Quality Index (CQI)	Compost Quality Classification
<2	Poor
2 - 4	Moderate
4 - 6	Good
6 - 8	Very Good
> 10	Extremely Good

Compost extract was prepared by add 10g of compost in 100ml distilled water. Extract doses of 30, 60, 100% were used, considering distilled water as a control. For germination index three different types of seeds (tomato, wheat and chickpeas), the percentage of germination and root elongation were measured for calculating germination index according to (Bera *et al.*, 2013):

Seed germination%
$$= \frac{No.of\ seeds\ germinated\ in\ compost\ extract}{No.of\ seeds\ germinated\ in\ control} * 100,$$

Root elongation%
$$= \frac{Mean\ of\ root\ length\ in\ compost\ extract}{Mean\ of\ root\ length\ in\ control} * 100,$$

Relative Germination index%
$$= \frac{Seed\ germination\% - Root\ elongation\%}{10000}.$$

The fertilizer index was calculated from the contents of the TOC, TN, TP, TK and C: N ratios as described Saha *et al.*, (2010). The MSW compost fertilization index is calculated using the formula:

Fertilizing index (FI) $=\Sigma \frac{SiWi}{Wi}$

where 'Si' is a score value of analytical data, and 'W' is weighing factor

of the 'i'th fertility parameter (Table 2).

Table (2). Criteria for 'weighing factor' to fertility parameters and 'score value' to compost (Saha *et al.,* 2010).

Fertility Parameters	Score Value (Si)					Weighting Factor (Wi)
	5	4	3	2	1	
TOC (% dm)	>20.0	15.1-20.0	12.1-15	9.1-12	>9.1	5
TN (% dm)	>1.25	1.01-1.25	0.81-1.0	0.51-0.80	>0.51	3
TP (% dm)	>0.60	0.41-0.60	0.21-0.40	0.11-0.20	>0.11	3
TK (% dm)	>1.00	0.76-1.00	0.51-0.75	0.26-0.50	>0.26	1
C:N ratio	<10.10	10.1-15	15.1-20	20.1-25	<25	3

Note: dm= dry matter.

For clean index calculation, heavy metal concentrations (Zn, Cu, Cd, Pb, Ni, Cr) was used according to (Mandal *et al.,* 2014). Clean index value was calculated by the following formula:

Clean index (CI) $=\Sigma \frac{SjWj}{Wj}$

where 'Sj' is the score value of analytical data, and 'Wj' is weighing factor of the 'j'th heavy metal (Table 3).

Table (3). Criteria for assigning 'weighing factor' to heavy metal parameters and 'score value' to analytical data (Saha *et al.,* 2010)

Heavy metal	Score Value (Si)						Weighting Factor (Wi)
	5	4	3	2	1	0	
Zn (mg/kg dm)	<151	151-300	301-500	501-700	701-900	>900	1
Cu (mg/kg dm)	<51	51-100	101-200	201-400	401-600	>600	2
Cd (mg/kg dm)	<0.3	0.3-0.6	0.7-1.0	1.1-2.0	2.0-4.0	>4.0	5
Pb (mg/kg dm)	<21	51-100	101-150	151-250	251-400	>400	3
Ni (mg/kg dm)	<10.10	21-40	41-80	81-120	121-160	>160	1
Cr (mg/kg dm)	<51	51-100	101-150	151-250	251-350	>350	3

2.6. Physico-chemical analysis:

The pH and electrical conductivity (EC) of composts extract measured by using pH-EC meter; while Nitrate content by using the colorimetric method using UV-spectrophotometer as described by APHA (1998). Organic carbon content by using potassium dichromate procedure (Richard, 1954); Cation exchange capacity was measured by using sodium acetate and ammonium acetate exchangeable method (Richard, 1954). Ash content by ignition method at 550°C according to (Allen, 1974), total nitrogen

determined by Kjeldahl method (Van Reeuwijk, 2002); total phosphorus by using the Olsen method (Allen, 1974); and potassium from composts extract by using flame photometer. Heavy metals were measured by using ICP (Inductive complex plasma) as described by (Punsu and Gantheyrou, 2006); while for biological analysis: pour plate count for heterotrophic bacterial count using nutrient agar as a medium as described by Atlas *et al.,* (1995). Total fungi by spread plate count using potato dextrose agar as described by (Aneja, 2012), and spread plate count for total actinomycetes as mentioned by Atlas *et al.,* (1995).

3.. RESULTS AND DISCUSSION

The result of household solid waste collection in Erbil city during this study showed an increase in generation rate of solid waste which was estimated by 0.632 kg/capita/day; 732.184 tons.day^{-1} for Erbil city inhabitants. Biodegradable organic matter represent 60% (0.377 kg/capita/day) from total SW generation (Figure 1). Erbil city rising SW generation is attributed to an increasing population, the unstable political situation in the country caused emigration from other Iraqi cities to Erbil city. This result is similar to that recorded by Aziz et al., (2011) and Wali (2014), but it is higher than noticed by Shekha (2011). According to data obtained from Erbil directorate municipality service and environment, the MSW collected from Erbil city and transported to Kani Qrzhala landfill reached to 2000 tons/day for 2015, while it was more than 2500 tons/day for 2014 and return this reduction in MSW generation to the economic crisis.
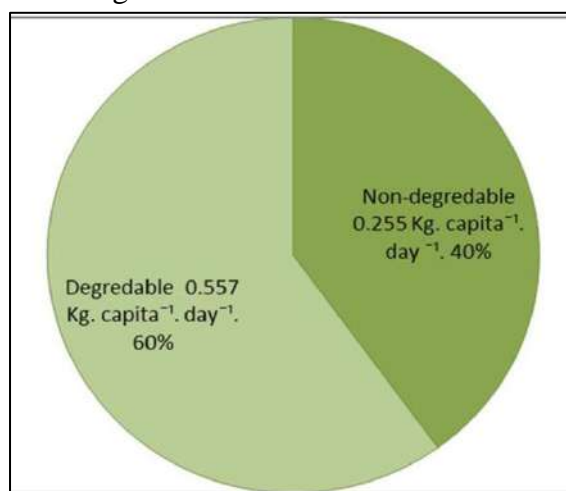

Figure 1: The degradable and non-degradable wastes in Erbil city in 2015.

3.1. Compost quality indices:

Compost quality index consists of three important parameters such as nutrient value, total microbial population, C/N ratio and germination index of compost. During the present study, the compost quality index ranged from 1.03 to 25.28 of the studied composts (Table 4). The minimum value recorded for pit compost of chickpeas seeds and maximum value for anaerobic compost of tomato seeds.

Table (4). Compost quality index of the studied composts.

Seeds	Doses %	Composting Types			
		Pit	Aerobic	Anaerobic	Worm
Tomato	30	2.88	3.29	25.28	11.41
	60	5.38	3.09	23.48	11.27
	100	3.79	4.15	19.23	12.45
Wheat	30	2.21	2.44	17.28	7.67
	60	2.10	1.89	14.87	7.05
	100	2.12	1.89	11.47	6.5
Chickpeas	30	1.44	1.42	10.30	5.33
	60	1.44	1.20	10.62	5.68
	100	1.03	1.55	10.94	3.97

According to Bera *et al.,* (2013) classified tomato and wheat seeds of pit compost as moderate quality, while chickpeas as poor quality. But in aerobic compost classified wheat and chickpeas as poor, while tomato seed as moderate. And in anaerobic compost classified all seeds as extremely good. Therefore, in worm compost classified tomato seed as extremely good, wheat seed as very good, and chickpeas as good quality. The fertilizer index can be taken as a measure of the nutrient supply potential, each analytical data affecting the fertilizer value (responsible for improving soil productivity) of compost. During the present study, the FI ranged from 3.3 to 4.06. The high amount FI in anaerobic compost resulted from a high amount of carbon, nitrogen, potassium and C/N ratio (Mandal *et al.,* 2014). Classification of MSW compost based on marketability and use the different area in accordance to FI value classify the aerobic and anaerobic composts as in class A which means the best quality, but other two types of compost pit and worm composts classify as class B which means very good quality. The present results agree with that found by Saha *et al.,* (2010).

The regulatory authority can use the Clean Index (CI) value to restrict the entry of heavy metals into sensitive environmental components (such as agricultural land and water bodies) (Mandal *et al.,* 2014). During our study, the CI value in all compost samples was 5, because all composts contain a very small amount of heavy metals (Fig.2). Depend on the MSW classification compost based on marketability and use in the different area in accordance to CI value classify the aerobic and anaerobic compost in class A type which means the best quality but pit and worm composts occur in class B type which means very good quality (Table 4). These results came in accordance with that found by (Saha *et al.,* 2010).
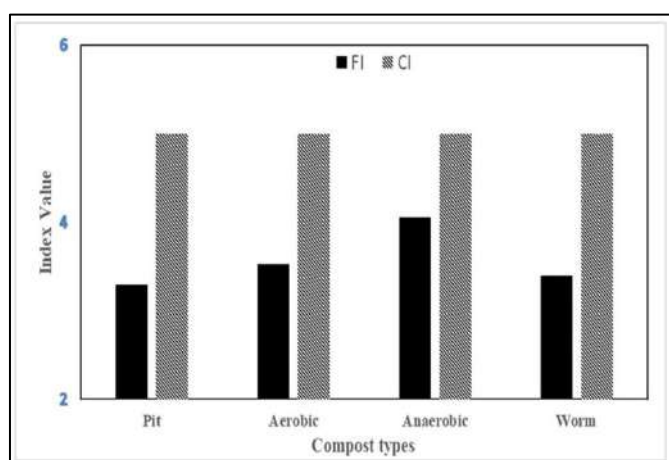

Figure 2: Clean Index and Fertilizing Index of the studied compost samples.

3.2. Physico-chemical parameters:

As shown in (Table 5) the pH value of different composts was in the alkaline side of neutrality. The minimum value was 7.57 recorded for pit compost, and the different compost types were within the stipulated range (7.2-8.5) for good quality. Change in pH value is due to metabolic activities resulted in the production of CO_2 from organic acids and releases of ammonia. While the electrical conductivity of compost extract was ranged from 244.8µs/cm in vermicompost to more than 1404µs/cm in anaerobic compost. The statistical analysis revealed significant differences ($P<0.05$) between the composts studied. High EC of composts probably due to the high concentration of soluble salts derived from food and meat waste due to degradation of organic matter (Campell *et al.,* 1997).

Total organic carbon varied from 15.76% recorded in anaerobic compost to 24.03% obtained in pit compost. Organic carbon content was found to be reduced in all compost sample degradation. Mondini *et al*. (2003) noted a decrease in the percentage of organic carbon, which shows the decomposition of the waste by the microbial population.

(Table 5). Physico-chemical parameters of the studied composts.

Variables	Pit	Aerobic	Anaerobic	Worm
pH	7.57	8.5	8.26	7.73
EC (µs.cm^{-1})	1110.83	1095	1404.66	244.83
TOC%	24.03	22.93	15.67	17.91
T.N%	0.617	0.846	2.188	0.846
T.P%	1.657	0.61	0.988	2.123
NO$_3$(mgNO$_3$.N.l^{-1})	22.2	7.94	17.59	16.43
C/N ratio	39.93	27.76	7.48	21.66
CEC(cmolc.kg^{-1})	51.19	33.37	37.08	9.2
Ash%	45.55	55.69	49.62	49.99
K$^+$%	0.002	0.001	0.004	0.001

The total nitrogen content in studied composts varied from 0.617% obtained in pit compost to 2.188% obtained in anaerobic compost. Sanedzie *et al.,* (2012) commented that low availability of nitrogen in pit compost would restrict the microbial activity and stabilization of the waste by composting, and a decrease in nitrogen level could be through volatilization of gaseous ammonium during mixing and processing of the compost heaps. On the other hand, total phosphorous concentration varied in different studied compost, and it was higher than that recommended standard. Maximum value recorded in worm compost (2.123%), In which phosphorus content gradually increased during worm composting process and phosphorus water solubility decreases with humification and immobilization factor (Elango *et al.,* 2009).

Nitrate is a form of inorganic nitrogen and is an important nutrient for plant growth, pit compost characterized by maximum nitrate content (22.2 mg NO_3 N/l) compared with other studied composts, high nitrate content may be attributed to nitrification occurs when all ammonium is mineralized to nitrate after maturation of compost (Bernal *et al.,* 2008). The C: N ratio is one of the most important parameters for the extent of composting and the degree of compost maturity (Dimambro *et al.,* 2007). The C/N ratio of compost sample recorded minimum

value 7.48 in anaerobic compost; this may be due to high moisture percentage. Saha *et al.,* (2010) recommended that too much moisture leads to luck of aeration and leaching. The maximum ratio obtained in pit compost (39.9); this would imply a high proportion of mineralizable carbon while the nature of the organic matter would influence the rate of the process. Shyamala and Belgali (2012) reported that the C/N ratio more than 25 likely indicated stable compost, then worm compost type is regarded as more stable kind.

Cation exchange capacity (CEC) is one of the factors used to describe soil properties and their importance in determining compost maturity and fertility. During composting, CEC is reported to increase (Iqbal *et al.,* 2012). CEC value of 9.209 cmolc/kg recorded in worm compost and maximum value 51.191 cmolc/kg was obtain from pit compost. CEC value in all types of composters, except worm, gradually increased and after became constant. The high CEC pit compost may be related to its organic matter content; particularly the stable organic matter is humus which contributes to cation exchange capacity.

Higher ash content 55.69% for aerobic compost, this may be due to the high amount of potassium. In the composts, high levels of minerals would suggest high ash content. On the other hand, potassium concentration was ranged from 0.36% recorded in pit compost to 0.51% recorded in aerobic compost. Gallardo-lara and Nogales (1987) It has been shown that potassium increases during anaerobic composting and the effective use of certain fibrous materials such as straw or wood chips that can absorb relatively large amounts of water and maintain structural integrity and porosity could prevent the loss of potassium from the compost formed. While, decrease K^+ in pit compost is due to run-off and leaching of the metal ions with water content present in the solid waste into the ground during the process (Pathak *et al.,* 2012).

CONCLUSION

The study was mainly focusing on performed several procedure for converting household solid wastes into compost, and using it as soil fertilizers. The results revealed that all produced compost types were classified as extremely good quality depending on CQI. The presence of a few amount of heavy metals in the studied compost confirming the good indicators of compost quality.

REFERENCES

ALLEN, S. E. 1974. Chemical analysis of ecological materials, a black well scientific publication. Osney Mead, Oxford.

ANEJA, K. R. 2012. Experiments in microbiology, plant pathology and biotechnology, 4th Ed. New Age International Publishers.

APHA (1998). Standard methods for the examination of water and wastewater, 20th Ed., APHA (American public health association), 1015, 15th. Street, NW, Washington, DC 20005.

ATLAS, R. M.; BROWN, A. E. & PARKS, L. C. 1995. Laboratory manual of experimental microbiology. Mosby-Year Book, Inc. USA.

AZIZ, S. Q.; AZIZ, H. A. BASHIR, M. J. & YUSOFF, M. S. 2011. Appraisal of domestic solid waste generation, components, and the feasibility of recycling in Erbil, Iraq. 29(8): p.880– 887.

BERA, R.; DATTA, A.; BOSE, S.; DOLUI, A. K.; CHATTERJEE, A. K.; DEY, G. C.; BARIK, A. K.; SARKAR, R. K.; MAJUMDAR, D. & SEAL, A. 2013. Comparative evaluation of compost quality, process convenience and cost under different composting methods to assess their large scale adoptability potential as also complemented by compost quality index, International Journal of Scientific and Research Publications. 3(6): 1–11.

CAMPELL, A. G.; FOLK, R. L. & TRIPEPI, R. R. 1997. Wood ash as an amendment in municipal sludge and yard composting processes. Compost Science and Utilization. 5(1): 62–73.

DIMAMBRO, M. E.; LILLYWHITE, R. & RAHN, C. 2007. The physical, chemical and microbial characteristics of biodegradable municipal waste derived composts. Compost Sci. Utiliz. 15(4): 243–252.

ELANGO, D.; THINAKARAN, N.; PANNEERSELVAM, P. & SIVANESAN, S. 2009. Thermophilic composting of municipal solid waste. Applied Energy. 86(5): 663–668.

Erbil Statistic Directorate. 2009. Erbil governorate population according to food card. *(*Archive).

GALLARDO-LARA, F. & NOGALES, R. 1987. Effect of application of town refuses compost on the soil-plant system-a review. Biological Wastes. 19: 35–62.

IQBAL, M. K.; KHAN, R. A.; NADEEM, A. & HUSSANIAN, A. 2012. Comparativestudy of different techniques of composting and their stability evaluation in municipal solid waste. The Chemical Society of Pakistan. 34(2): 273–282.

MANDAL, P.; CHATURVEDI, M. K.; BASSIN, J. K.; VAIDYA, A. N. & GUPTA, R. K. 2014. Estimating the quantity of solid waste generation in Oyo. Int J Recycl Org Waste Agricult. 3: 133–139.

MISRA, R. V. & ROY, R. N. 2002. On-farm composting methods. FAO 1980 a manual of rural composting. FAO/UNDP Regional Project RAS/75/004 Field Document 15, pp.1–26.

MONDINI, C.; DELL'ABATE, M. T.; LEITA, L. & BENEDETTI, A. 2003. An integrated chemical, thermal and microbiological approach to compost stability evaluation. Journal of Environmental Quality. 32: 2379–2386.

PATHAK, A. K.; SINGH, M. M.; KUMARA, V.; ARYA, S. & TRIVEDIC, A. K. 2012. Assessment of physico- chemical properties and microbial community during composting of municipal solid waste (viz. kitchen waste) at Jhansi city, u.p. (India). Recent Research in Science and Technology. 4(4):10–14.

PANSU, M. & GAUTHEYROU, J. 2006. Handbook of soil analysis. Springer velage Berlin Heidelberg.

PREDA, G.; LIXANDRU, B. & POPESCU, D. 2013. Practical methods for aerobic composting of cattle manure. Animal science and biotechnologies. Animale Science and Biotechnologies. 46(1): 204–208.

RAJESHWARI, K. V. & BALAKRISHNAN, M. 2000. Aerobic and anaerobic systems for solid waste treatment. Biochemical methods of conversion. pp. 839–851.

RICHARDS, L. A. 1954. Diagnosis and improvement of saline and alkaline soils. United States Salinity Laboratory Staff, USA. Hand Book.

SAHA, J. K.; PANWAR, N. & SINGH, M. V. 2010. An assessment of municipal solid waste compost quality produced in different cities of India in the perspective of developing quality control indices. Waste Management. 30: 192–201.

SANEDZIE, F.; ROCKSON, G. N. & ACHIO, S. 2012. Comparison of compost maturity, microbial survival and health hazards in two composting systems. J. Microbiol. Biotechnol. Food Sci. 2(1): 175–193.

SHEKHA, Y. A. 2011. Household solid waste content in Erbil city, Iraqi Kurdistan Region, Iraq. Zanco J. 23(3): 1–10.

SHYAMALA, D. C. & BELAGALI, S. L. 2012. Studies on variations in physicochemical and biological characteristics at different maturity stages of municipal solid waste compost. International Journal of Environmental Sciences. 2(4): 1984–1997.

SHYAMALA, D. C. & BELAGALI, S. L. 2015. Effect of municipal solid waste and agricultural composts on growth and yield of fenugreek seeds (*Trigonella foenum* graecum), Research Journal of Pharmaceutical Biological and Chemical Sciences. 6(3): 418–426.

SOUFAN, B. A. 2012. Solid waste management in the west bank: Institutional, legal, financial assessment and framework development, MSc. Thesis. Nablus, Palestine: An-Najah National University.

VANREEUWIJK, L. P. 2002. Procedures for soil analysis, Technical Paper 9. 6th Ed. International Soil Reference and Information Centre. The Netherlands. pp.101.

WALI, K. I. 2011. The domestic solid waste generation management in Erbil city. Zanco Journal of Pure and Applied Sciences. 22(6): 37–52.